

The Role of Monocytes and Macrophages Pathogenesis of HIV and SIV-Associated Cardiovascular Disease

Author: Joshua Aaron Walker

Persistent link: <http://hdl.handle.net/2345/bc-ir:107030>

This work is posted on [eScholarship@BC](#),
Boston College University Libraries.

Boston College Electronic Thesis or Dissertation, 2016

Copyright is held by the author, with all rights reserved, unless otherwise noted.

The Role of Monocytes and Macrophages Pathogenesis of HIV and SIV-Associated Cardiovascular Disease

Joshua Aaron Walker

A dissertation
by
Joshua A. Walker

Submitted to the Faculty of
the Department of Biology
in Partial Fulfillment
of the Requirements for the Degree of
Doctor of Philosophy

Boston College
Morrissey College of Arts and Sciences
Graduate School

June 2016

Monocyte/Macrophage Activation in the Development of HIV and SIV-Associated Cardiovascular Pathogenesis

Joshua A. Walker

Principal Investigator: Kenneth Williams, Ph.D.

Advisory Committee: Welkin Johnson, Ph.D.
Thomas Seyfried, Ph.D.

Readers: Tricia Burdo, Ph.D.
Susan Westmoreland, VMD.



The studies described in this thesis were performed in the Biology Department of Boston College, Chestnut Hill, MA.

ABSTRACT

HIV associated cardiovascular disease is likely due to multiple factors ranging from accelerated aging, the direct effects of HIV proteins, and increased inflammation and immune activation. Monocytes/macrophages play roles in the development and progression of HIV and cardiovascular disease. Increased monocyte/macrophage inflammation and immune activation associated with HIV infection likely contributes to the increased risk of cardiovascular disease development associated with HIV infection. To further understand the role of monocytes/macrophages in the development of HIV-associated cardiovascular disease we: 1) assessed monocyte activation longitudinally to determine if they correlate with and can be predictive of cardiac fibrosis and inflammation; 2) we examined cardiac tissues from the SIV-infected CD8+ T-lymphocyte depleted animals to determine the effects of monocyte/macrophage inflammation on cardiac fibrosis; 3) in parallel we examined cardiovascular tissues from HIV+ individuals on durable cART to determine if aortic and cardiac inflammation persists with infection and if soluble factors (sCD163) correlated with intima-media thickness and fibrosis; 4) we next examined the effects of blocking leukocytes trafficking to the heart on SIV-associated cardiac inflammation and fibrosis; 5) and finally we examined if targeting monocyte/macrophage activation (as opposed to traffic) directly using MGBG decreases SIV-associated cardiovascular pathology, inflammation and fibrosis. We found that early increased monocyte activation was predictive of animals that developed cardiac fibrosis and SIV encephalitis (SIVE). Animals with both cardiac fibrosis and SIVE had increased macrophage inflammation in the heart, suggesting that there is a link between cardiac and CNS inflammation seen with HIV infection (Chapter 2). We found in a SIV-infected CD8+ T-lymphocyte depletion model of rapid AIDS increased prevalence of cardiac disease compared to nondepleted animals, and increased cardiac inflammation that correlated with cardiac fibrosis. Monocyte/macrophage traffic to the heart occurred later with SIV infection, possibly with the

development of AIDS (Chapter 3). In post-mortem human tissues studies we found that inflammation in aorta and heart correlated with increased soluble CD163, and correlated with aortic intima-media thickness and cardiac fibrosis with HIV infection (Chapter 4). Blocking leukocyte traffic to the heart using an anti- α 4 antibody decreased macrophage inflammation in the heart that correlated with decreased cardiac fibrosis (Chapter 5). Using MGBG, a polyamine biosynthesis inhibitor that directly targets monocyte/macrophage activation, we found decreased inflammation in the carotid artery and heart correlated with decreased carotid artery intima-media thickness and cardiac fibrosis (Chapter 6). Overall these studies provide evidence for ongoing monocyte/macrophage cardiovascular inflammation with HIV and SIV infection. Macrophage inflammation correlates with markers of cardiovascular disease (fibrosis and intima-media thickness, cardiomyocyte damage). Directly targeting monocyte/macrophage traffic (anti- α 4 antibody) and activation (MGBG) decreased cardiovascular pathology, inflammation, fibrosis, and intima-media thickness. Taken together, the data in this thesis indicate that targeting monocytes/macrophages in conjunction with combination anti-retroviral therapy could alleviate cardiovascular disease in HIV-infected individuals.

TABLE OF CONTENTS

Abstract	iv
Table of Contents	vi
Acknowledgements	xi
List of Tables	xii
List of Figures	xiv
List of Abbreviations	xvii
Chapter 1: Introduction	
I. HIV Biology	
A. HIV Clinical Progression	1
B. HIV Genome and Replication	4
II. HIV Infection in the cART Era	
A. Increased Lifespan with Effective cART	6
B. Increased Immune Activation with cART	8
III. Cardiovascular Manifestations of HIV Infection	
A. HIV in the Pre-cART Era	9
B. HIV in the Post-cART Era	10
IV. Role of Immune Cells in Cardiovascular Disease	

A.	T-lymphocytes	12
B.	B-lymphocytes	14
C.	Monocytes/Macrophages	16
V.	Plaque Stability is Influenced by Immune Cells	
A.	Characteristics of Stable vs Unstable Atherosclerotic Plaques	19
B.	Atherosclerotic Plaques Associated with HIV Infection	20
VI.	Imaging Modalities to Diagnose Cardiovascular Disease	
A.	Positron Emission Tomography	21
B.	Tilmanocept as Direct Diagnostic Imaging Agent	22
C.	B-mode ultrasound	23
B.	Cardiac Magnetic Resonance Spectroscopy	23
VII.	Therapies Targetting Macrophage Inflammation	
A.	3-hydroxy-3-methylglutaryl-coenzyme A reductase inhibitors	23
B.	Altering Macrophage Polarization	24
VIII.	SIV-Infected, CD8⁺ T-lymphocyte Depletion Model of AIDS	25
IX.	Summary	26
X.	References	30

Chapter 2: Expansion of CD14⁺CD16⁺ Monocyte Subset Correlates with Increased Cardiac Fibrosis, Inflammation, and SIV Encephalitis in SIV-infected Rhesus Macaques

Abstract	56
Introduction	57
Results	60
Discussion	64

Materials and Methods	68
Tables, Figures, Figure Legends	72
References	86
Acknowledgements and Funding	96

Chapter 3: Elevated Numbers of CD163+ Macrophages in Hearts of SIV Infected Monkeys

Correlates with Cardiac Pathology and Fibrosis

Abstract	98
Introduction	99
Results	101
Discussion	104
Materials and Methods	108
Tables, Figures, Figure Legends	112
References	125
Acknowledgements and Funding	131

Chapter 4: Increased Aortic Intima Media Thickness and Cardiac Fibrosis Correlates with

Soluble CD163: A Role for Monocytes/Macrophages in HIV-Associated Cardiovascular Disease

Progression

Abstract	133
Introduction	134
Results	136
Discussion	138
Materials and Methods	141
Tables, Figures, Figure Legends	143
References	152

Acknowledgement and Funding	158
Chapter 5: An Anti-α4 Antibody Blocks Monocyte/Macrophage Traffic to the Heart and Decreases Cardiac Pathology in a SIV Infection Model of AIDS	
Abstract	160
Introduction	161
Results	164
Discussion	169
Materials and Methods	174
Tables, Figures, Figure Legends	177
References	188
Acknowledgements and Funding	197
Chapter 6: Direct Targeting of Macrophages with Methyglyoxal-bis-Guanylhydrazone Decreases SIV-Associated Cardiovascular Inflammation and Pathology	
Abstract	199
Introduction	200
Results	203
Discussion	206
Materials and Methods	210
Tables, Figures, Figure Legends	215
References	225
Acknowledgements and Funding	234
Chapter 7: Summary and Discussion	230
Appendices	

Tilmanocept as a diagnostic imaging agent	240
Publications	251
Conferences and Awards	253

ACKNOWLEDGEMENTS

First and foremost I would like to extend my sincerest gratitude to my advisor, Dr. Kenneth Williams for the opportunities he has given me by being a part of his research lab. He has consistently impressed me with his dedication to his work and challenged me to exceed beyond my expectations on a daily basis. I sincerely thank him for his mentorship over the years.

I would also like to thank past and current lab members who have supported me during my time at Boston College. Dr. Caroline Soulas was instrumental in teaching and helping me learn when I first started at Boston College. I am particularly thankful for the guidance and day to day mentorship from Dr. Tricia Burdo. I would like to extend my thanks to the other lab members, past and present, that I have had the pleasure of working with over the past 6 years in the lab; Dr. Brian Nowlin, Dr. Jennifer Campbell, Jaclyn Mallard, Jessica Lakritz, and Dr. Jamie Schafer. And of course I have to thank the undergraduate research assistants in the Williams lab that have been an integral part my research. Thank you to Katherine Nowicki, Megan Sulciner, John Wang, and Graham Beck for your thoughtful questions and dedication to the lab, and your willingness to count thousands of cells without complaint.

I thank the members of my committee for their time and valuable insight into my projects. And last, but surely not least, I want to thank my family and friends for their support and encouragement during my graduate career.

LIST OF TABLES

Table 2.1. Cardiac and CNS pathology of animals used in this study	72
Table 2.2. Numbers of macrophages and T-lymphocytes in cardiac tissues of animals with and without cardiac disease	74
Table 2.3. Numbers of cardiac macrophages and T-lymphocytes present in animals with and without SIV encephalitis	75
Table 3.1 Rhesus macaques used in this study	112
Table 3.2 Comparison of the numbers of macrophages and T-lymphocytes in Uninfected, SIV+, and SIV+ CD8+ T-lymphocyte depleted rhesus macaques	113
Table 3.3. Increased numbers of macrophages and T-lymphocytes in SIV-infected CD8+ T-lymphocyte depleted rhesus macaques with cardiac pathology compared to SIV-infected CD8+ T-lymphocyte depleted rhesus macaques without cardiac pathology	115
Table 3.4. BrdU+ cells in the heart of SIV-infected CD8+ T-lymphocyte depleted rhesus macaques are of myeloid lineage	116
Table 4.1. Increased numbers of macrophages in the aorta and cardiac tissues with HIV infection	143
Table 5.1. Cardiac pathology of natalizumab treated and control animals used in this study	177

Table 5.2. Numbers of macrophages and T-lymphocytes in natalizumab treated and control animals	179
Table 5.3. Numbers of macrophages and T-lymphocytes in late natalizumab treated animals and controls with and without cardiac pathology	181
Table 6.1. MGBG and placebo control animals used in this study	215
Table 6.2. Cardiovascular pathology of MGBG and placebo control animals	217

LIST OF FIGURES

Figure 1.1. Replication of HIV virus in Mucosa and Submucosa Tissue	2
Figure 1.2. Time Course of HIV Infection	3
Figure 1.3. Organization of HIV-1 Genome	4
Figure 1.4. HIV-1 Replication Cycle	6
Figure 1.5. Mortality in the cART Use Over Time	7
Figure 1.6. Time Course of HIV-1 Infection with cART Use	7
Figure 1.7. Increased Levels of Biomarkers of Immune Activation	9
Figure 1.8. The Role of T-lymphocytes in Atherosclerotic Plaque Development	13
Figure 1.9. Adaptive Immune Pathways in the Development of Fibrosis	14
Figure 1.10. The Role of B-lymphocytes and immunoglobins with Atherosclerotic Plaques Development	15
Figure 1.11. Monocyte Recruitment and Macrophage Differentiation within Atherosclerotic Lesion	18
Figure 1.12. Pathophysiology of Plaque Progression and Rupture	20
Figure 1.13. Comparison of Stable and Unstable Atherosclerotic Plaques	21

Figure 2.1. Significant increase in myocardial fibrosis in SIV-infected, CD8⁺ T-lymphocyte depleted rhesus macaques with cardiac pathology	76
Figure 2.2. Gating strategy to identify monocyte subsets in blood plasma	78
Figure 2.3. Elevated CD14⁺CD16⁺ monocyte expression early correlates with myocardial fibrosis in SIV-infected, CD8⁺ T-lymphocyte depleted rhesus macaques with cardiac pathology and SIVE	80
Figure 2.4. Plasma SIV-RNA does not distinguish between animals with and without cardiac disease or with and without SIV encephalitis	82
Figure 2.5. Animals with cardiac disease have increased CCR2 expression on activated CD14⁺CD16⁺ monocytes	84
Figure 3.1. Increased numbers of CD163⁺ macrophages and amount of collange in heart tissue in SIV infected rhesus macaques with cardiac pathology	117
Figure 3.2. Correlations between the percentage of collagen per total tissue area and numbers of CD163⁺, CD68⁺ and MAC387⁺ macrophages in SIV infected rhesus macaques	119
Figure 3.3. Increased traffic of macrophages to the heart during late SIV infection	121
Figure 3.4. SIV plasma virus does not distinguish between animals with and without cardiac pathology	123
Figure 4.1. HIV infection results in increased macrophage inflammation in the aorta and cardiac tissue compared to uninfected individuals	144
Figure 4.2. HIV infection results in an increased aortic intima-media thickness which correlates with increased numbers of macrophages	146

Figure 4.3. HIV infection results in increasing levels of fibrosis in cardiac tissues which correlates with increased numbers of macrophages	148
Figure 4.4. Plasma soluble CD163 correlates with increased inflammation, fibrosis, and aortic intima-media thickness in aorta and cardiac tissues	150
Figure 5.1. Natalizumab treatment decreases the numbers of macrophages in cardiac tissues in SIV-infected CD8+ T-lymphocyte depleted rhesus macaques	183
Figure 5.2. Natalizumab treatment decreases fibrosis in cardiac tissues in SIV-infected CD8+ T-lymphocyte depleted rhesus macaques	184
Figure 6.1. Daily treatment with MGBG results in a trend of decreased cardiovascular inflammation in the carotid artery and a significant decrease in inflammation in cardiac tissue from SIV-infected CD8+ T-lymphocyte depleted rhesus macaques	219
Figure 6.2. MGBG treatment prevents an increase in carotid artery intima-media thickness which correlates with a decreased trend in macrophage inflammation	221
Figure 6.3. MGBG treatment prevents an increase in cardiac fibrosis in cardiac tissues similar to levels seen in uninfected controls	223

LIST OF ABBREVIATION

AIDS	Acquired immunodeficiency syndrome
aIMT	Aortic intima-media thickness
BrdU	5'-bromo-2'-deoxyuridine
CA	Capsid
CAC	Coronary artery calcium
cART	Combination antiretroviral therapy
CCR	Chemokine (C-C motif) receptor
CCR2	Chemokine (C-C motif) receptor-2
CCR5	Chemokine (C-C motif) receptor-5
ciMT	Carotid artery intima-media thickness
CMV	Cytomegalovirus
CNS	Central nervous system
CVD	Cardiovascular disease
DAB	3,3'-diaminobenzidine tetrahydrochloride
DC	Dendritic cell
Dpi	Days post infection
ELISA	Enzyme-linked immunosorbent assay
ENV	Envelope polyprotein
FDG	Fluorodeoxyglucose
FDM	Fluorodeoxymannose
GAG	Group-specific antigen polyprotein
HAND	HIV-associated neurocognitive disorders
HIV	Human immunodeficiency virus
HIVE	Human immunodeficiency virus encephalitis
HRP	Horseradish peroxidase
IF	Immunofluorescence
IHC	Immunohistochemistry
IMT	Intima-media thickness
IN	Integrase
IL-3	Interleukin-3
IL-4	Interleukin-4
IL-5	Interleukin-5
IL-15	Interleukin-15
IL-6	Interleukin-6
LTR	Long terminal repeat
MA	Matrix
MCP-1	Monocyte chemotactic protein-1

MFI	Mean fluorescence intensity
MGBG	Methylglyoxal-bi-guanylhydrazone
MRS	Magnetic resonance spectroscopy
Nef	Negative factor
NK	Natural killer
OI	Opportunistic infection
PBMC	Peripheral blood mononuclear cell
PET	Positron emission tomography
POL	Pol polyprotein
sCD163	Soluble CD163
sCD14	Soluble CD14
SIV	Simian immunodeficiency virus
SIVE	Simian immunodeficiency virus encephalitis
SU	Surface or gp120 protein
Tat	Trans-activator
TLO	Tertiary lymphoid organ
TM	Transmembrane or gp41 protein
TNF- α	Tumor necrosis factor-alpha
VCAM-1	Vascular cell adhesion molecule-1
Vif	Viral infectivity factor
Vpr	Viral protein R
Vpu	Viral protein U
Vpx	Viral protein X
Rev	Regulator of expression of viral proteins

CHAPTER 1. Introduction

I. HIV Biology

A. HIV clinical progression in the Pre-cART era

Approximately 80% of HIV infections are accounted for through gastrointestinal and reproductive tract mucosal exposure with the remaining 20% of infections due to percutaneous or intravenous infections or direct mother to infant transmission¹⁻³. While the exposure route can differ from person to person, the timing of detection of viral and host biomarkers of infection in untreated cases of HIV is relatively uniform.⁴ During the first 7 to 21 days, while HIV is replicating in the mucosa, submucosa, and lymphatic tissue (**Figure 1.1**), the virus cannot be detected in plasma¹. During this early asymptomatic phase, there is uncontrolled viral spread within the body and establishment of viral reservoirs^{2,3}. Acute infection occurs within 2 to 4 weeks after infection and is characterized by a rapid increase in plasma HIV RNA as well as decreases in CD4+ T-lymphocytes in the blood and gut. Following this, the virus enters into a latent stage where viral RNA is decreased and remains relatively stable while there is a recovery of CD4+ T-lymphocytes. This period can last on average 10 years, which is then followed by progression to AIDS, the final stage. Here, viral RNA in the blood increases rapidly along with continued decrease of CD4+ T-lymphocytes. It is at this time where individuals experience symptoms of AIDS and development of opportunistic infections (**Figure 1.2**)^{5,6}.

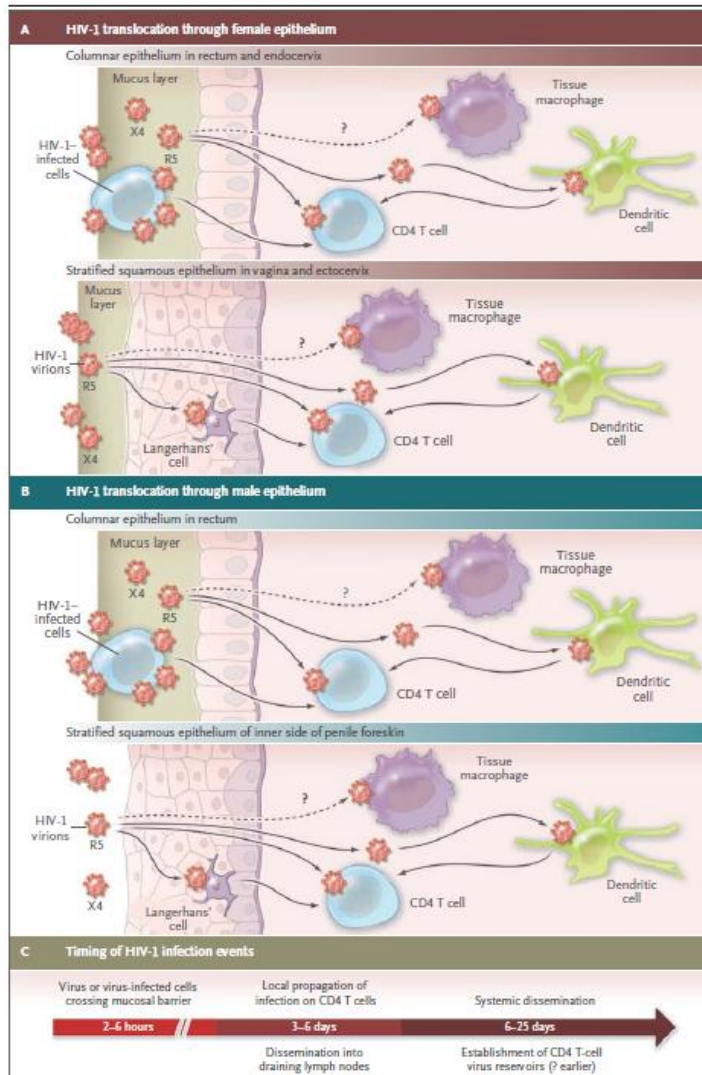


Figure 1.1 Replication of HIV virus in mucosa and submucosa tissue. A schematic diagram of HIV-1 virus infection and replication during the early stages of disease (Reproduced with permission from Cohen MS et al. Acute HIV-1 Infection. *N Engl Med* 2011,**364**:1943-1954, Copyright Massachusetts Medical Society)

Upon initial HIV infection, the host mounts an immune response that includes the production of acute-phase reactants and inflammatory cytokines and the beginning of CD8+ T-lymphocyte cytotoxic response⁷. Interferon (IFN)- α and interleukin (IL)-15 are both elevated prior to peak viremia along with tumor necrosis factor (TNF)- α and IFN- γ that are secreted by a mix of dendritic cells (DCs), monocytes, and natural killer (NK) cells⁷⁻¹⁰. Cytotoxic CD8+ T-lymphocyte responses appear days before peak viremia along with the production of cytokines

and contribute to the initial control of the spread of the virus¹¹⁻¹³. Approximately 3 months after infection, neutralizing antibodies begin to be detected within the blood^{1,14}. The initial neutralizing antibodies recognize the surface glycoprotein (gp)41 of HIV-1, but many neutralizing antibodies are eventually generated that recognize gp120. It is during the asymptomatic period when the virus is in a latent stage, that the host immune responses are able to keep viral replication in control¹⁵. However, continued viral replication eventually leads to reduced CD4+ T-lymphocytes and chronic dysregulated immune activation that can result in susceptibility to opportunistic infections (OIs), including tuberculosis, Kaposi sarcoma, and cytomegalovirus (CMV). Both infected and uninfected CD4+ T-lymphocytes die during HIV infection, with uninfected cells dying through apoptosis, possibly due to cytotoxicity of HIV proteins. CD4+ cells can also enter apoptosis due to an abortive infection or due to expression of HIV proteases after viral integration. AIDS is defined by the number of CD4+ T-lymphocytes falling below 200 cells/mL of blood. As numbers of CD4+ T-lymphocytes decrease, plasma virus also increases, along with the development of OIs (**Figure 1.2**).

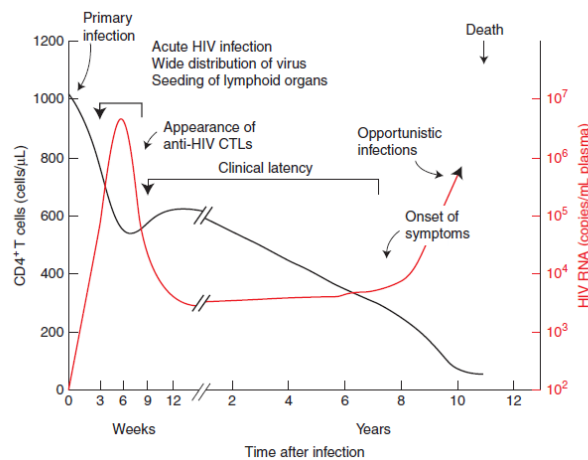


Figure 1.2 Time course of typical HIV infection. Patterns of CD4+ T cell decline and viremia vary greatly from one patient to another

(Reprinted by permission from Cold Spring Harbor Laboratory Press, *Cold Spring Harb Perspect Med*, 3(1), Coffin J, Swanstrom R, HIV Pathogenesis: Dynamics and Genetics of Viral Populations and Infected Cells, a012526-a012526, 2013)

B. HIV Genome and replication

HIV is a complex enveloped retrovirus that encodes for 15 distinct proteins. The genome has 9 open reading frames, 3 of which encode Gag, Pol, and Env polyproteins, which are proteolyzed into proteins that are common to all retroviruses¹⁶. The core of the virion and the outer membrane are made of the four Gag proteins, MA (matrix), CA (capsid), NC (nucleocapsid), and p6, along with the two Env proteins, SU (surface or gp120) and TM (transmembrane of gp41). PR (protease), RT (reverse transcriptase), and IN (integrase) are the three Pol proteins that are encapsulated within the virion and provide necessary enzymatic functions for genome integration and replication of the virus. The remaining proteins encoded by the genome are 6 accessory proteins. Vif, Vpr, and Nef, which are found within the viral particle. Tat and Rev assist in gene regulatory functions while Vpu assists in the assembly of the virion. Long terminal repeats (LTR) at the 5' and 3' ends of the genome help to regulate transcription of the viral genes (**Figure 1.3**)¹⁶⁻¹⁸.

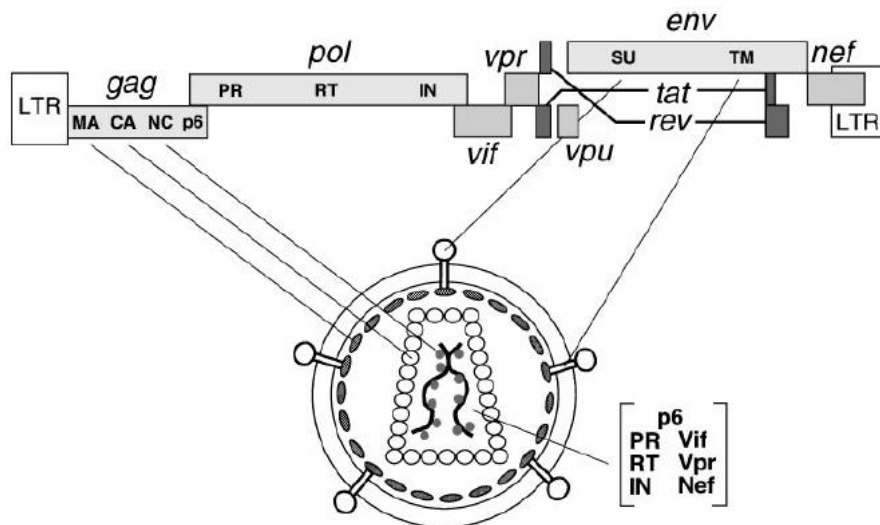


Figure 1.3 Organization of HIV-1 genome and virion showing the 15 proteins and open reading frames (Reproduced with permission from Frankel AD and Young JAT. HIV-1 Fifteen Proteins and an RNA. *Ann Rev Biochem* 1998,**67**:1-25).

Historically, the CD4 cell surface molecule was initially discovered to be the main cellular receptor for HIV-1 shortly after the virus was isolated¹⁹⁻²¹. Following this, it was discovered that HIV uses one of two coreceptors to gain entry into a cell, either the CXC-chemokine receptor 4 (CXCR4) or the CC-chemokine receptor 5 (CCR5)^{22,23}. Viral infection of a cell first begins with the recognition of the envelope protein gp120 to the CD4 receptor on a target cell²⁴. Binding of the CD4 receptor on a target cell results in a conformational change in gp120 that allows it to interact and bind with the CXCR4 or CCR5 co-receptor, followed by the insertion of the gp41 protein into the host cell membrane²⁵. When the membranes of the virion and the target cell fuse, the core proteins begin to uncoat and the HIV genome, reverse transcriptase, and integrase are released into the cytoplasm of the target cell^{26,27}. Within the nucleus of the target cell, the viral enzyme, integrase, allows incorporation of HIV intermediate DNA (provirus) into the cellular DNA where it is used as a template for the production of new virions. New viral transcripts and the full length RNA genome of HIV are transcribed and exported from the nucleus and into the cytoplasm. Using both viral and cellular proteins, HIV RNA is spliced and assembled into new virions that bud from the surface of the target cell and can then infect new cells (**Figure 1.4**)²⁸⁻³⁰.

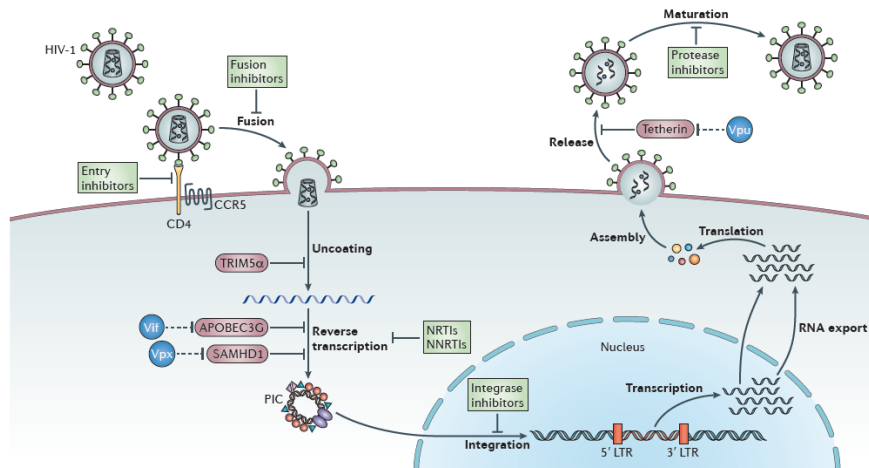


Figure 1.4 Overview of the HIV-1 replication cycle along with antiretroviral drugs and the steps that they target (green boxes)

(Reprinted by permission from Macmillan Publishers Ltd: Barre-Sinoussi F et al., Past, present and future: 30 years of HIV research, *Nat Rev Microbiol*, 11(12) 877-883, 2013).

II. HIV infection in the cART era

A. Increased lifespan with effective cART

With the emergence of combination anti-retroviral therapy (cART) the health and lifespan of HIV infected individuals has dramatically increased³¹⁻³⁴ (**Figure 1.5**). The goal of an effective drug regimen is to improve immune function and decrease plasma viral load below the limit of detection of commercial assays, 50 copies of HIV RNA/mL (**Figure 1.6**)^{35,36}. Because of effective cART, reduced plasma viral load, and recovery of CD4+ T-lymphocytes, the patterns of morbidity and mortality with HIV infection has shifted in the post-cART era^{37,38}. Previously, in the pre-cART era the healthcare focus in AIDS management centered on AIDS specific malignancies such as Kaposi sarcoma and lymphomas, tuberculosis, CMV, Pneumocystis carinii, and complications arising from early anti-retroviral therapy associated drug toxicities, drug-drug interactions, and drug resistance. In the cART era, with a longer lifespan, HIV has become a chronic condition, leading to a rise in a number of significant non-AIDS co-morbidities³⁹. These entail, but are not limited to, AIDS-related cancers, renal⁴⁰, hepatic⁴¹, neurological⁴²⁻⁴⁴, and

cardiovascular complications⁴⁵⁻⁵⁰. While the cause of these secondary diseases is most likely multi-factorial, growing evidence in recent years has implicated prolonged immune activation and chronic inflammation as central to the development of chronic HIV pathologies, with monocytes/macrophages postulated to play an important role.

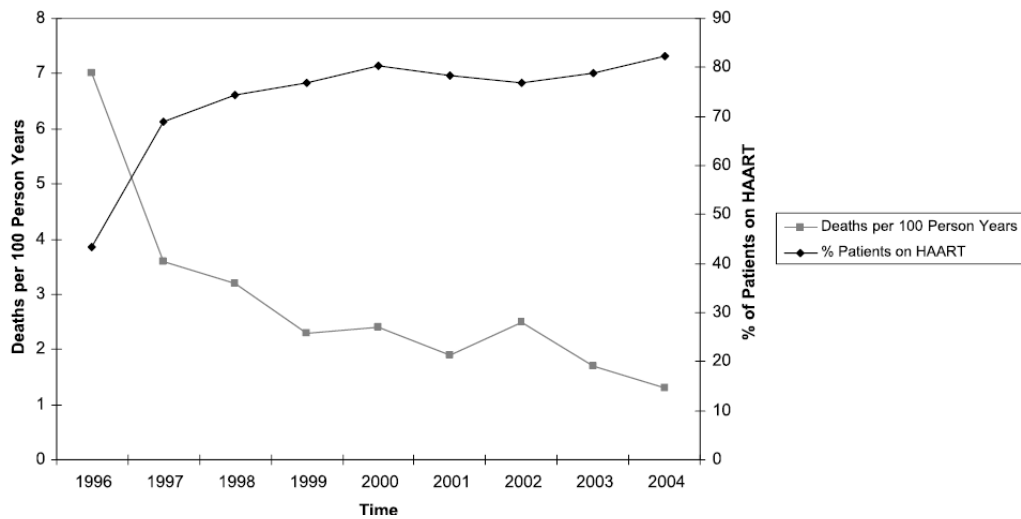


Figure 1.5 Mortality and cART use over time
(Palella FJ et al., Mortality in the Highly Active Antiretroviral Therapy Era Changing Causes of Death and Disease in the HIV Outpatient Study. *J Acquir Immune Defic Syndr.* 2006;43(1):27-34).

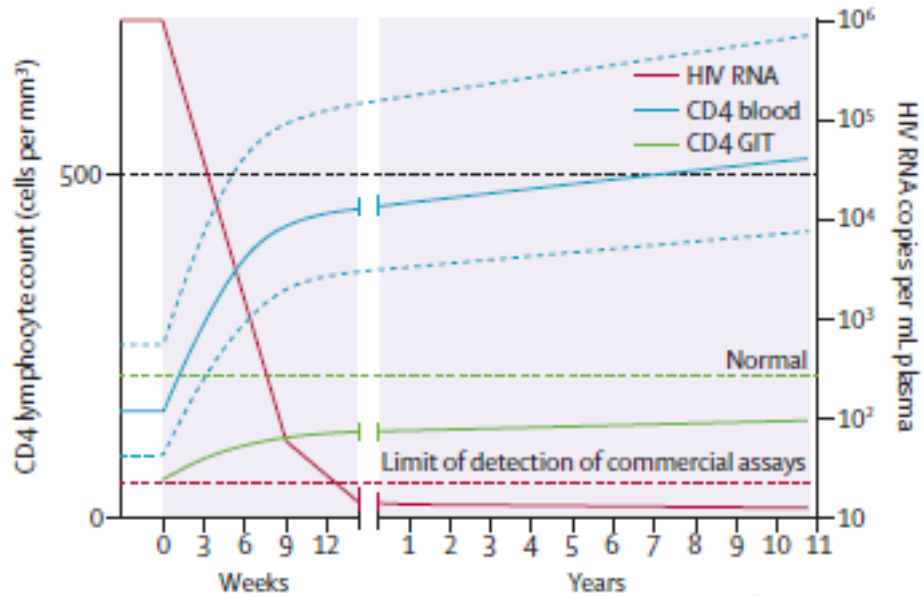


Figure 1.6 Time course of HIV infection with combination antiretroviral therapy
(Reprinted from *Lancet*, 384(9939), Maartens G, et al., HIV infection: epidemiology, pathogenesis, treatment, and prevention, 258-271, 2014, with permission from Elsevier)

B. Increased immune activation with HIV infection

Durable cART can decrease plasma viral load to low or undetectable levels in patients that adhere to the drug regimen. However, low level viremia still exists⁵¹⁻⁵³ in these patients possibly due to ongoing viral replication or release of virus from latent tissue or cellular reservoirs^{54,55}. Low level viral replication can lead to prolonged immune activation. Several studies have showed that HIV infected individuals on suppressive cART still have elevated markers of immune activation that remain elevated after initiation of cART and do not return to levels seen in HIV negative individuals.⁵⁶⁻⁵⁸ (**Figure 1.7**). In particular, soluble CD163 (sCD163) in the blood has become a useful biomarker of HIV activity. CD163 is a hemoglobin/haptoglobin receptor that is expressed solely on monocytes/macrophages⁵⁹⁻⁶¹. Soluble CD163 is proteolytically cleaved from the surface of activated CD163+ macrophages in response to pro-inflammatory stimuli^{62,63}. Serum levels of sCD163 correlated with HIV-1 activity where they are elevated in acutely (<1yr) and chronically (>1yr) infected individuals and remain elevated even after initiation of cART in chronically infected individuals⁶⁴. Chronic immune activation, based on elevated sCD163, is also seen in HIV-1 elite controllers (who spontaneously control virus without being on cART) with higher sCD163 in elite controllers than in patients on durable cART.⁶⁵

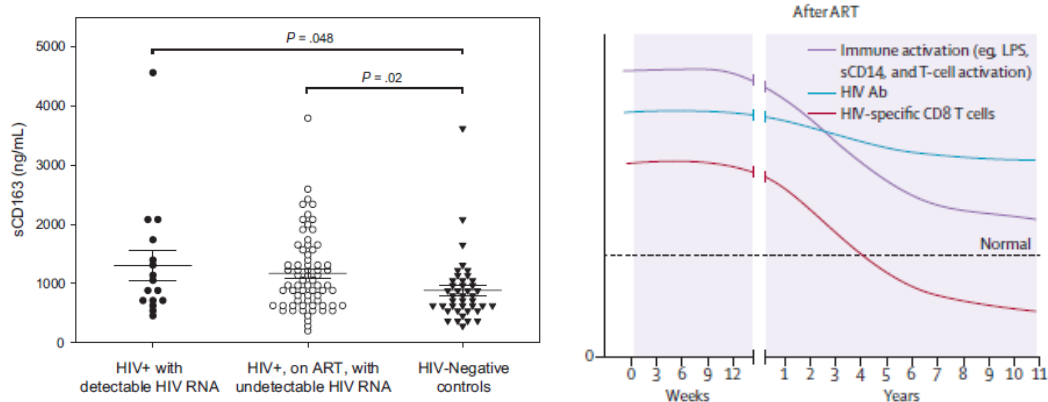


Figure 1.7 Increased levels of biomarkers of immune activation sCD163 and sCD14 in HIV infected individuals on cART

(Left. Burdo TH, et al., Soluble CD163 made by monocyte/macrophages is a novel marker of HIV activity in early and chronic infection prior to and after anti-retroviral therapy. *J Infect Dis.* 2011;204(1):154-163, by permission of Oxford Press. Right. Reprinted from *Lancet*, 384(9939), Maartens G at al., HIV infection: epidemiology, pathogenesis, treatment, and prevention, 258-271, 2014, with permission from Elsevier)

III. Cardiovascular manifestations of HIV infection

A. Pre-cART era

The focus of research on cardiovascular disease associated with HIV infection has shifted in the pre- and post-cART era. In the pre-cART era many of the manifestations have been associated with the cardiac muscle itself. In the pre-cART era dilated cardiomyopathy (DCM), an enlargement of the heart resulting in deficiencies in pumping blood, had been diagnosed in 8-30% of HIV infected individuals and in 25% of patients at necropsy⁶⁶⁻⁶⁸. Myocarditis, inflammation of the heart muscle, has been documented in as low as 6% and as high as 50% of HIV infected individuals^{66,69,70}. Magnetic resonance imaging (MRI) showed that with HIV infection there is increased inflammation in early stages of HIV infection and increased fibrosis in the later stages⁷¹. The prevalence of myocarditis and fibrosis among HIV+ individuals has increased as HIV+ individuals on cART live longer. Similar rates of endocarditis and pericardial effusion are seen in HIV+ individuals as well^{72,73}. It was initially believed that much of the

myocardial disease associated with HIV and AIDS was due to Kaposi Sarcoma, a tumor caused by infection with human herpesvirus-8^{74,75}. However, with effective cART, many of these manifestations of the myocardial disease has been significantly reduced, in some cases by as much as 30%^{69,76,77}.

B. Post-cART era

While the prevalence of some types of myocardial disease associated with HIV have decreased with cART^{76,77} recent reports have begun to show that there still exists a significant burden of myocardial disease associated with chronic HIV infection^{50,78}. Magnetic resonance spectroscopy (MRS) studies demonstrated that HIV infected individuals continue to have subclinical myocardial disease, fibrosis, and alterations in cardiac function^{50,78-80}. Significant myocardial fibrosis was prevalent in 76% of HIV infected individuals on cART compared to only 13% of age-matched control individuals⁷⁸. Similar findings were presented in a recent study examining asymptomatic HIV infected individuals on suppressive cART with HIV plasma RNA below 200 copies/mL and CD4+ T-lymphocytes greater than 400 cells/ μ L where cardiac magnetic resonance (CMR) showed that myocardial fibrosis was seen in 82.1% of HIV infected individuals compared to 27.3% of healthy controls^{81,82}.

HIV has become there has also been an increase in vascular disease due to continued immune activation and systemic inflammation. Compared to the general population, HIV infected individuals are at an increased risk of atherosclerosis⁸³⁻⁸⁵. FDG-PET imaging of HIV infected individuals showed increased inflammation in the ascending aorta consistent with atherosclerosis which correlated with elevated serum levels of sCD163, suggesting a role for inflammation, specifically monocytes/macrophages, in the development of HIV-associated cardiovascular disease (CVD)⁸⁶. It has previously been shown that traditional risk factors of CVD,

(elevated D-dimer, C-Reactive protein (CRP), and interleukin (IL)-6) are not associated with atherosclerotic plaques in HIV patients, but markers of immune activation, sCD14 and sCD163⁶⁴ are, suggesting that chronic immune activation of monocytes/macrophages play a role in the development of HIV-associated CVD.

Levels of sCD14 are associated with coronary artery calcium (CAC), a marker of CVD, among HIV infected individuals⁸⁷. In a study examining men with and without HIV, it was found that sCD14 and sCD163 are elevated in those with HIV and associated with subclinical atherosclerosis⁸⁸. Early during the cART era it was thought that drug toxicities were responsible for the increase in CVD associated with HIV infection⁸⁹⁻⁹². However, it is interesting to note that HIV-1 elite controllers, who spontaneously maintain low levels of viremia without cART still experience an increase in CVD⁹³. Reportedly elite controllers had an increase in non-calcified, vulnerable plaques that are prone to rupture compared to uninfected controls, as well as chronically infected individuals on cART, accompanied by elevated serum markers of inflammation and immune activation, sCD14, sCD163^{65,94}. This supports the notion that cART toxicity is not the sole cause of HIV-associated CVD, but inflammation and immune activation play a role in the development of CVD.

As the prognosis of HIV+ individuals has improved with the development of effective cART this population is now aging, with approximately 50% of HIV+ individuals in the United States and Europe being 50 years old or older.⁹⁵ Data shows that mortality due to AIDS-related causes has decreased in the cART era but there has been a proportional increase in mortality due to non AIDS-related illnesses,^{45,96,97} and in particular the proportion of deaths due to CVD among HIV+ individuals has increased.⁴⁵ In a large population study examining HIV+ individuals on cART compared to uninfected controls it was demonstrated that with HIV infection there is an increase in noninfectious comorbidities, in particular CVD, compared to controls.^{98,99}

Additionally, HIV+ individuals were more likely to suffer from multiple pathologies simultaneously (poly pathology). The prevalence of poly pathology among HIV+ individuals was similar to that seen in uninfected individuals that are 10 to 15 years older⁹⁸. The results from this study suggest that HIV infection can lead to the early aging of an infected individual, potentially leading to the development of CVD at an earlier age compared to the general population.

IV. Role of Immune Cells in Cardiovascular Disease

A. T-lymphocytes

Early evidence of increased expression of MHC-II molecular human leukocyte antigen D-related (HLA-DR) in human atheromas along with large numbers of T-lymphocytes provided insight into the role of the adaptive immune system in the development of atherosclerosis¹⁰⁰⁻¹⁰². The majority of T-lymphocytes within the atheroma are CD4+ T helper cells¹⁰³. T-lymphocytes are one of the first cell types to be recruited into a developing atheroma and they are increased in unstable plaques that are prone to rupture compared to more stable atherosclerotic plaques^{104,105}.

Within atherosclerotic plaques the most abundant subset of T-lymphocytes are CD4+ T-lymphocytes. Naïve T-lymphocytes mature into effector or helper cells (Th), with the most well known Th cells being Th1, that express IFN- γ , Th2, which produce and secrete interleukin (IL)-5, IL-4, and IL-3, and Th17, cells which secrete IL-17 and IL-22^{106,107}. In a large proportion of plaques, Th-1 T-lymphocytes were found to be the most abundant subset and IFN- γ has been shown to be expressed and play a role in promoting atherosclerosis and ongoing inflammation¹⁰⁸. IFN- γ promotes atherosclerosis by altering endothelial function, necessary for the recruitment of inflammatory cells to the developing lesion, and alters cholesterol export

from macrophages resulting in increased foam cell formation¹⁰⁹. Conversely, Th2 cells appear to have a protective effect in regards to the development of atherosclerosis. Th2 cells secrete IL-4 which can inhibit Th1 differentiation as well as IFN- γ production^{110,111}. While not as abundant as CD4+ T-lymphocytes, CD8+ cytotoxic T-lymphocytes are also present in atherosclerotic plaques and have a pro-atherogenic effect by initiating cell death (**Figure 1.8**)¹⁰⁶.

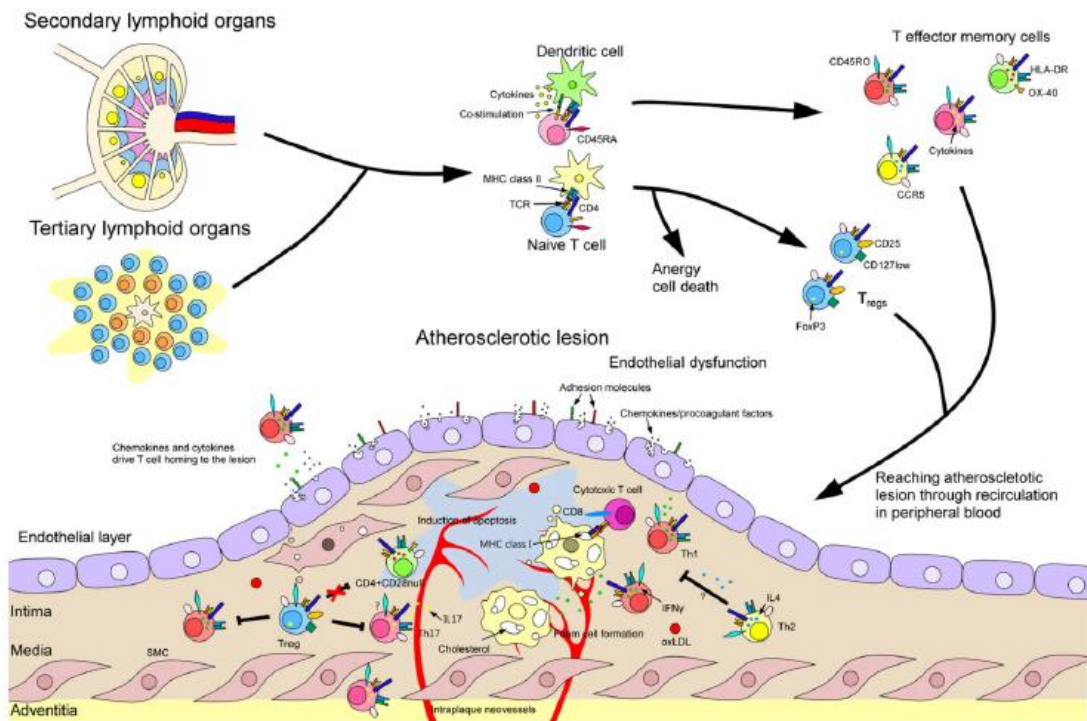


Figure 1.8 The role of T-lymphocytes within atherosclerotic plaque development
 (Reprinted by permission from John Wiley and Sons, *Clin Exp Immunol*, 179(2), Ammirati E et al., The role of T and B cells in human atherosclerosis and atherothrombosis, 173-187, 2015)

Within the heart itself, T-lymphocytes are also important in the development of cardiac inflammation and fibrosis, accumulation of fibrillar extracellular matrix (ECM) in the myocardium^{112,113}. It has been proposed that Th2 cells promote the development of cardiac fibrosis while Th1 cells, and the cytokines that they produce, are anti-fibrotic under inflammatory conditions¹¹⁴. However, other reports have shown evidence that Th1 T-lymphocytes have pro-fibrotic effects as well¹¹⁵. IFN- γ produced by Th1 cells is known to help in

the differentiation, migration, and activation of macrophages as well as expressing MCP-1 which aids in the recruitment of cells to the heart leading to active inflammation and the development of fibrosis (Figure 1.9)^{116,117}.

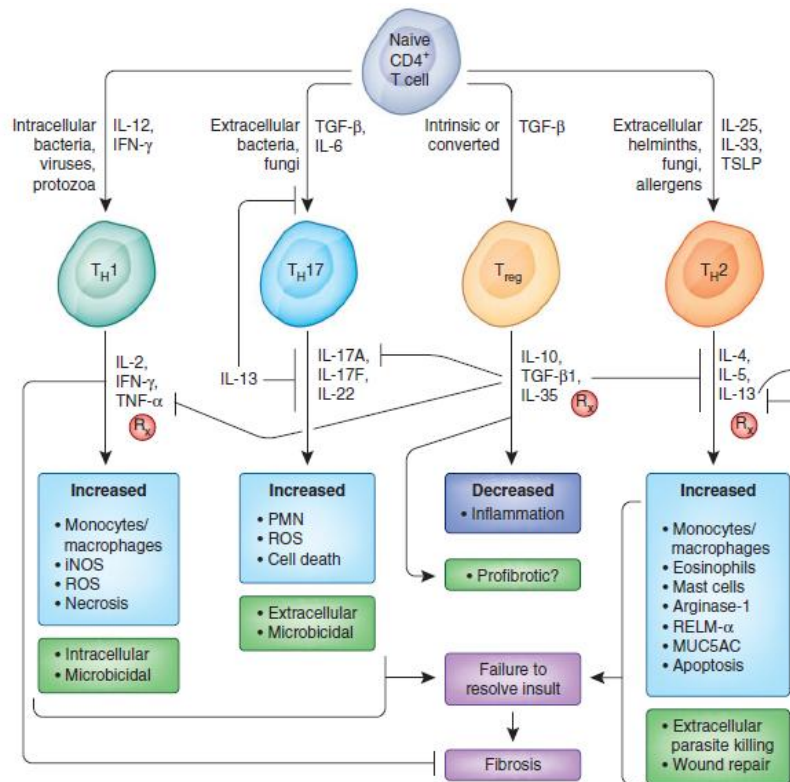


Figure 1.9 Adaptive immune pathways in the development of fibrosis
 (Reprinted by permission from Macmillan Publishers Ltd: *Nat Med*, 18(7), Wynn TA and Ramalingam TR, Mechanisms of fibrosis: therapeutic translation for fibrotic disease, 1028-1040, 2012)

B. B-lymphocytes

Much of the clinical research involving the immune system and its role in the development of atherosclerosis and subsequent CVD has focused on T-lymphocytes. However, rodent studies suggest that B-lymphocytes may play a protective role in atherosclerosis^{118,119}. While T-lymphocytes are numerous in a developing plaque, there are fewer B-lymphocytes but their numbers are increased in the outer adventitial layer of the vessel wall^{120,121}. B-lymphocytes are found in both the intima and adventitia of a vessel wall in human and animal

studies, but they are more prevalent in the adventitia than the intima¹²². In the adventitia associated with an atherosclerotic plaque, B and T-lymphocytes have been described as forming tertiary lymphoid organs (TLO)¹²³. B-lymphocytes present in the intima produce antibodies against low-density lipoprotein (LDL,) which can aid in LDL clearance by monocytes/macrophages and neutrophils¹²³. B-lymphocytes in the adventitia are thought to accumulate later during the course of the disease, and their numbers are increased when TLO are present (**Figure 1.10**).

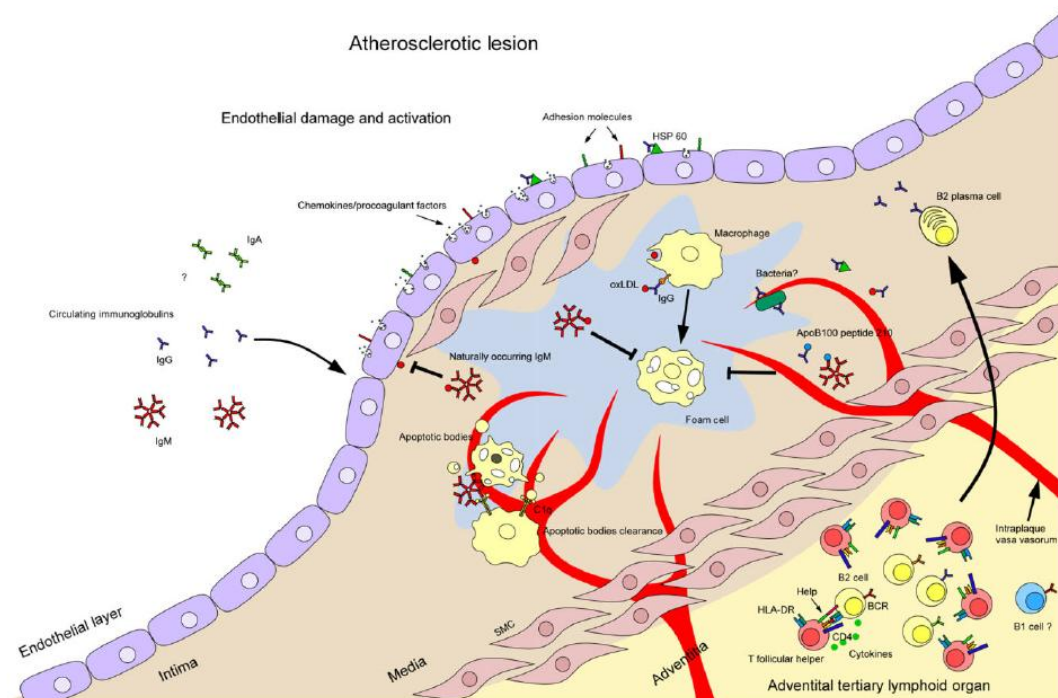


Figure 1.10 The role of B cells and immunoglobulins within atherosclerotic plaque development (Reprinted by permission from John Wiley and Sons, *Clin Exp Immunol*, 179(2), Ammirati E et al., The role of T and B cells in human atherosclerosis and atherothrombosis, 173-187, 2015)

Similar to T-lymphocytes, which can be classified as Th1 and Th2, B-lymphocytes can be classified as either B1 or B2 that potentially have different functions^{101,118}. B2 cells are thought to be pro-atherogenic. When B2 cells were isolated, purified, and transferred into lymphocyte-deficient mouse models atherosclerosis was significantly increased, suggesting a proatherogenic

role for B2 cells in the absence of other immune cells types¹¹⁹. Conversely B1 cells that secrete nonspecific natural IgM antibodies are protective against atherosclerosis. Natural IgM antibodies inversely correlate with atherosclerotic burden in carotid arteries and carotid artery intima-media thickness^{101,120}. This suggests a protective role for B1 cells in human atherosclerosis.

In contrast to their possible protective role in preventing or reducing atherosclerotic disease, B-lymphocytes may contribute to cardiac disease. B-lymphocytes can generate cardiac specific antibodies that can bind to cardiomyocytes causing apoptosis¹²⁴. Additionally, in mice that are lacking both T and B-lymphocytes, there is a delay in the development of acute cardiomyopathy as well as decreased levels of myocardial fibrosis. With injury to the heart, B-lymphocytes selectively secrete the chemokine CCL7 which triggers monocyte mobilization and recruitment from the bone marrow. In mice depleted of B-lymphocytes, there is decreased CCL7 and subsequently a reduction in monocyte/macrophage infiltration of the heart and improves myocardial function¹²⁵.

C. Monocytes/Macrophages

Monocytes are mononuclear phagocytes that comprise 5-10% of leukocytes in circulation in humans¹²⁶. They are a heterogeneous population and classified based on their expression of various surface antigens, size, morphology, and function¹²⁶⁻¹³⁰. Monocytes have been identified by their expression of CD14, the lipopolysaccharide co-receptor, and their expression of CD16, the low affinity Fcγ-III receptor that acts as a marker of activated monocytes,^{127,131-133} resulting in populations of monocytes as being defined as either CD14⁺CD16⁻ or CD14⁺CD16⁺. More recently, research showed that CD16⁺ monocytes are a heterogeneous population, leading to new nomenclature dividing monocytes into three

populations: CD14⁺⁺CD16⁻ (classical), CD14⁺⁺CD16⁺ (intermediate) and CD14⁺CD16⁺⁺ (non-classical) monocytes. Monocytes are a key component in the development of CVD and previously have been shown to be predictive of CVD^{134,135}. CD14⁺⁺CD16⁺ monocytes were independently related to the occurrence of myocardial infarction and non-hemorrhagic stroke¹³⁵, and CD14⁺CD16⁺ monocytes were associated with the development of coronary artery disease¹³⁶. CD14⁺⁺CD16⁺ monocytes are also increased in patients experiencing congestive heart failure and increased numbers in circulation could reflect deterioration of the heart muscle¹³⁷. Studies have defined the role of monocytes/macrophages that express surface markers such as CD68, CD163, and CD206 in the development of coronary artery disease,¹³⁸ cardiac fibrosis,¹³⁹ myocarditis^{76,140} and atherosclerotic plaque progression^{141,142,143-145}. In the initial stages of atherosclerosis, activated endothelium results in increased expression of surface adhesion molecules, such as E-selectin, P-selectin¹⁴⁶, and VCAM-1^{138,147}, and secrete chemokines CCL2, CCL5, and CX3CL1¹⁴⁸, promoting the recruitment of leukocytes and monocytes to the arterial wall^{103,149}. Here, monocytes differentiate into macrophages where they can phagocitize low density lipoprotein (LDL) and develop into foam cells,¹⁵⁰ which contribute to the development of an atheroma core^{149,151}. Within atherosclerotic plaques there are a range of monocyte/macrophage phenotypes, where M1 inflammatory macrophages are thought to play a role in plaque rupture¹⁵², while M2, characterized by CD163 and CD206 expression, macrophages are thought to be athero-protective¹⁵³. However, the distinction between M1 and M2 polarized macrophages based on their surface markers is not distinct and monocytes/macrophages should be distinguished based on their actual function within tissues. Studies using optical coherence tomography have shown that vulnerable plaques have a lipid rich core and more macrophages present in the cap and shoulder regions than stable plaques within the same individual¹⁵⁴. Histological studies showed that macrophages in vulnerable

plaques (those that are prone to rupture) M2 CD163 and CD206 positive macrophages¹⁵⁵. It is possible that while these macrophages express classical markers of M2 polarized cells they are in fact having a pro-inflammatory effect and that the definitions of M1 and M2 macrophages will need to be altered based on actual function. Work by our lab showed that numbers of CD163+ and CD206+ macrophages in the *intima* of the aorta correlate with increased intima-media thickness, a CVD marker (Chapter 4). Additionally, macrophages within an atherosclerotic plaque secrete matrix metalloproteinases (MMPs), promoting plaque instability and rupture (Figure 1.11)^{156,157}.

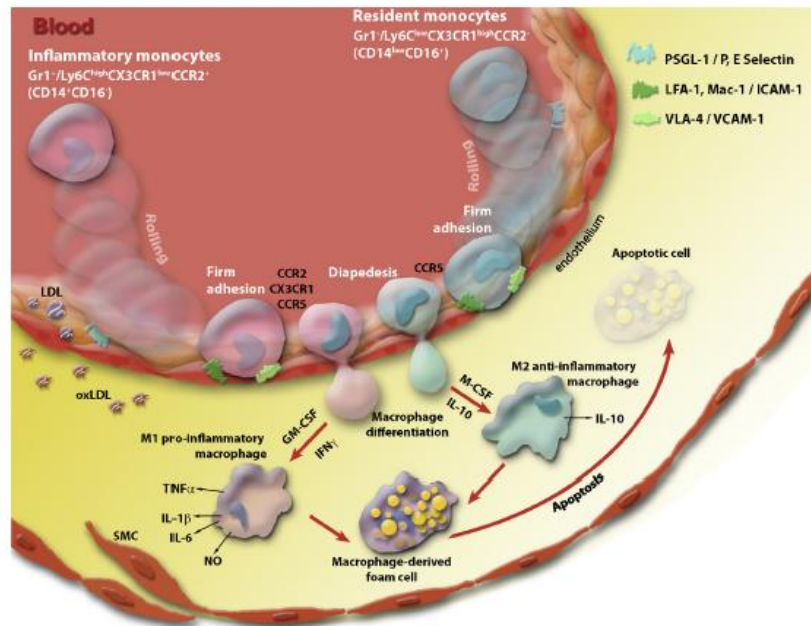


Figure 1.11 Monocyte recruitment and macrophage differentiation within an atherosclerotic lesion (Reprinted from *Immunobiology*, 218(11), Fenyo IM and Gafencu AV. The involvement of the monocytes/macrophages in chronic inflammation associated with atherosclerosis, 1376-1384, 2013, with permission from Elsevier)

In the normal heart there are few macrophages present in the ventricles and atria that express CD68 and are likely resident tissue macrophages.¹⁵⁸ Numbers of macrophages are increased with cardiovascular disease with and without HIV infection^{159,160}. Growing evidence

supports the role of monocytes and macrophages in the development of cardiac fibrosis. In response to injury or infection monocytes traffic to the myocardium and develop into tissue macrophages that secrete pro-inflammatory and fibrotic factors. We showed that increased numbers of macrophages in the heart correlate with increased cardiac fibrosis¹⁶¹.

Monocytes/macrophages can secrete high levels of pro-inflammatory cytokines interleukin (IL)- 1β ¹⁶², tumor necrosis factor (TNF)- α ^{163,164} as well as pro-fibrotic growth factors transforming growth factor (TGF)- β ^{165,166}. TNF- α and IL- 1β are expressed in fibrotic heart tissue and levels of TNF- α in circulation correlated with collagen turnover suggesting a role for the cytokine in cardiac remodeling¹⁶⁷.

V. Plaque stability is influenced by immune cells

A. Characteristics of stable and unstable atherosclerotic plaques

Atherosclerosis comprises the bulk of CVD and is now considered a chronic inflammatory disease affecting the walls of mid to large arteries¹⁶⁸. Typically, atherosclerotic plaques remain dormant for years and may not even result in clinical manifestations such as myocardial infarction (MI). However, the surface of a plaque can be damaged or degraded and is then prone to rupture resulting in a thrombosis and eventually result in myocardial infarction (MI) (**Figure 1.12**)¹⁶⁹. Stable plaques tend to be more calcified and have reduced macrophage content compared to unstable, vulnerable, plaques which have large lipid filled cores with apoptotic cells and increased numbers of macrophages in the shoulder and cap regions (**Figure 1.13**)^{154,155}. Macrophages located in atherosclerotic plaques secrete matrix metalloproteinases (MMPs) which can degrade collagen and other components of the ECM that give a plaque its strength¹⁷⁰⁻¹⁷². While MMPs can be secreted by numerous cells types within a plaque,

macrophages have been shown to secrete MMP-1, -3, and -8, which colocalized with cleaved collagen suggesting that MMPs are not only secreted but also activate^{173,174}.

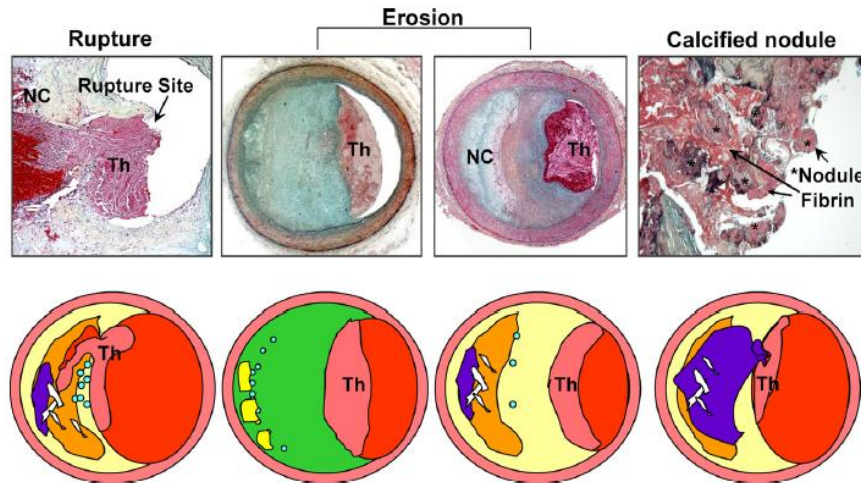


Figure 1.12 Pathophysiology of plaque progression and rupture
 (Reprinted from *Heart Lung Circ*, 22(6), Sakakura K et al., Pathophysiology of atherosclerosis plaque progression, 399-411, 2013, with permission from Elsevier)

B. Atherosclerotic plaques associated with HIV infection

Within HIV infected populations there is an increased risk of CVD due in part to monocyte/macrophage accumulation¹⁷⁵⁻¹⁷⁷, resulting in a phenotype of plaques that are vulnerable, non-calcified, and prone to rupture^{64,86}. FDG-PET imaging showed that HIV infection results in increased inflammation in the ascending aorta, which correlated with increased levels of sCD163, proteolytically cleaved specifically by monocytes/macrophages⁸⁶. In addition to increased aortic inflammation in HIV patients, there is elevated high-risk plaque morphology defined as an increase in the number of low attenuated plaques and positive remodeling¹⁷⁸. Noncalcified vulnerable plaques among HIV+ individuals are linked to markers of monocyte/macrophage activation including sCD163⁸⁶. This suggests that targeting

monocytes/macrophages in HIV infected individuals could provide a benefit in reducing the number and extent of noncalcified plaques and decrease clinical sequelae of CVD such as MI.

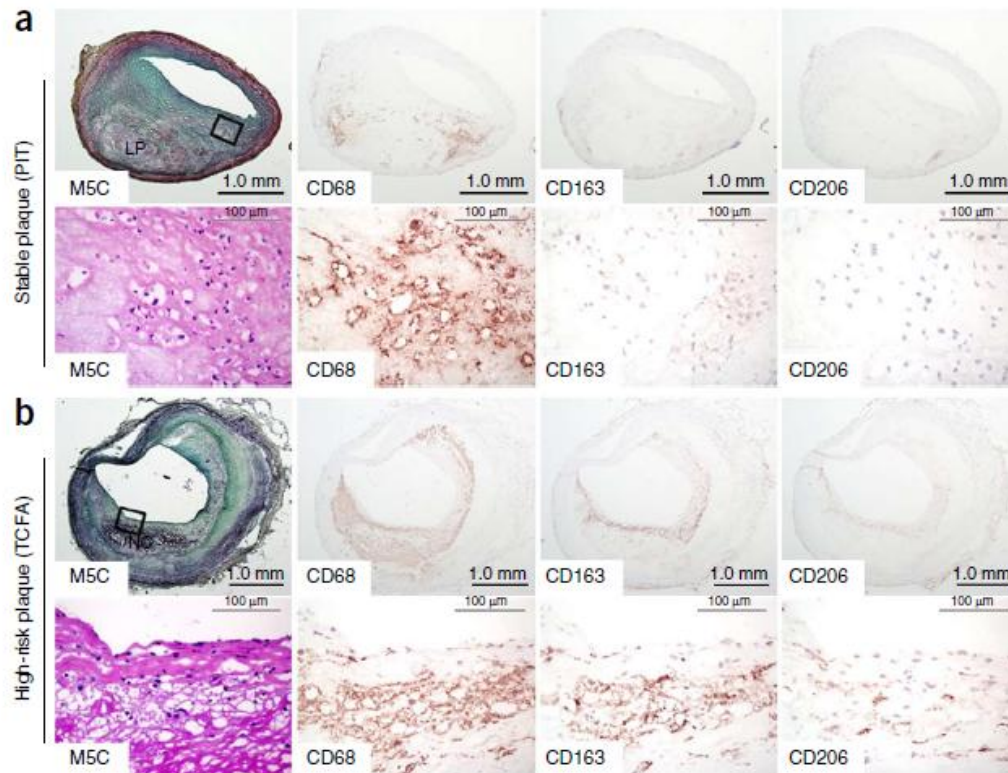


Figure 1.13 Comparison of stable and unstable atherosclerotic plaques
 (Reprinted by permission from Macmillan Publishers Ltd: *Nat Med*, 20(2), Tahara N et al., 2-deoxy-2-[F]fluoro-d-mannose positron emission tomography imaging in atherosclerosis, 215-219, 2014)

VI. Imaging modalities to diagnose cardiovascular disease

A. Positron Emission Tomography

Radiolabeled ^{18}F -fluorodeoxyglucose (FDG) with positron emission tomography (PET) has been employed as a technique to visualize vascular inflammation in animal models and human cases of atherosclerosis¹⁷⁹⁻¹⁸¹. Metabolically active cells readily take up and accumulate the radiolabeled glucose through glucose transporters (GLUTs). Because macrophages are more metabolically active than surrounding cells they will take up glucose in excess and can then be

visualized using PET imaging to show vascular inflammation due to macrophage accumulation¹⁵⁵. Macrophages are polarized into either M1 pro-inflammatory or M2 anti-inflammatory subsets that express different surface markers^{153,182}. M2 macrophages express the mannose receptor (MR), CD206, on their cell surface, which provides a target for using radiolabeled mannose, ¹⁸[F]FDM, as an imaging agent. As previously discussed, CD206+ macrophages present in unstable atherosclerotic plaques¹⁵⁵. Animal studies showed that ¹⁸[F]FDM was readily taken up by M2 macrophages in atherosclerotic plaques at a higher rate than ¹⁸[F]FDG resulting in better sensitivity and diagnosis following PET imaging¹⁵⁵. In addition, by using ¹⁸[F]FDM it is possible to specifically target those macrophages that are responsible for plaque stability and distinguish high risk plaques.

B. Use of Tilmanocept as a direct diagnostic imaging agent

^{99m}Tc-tilmanocept (Lymphoseek®, Navidea Biopharmaceuticals, Inc.) is a sensitive and specific diagnostic imaging agent that binds specifically to CD206, the MR on the surface of macrophages and dendritic cells¹⁸³. Tilmanocept has previously been approved for and used in human studies in sentinel lymph node (SLN) biopsies to detect various types of cancers that express CD206¹⁸⁴⁻¹⁸⁶. Expression of CD206 on macrophages is not specific to cancers, but is also expressed on macrophages in various other diseases such as rheumatoid arthritis and cardiovascular disease¹⁸³. As numbers of macrophages expressing CD206 are increased in unstable atherosclerotic plaques it is possible that ^{99m}Tc-tilmanocept to directly identify macrophages in vascular inflammation and discriminate between stable and unstable atherosclerotic plaques¹⁵⁵.

C. B-mode ultrasound to measure intima-media thickness of arteries

The development of ultrasound techniques has made it possible to noninvasively measure the intima-media thickness (IMT) of an artery *in vivo*¹⁸⁷. Measurements in both the carotid artery and aorta of IMT effectively determine the risk of atherosclerosis in people¹⁸⁸⁻¹⁹⁰. A longitudinal study using therapies designed to reduce vascular inflammation in HIV+ patients effectively reduced IMT, reducing CVD risk due to atherosclerosis¹⁹¹.

D. Cardiac magnetic resonance spectroscopy

Cardiac magnetic resonance spectroscopy (MRS) not only can be used to gain anatomical and functional information about the heart, but also information on the composition of the tissue itself including the presence of inflammation and fibrosis^{81,192}. Cardiac biopsy samples from healthy individuals were stained with picosirius red to quantify the amount of myocardial fibrosis. The amount of fibrosis measured in the biopsy samples strongly correlated with results from cardiac MRS¹⁹³.

VII. Therapies targeting macrophage inflammation for cardiovascular disease

A. 3-hydroxy-3-methylglutaryl-coenzyme A reductase inhibitors (statins)

Statins are commonly used to lower low-density lipoprotein (LDL) cholesterol to prevent CVD^{194,195}, but have also been shown to have pleiotropic properties that are anti-inflammatory and immune modulatory¹⁹⁶. In monkeys fed a pro-atherogenic diet for 12 months, pravastatin and simvastatin decreased the number of macrophages present in developing atheromas,

independent of their effects to lower plasma LDL cholesterol¹⁹⁷. Here, monkeys were divided into groups and fed atherogenic diets to keep levels of plasma total cholesterol, HDL, and LDL similar. Statin treatment reduced expression of IL-1 β that can increase vascular cell adhesion molecule-1 (VCAM-1) on endothelial cells and result in increased adhesion of monocytes to the vessel wall. Additional studies using apolipoprotein E*3 (apoE*3)-Leiden mice, which develop atherosclerotic plaques similar to humans, showed that rosuvastatin and atorvastatin treatment reduced the density of macrophages within atherosclerotic plaque regions and prevented their progression^{198,199}. In humans, rosuvastatin use in the Measuring Effects on Intima-Media Thickness (METEOR) trial resulted in a decreased rate of progression of carotid artery intima-media thickening,²⁰⁰ and specifically among HIV+ individuals on ART with a moderate risk of CVD, rosuvastatin decreased cIMT thickness over a two year period¹⁹¹. However, these studies did not examine if a reduction in cIMT was related to decreased macrophage inflammation the carotid artery. A study using atorvastatin on HIV+ individuals with subclinical atherosclerosis showed that over a 12 month time period while non-calcified plaque volume was decreased arterial inflammation of the aorta was not²⁰¹.

B. Altering macrophage polarization

Macrophages are divided into either M1 or M2 phenotypes based on the expression of surface molecules and, in CVD, based on their different functions in the development of cardiac fibrosis and atherosclerotic plaque development and rupture. Because it has been suggested that M1 and M2 macrophage phenotypes may actually be the ends of a spectrum it might be possible to alter macrophage polarization to diminish tissue specific pathologies. In one such attempt, fasudil, a rho-kinase inhibitor, inhibited M1 macrophages in EAE mice and increased expression of M2 macrophage markers while decreasing expression of pro-inflammatory

cytokines IL-1 β , TNF- α , and MCP-1²⁰². Small interfering RNAs (siRNAs), in animals, have been used to inhibit TNF- α expression by macrophages. When delivered orally, siRNAs decreased expression of TNF- α and IL-1 β when mice were challenged with lipopolysaccharide (LPS) and successfully decreased inflammation²⁰³.

VIII. SIV-infected, CD8+ T-lymphocyte depletion model of AIDS in rhesus macaques

Simian immunodeficiency virus infection (SIV) in rhesus macaques induces a disease that is similar to HIV in humans²⁰⁴. SIV infected macaques follow a similar progression to HIV in humans including loss of CD4+ T-lymphocytes, opportunistic infections with progression to AIDS, and SIV encephalitis (SIVE)²⁰⁵⁻²⁰⁷. SIV infection of rhesus macaques could be used to effectively study the effects of CVD associated with HIV infection^{91,208-210}. Intravenous (iv) infection with SIVmac251 in rhesus macaques results in the development of AIDS in 1 to 3 years, and a high incidence of macrophage mediated disease, including CNS and cardiovascular disease²¹¹. Administration of a chimeric humanized mouse anti-CD8 monoclonal antibody at days 6, 8, and 12 post infection (dpi) successfully depleted CD8+ T-lymphocytes and NK cells²¹². This leads to viremia by 12 dpi that does not subside and the development of AIDS in 3-4 months with increased incidences of macrophage mediated diseases when animals are persistently depleted of CD8+ T-lymphocytes²¹¹.

We have previously used the CD8+ T-lymphocyte depletion model of AIDS to study SIVE²¹³⁻²¹⁸, and cardiovascular inflammation¹⁶¹. SIV infection of nonhuman primates results in cardiovascular pathology similar to that seen with HIV infection^{161,208,219}. Studies showed that SIV infected nonhuman primates develop a spectrum of cardiovascular disease found in HIV infected individuals, ranging from myocarditis, fibrosis, atherosclerosis and acute MI²²⁰⁻²²².

The pathophysiology and etiology of CVD associated with HIV is poorly understood and limitation of studying the cardiovascular effects of HIV is due to the high number of confounding factors in patients²²³. In humans, cardiovascular disease could be due to HIV or the effects of cART²²⁴⁻²²⁶. As most of the HIV infected individuals are treated it is difficult to distinguish cardiovascular disease being caused by the virus itself or the toxic side effects of cART that can result in changes in lipid levels or be directly toxic to the vasculature²²³. Using a nonhuman primate model to study HIV is beneficial in that it allows the study of and relationships between HIV infection and increased immune activation and inflammation and CVD without any confounding factors. Due to the shorter time course for the development of SIV-associated CVD, it can also be used as a model to test new therapies used in conjunction with cART to alleviate HIV-associated CVD.

IX. Summary of studies in this thesis

Monocytes/macrophages play important roles in both atherosclerosis and myocardial fibrosis. We hypothesized that the increased CVD risk seen among HIV+ patients is due to chronic monocyte/macrophage activation and inflammation. Studies in this thesis examined how monocytes/macrophages contribute to the development of cardiovascular disease with SIV and HIV. We first asked if changes in monocyte activation predict development of cardiac disease, specifically cardiac fibrosis (Chapter 2). We also asked if there is a link between SIVE and cardiac inflammation that could possibly be due to increased monocyte/macrophage traffic and accumulation (Chapter 2). We next asked if increased macrophage inflammation in the heart of SIV-infected correlates with cardiac fibrosis (Chapter 3). In parallel we examined cardiovascular inflammation in post-mortem human tissues of HIV-infected individuals on durable cART and whether soluble factors correlate with markers of cardiovascular disease

(Chapter 4). The final two chapters of this thesis examined whether or not blocking traffic of monocytes/macrophages (Chapter 5) to the heart and monocyte/macrophage activation (Chapter 6) can alleviate cardiovascular disease.

We first began by examining if changes in circulating monocytes can predict the development of cardiac fibrosis in SIV-infected CD8+ T-lymphocyte depleted animals (Chapter 2). In these studies, we show that there are indeed early changes in the numbers of activated CD14+CD16+ monocytes in animals that develop cardiac disease compared to those that do not. As early as 8 days post infection (dpi) the numbers of circulating CD14+CD16+ monocytes are significantly increased, and remain elevated through infection. The numbers of CD14+CD16+ monocytes at 8 dpi and terminally correlated with cardiac fibrosis, suggesting that monocytes can predict cardiac fibrosis development. In the studies in this chapter we also show an increased prevalence of CNS disease in animals with cardiac disease compared to those without. Animals with SIV encephalitis (SIVE) have increased cardiac fibrosis compared to animals without encephalitis and increased inflammation in the heart (myocarditis). These data suggest a link between cardiac and CNS disease, possibly caused by increased inflammation associated with SIV and HIV infection.

In chapter 3 of this thesis we examined the role of macrophage inflammation and traffic to the heart. In these studies we found that SIV-infected, CD8+ T-lymphocyte depleted animals had a higher prevalence of cardiac disease and inflammation compared to non-depleted animals. This further suggests that the immune system plays a role in the development of cardiac disease. In these experiments plasma viral load for all CD8+ T-lymphocyte depleted animals peaked at 8 dpi and remained elevated throughout infection, regardless of whether the animal developed cardiac disease or not. Additionally, we did not find evidence of either SIV RNA or protein in inflammatory cells in cardiac tissues, which had previously been reported to

occur infrequently in other studies.^{209,210,219} In this study we still found significant inflammation in the heart which correlated with increased cardiac fibrosis. As we do not find virally infected cells in the heart but still saw significant inflammation we can conclude that damage to the heart is not due solely to toxic effects of viral proteins and that macrophages themselves are mediating damage, possibly due to secreting pro-fibrotic cytokines. We found that increased inflammation in cardiac tissues correlated with increased cardiac fibrosis. Using BrdU we found that there is increased traffic to the heart of macrophages later (>21 dpi) during infection with the development of AIDS.

In parallel to the studies in chapter 3, we examined age and sex-matched samples from HIV+ and HIV- individuals (Chapter 4). Here we found that inflammation in the heart and inflammation in the aorta are correlated. We found that with HIV infection there was an increase in cardiac fibrosis which correlated with increased inflammation in the heart and increased aortic intima-media thickness (aIMT) correlated with increased inflammation as well. We also found that increased blood levels of soluble CD163 (sCD163) seen with HIV infection correlated with increased cardiac fibrosis and aIMT.

In the previous chapters of this thesis we show evidence that monocytes/macrophages play a role in the development of cardiovascular associated with HIV. In chapters 5 and 6 of this thesis we next examined the effects on the heart and vasculature when we block monocytes/macrophages. In chapter 5, we blocked leukocyte traffic to the heart using an anti- α 4 antibody, natalizumab. We found that when natalizumab was administered at the time of SIV infection, there were no differences in numbers of macrophages in the heart or degree of fibrosis in treated animals compared to untreated. We showed in chapter 3 that the majority of macrophage traffic to the heart occurs later (>21 dpi) during infection and that numbers of macrophages correlate with fibrosis. Blocking traffic to the heart early showed no significant

differences compared to SIV+ infected animals that were sacrificed at 21 dpi because there is little cardiac inflammation at this time point. When animals began treatment with the natatlizumab late, at 21 dpi, we found that there was a significant decrease in macrophage inflammation compared to uninfected animals which correlated with a decrease in cardiac fibrosis.

In chapter 6 we targeted macrophages specifically using a polyamine biosynthesis inhibitor, methylglyoxal-bis-guanylhydrazone (MGBG). SIV-infected, CD8+ T-lymphocyte depleted macaques were treated daily with either an oral placebo or MGBG beginning at 21 dpi, when cardiac inflammation occurs, as shown in chapter 3. Sections of the aorta from treated and control animals were all normal, possibly due to the acute infection model used in this study. In the carotid artery and the heart we found that MGBG significantly decreased macrophage inflammation compared to paired placebo control animals. We noted that MGBG also decreased cardiac fibrosis and carotid artery intima-media thickness (cIMT), both markers of cardiovascular disease. Used in conjunction with cART, these experiments show that therapeutics targeting macrophages directly could be beneficial in treating HIV-associated CVD.

X. References

1. Cohen MS, Shaw GM, McMichael AJ, Haynes BF. Acute HIV-1 Infection. *N Engl J Med*. 2011;364(20):1943-1954.
2. Pope M, Haase AT. Transmission, acute HIV-1 infection and the quest for strategies to prevent infection. *Nat Med*. 2003;9(7):847-852.
3. Shaw GM, Hunter E. HIV transmission. *Cold Spring Harb Perspect Med*. 2012;2(11).
4. Fiebig EW, Wright DJ, Rawal BD, et al. Dynamics of HIV viremia and antibody seroconversion in plasma donors: implications for diagnosis and staging of primary HIV infection. *Aids*. 2003;17(13):1871-1879.
5. Coffin J, Swanstrom R. HIV Pathogenesis: Dynamics and Genetics of Viral Populations and Infected Cells. *Cold Spring Harb Perspect Med*. 2013;3(1):a012526-a012526.
6. Hollingsworth TD, Anderson RM, Fraser C. HIV-1 transmission, by stage of infection. *J Infect Dis*. 2008;198(5):687-693.
7. Borrow P, Bhardwaj N. Innate immune responses in primary HIV-1 infection. *Curr Opin HIV AIDS*. 2008;3(1):36-44.
8. Gaines H, von Sydow MA, von Stedingk LV, et al. Immunological changes in primary HIV-1 infection. *Aids*. 1990;4(10):995-999.
9. von Sydow M, Sonnerborg A, Gaines H, Strannegard O. Interferon-alpha and tumor necrosis factor-alpha in serum of patients in various stages of HIV-1 infection. *AIDS Res Hum Retroviruses*. 1991;7(4):375-380.
10. Norris PJ, Pappalardo BL, Custer B, Spotts G, Hecht FM, Busch MP. Elevations in IL-10, TNF-alpha, and IFN-gamma from the earliest point of HIV Type 1 infection. *AIDS Res Hum Retroviruses*. 2006;22(8):757-762.

11. Goonetilleke N, Liu MK, Salazar-Gonzalez JF, et al. The first T cell response to transmitted/founder virus contributes to the control of acute viremia in HIV-1 infection. *J Exp Med.* 2009;206(6):1253-1272.
12. Borrow P, Lewicki H, Wei X, et al. Antiviral pressure exerted by HIV-1-specific cytotoxic T lymphocytes (CTLs) during primary infection demonstrated by rapid selection of CTL escape virus. *Nat Med.* 1997;3(2):205-211.
13. Schmitz JE, Kuroda MJ, Santra S, et al. Control of viremia in simian immunodeficiency virus infection by CD8+ lymphocytes. *Science.* 1999;283(5403):857-860.
14. Wei X, Decker JM, Wang S, et al. Antibody neutralization and escape by HIV-1. *Nature.* 2003;422(6929):307-312.
15. Deeks SG, Kitchen CM, Liu L, et al. Immune activation set point during early HIV infection predicts subsequent CD4+ T-cell changes independent of viral load. *Blood.* 2004;104(4):942-947.
16. Frankel AD, Young JAT. HIV-1 Fifteen Proteins and an RNA. *Annu Rev Biochem.* 1998;67:1-25.
17. Sundquist WI, Krausslich HG. HIV-1 assembly, budding, and maturation. *Cold Spring Harb Perspect Med.* 2012;2(7):a006924.
18. Ganser-Pornillos BK, Yeager M, Sundquist WI. The structural biology of HIV assembly. *Curr Opin Struct Biol.* 2008;18(2):203-217.
19. Barre-Sinoussi F, Ross AL, Delfraissy JF. Past, present and future: 30 years of HIV research. *Nat Rev Microbiol.* 2013;11(12):877-883.
20. Dalglish AG, Beverley PC, Clapham PR, Crawford DH, Greaves MF, Weiss RA. The CD4 (T4) antigen is an essential component of the receptor for the AIDS retrovirus. *Nature.* 1984;312(5996):763-767.

21. Klatzmann D, Champagne E, Chamaret S, et al. T-lymphocyte T4 molecule behaves as the receptor for human retrovirus LAV. *Nature*. 1984;312(5996):767-768.
22. Deng H, Liu R, Ellmeier W, et al. Identification of a major co-receptor for primary isolates of HIV-1. *Nature*. 1996;381(6584):661-666.
23. Feng Y, Broder CC, Kennedy PE, Berger EA. HIV-1 entry cofactor: functional cDNA cloning of a seven-transmembrane, G protein-coupled receptor. *Science*. 1996;272(5263):872-877.
24. Kwong PD, Wyatt R, Robinson J, Sweet RW, Sodroski J, Hendrickson WA. Structure of an HIV gp120 envelope glycoprotein in complex with the CD4 receptor and a neutralizing human antibody. *Nature*. 1998;393(6686):648-659.
25. Buzon V, Natrajan G, Schibli D, Campelo F, Kozlov MM, Weissenhorn W. Crystal structure of HIV-1 gp41 including both fusion peptide and membrane proximal external regions. *PLoS Pathog*. 2010;6(5):e1000880.
26. Miller MD, Farnet CM, Bushman FD. Human immunodeficiency virus type 1 preintegration complexes: studies of organization and composition. *J Virol*. 1997;71(7):5382-5390.
27. Forshey BM, von Schwedler U, Sundquist WI, Aiken C. Formation of a human immunodeficiency virus type 1 core of optimal stability is crucial for viral replication. *J Virol*. 2002;76(11):5667-5677.
28. Ruelas DS, Greene WC. An integrated overview of HIV-1 latency. *Cell*. 2013;155(3):519-529.
29. Karn J, Stoltzfus CM. Transcriptional and posttranscriptional regulation of HIV-1 gene expression. *Cold Spring Harb Perspect Med*. 2012;2(2):a006916.

30. Freed EO. HIV-1 assembly, release and maturation. *Nat Rev Microbiol.* 2015;13(8):484-496.
31. Collaboration TATC. Life expectancy of individuals on combination antiretroviral therapy in high-income countries: a collaborative analysis of 14 cohort studies. *Lancet.* 2008;372(9635):293-299.
32. Zwahlen M, Harris R, May M, et al. Mortality of HIV-infected patients starting potent antiretroviral therapy: comparison with the general population in nine industrialized countries. *Int J Epidemiol.* 2009;38(6):1624-1633.
33. Engsig FN, Zangerle R, Katsarou O, et al. Long-term mortality in HIV-positive individuals virally suppressed for >3 years with incomplete CD4 recovery. *Clin Infect Dis.* 2014;58(9):1312-1321.
34. Palella FJJ, Delaney KM, Moorman AC, et al. Declining Morbidity and Mortality among Patients with Advanced Human Immunodeficiency Virus Infection. *N Engl J Med.* 1998;338(13):853-860.
35. Maartens G, Celum C, Lewin SR. HIV infection: epidemiology, pathogenesis, treatment, and prevention. *Lancet.* 2014;384(9939):258-271.
36. Deeks SG, Autran B, Berkhout B, et al. Towards an HIV cure: a global scientific strategy. *Nat Rev Immunol.* 2012;12(8):607-614.
37. Ray M, Logan R, Sterne JA, et al. The effect of combined antiretroviral therapy on the overall mortality of HIV-infected individuals. *Aids.* 2010;24(1):123-137.
38. d'Arminio Monforte A, Sabin CA, Phillips A, et al. The changing incidence of AIDS events in patients receiving highly active antiretroviral therapy. *Arch Intern Med.* 2005;165(4):416-423.

39. Deeks SG, Phillips AN. HIV infection, antiretroviral treatment, ageing, and non-AIDS related morbidity. *Bmj*. 2009;338:a3172.
40. George E, Lucas GM, Nadkarni GN, Fine DM, Moore R, Atta MG. Kidney function and the risk of cardiovascular events in HIV-1-infected patients. *Aids*. 2010;24(3):387-394.
41. Weber R, Sabin CA, Friis-Møller N, et al. Liver-related deaths in persons infected with the human immunodeficiency virus: the D:A:D study. *Arch Intern Med*. 2006;166(15):1632-1641.
42. Simioni S, Cavassini M, Annoni JM, et al. Cognitive dysfunction in HIV patients despite long-standing suppression of viremia. *Aids*. 2010;24(9):1243-1250.
43. Harezlak J, Buchthal S, Taylor M, et al. Persistence of HIV-associated cognitive impairment, inflammation, and neuronal injury in era of highly active antiretroviral treatment. *Aids*. 2011;25(5):625-633.
44. Gonzalez-Scarano F, Martin-Garcia J. The neuropathogenesis of AIDS. *Nat Rev Immunol*. 2005;5(1):69-81.
45. Feinstein MJ, Bahiru E, Achenbach C, et al. Patterns of Cardiovascular Mortality for HIV-Infected Adults in the United States: 1999-2013. *Am J Cardiol*. 2016;117(2):214-220.
46. Petoumenos K, Reiss P, Ryom L, et al. Increased risk of cardiovascular disease (CVD) with age in HIV-positive men: a comparison of the D:A:D CVD risk equation and general population CVD risk equations. *HIV Med*. 2014;15(10):595-603.
47. Sackoff JE, Hanna DB, Pfeiffer MR, Torian LV. Causes of death among persons with AIDS in the era of highly active antiretroviral therapy: New York City. *Ann Intern Med*. 2006;145(6):397-406.
48. Peters B, Post F, Wierzbicki AS, et al. Screening for chronic comorbid diseases in people with HIV: the need for a strategic approach. *HIV Med*. 2013;14 Suppl 1:1-11.

49. Paula AA, Schechter M, Tuboi SH, et al. Continuous increase of cardiovascular diseases, diabetes, and non-HIV related cancers as causes of death in HIV-infected individuals in Brazil: an analysis of nationwide data. *PLoS One*. 2014;9(4):e94636.
50. Cheruvu S, Holloway CJ. Cardiovascular disease in human immunodeficiency virus. *Intern Med J*. 2014;44(4):315-324.
51. Dahl V, Peterson J, Fuchs D, Gisslen M, Palmer S, Price RW. Low levels of HIV-1 RNA detected in the cerebrospinal fluid after up to 10 years of suppressive therapy are associated with local immune activation. *Aids*. 2014;28(15):2251-2258.
52. Hofstra LM, Mudrikova T, Stam AJ, et al. Residual viremia is preceding viral blips and persistent low-level viremia in treated HIV-1 patients. *PLoS One*. 2014;9(10):e110749.
53. Pomerantz RJ, Zhang H. Residual HIV-1 persistence during suppressive HAART. *Curr Clin Top Infect Dis*. 2001;21:1-30.
54. Siliciano JD, Siliciano RF. A long-term latent reservoir for HIV-1: discovery and clinical implications. *J Antimicrob Chemother*. 2004;54(1):6-9.
55. Blankson JN, Persaud D, Siliciano RF. The challenge of viral reservoirs in HIV-1 infection. *Annu Rev Med*. 2002;53:557-593.
56. Wada NI, Jacobson LP, Margolick JB, et al. The effect of HAART-induced HIV suppression on circulating markers of inflammation and immune activation. *Aids*. 2015;29(4):463-471.
57. Hattab S, Guiguet M, Carcelain G, et al. Soluble biomarkers of immune activation and inflammation in HIV infection: impact of 2 years of effective first-line combination antiretroviral therapy. *HIV Med*. 2015;16(9):553-562.

58. Mooney S, Tracy R, Osler T, Grace C. Elevated Biomarkers of Inflammation and Coagulation in Patients with HIV Are Associated with Higher Framingham and VACS Risk Index Scores. *PLoS One*. 2015;10(12):e0144312.
59. Kristiansen M, Graversen JH, Jacobsen C, Hoffma nÈ, Lawk SKA, Moestrup SK. Identification of the haemoglobin scavenger receptor. *Nature*. 2001;409:1999-2002.
60. Onofre G, Koláčková M, Jankovičová K, Krejsek J. Scavenger Receptor CD163 and its Biological Function. *Acta Medica*. 2009;52(2):57-61.
61. Moller HJ. Soluble CD163. *Scand J Clin Lab Invest*. 2012;72(1):1-13.
62. Buechler C, Ritter M, Orsó E, Langmann T, Klucken J, Schmitz G. Regulation of scavenger receptor CD163 expression in human monocytes and macrophages by pro- and antiinflammatory stimuli. *Journal of Leukocyte Biology*. 2000;67(1):97-103.
63. Etzerodt A, Moestrup SK. CD163 and inflammation: biological, diagnostic, and therapeutic aspects. *Antioxid Redox Signal*. 2013;18(17):2352-2363.
64. Burdo TH, Lo J, Abbara S, et al. Soluble CD163, a novel marker of activated macrophages, is elevated and associated with noncalcified coronary plaque in HIV-infected patients. *J Infect Dis*. 2011;204(8):1227-1236.
65. Pereyra F, Lo J, Triant V, et al. Increased coronary atherosclerosis and immune activation in HIV-1 elite controllers. *Aids*. 2012;26:2409-2415.
66. Nakazono T, Jeudy J, White CS. HIV-related cardiac complications: CT and MRI findings. *AJR. American journal of roentgenology*. 2012;198(2):364-369.
67. Barbaro G, di Lorenzo G, Grisorio B, Barbarini G. Incidence of Dilated Cardiomyopathy and Detection of HIV in Myocardial Cells of HIV-Positive Patients. *N Engl J Med*. 1998;339(16):1093-1099.

68. Enakpena E, John J, Obiagwu C, et al. Hiv Disease and the Heart: A Review. *Journal of Cardiology and Therapy*. 2015;2:279-284.
69. Khunnawat C, Mukerji S, Havlichek D, Jr., Touma R, Abela GS. Cardiovascular manifestations in human immunodeficiency virus-infected patients. *Am J Cardiol*. 2008;102(5):635-642.
70. Sani MU. Myocardial disease in human immunodeficiency virus (HIV) infection: a review. *The Middle European Journal of Medicine*. 2008;120(3-4):77-87.
71. Raj V, Joshi S, Pennell DJ. Images in Cardiovascular Medicine. Cardiac magnetic resonance of acute myocarditis in an human immunodeficiency virus patient presenting with acute chest pain syndrome. *Circulation*. 2010;121(25):2777-2779.
72. Barbaro G. Cardiovascular Manifestations of HIV Infection. *Circulation*. 2002;106(11):1420-1425.
73. Restrepo CS, Diethelm L, Lemos JA, et al. Cardiovascular complications of human immunodeficiency virus infection. *Radiographics : a review publication of the Radiological Society of North America, Inc*. 2006;26(1):213-231.
74. Escarcega RO, Franco JJ, Mani BC, Vyas A, Tedaldi EM, Bove AA. Cardiovascular disease in patients with chronic human immunodeficiency virus infection. *Int J Cardiol*. 2014;175(1):1-7.
75. Silver MA, Macher AM, Reichert CM, et al. Cardiac involvement by Kaposi's sarcoma in acquired immune deficiency syndrome (AIDS). *Am J Cardiol*. 1984;53(7):983-985.
76. Esser S, Gelbrich G, Brockmeyer N, et al. Prevalence of cardiovascular diseases in HIV-infected outpatients: results from a prospective, multicenter cohort study. *Clin Res Cardiol*. 2013;102(3):203-213.

77. Silwa K, Carrington MJ, Becker A, Thienemann F, Ntsekhe M, Stewart S. Contribution of the human immunodeficiency virus acquired immunodeficiency syndrome epidemic to de novo presentations of heart disease in the Heart of Soweto Study cohort. *Eur Heart J*. 2012;33(7):866-874.
78. Holloway CJ, Ntusi N, Suttie J, et al. Comprehensive cardiac magnetic resonance imaging and spectroscopy reveal a high burden of myocardial disease in HIV patients. *Circulation*. 2013;128(8):814-822.
79. Frustaci A, Petrosillo N, Vizza D, et al. Myocardial and microvascular inflammation/infection in patients with HIV-associated pulmonary artery hypertension. *Aids*. 2014;28(17):2541-2549.
80. Remick J, Georgiopolou V, Marti C, et al. Heart failure in patients with human immunodeficiency virus infection: epidemiology, pathophysiology, treatment, and future research. *Circulation*. 2014;129(17):1781-1789.
81. Luetkens JA, Doerner J, Schwarze-Zander C, et al. Cardiac Magnetic Resonance Reveals Signs of Subclinical Myocardial Inflammation in Asymptomatic HIV-Infected Patients. *Circ Cardiovasc Imaging*. 2016;9(3):e004091.
82. Hsue PY, Tawakol A. Inflammation and Fibrosis in HIV: Getting to the Heart of the Matter. *Circ Cardiovasc Imaging*. 2016;9(3):e004427.
83. Lo J, Abbara S, Shturman L, et al. Increased prevalence of subclinical coronary atherosclerosis detected by coronary computed tomography angiography in HIV-infected men. *Aids*. 2010;24(2):243-253.
84. Post WS, Budoff M, Kingsley L, et al. Associations Between HIV Infection and Subclinical Coronary Atherosclerosis. *Ann Intern Med*. 2014;160(7):458-467.

85. Baker JV, Henry WK, Patel P, et al. Progression of carotid intima-media thickness in a contemporary human immunodeficiency virus cohort. *Clin Infect Dis*. 2011;53(8):826-835.
86. Subramanian S, Tawakol A, Abbara S, et al. Arterial Inflammation in Patients With HIV. *JAMA*. 2012;308:379-386.
87. Longenecker CT, Jiang Y, Orringer CE, et al. Soluble CD14 is independently associated with coronary calcification and extent of subclinical vascular disease in treated HIV infection. *Aids*. 2014;28(7):969-977.
88. McKibben RA, Margolick JB, Grinspoon S, et al. Elevated Levels of Monocyte Activation Markers Are Associated With Subclinical Atherosclerosis in Men With and Those Without HIV Infection. *J Infect Dis*. 2015;211(8):1219-1228.
89. Carr A, Cooper DA. Adverse effects of antiretroviral therapy. *Lancet*. 356(9239):1423-1430.
90. Friis-Møller N, Reiss P, Sabin CA, et al. Class of antiretroviral drugs and the risk of myocardial infarction. *N Engl J Med*. 2007;356(17):1723-1735.
91. Annamalai L, Westmoreland SV, Domingues HG, Walsh DG, Gonzalez RG, O'Neil SP. Myocarditis in CD8-Depleted SIV-Infected Rhesus Macaques after Short-Term Dual Therapy with Nucleoside and Nucleotide Reverse Transcriptase Inhibitors. *PLoS One*. 2010;5(12):e14429.
92. Currier JS, Lundgren JD, Carr A, et al. Epidemiological evidence for cardiovascular disease in HIV-infected patients and relationship to highly active antiretroviral therapy. *Circulation*. 2008;118(2):e29-35.
93. Crowell TA, Gebo KA, Blankson JN, et al. Hospitalization Rates and Reasons among HIV Elite Controllers and Persons With Medically Controlled HIV Infection. *J Infect Dis*. 2014.

94. Li JZ, Arnold KB, Lo J, et al. Differential Levels of Soluble Inflammatory Markers by Human Immunodeficiency Virus Controller Status and Demographics. *Open Forum Infect Dis.* 2014;2(1):ofu117-ofu117.
95. Martin-Iguacel R, Llibre JM, Friis-Moller N. Risk of Cardiovascular Disease in an Aging HIV Population: Where Are We Now? *Curr HIV/AIDS Rep.* 2015.
96. Palella FJB, R. K., Moorman AC, Chmiel JS, et al. Mortality in the Highly Active Antiretroviral Therapy Era Changing Causes of Death and Disease in the HIV Outpatient Study. *J Acquir Immune Defic Syndr.* 2006;43(1):27-34.
97. Alejos B, Hernando V, Lopez-Aldeguer J, et al. Overall and cause-specific mortality in HIV-positive subjects compared to the general population. *Journal of the International AIDS Society.* 2014;17(4 Suppl 3):19711.
98. Guaraldi G, Orlando G, Zona S, et al. Premature age-related comorbidities among HIV-infected persons compared with the general population. *Clin Infect Dis.* 2011;53(11):1120-1126.
99. Capeau J. Premature Aging and Premature Age-Related Comorbidities in HIV-Infected Patients: Facts and Hypotheses. *Clin Infect Dis.* 2011;53(11):1127-1129.
100. Jonasson L, Holm J, Skalli O, Bondjers G, Hansson GK. Regional accumulations of T cells, macrophages, and smooth muscle cells in the human atherosclerotic plaque. *Arteriosclerosis.* 1986;6(2):131-138.
101. Jonasson L, Holm J, Skalli O, Gabbiani G, Hansson GK. Expression of class II transplantation antigen on vascular smooth muscle cells in human atherosclerosis. *J Clin Invest.* 1985;76(1):125-131.
102. Hansson GK, Holm J, Jonasson L. Detection of activated T lymphocytes in the human atherosclerotic plaque. *Am J Pathol.* 1989;135(1):169-175.

103. Hansson GK, Hermansson A. The immune system in atherosclerosis. *Nat Immunol.* 2011;12(3):204-212.
104. Arbab-Zadeh A, Nakano M, Virmani R, Fuster V. Acute coronary events. *Circulation.* 2012;125(9):1147-1156.
105. Virmani R, Kolodgie FD, Burke AP, Farb A, Schwartz SM. Lessons from sudden coronary death: a comprehensive morphological classification scheme for atherosclerotic lesions. *Arterioscler Thromb Vasc Biol.* 2000;20(5):1262-1275.
106. Ammirati E, Moroni F, Magnoni M, Camici PG. The role of T and B cells in human atherosclerosis and atherothrombosis. *Clin Exp Immunol.* 2015;179(2):173-187.
107. Daugherty A. T Lymphocytes in Atherosclerosis: The Yin-Yang of Th1 and Th2 Influence on Lesion Formation. *Circ Res.* 2002;90(10):1039-1040.
108. Frostegard J, Ulfgren AK, Nyberg P, et al. Cytokine expression in advanced human atherosclerotic plaques: dominance of pro-inflammatory (Th1) and macrophage-stimulating cytokines. *Atherosclerosis.* 1999;145(1):33-43.
109. Ait-Oufella H, Taleb S, Mallat Z, Tedgui A. Recent Advances on the Role of Cytokines in Atherosclerosis. *Arterioscler Thromb Vasc Biol.* 2011;31(5):969-979.
110. Paul WE, Seder RA. Lymphocyte responses and cytokines. *Cell.* 1994;76(2):241-251.
111. Libby P, Lichtman AH, Hansson GK. Immune effector mechanisms implicated in atherosclerosis: from mice to humans. *Immunity.* 2013;38(6):1092-1104.
112. Wei L. Immunological aspect of cardiac remodeling: T lymphocyte subsets in inflammation-mediated cardiac fibrosis. *Experimental and molecular pathology.* 2011;90(1):74-78.

113. Brower GL, Gardner JD, Forman MF, et al. The relationship between myocardial extracellular matrix remodeling and ventricular function. *Eur J Cardiothorac Surg*. 2006;30(4):604-610.
114. Marra F, Aleffi S, Galastri S, Provenzano A. Mononuclear cells in liver fibrosis. *Semin Immunopathol*. 2009;31(3):345-358.
115. Amoah BP, Yang H, Zhang P, Su Z, Xu H. Immunopathogenesis of Myocarditis: The Interplay Between Cardiac Fibroblast Cells, Dendritic Cells, Macrophages and CD4+ T Cells. *Scand J Immunol*. 2015;82(1):1-9.
116. Wynn TA. Cellular and molecular mechanisms of fibrosis. *J Pathol*. 2008;214(2):199-210.
117. Han YL, Li YL, Jia LX, et al. Reciprocal interaction between macrophages and T cells stimulates IFN-gamma and MCP-1 production in Ang II-induced cardiac inflammation and fibrosis. *PLoS One*. 2012;7(5):e35506.
118. Caligiuri G. Protective immunity against atherosclerosis carried by B cells of hypercholesterolemic mice. *J Clin Invest*. 2002;109(6):745-753.
119. Rotzius P, Thams S, Soehnlein O, et al. Distinct Infiltration of Neutrophils in Lesion Shoulders in ApoE^{-/-} Mice. *Am J Pathol*. 2010;177(1):493-500.
120. Huan T, Zhang B, Wang Z, et al. A systems biology framework identifies molecular underpinnings of coronary heart disease. *Arterioscler Thromb Vasc Biol*. 2013;33(6):1427-1434.
121. Houtkamp MA, de Boer OJ, van der Loos CM, van der Wal AC, Becker AE. Adventitial infiltrates associated with advanced atherosclerotic plaques: structural organization suggests generation of local humoral immune responses. *J Pathol*. 2001;193(2):263-269.
122. !!! INVALID CITATION !!! {}.

123. Kyaw T, Tipping P, Toh BH, Bobik A. Current understanding of the role of B cell subsets and intimal and adventitial B cells in atherosclerosis. *Curr Opin Lipidol.* 2011;22(5):373-379.
124. Cordero-Reyes AM, Youker KA, Torre-Amione G. The role of B-cells in heart failure. *Methodist DeBakey cardiovascular journal.* 2013;9(1):15-19.
125. Zouggari Y, Ait-Oufella H, Bonnin P, et al. B lymphocytes trigger monocyte mobilization and impair heart function after acute myocardial infarction. *Nat Med.* 2013;19(10):1273-1280.
126. Gordon S, Taylor PR. Monocyte and macrophage heterogeneity. *Nat Rev Immunol.* 2005;5(12):953-964.
127. Kim WK, Sun Y, Do H, et al. Monocyte heterogeneity underlying phenotypic changes in monocytes according to SIV disease stage. *J Leukoc Biol.* 2010;87(4):557-567.
128. Ziegler-Heitbrock L, Ancuta P, Crowe S, et al. Nomenclature of monocytes and dendritic cells in blood. *Blood.* 2010;116(16):e74-80.
129. Wong KL, Tai JJ, Wong WC, et al. Gene expression profiling reveals the defining features of the classical, intermediate, and nonclassical human monocyte subsets. *Blood.* 2011;118(5):e16-31.
130. Grage-Griebenow E, Flad HD, Ernst M. Heterogeneity of human peripheral blood monocyte subsets. *J Leukoc Biol.* 2001;69(1):11-20.
131. Ziegler-Heitbrock L, Hofer TP. Toward a refined definition of monocyte subsets. *Front Immunol.* 2013;4:23.
132. Ziegler-Heitbrock L. The CD14+ CD16+ blood monocytes: their role in infection and inflammation. *J Leukoc Biol.* 2007;81(3):584-592.

133. Serbina NV, Jia T, Hohl TM, Pamer EG. Monocyte-mediated defense against microbial pathogens. *Annu Rev Immunol.* 2008;26:421-452.
134. Gratchev A, Sobenin I, Orekhov A, Kzhyskowska J. Monocytes as a diagnostic marker of cardiovascular diseases. *Immunobiology.* 2012;217(5):476-482.
135. Rogacev KS, Cremers B, Zawada AM, et al. CD14⁺⁺CD16⁺ monocytes independently predict cardiovascular events: a cohort study of 951 patients referred for elective coronary angiography. *J Am Coll Cardiol.* 2012;60(16):1512-1520.
136. Schlitt A, Heine GH, Blankenberg S, et al. CD14⁺CD16⁺ monocytes in coronary artery disease and their relationship to serum TNF-alpha levels. *Thromb Haemost.* 2004;92(2):419-424.
137. Barisione C, Garibaldi S, Ghigliotti G, et al. CD14CD16 monocyte subset levels in heart failure patients. *Disease Markers.* 2010;28:115-124.
138. Pamukcu B, Lip GYH, devitt A, Griffiths H, Shantsila E. The role of monocytes in atherosclerotic coronary artery disease. *Ann Med.* 2010;42(6):394-403.
139. Lech M, Anders HJ. Macrophages and fibrosis: How resident and infiltrating mononuclear phagocytes orchestrate all phases of tissue injury and repair. *Biochim Biophys Acta.* 2013;1832(7):989-997.
140. Patanè S, Marte F, Sturiale M, Dattilo G, Albanese A. Myocarditis and cardiomyopathy HIV associated. *Int J Cardiol.* 2011;146(3):e56-57.
141. Moore KJ, Sheedy FJ, Fisher EA. Macrophages in atherosclerosis: a dynamic balance. *Nat Rev Immunol.* 2013;13(10):709-721.
142. Woollard KJ, Geissmann F. Monocytes in atherosclerosis subsets and functions. *Nature Reviews Cardiology.* 2010;7(2):77-86.

143. Andersson J, Libby P, Hansson GK. Adaptive immunity and atherosclerosis. *Clin Immunol.* 2010;134(1):33-46.
144. Ross R. Atherosclerosis — An Inflammatory Disease. *N Engl J Med.* 1999;340(2):115-126.
145. Kzhyshkowska J, Neyen C, Gordon S. Role of macrophage scavenger receptors in atherosclerosis. *Immunobiology.* 2012;217(5):492-502.
146. Ramos CL, Huo Y, Jung U, et al. Direct Demonstration of P-Selectin and VCAM-1 Dependent Mononuclear Cell Rolling in Early Atherosclerotic Lesions of Apolipoprotein E Deficient Mice. *Circ Res.* 1999;84(11):1237-1244.
147. Mestas J, Ley K. Monocyte-Endothelial Cell Interactions in the Development of Atherosclerosis. *Trends Cardiovasc Med.* 2008;18(6):228-232.
148. Zernecke A, Shagdarsuren E, Weber C. Chemokines in atherosclerosis: an update. *Arterioscler Thromb Vasc Biol.* 2008;28(11):1897-1908.
149. Fernandez-Velasco M, Gonzalez-Ramos S, Bosca L. Involvement of monocytes/macrophages as key factors in the development and progression of cardiovascular diseases. *Biochem J.* 2014;458(2):187-193.
150. Dushkin MI. Macrophage/foam cell is an attribute of inflammation: mechanisms of formation and functional role. *Biochemistry. Biokhimiia.* 2012;77(4):327-338.
151. Woollard KJ. Immunological aspects of atherosclerosis. *Clin Sci (Lond).* 2013;125(5):221-235.
152. Bobryshev YV. Dendritic cells and their role in atherogenesis. *Lab Invest.* 2010;90(7):970-984.
153. Bouhlel MA, Derudas B, Rigamonti E, et al. PPARgamma activation primes human monocytes into alternative M2 macrophages with anti-inflammatory properties. *Cell Metab.* 2007;6(2):137-143.

154. MacNeill BD, Jang IK, Bouma BE, et al. Focal and multi-focal plaque macrophage distributions in patients with acute and stable presentations of coronary artery disease. *J Am Coll Cardiol.* 2004;44(5):972-979.
155. Tahara N, Mukherjee J, de Haas HJ, et al. 2-deoxy-2-[F]fluoro-d-mannose positron emission tomography imaging in atherosclerosis. *Nat Med.* 2014;20(2):215-219.
156. Tan C, Liu Y, Li W, et al. Associations of matrix metalloproteinase-9 and monocyte chemoattractant protein-1 concentrations with carotid atherosclerosis, based on measurements of plaque and intima-media thickness. *Atherosclerosis.* 2014;232(1):199-203.
157. Ma Y, Yabluchanskiy A, Hall ME, Lindsey ML. Using plasma matrix metalloproteinase-9 and monocyte chemoattractant protein-1 to predict future cardiovascular events in subjects with carotid atherosclerosis. *Atherosclerosis.* 2014;232(1):231-233.
158. Azzawi M, Hasleton PS, Kan SW, Hillier VF, Quigley A, Hutchinson IV. Distribution of myocardial macrophages in the normal human heart. *J Anat.* 1997;191:417-423.
159. Swirski FK, Nahrendorf M. Leukocyte behavior in atherosclerosis, myocardial infarction, and heart failure. *Science.* 2013;339(6116):161-166.
160. Nahrendorf M, Swirski FK, Aikawa E, et al. The healing myocardium sequentially mobilizes two monocyte subsets with divergent and complementary functions. *J Exp Med.* 2007;204(12):3037-3047.
161. Walker JA, Sulciner ML, Nowicki KD, Miller AD, Burdo TH, Williams KC. Elevated numbers of CD163+ macrophages in hearts of simian immunodeficiency virus-infected monkeys correlate with cardiac pathology and fibrosis. *AIDS Res Hum Retroviruses.* 2014;30(7):685-694.

162. Francis SE, Holden H, Holt CM, Duff GW. Interleukin-1 in myocardium and coronary arteries of patients with dilated cardiomyopathy. *J Mol Cell Cardiol.* 1998;30(2):215-223.
163. Torre-Amione G, Kapadia S, Lee J, et al. Tumor necrosis factor-alpha and tumor necrosis factor receptors in the failing human heart. *Circulation.* 1996;93(4):704-711.
164. Habib FM, Springall DR, Davies GJ, Oakley CM, Yacoub MH, Polak JM. Tumour necrosis factor and inducible nitric oxide synthase in dilated cardiomyopathy. *Lancet.* 1996;347(9009): 1151–1155.
165. Pauschinger M, Knopf D, Petschauer S, et al. Dilated Cardiomyopathy Is Associated With Significant Changes in Collagen Type I/III ratio. *Circulation.* 1999;99(21):2750-2756.
166. Li RK, Li G, Mickle DA, et al. Overexpression of transforming growth factor-beta1 and insulin-like growth factor-I in patients with idiopathic hypertrophic cardiomyopathy. *Circulation.* 1997;96(3):874-881.
167. Timonen P, Magga J, Risteli J, et al. Cytokines, interstitial collagen and ventricular remodelling in dilated cardiomyopathy. *Int J Cardiol.* 2008;124(3):293-300.
168. Silvestre-Roig C, de Winther MP, Weber C, Daemen MJ, Lutgens E, Soehnlein O. Atherosclerotic plaque destabilization: mechanisms, models, and therapeutic strategies. *Circ Res.* 2014;114(1):214-226.
169. Hansson GK, Libby P, Tabas I. Inflammation and plaque vulnerability. *J Intern Med.* 2015;278(5):483-493.
170. Newby AC. Metalloproteinase Expression in Monocytes and Macrophages and its Relationship to Atherosclerotic Plaque Instability. *Arterioscler Thromb Vasc Biol.* 2008;28(12):2108-2114.
171. Newby AC. Metalloproteinases promote plaque rupture and myocardial infarction: A persuasive concept waiting for clinical translation. *Matrix Biol.* 2015;44-46:157-166.

172. Knox JB, Sukhova GK, Whittamore AD, Libby P. Evidence for altered balance between matrix metalloproteinases and their inhibitors in human aortic diseases. *Circulation*. 1997;95(1):205-212.
173. Herman MP, Sukhova GK, Libby P, et al. Expression of neutrophil collagenase (matrix metalloproteinase-8) in human atheroma: a novel collagenolytic pathway suggested by transcriptional profiling. *Circulation*. 2001;104(16):1899-1904.
174. Sukhova GK, Schonbeck U, Rabkin E, et al. Evidence for increased collagenolysis by interstitial collagenases-1 and -3 in vulnerable human atheromatous plaques. *Circulation*. 1999;99(19):2503-2509.
175. Crowe SM, Westhorpe CL, Mukhamedova N, Jaworowski A, Sviridov D, Bukrinsky M. The macrophage: the intersection between HIV infection and atherosclerosis. *J Leukoc Biol*. 2010;87(4):589-598.
176. Anzinger JJ, Butterfield TR, Angelovich TA, Crowe SM, Palmer CS. Monocytes as regulators of inflammation and HIV-related comorbidities during cART. *J Immunol Res*. 2014;2014:569819.
177. van der Wal AC, Becker AE, van der Loos CM, Das PK. Site of Intimal Rupture or Erosion of Thrombosed Coronary Atherosclerotic Plaques Is Characterized by an Inflammatory Process irrespective of the Dominant Plaque Morphology. *Circulation*. 1994;89(1):36-44.
178. Tawakol A, Lo J, Zanni MV, et al. Increased Arterial Inflammation Relates to High-risk Coronary Plaque Morphology in HIV-Infected Patients. *J Acquir Immune Defic Syndr*. 2014;66(2):164-171.
179. Lederman RJ, Raylman RR, Fisher SJ, et al. Detection of atherosclerosis using a novel positron-sensitive probe and 18-fluorodeoxyglucose (FDG). *Nucl Med Commun*. 2001;22(7):747-753.

180. Tawakol A, Grinspoon SK. Imaging atherosclerotic burden and inflammation: insights into the spectrum of atherosclerotic disease in HIV. *J Nucl Cardiol.* 2015;22(2):381-384.
181. Tawakol A, Migrino RQ, Hoffmann U, et al. Noninvasive in vivo measurement of vascular inflammation with F-18 fluorodeoxyglucose positron emission tomography. *J Nucl Cardiol.* 2005;12(3):294-301.
182. Burdo TH, Walker JA, Williams KC. Macrophage Polarization in AIDS: Dynamic Interface between Anti-Viral and Anti-Inflammatory Macrophages during Acute and Chronic Infection. *J Clin Cell Immunol.* 2015;6(3).
183. Cope FO, Abbruzzese B, Sanders J, et al. The inextricable axis of targeted diagnostic imaging and therapy: An immunological natural history approach. *Nucl Med Biol.* 2016;43(3):215-225.
184. Leong SP, Kim J, Ross M, et al. A phase 2 study of (99m)Tc-tilmanocept in the detection of sentinel lymph nodes in melanoma and breast cancer. *Ann Surg Oncol.* 2011;18(4):961-969.
185. Sondak VK, King DW, Zager JS, et al. Combined analysis of phase III trials evaluating [(99m)Tc]tilmanocept and vital blue dye for identification of sentinel lymph nodes in clinically node-negative cutaneous melanoma. *Ann Surg Oncol.* 2013;20(2):680-688.
186. Wallace AM, Hoh CK, Ellner SJ, Darrah DD, Schulteis G, Vera DR. Lymphoseek a molecular imaging agent for melanoma sentinel lymph node mapping. *Ann Surg Oncol.* 2007;14(2):913-921.
187. Åstrand H, Sandgren T, Ahlgren ÅR, Länne T. Noninvasive ultrasound measurements of aortic intima-media thickness: implications for in vivo study of aortic wall stress1
1Competition of interest: none. *J Vasc Surg.* 2003;37(6):1270-1276.

188. Jarvisalo MJ, Jartti L, Nanto-Salonen K, et al. Increased Aortic Intima-Media Thickness: A Marker of Preclinical Atherosclerosis in High-Risk Children. *Circulation*. 2001;104(24):2943-2947.
189. O'Leary DH, Polak JF, Kronmal RA, Manolio TA, Burke GL, Wolfson SK, Jr. Carotid-artery intima and media thickness as a risk factor for myocardial infarction and stroke in older adults. Cardiovascular Health Study Collaborative Research Group. *N Engl J Med*. 1999;340(1):14-22.
190. Homma S, Hirose N, Ishida H, Ishii T, Araki G. Carotid plaque and intima-media thickness assessed by b-mode ultrasonography in subjects ranging from young adults to centenarians. *Stroke*. 2001;32(4):830-835.
191. Calza L, Manfredi R, Colangeli V, et al. Two-year treatment with rosuvastatin reduces carotid intima-media thickness in HIV type 1-infected patients receiving highly active antiretroviral therapy with asymptomatic atherosclerosis and moderate cardiovascular risk. *AIDS Res Hum Retroviruses*. 2013;29(3):547-556.
192. Luetkens JA, Doerner J, Thomas DK, et al. Acute myocarditis: multiparametric cardiac MR imaging. *Radiology*. 2014;273(2):383-392.
193. de Meester de Ravenstein C, Bouzin C, Lazam S, et al. Histological Validation of measurement of diffuse interstitial myocardial fibrosis by myocardial extravascular volume fraction from Modified Look-Locker imaging (MOLLI) T1 mapping at 3 T. *J Cardiovasc Magn Reson*. 2015;17:48.
194. Smith SC, Jr., Benjamin EJ, Bonow RO, et al. AHA/ACCF secondary prevention and risk reduction therapy for patients with coronary and other atherosclerotic vascular disease: 2011 update: a guideline from the American Heart Association and American College of

- Cardiology Foundation endorsed by the World Heart Federation and the Preventive Cardiovascular Nurses Association. *J Am Coll Cardiol*. 2011;58(23):2432-2446.
195. Taylor FC, Huffman M, Ebrahim S. Statin therapy for primary prevention of cardiovascular disease. *JAMA*. 2013;310(22):2451-2452.
 196. Wang CY, Liu PY, Liao JK. Pleiotropic effects of statin therapy: molecular mechanisms and clinical results. *Trends Mol Med*. 2008;14(1):37-44.
 197. Sukhova GK. Statins Reduce Inflammation in Atheroma of Nonhuman Primates Independent of Effects on Serum Cholesterol. *Arterioscler Thromb Vasc Biol*. 2002;22(9):1452-1458.
 198. Verschuren L, Kleemann R, Offerman EH, et al. Effect of low dose atorvastatin versus diet-induced cholesterol lowering on atherosclerotic lesion progression and inflammation in apolipoprotein E*3-Leiden transgenic mice. *Arterioscler Thromb Vasc Biol*. 2005;25(1):161-167.
 199. Kleemann R, Princen HM, Emeis JJ, et al. Rosuvastatin reduces atherosclerosis development beyond and independent of its plasma cholesterol-lowering effect in APOE*3-Leiden transgenic mice: evidence for antiinflammatory effects of rosuvastatin. *Circulation*. 2003;108(11):1368-1374.
 200. Crouse JR, 3rd, Raichlen JS, Riley WA, et al. Effect of rosuvastatin on progression of carotid intima-media thickness in low-risk individuals with subclinical atherosclerosis: the METEOR Trial. *JAMA*. 2007;297(12):1344-1353.
 201. Lo J, Lu MT, Ihenachor EJ, et al. Effects of statin therapy on coronary artery plaque volume and high-risk plaque morphology in HIV-infected patients with subclinical atherosclerosis: a randomised, double-blind, placebo-controlled trial. *Lancet HIV*. 2015;2(2):e52–e63.

202. Liu C, Li Y, Yu J, et al. Targeting the shift from M1 to M2 macrophages in experimental autoimmune encephalomyelitis mice treated with fasudil. *PLoS One*. 2013;8(2):e54841.
203. Aouadi M, Tesz GJ, Nicoloso SM, et al. Orally delivered siRNA targeting macrophage Map4k4 suppresses systemic inflammation. *Nature*. 2009;458(7242):1180-1184.
204. Lackner AA. Pathology of simian immunodeficiency virus induced disease. *Current topics in microbiology and immunology*. 1994;188:35-64.
205. Letvin NL, Daniel MD, Sehgal PK, et al. Induction of AIDS-like disease in macaque monkeys with T-cell tropic retrovirus STLV-III. *Science*. 1985;230(4721):71-73.
206. Kanki PJ, McLane MF, King NW, Jr., et al. Serologic identification and characterization of a macaque T-lymphotropic retrovirus closely related to HTLV-III. *Science*. 1985;228(4704):1199-1201.
207. Daniel MD, Letvin NL, King NW, et al. Isolation of T-cell tropic HTLV-III-like retrovirus from macaques. *Science*. 1985;228(4704):1201-1204.
208. Kelly KM, Tocchetti CG, Lyashkov A, et al. CCR5 Inhibition Prevents Cardiac Dysfunction in the SIV/Macaque Model of HIV. *J Am Heart Assoc*. 2014;3(2):e000874.
209. Yearley JH, Pearson C, Carville A, Shannon RP, Mansfield K. SIV-Associated Myocarditis: Viral and Cellular Correlates of Inflammation Severity. *AIDS Res Hum Retroviruses*. 2006;22(6):529-540.
210. Yearley JH, Pearson C, Carville A, Shannon RP, Mansfield K. Phenotypic Variation in Myocardial Macrophage Populations Suggests a Role for Macrophage Activation in SIV-Associated Cardiac Disease. *AIDS Res Hum Retroviruses*. 2007;23(4):512-524.
211. Williams K, Burdo TH. Monocyte mobilization, activation markers, and unique macrophage populations in the brain: observations from SIV infected monkeys are

- informative with regard to pathogenic mechanisms of HIV infection in humans. *J Neuroimmune Pharmacol.* 2012;7(2):363-371.
212. Williams KC, Corey S, Westmoreland SV, et al. Perivascular macrophages are the primary cell type productively infected by simian immunodeficiency virus in the brains of macaques: implications for the neuropathogenesis of AIDS. *J Exp Med.* 2001;193(8):905-915.
213. Campbell JH, Burdo TH, Autissier P, et al. Minocycline inhibition of monocyte activation correlates with neuronal protection in SIV neuroAIDS. *PLoS One.* 2011;6(4):e18688.
214. Campbell JH, Ratai E-M, Autissier P, et al. Anti- α 4 Antibody Treatment Blocks Virus Traffic to the Brain and Gut Early, and Stabilizes CNS Injury Late in Infection. *PLoS Pathog.* 2014;10(12):e1004533.
215. Nowlin BT, Burdo TH, Midkiff CC, Salemi M, Alvarez X, Williams KC. SIV encephalitis lesions are composed of CD163(+) macrophages present in the central nervous system during early SIV infection and SIV-positive macrophages recruited terminally with AIDS. *Am J Pathol.* 2015;185(6):1649-1665.
216. Soulas C, Conerly C, Kim WK, et al. Recently infiltrating MAC387(+) monocytes/macrophages a third macrophage population involved in SIV and HIV encephalitic lesion formation. *Am J Pathol.* 2011;178(5):2121-2135.
217. Burdo TH, Soulas C, Orzechowski K, et al. Increased monocyte turnover from bone marrow correlates with severity of SIV encephalitis and CD163 levels in plasma. *PLoS Pathog.* 2010;6(4):e1000842.
218. Burdo TH, Lackner AA, Williams KC. Monocyte/macrophages and their role in HIV neuropathogenesis. *Immuno Rev.* 2013;254(1):102-113.

219. Kelly KM, Tarwater PM, Karper JM, et al. Diastolic dysfunction is associated with myocardial viral load in simian immunodeficiency virus-infected macaques. *Aids*. 2012;26(7):815-823.
220. Butt AA, Chang CC, Kuller L, et al. Risk of heart failure with human immunodeficiency virus in the absence of prior diagnosis of coronary heart disease. *Arch Intern Med*. 2011;171(8):737-743.
221. De Castro S, d'Amati G, Gallo P, et al. Frequency of development of acute global left ventricular dysfunction in human immunodeficiency virus infection. *J Am Coll Cardiol*. 1994;24(4):1018-1024.
222. Cohen IS, Anderson DW, Virmani R, et al. Congestive cardiomyopathy in association with the acquired immunodeficiency syndrome. *N Engl J Med*. 1986;315(10):628-630.
223. Pandrea I, Landay A, Wilson C, Stock J, Tracy R, Apetrei C. Using the Pathogenic and Nonpathogenic Nonhuman Primate Model for Studying Non-AIDS Comorbidities. *Curr HIV/AIDS Rep*. 2015.
224. El-Sadr WM, Lundgren J, Neaton JD, et al. CD4+ count-guided interruption of antiretroviral treatment. *N Engl J Med*. 2006;355(22):2283-2296.
225. Kuller LH, Tracy R, Belloso W, et al. Inflammatory and coagulation biomarkers and mortality in patients with HIV infection. *PLoS Med*. 2008;5(10):e203.
226. Lipshultz SE, Mas CM, Henkel JM, Franco VI, Fisher SD, Miller TL. HAART to heart: highly active antiretroviral therapy and the risk of cardiovascular disease in HIV-infected or exposed children and adults. *Expert Rev Anti Infect Ther*. 2012;10(6):661-674.

CHAPTER 2. Expansion of Circulating CD14+CD16+ Monocyte Subset Correlates with Increased Cardiac Fibrosis, Inflammation, and SIV Encephalitis in SIV-infected Rhesus Macaques

Joshua A. Walker, John Wang,

Andrew D. Miller, Patrick Autissier,

Kenneth C. Williams

ABSTRACT

HIV infection with cART is associated with subclinical myocardial disease and increased prevalence of HIV-associated neurological disorders (HAND). Increased frequency of activated CD14⁺CD16⁺ monocytes in circulation are associated with cardiovascular disease, HAND, and SIV encephalitis (SIVE). Cross sectional studies implicated monocytes/macrophages with cardiovascular disease, but longitudinal studies have not been done. We conducted a longitudinal study of 14 SIV-infected, CD8⁺ T-lymphocyte depleted rhesus macaques with AIDS and assessed circulating monocyte subsets as possible correlations of cardiac disease and SIVE. Cardiac tissues were examined for inflammation, fibrosis, and cardiomyocyte degeneration and CNS tissues were assessed for the presence of SIVE. Five of 14 (36%) animals had no significant findings in the heart while 9 of 14 (64%) had increased inflammation, fibrosis, and cardiomyocyte degeneration. Six of 9 (66%) animals with cardiac disease had SIVE compared to 1 of 5 (20%) animals with no significant findings in the heart. In animals with SIVE there was a significant 2.46-fold increase in numbers of circulating CD14⁺CD16⁺ monocytes as early as 8 dpi. There was a significant increase in cardiac macrophage inflammation in SIVE animals compared to those without encephalitis (SIV no E). There was a significant 2.26-fold increase in the percentage of collagen and a significant 2.28-fold increase in the absolute numbers of activated CD14⁺CD16⁺ monocytes in animals with cardiac disease as early as 8 dpi. There were positive correlations between numbers of CD14⁺CD16⁺ monocytes and cardiac fibrosis seen as early as 8 dpi and continued throughout infection. These data show that numbers of activated circulating monocytes could predict cardiac fibrosis, cardiac inflammation, and SIVE. Cardiac inflammation and fibrosis and SIVE could potentially be linked by increased monocyte/macrophage traffic and accumulation.

INTRODUCTION

Monocytes are mononuclear phagocytes that comprise 5-10% of leukocytes in circulation in humans.¹ They are a heterogeneous population and classified based on their expression of surface antigens, size, morphology, and function.¹⁻⁵ Monocytes are identified by their expression of CD14, the lipopolysaccharide co-receptor, and expression of CD16, a low affinity Fc γ -III receptor that acts as a marker of activated monocytes,^{2,6-8} Three populations of circulating monocytes are recognized in humans and rhesus macaques based on CD14 and CD16 expression: CD14⁺CD16⁻ classical monocytes, CD14⁺CD16⁺ intermediate monocytes, and CD14⁺CD16⁺⁺ nonclassical monocytes.^{3,4} Under normal physiological conditions, classical CD14⁺⁺CD16⁻ monocytes are the predominant phenotype and activated monocytes expressing CD16 comprise a minor population.^{2-4,8} Increased CD16 expression in monocytes occurs with inflammation and infection,^{7,9,10} leading to their status as “pro-inflammatory”. With HIV and SIV infection, there is increased monocyte egress from the bone marrow⁹, an increased turnover rate¹¹, and activation.^{2,12-14} Expansion of the circulating CD14⁺CD16⁺ monocyte population is a marker of HIV and SIV disease progression to AIDS.^{9,15,16}

Monocytes/macrophages are implicated in the development of cardiac fibrosis and myocarditis with and without HIV infection.¹⁷⁻²¹ In response to injury or infection monocytes traffic to the myocardium and develop into tissue macrophages which secrete pro-inflammatory and pro-fibrotic factors²²⁻²⁷ that are increased with HIV infection.²⁸⁻³⁰ Increased macrophage inflammation and pro-inflammatory cytokine production in the heart play roles in the approximate two-fold increase in relative risk of atherosclerosis, stroke, and myocarditis among HIV+ individuals on combination anti-retroviral (cART) era.³¹⁻³⁷ Although the prevalence of myocardial disease in HIV infected patients decreased with cART,^{38,39} a significant burden of myocardial inflammation and fibrosis still exists in this population.⁴⁰⁻⁴³ Magnetic resonance spectroscopy (MRS) studies found increased subclinical myocardial disease, fibrosis, and a

decline in cardiac function in HIV infected individuals compared to uninfected individuals.^{40, 44}

We examined post-mortem tissue of HIV infected individuals and demonstrated significant macrophage inflammation in cardiac tissues which correlated with inflammation in the aorta and increased levels of plasma sCD163 (Unpublished data).

In addition to a greater risk of CVD with HIV infection, there is an increased prevalence HIV-associated neurological disorders (HAND),⁴⁵ for which chronic monocyte/macrophage activation and inflammation plays a role. HAND with HIV results in increased accumulation of intracranial and/or spinal cord CD14⁺ CD16⁺ CD163⁺ perivascular macrophages, and increased soluble CD14 (sCD14) and soluble CD163 (sCD163) in plasma.^{16, 46-49} Soluble CD163, a marker of monocyte/macrophage activation, is increased in chronically HIV-infected individuals with neurocognitive impairment, despite being on cART.⁵⁰ Additionally, sCD14 and sCD163 are associated with noncalcified plaques in HIV+ individuals on cART.⁵¹ Increased plasma sCD163 is associated with aortic inflammation with HIV.⁵² Studies reported that increased CVD risk factors, high density lipoprotein (HDL), smoking and Framingham Risk Score (FRS), are associated with neuroinflammation in HIV+ individuals.^{45, 53} Carotid artery intima-media thickness, a measurement of CVD⁵⁴⁻⁵⁶ is increased with HIV infection^{34, 57} and associated with a decline in neurocognition.⁵⁸ It is possible that there is a link between cardiovascular disease and neurocognitive decline in the setting of HIV where chronic monocyte/macrophage activation plays a role.

We reported in a model of rapid AIDS in rhesus macaques that increased numbers of CD163⁺, CD68⁺ and newly infiltrating macrophages expressing MAC387, cardiac macrophages correlated with increased cardiac fibrosis.⁵⁹ In the current study we used 14 SIV-infected rhesus macaques and examined blood monocyte/macrophage activation longitudinally to determine if they are predictive of cardiac fibrosis, cardiac inflammation, cardiomyocyte degeneration and

SIV encephalitis (SIVE). Sections of the left ventricle were examined blindly by histology and scored for the degree of cardiac fibrosis, inflammation, and cardiomyocyte degeneration. Animals with cardiac disease (based on the presence of fibrosis, inflammation, and cardiomyocyte degeneration at necropsy) had significantly elevated numbers of circulating activated CD14⁺CD16⁺ monocytes as early as 8 days post infection (dpi), which remained consistently elevated throughout the course of infection and correlated with cardiac fibrosis. Additionally C-C chemokine receptor 2 (CCR2) mean fluorescence intensity (MFI) was also increased in animals with cardiac disease compared to those without. Early increases in CD14⁺CD16⁺ monocytes also separated animals with SIVE compared to animals without encephalitis (SIV no E). There was a higher incidence SIVE in animals with cardiac fibrosis and inflammation (66%) compared to animals with no significant findings in the heart (20%), suggesting that development of cardiac and encephalitis are linked by monocyte/macrophage activation and accumulation.

RESULTS

Assessment of cardiac and CNS pathology

All 14 animals used in this study were sacrificed with AIDS. Nine of 14 (64%) animals had cardiac inflammation and fibrosis. Four of these 9 (44%) animals had cardiomyocyte degeneration. Five of 14 (36%) animals had no significant findings with regards to inflammation, fibrosis, and cardiomyocyte degeneration (Table 2.1). Of the 9 animals with cardiac inflammation, fibrosis, and cardiomyocyte degeneration, 6 also had SIVE (66%). Four had mild SIVE and 2 had severe SIVE. Only 1 of the 5 animals with no cardiac findings had SIVE (20%), which was mild (Table 2.1).

There is increased macrophage inflammation and fibrosis in animals with cardiac and CNS disease

Cardiac disease

By immunohistochemistry there was a significant 1.62-fold increase in CD163⁺ macrophages, a 1.97-fold increase in CD68⁺ macrophages, a 1.57-fold increase in MAC387⁺ monocytes/macrophages, and a 2.72-fold increase in CD206⁺ macrophages in cardiac tissues of animals with cardiac pathology. There were no differences in the numbers of CD3⁺ T-lymphocytes in cardiac tissues between those monkeys with and without cardiac disease (Table 2.2). We did not find SIV-p28⁺ or SIV-RNA⁺ cells in cardiac tissues consistent with our previous findings^{59, 64} and others that show a low level of cardiac infection.⁶⁷⁻⁶⁹ We found a 2.26-fold increase in cardiac fibrosis, measured as the percentage collagen per tissue area, in animals with cardiac pathology (Fig. 2.1A, *left*) compared to animals with no significant findings (NSF) (Fig.

2.1A, *right*). Animals with cardiac pathology had an average percent collagen per total tissue area of $18.99 \pm 1.56\%$ (n=9) compared to $8.38 \pm 0.52\%$ (n=5) in (Fig. 2.1B).

CNS disease

Animals were grouped based on whether or not they developed SIV encephalitis (SIVE). Previously we reported that the animals in this study with SIVE had increased numbers of CD163⁺ macrophages and MAC387⁺ monocytes/macrophages in the CNS meninges, perivascular space, and SIVE lesions compared to SIV no E animals. It is possible that cardiac and CNS disease are linked by increased monocyte/macrophage inflammation in both tissue compartments. We found that animals with SIVE (n=7) had significant macrophage inflammation in the heart compared to SIV no E animals (n=7). There was a significant 1.53-fold increase in CD163⁺ macrophages, a 1.49-fold increase in MAC387⁺ monocytes/macrophages, and a 1.96-fold increase in CD206⁺ macrophages in cardiac tissues in animals that developed SIVE compared to animals without CNS disease (Table 2.3). There was a significant 1.54-fold increase in the level of cardiac fibrosis in SIVE animals compared to SIV no E animals.

SIV+ animals with cardiac disease and encephalitis have significant early increases in activated CD14⁺CD16⁺ monocytes that persist throughout infection

The absolute numbers of activated CD14⁺CD16⁺ monocytes increased for animals with and without cardiac fibrosis after 0 dpi. There was a significant 2.28-fold increase in the number of blood CD14⁺CD16⁺ monocytes in animals with cardiac fibrosis compared to those with no cardiac findings. While the numbers of CD14⁺CD16⁺ monocyte subsets fluctuates over the course of disease significant differences between animals with and without cardiac fibrosis were found at 8, 19, 26, 35, 42, 54, and 61 dpi (Fig 2.3A). There were no differences in the absolute

numbers of classical CD14⁺CD16⁻ monocytes between these groups. The percentage of classical CD14⁺CD16⁻ monocytes decreased after infection but was not statistically different between the groups (Fig. 2.3B). There was a significant 2.46-fold increase in the number of CD14⁺CD16⁺ monocytes in animals with SIVE (n=7) compared to SIV no E (n=7) animals that was detected as early as 8dpi (Fig. 2.3C). The numbers of CD14⁺CD16⁻ monocytes did not significantly differ with infection between the two groups (Fig. 2.3D). Plasma viral load for all animals peaked at 8 dpi and remained elevated. Plasma viral load did not distinguish between animals with and without cardiac disease or with and without SIVE (Fig. 2.4).

There are positive correlations between increased number of CD14⁺CD16⁺ monocytes early and late and increased cardiac fibrosis in animals with cardiac pathology

By 8 dpi there are significant differences in the percentage of CD14⁺CD16⁺ monocytes between animals with and without cardiac pathology as well as significant differences in the percentage of collagen per total tissue area (fibrosis). Examining the percentage of CD14⁺CD16⁺ monocytes at 8 dpi, we found positive correlations between increased CD14⁺CD16⁺ monocytes and increased cardiac fibrosis ($r=.65$, $p<0.05$) (Fig. 2.3C). A positive correlation between numbers of CD14⁺CD16⁺ monocytes at necropsy and fibrosis was found ($r=.60$, $p<0.05$) (Fig. 2.3D).

SIV+ animals with increased cardiac fibrosis have increased expression of CCR2 on CD14⁺CD16⁺

Chemokine receptor 2 (CCR2) is unregulated on activated monocytes. Expression of CCR2 mean fluorescence intensity (MFI) on CD14⁺CD16⁺ monocytes was analyzed by flow

cytometry and compared between animals housed at NERPC or TNRPC. In both cohorts (Fig. 2.5A, B), there was an increase in CD14⁺CD16⁺ CCR2 MFI mean fluorescence during late infection. For cohort 1 at NERPC (Fig. 2.5A), CCR2 expression was increased at 35, 42, 47, and 54 dpi for animals with cardiac fibrosis compared to those with no significant findings. For cohort 2 at TNRPC (Fig. 2.5B), CCR2 expression was increased at 54, 61, 82, and 89 dpi.

DISCUSSION

In this study we found early expansion of activated CD14⁺CD16⁺ monocytes correlated with the development of SIV-associated cardiac and CNS disease. Increases in activated CD14⁺CD16⁺ monocytes correlated with increased cardiac fibrosis, inflammation, cardiomyocyte degeneration, and the presence of SIVE.

Results from this study demonstrate a correlation between cardiac disease, encephalitis, and activated monocytes. Of the 9 animals with cardiac disease (increased cardiac fibrosis and inflammation) 6 also developed SIVE. In contrast only 1 of 5 animals that had no significant cardiac findings developed SIVE, which was found to be mild. Additionally, when animals are grouped based on SIVE or SIVE no E we found that animals with SIVE had significantly more macrophage inflammation in the heart compared to SIV no E animals. SIVE animals also had significant early increases in numbers of CD14⁺CD16⁺ monocytes in blood and significantly more cardiac fibrosis in the heart. This suggests that the development of CNS and cardiac disease are possibly linked and caused by increased monocyte/macrophage accumulation with HIV and SIV infection.

HIV has been associated with a spectrum of cardiac disease comprising but not limited to dilated cardiomyopathy, myocarditis, and pericardial effusion.⁷⁰ Comparing the incidences of the pre- and post-cART era, the rates of cardiac disease has declined.^{38, 39, 71} However, recent studies have shown that even in the cART era incidences of subclinical myocardial disease in patients with HIV remains.^{43, 44, 72, 73}

In a CD8⁺ T-lymphocyte depletion model of rapid AIDS, plasma SIV viral load of all animals peaked early during infection (8 days post infection), and remained consistently high due to the lack of CD8⁺ T-lymphocyte immune control,⁷⁴⁻⁷⁶ thus there was no difference in

plasma viral load between animals with myocardial fibrosis and animals that had no significant findings in the heart. Although plasma viral load has been shown to correlate with functional cardiac decline⁶⁷, few studies have found infection of cardiac macrophages.^{67, 68} The few SIV-infected and HIV-infected cells in the heart are consistently demonstrated as CD163+ macrophages.⁶⁷⁻⁶⁹

In the CNS, virus enters the brain as early as 3 to 7 days after infection in both humans and nonhuman primates.^{61, 77} Levels of viral RNA in the CNS decrease during acute infection while the levels of viral DNA remain unchanged.^{77, 78} During the later stages of infection it is believed that viral replication is reactivated, which coincides with macrophage activation and recruitment of perivascular macrophages to the CNS.⁷⁸ Additionally, our lab has shown that in SIV-infected rhesus macaques that MAC387+ macrophages (a marker of active inflammation) are recruited to the CNS after 21 dpi, possibly when viral replication is reactivated and encephalitis begins to develop.⁷⁹ These data suggest that the presence of actively replicating viral RNA is necessary for the development of HIV and SIV encephalitis. In the heart itself we did not find SIV protein or RNA, but significant inflammation was present. This suggests that monocyte/macrophage accumulation more so than viral replication is important for the development of cardiac pathology with AIDS. However, we do acknowledge that the level of viral infection in the heart may be below the detection limit of immunohistochemistry or *in situ* hybridization.

Previous cross sectional studies have demonstrated the ability of monocytes to indicate a previous history of cardiovascular⁸⁰⁻⁸⁴ and CNS disease.^{2, 11, 15} In this study we show that activated monocytes longitudinally correlated with increased fibrosis and inflammation in cardiac tissues. Significant early changes in the absolute number of activated CD14⁺CD16⁺ monocytes were found in animals with increased cardiac fibrosis, inflammation, and

cardiomyocyte degeneration compared to animals that had no significant findings in the heart. While the total number of activated CD14⁺CD16⁺ monocytes fluctuated throughout infection, they remained significantly elevated in animals with cardiac and CNS disease. Additionally we found positive correlations between the number of CD14⁺CD16⁺ monocytes early and late and levels of cardiac fibrosis suggesting that monocyte/macrophage activation is predictive of myocardial disease.

In this study we found that expression of chemokine receptor-2 (CCR2) on CD14⁺CD16⁺ monocytes was increased later in infection in animals with increased cardiac fibrosis. CCR2 signaling is necessary for cells to leave the bone marrow and be recruited to sites of active inflammation.^{85,86} CCR2 is highly expressed on a subset of monocytes/macrophages and when it is reduced there is a delay in the development of atherosclerosis and myocarditis in rodent models.^{87,88} In patients with myocarditis the number of blood monocytes/macrophages positive for CCR2 are also increased.⁸⁷ CCR2 expression is also increased on CD14⁺CD16⁺ monocytes from patients with HAND, suggesting that it is a marker for HAND.⁸⁹ Increased CCR2 expression on monocytes from a subset of animals in this study may account for increased traffic to the heart and the CNS. Previously, using BrdU, we showed that there is an increase in monocyte/macrophage traffic to the heart later during SIV infection (>21 dpi), possibly with the development of AIDS.⁵⁹ Data of CCR2 expression from this study appears to support this idea of monocytes/macrophages trafficking to the heart later during infection and possibly resulting in increased fibrosis as we do not see early differences in CCR2 expression between the two groups of animals.

In our study we examined if changes in monocytes correlate with increased cardiac fibrosis during SIV infection. We found an increased incidence of encephalitis in animals that developed cardiac disease. In animals with SIVE, characterized by accumulation of perivascular

macrophages and multinucleate giant cells (MNGCs), we found increased macrophage inflammation in the heart suggesting a possible link between the development of encephalitis and cardiac disease with HIV and SIV infection mediated by monocyte/macrophage accumulation. We found that in SIV-infected animals with increased cardiac fibrosis and SIVE there indeed were significant early changes in the numbers of CD14⁺CD16⁺ monocytes that persisted throughout the course of infection. Increased numbers of CD14⁺CD16⁺ monocytes correlated with increased cardiac fibrosis. There was also an increase in CCR2 MFI in animals with cardiac disease used in this study. CCR2 MFI on activated CD14⁺CD16⁺ could be used as biomarker to predict cardiac inflammation similar to how it has been used to predict monocyte traffic to the CNS.⁸⁹ While this would have to be examined in HIV-infected individuals, it is possible that absolute numbers CD14⁺CD16⁺ monocytes and CCR2 expression could be used as a non-invasive method to determine the presence of cardiac fibrosis and inflammation with HIV infection.

MATERIALS AND METHODS

Ethical treatment of animals

Animals were housed at Harvard University's New England Primate Research Center (NEPRC) or Tulane University's National Primate Center (TNPRC) and handled in strict accordance with Harvard University's and Tulane University's National Primate Research Center Institutional Animal Care and Use Committee (IACUC). Animal IACUC approval from NEPRC and TNPRC was granted for all procedures. The NEPRC protocol number for this study was 04420 and the animal welfare assurance number was A3431-01. The TNPRC the protocol number is 3497 and the animal welfare assurance number is A4499-01.

Animals, SIV infection, and CD8+ T-lymphocyte depletion

Fourteen rhesus macaques were utilized in this study. Five were housed at Harvard University's New England Primate Research Center (NEPRC) and nine were housed at Tulane University's National Primate Research Center (TNPRC) in accordance with standards of the American Association for Accreditation of Laboratory Animal Care. The animals were intravenously (i.v.) inoculated with SIVmac251 (20ng of SIV p28) provided by Ronald Desrosiers. Blood samples were taken prior to, on the day of infection, and weekly thereafter. CD8+ T lymphocyte depletion was achieved with subcutaneous administration of human anti-CD8 antibody cM-T807 (10mg/kg) at day 6 post-infection, and i.v. administration (5mg/kg) on days 8 and 12 post-infection. Animals were anesthetized with ketamine-HCl and euthanized with AIDS with intravenous pentobarbital overdose and exsanguinated.

Plasma viral load and viral infection in the heart

Plasma SIV-RNA was quantified using real-time PCR for all animals used in this study, as previously described.⁶⁰ 500µL of EDTA plasma was collected and SIV virions were pelleted by centrifugation at 20,000 g for 1 hour. The threshold sensitivity was 100 copy Eq/mL, with an average interassay coefficient variation of less than 25%. The presence of SIV infected cells in the heart was evaluated by immunohistochemistry with an SIV-p28 antibody (SIVmac251, Fitzgerald Industries) and *in situ* hybridization with digoxigenin-labeled riboprobes to detect SIV-RNA as previously described.⁵⁹

Assessment of inflammation and fibrosis in cardiac tissues and SIV Encephalitis in CNS

Following exsanguination, standard necropsy was performed and lymph nodes and critical organs including heart and brain, were fixed in 10% neutral buffered formalin. Following fixation, tissues were paraffin embedded, sectioned at 5µm, and stained with hematoxylin and eosin. Sections of cardiac tissue (left ventricle) were analyzed blindly by a veterinary pathologist. Cardiac tissues were scored based upon 10 randomly chosen 400x fields. The degree of inflammation, fibrosis, and cardiomyocyte degeneration in each tissue section was assessed graded as having: A) no significant findings (NSF); B) mild; C) moderate; D) or severe. SIV encephalitis (SIVE) was diagnosed based on the presence of multinucleated giant cells (MNGCs), accumulation of perivascular macrophages, and productive SIV infection.^{11, 61-63}

Single label immunohistochemistry of cardiac tissues

Numbers of macrophages and T-lymphocytes in formalin-fixed, paraffin-embedded cardiac tissues for all animals were determined through immunohistochemistry and cell

counting, as previously described⁶⁴. Macrophages were identified using monoclonal antibodies against CD163 (clone EdHu-1, Serotec), CD68 (clone KP1, Dako), Myeloid/Histiocyte Antigen (clone MAC387, Dako), and CD206 (clone 685645, R&D systems) and T-lymphocytes were identified using a polyclonal antibody against CD3 (Dako). Data are presented as the mean positive number of cells/mm² from 20 non-overlapping fields of view plus or minus the standard error of the mean (SEM).

Measurement of myocardial fibrosis

Myocardial fibrosis was determined as the percent collagen per tissue area of cardiac tissue.^{65, 66} Sections were analyzed using a modified Massons Trichrome stain as previously described.⁶⁴ Sections were imaged using a Zeiss Axio Imager M1 microscope using Plan-Apochromat x20/0.8 Korr objectives. The percent collagen (blue dye) per total tissue area was determined using ImageJ Analysis software from 20 non-overlapping 200x microscopic fields (field area=0.148mm²). Data are presented as the percent collagen per total tissue area plus or minus the SEM.

Flow cytometry

Flow cytometric analysis was conducted on 100ul aliquots of peripheral whole blood collected in EDTA-coated tubes from all animals. Blood samples were taken at -7, 0, 5, 8, 12, weekly thereafter, until necropsy. Samples from animals housed at the NERPC were shipped and analyzed the same day and samples from animals at the TNPRC were shipped overnight. Erythrocyte lysis was performed (ImmunoPrep Reagent System, Beckman Coulter), followed by 2 washes with PBS, and incubation with fluorochrome-conjugated antibodies including anti-

CCR2-APC (clone: 48607, R&D Systems), anti-CD14-APC (clone: M5E2, BD Pharmingen), anti-CD16-PE (clone: 3G8, BD Pharmingen) anti-HLA-DR-PerCP-Cy5.5 (clone: L243, BD Pharmingen). All samples were fixed in 2% paraformaldehyde and results acquired on a BD FACS Aria (BD Biosciences) and analyzed with Tree Star Flow Jo version 8.7. Monocytes are first selected based on size and granularity (FSC vs SSC), followed by selection of HLA-DR⁺ CD14⁺ cells. From this gate the percentage of monocyte subsets expressing CD14 and/or CD16 could be determined.

Absolute Monocyte counts from whole blood

The absolute number of peripheral blood monocytes for each animal was calculated by multiplying the total white blood cell count by the total percentage of each monocyte subset as determined by flow cytometric analysis.

Statistical analysis

Statistical analyses were done using Prism version 5.0a (Graphpad Software, Inc., San Diego, CA) software. Comparisons between groups at each time point were made using a non-parametric Mann-Whitney *t*-test with significant accepted at $p < 0.05$. A Spearman rank test was used for all correlations.

Table 2.1. Cardiac and CNS pathology of animals used in this study.

Animal ID	Cardiac Inflammation	Cardiac Fibrosis	Cardiomyocyte Degeneration	Fibrosis (Percent collagen per total tissue area)	CNS Pathology
185-05	NSF	NSF	NSF	10.01%	SIV no E
168-05	NSF	NSF	NSF	8.8%	SIV no E
288-07	NSF	NSF	NSF	8.6%	SIV no E
FD80	NSF	NSF	NSF	7.4%	SIVE (Mild)
FT73	NSF	NSF	NSF	7.1%	SIV no E
FD05	Severe	Severe	Moderate	28.72%	SIVE (Mild)
55-05	Moderate	Severe	Mild	21.90%	SIVE (Mild)
DB79	Mild	Mild	NSF	20.5%	SIVE (Severe)
FB92	Mild	Severe	NSF	19.98%	SIV no E
CM07	Mild	Moderate	NSF	18.93%	SIVE (Mild)
FR56	Mild	Mild	Mild	17.54%	SIVE (Mild)
FC42	Mild	Mild	Moderate	15.7%	SIV no E
244-96	Moderate	Mild	NSF	14.32%	SIVE (Severe)
FD37	Mild	Mild	NSF	13.4%	SIV no E

Fourteen SIV-infected, CD8⁺T-lymphocyte depleted rhesus macaques were used in this study, all of which were sacrificed with AIDS. Sections of left ventricular tissue (cardiac tissue) were examined by a veterinary pathologist to determine the presence and severity of cardiac inflammation and cardiomyocyte degeneration. Each criteria was scored as having no significant findings (NSF) or mild, moderate, or severe. Five animals were found to have no

significant cardiac findings. Nine animals were found to have cardiac pathology. Fibrosis was determined as the percentage of collagen per total tissue area after sections of cardiac tissue were stained with a Massons Trichrome stain. SIV encephalitis (SIVE) was diagnosed post mortem and based on the presence of SIV virus in the CNS and multi-nucleated giant cells. Of the 5 animals with no significant cardiac findings only 1 animal had SIVE (20%) compared to 6 of 9 (66%) animals with cardiac pathology having SIVE.

Table 2.2. Numbers of macrophages and T-lymphocytes present in cardiac tissues

	With Cardiac Pathology (n=9)	NSF (n=5)	<i>p</i> -value
CD163	269.81±26.72	166.2±18.48	*
CD68	109.30±8.66	55.7±10.24	**
MAC387	22.62±2.51	14.35±1.40	*
CD206	154.27±14.56	84.56±25.33	*
CD3	19.44±4.69	15.08±5.41	NS

Sections of cardiac tissue from all animals were immunohistochemically stained with antibodies recognizing CD163⁺, CD68⁺, MAC387⁺, CD206⁺ macrophages and CD3⁺ T-lymphocytes. Twenty random, non-overlapping 200x fields of view were sampled for each animal and the average number of cells/mm² were calculated and expressed as plus or minus the standard error of the mean. P-values were calculated using a non-parametric Mann-Whitney *t*-test with significant accepted at $p < 0.05$ (* $p < 0.05$, ** $p < 0.01$). NSF, no significant findings.

Table 2.3 Numbers of cardiac macrophages and T-lymphocytes present in animals with and without SIV encephalitis

	SIVE (n=7)	SIV no E (n=7)	p-value
CD163	181.18±22.13	281.42±30.51	*
CD68	73.3±13.85	107.83±10.59	NS
MAC387	14.92±1.21	22.26±2.99	*
CD206	87.41±9.03	171.35±9.03	**
CD3	20.03±3.11	17.17±3.11	NS

Animals were grouped based on if they developed SIV encephalitis (SIVE, n=7) or did not develop encephalitis (SIV no E, n=7). Sections of cardiac tissue from all animals were immunohistochemically stained with antibodies recognizing CD163⁺, CD68⁺, MAC387⁺, CD206⁺ macrophages and CD3⁺ T-lymphocytes. Twenty random, non-overlapping 200x fields of view were sampled for each animal and the average number of cells/mm² were calculated and expressed as plus or minus the standard error of the mean. P-values were calculated using a non-parametric Mann-Whitney *t*-test with significant accepted at p<0.05 (*p<0.05, **p<0.01).

Figure 2.1

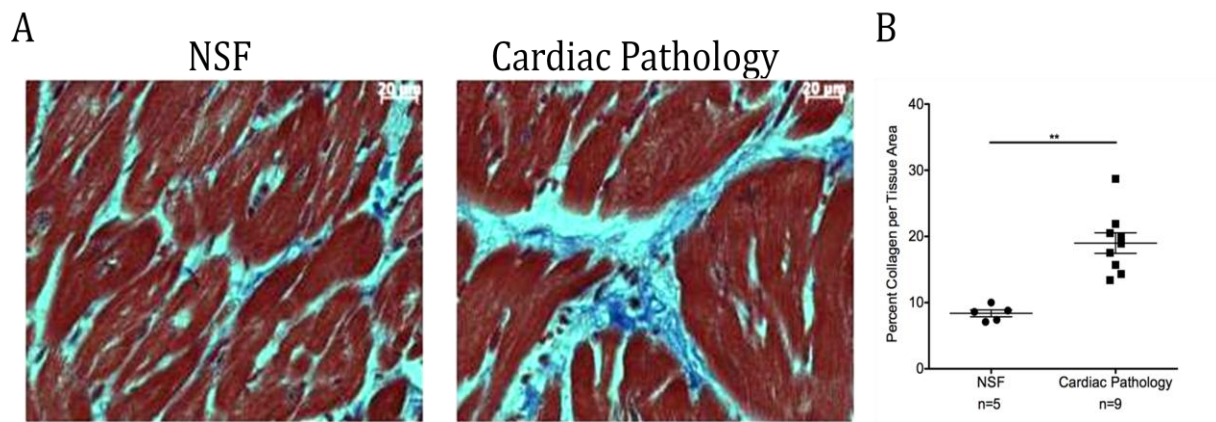


Figure 2.1. There is a significant increase in myocardial fibrosis in SIV-infected, CD8⁺T-lymphocyte depleted rhesus macaques with cardiac pathology

(A). Sections of cardiac tissue were stained with a Massons trichrome stain to visualize cardiomyocyte cytoplasm (red) and collagen (blue) from SIV-infected CD8⁺ T-lymphocyte depleted rhesus macaques that had no significant findings (NSF) in the heart (*left n=5*) or had cardiac pathology based on scorings from a veterinary pathologist (*right n=9*) (400x magnification). Fibrosis, determined as the percentage of collagen per total tissue area was quantified for each animal. (B) For animals with no significant findings in the heart, the average percentage of collagen per total tissue area was $8.38 \pm 0.52\%$ ($n=5$) compared to $18.99 \pm 1.56\%$ ($n=9$), a significant 2.26-fold increase (non-parametric Mann-Whitney t-test, ** $p < 0.01$). The percentage of collagen per total tissue area was averaged from 20 non-overlapping 200x fields of view and expressed as the average plus or minus the standard error of the mean.

Figure 2.2

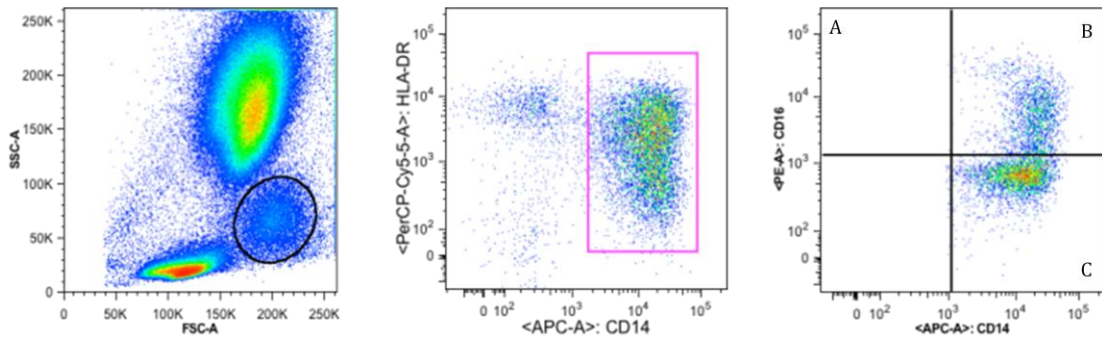


Figure 2.2. Gating strategy to identify monocyte subsets in blood plasma

Following infection, blood was drawn weekly until necropsy. Using Flow Jo version 8.7, monocytes were selected based on forward and side scatter. Cells positive for CD14 and HLA-DR expression were selected, followed by analysis of monocyte subsets based on CD14 and CD16 expression. A) non-classical CD14⁺CD16⁺, B) intermediate CD14⁺⁺CD16⁺ monocytes, C) classical monocytes CD14⁺CD16⁻.

Figure 2.3

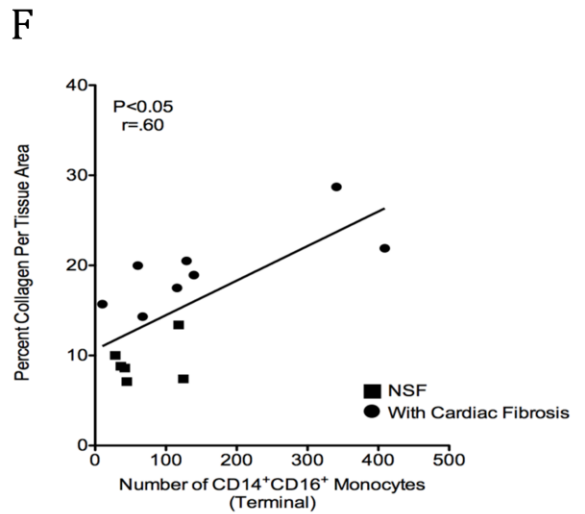
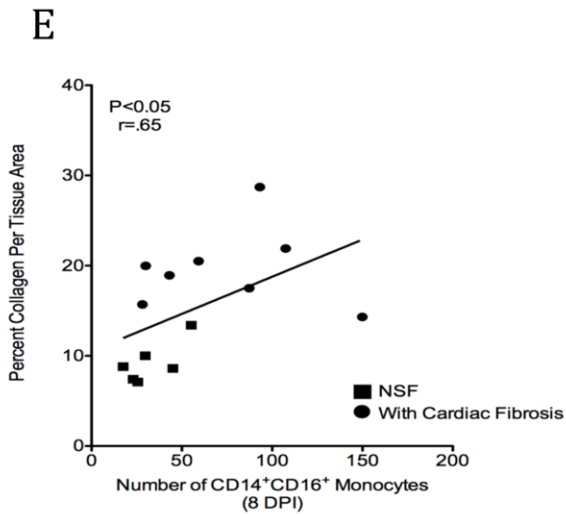
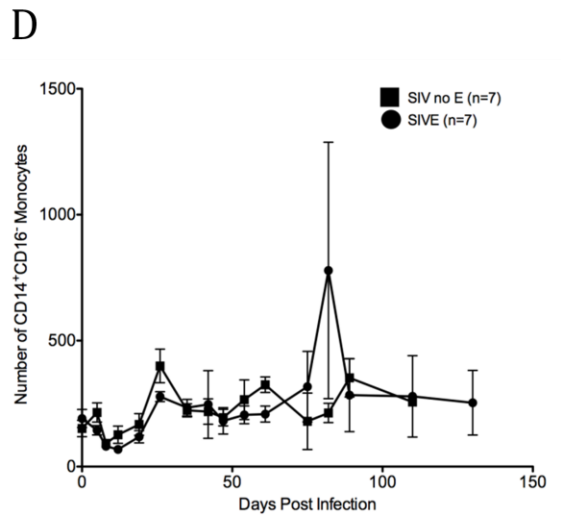
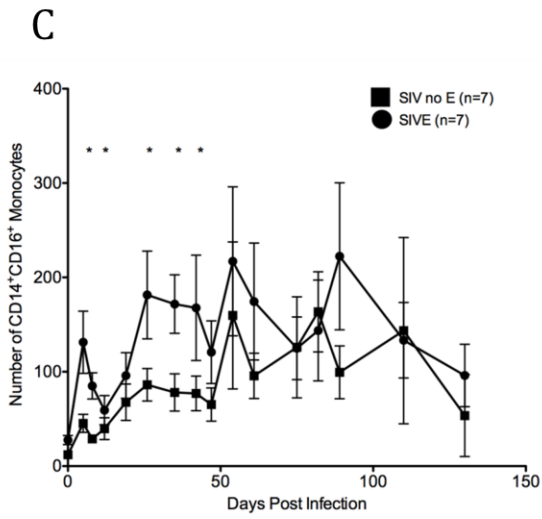
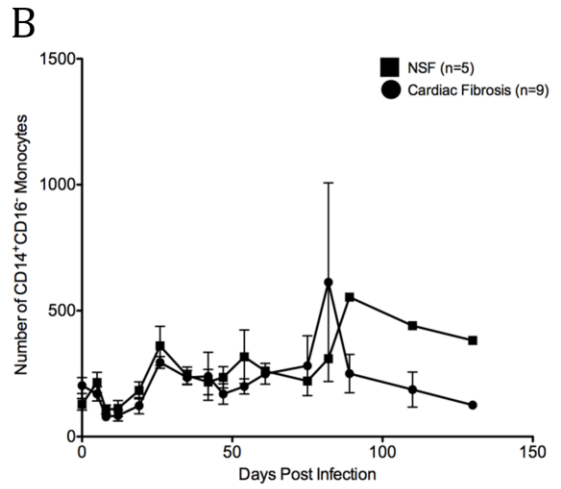
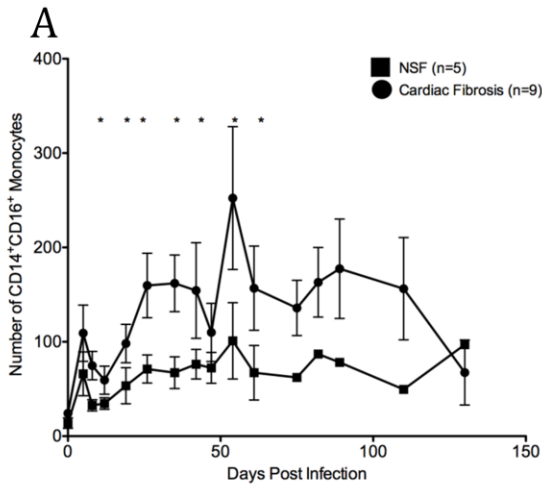


Figure 2.3. Elevated CD14⁺CD16⁺ monocyte expression early correlates with myocardial fibrosis in SIV-infected, CD8⁺ T-lymphocyte depleted rhesus macaques with cardiac pathology and SIVE

Animals were grouped based the presence of absence of cardiac pathology (NSF=square, Cardiac pathology=circle). (A) By 8 dpi CD14⁺CD16⁺ monocyte subset were significantly differences between animals with cardiac pathology and those without. The absolute number of CD14⁺CD16⁺ monocytes in animals with no significant findings in the heart was 32.68±5.89 cells/μL of blood, compared to 74.70±15.02 for animals with cardiac pathology, a significant 2.28-fold increase (*, p<0.05). There were significant differences in the numbers of CD14⁺CD16⁺ monocytes at day 8, 19, 26, 35, 42, 54, 61 post infection (non-parametric Mann-Whitney t-test, * p<0.05). (B) While the absolute number of CD14⁺CD16⁻ monocyte subsets decreased over the course of SIV infection, there were no significant differences between the groups. Animals were also grouped and analyzed based on if the developed SIV encephalitis (SIVE) or did not develop CNS disease (SIV no E). (C) There were significant increases in the numbers of CD14⁺CD16⁺ monocytes at days 5, 8, 26, 35, and 42 post infection in animals that developed SIVE compared to SIV no E animals (non-parametric Mann-Whitney t-test, *p<0.05). (D) There were no significant differences in numbers of CD14⁺CD16⁻ monocytes during infection between animals that did and did not develop SIVE. Spearman rank correlation was used to examine correlations between the percentage of CD14⁺CD16⁺ monocytes and myocardial fibrosis (E, F) There were positive correlations between the number of CD14⁺CD16⁺ monocytes at early (r= .65, p<0.05) and terminally and cardiac fibrosis (r=.60, p<0.05).

Figure 2.4

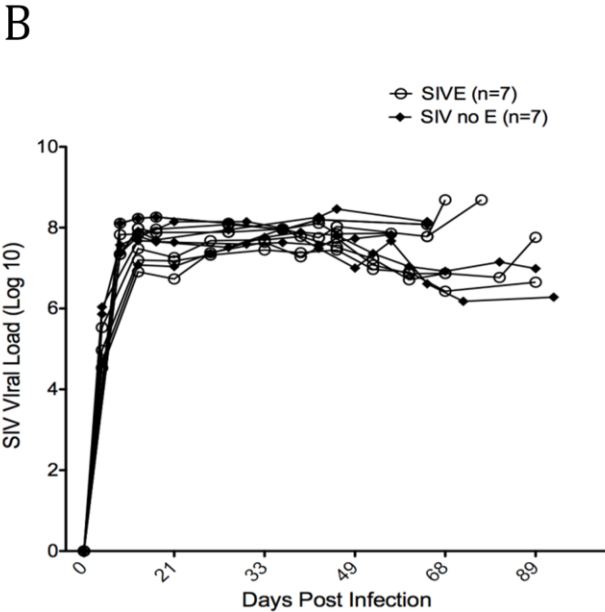
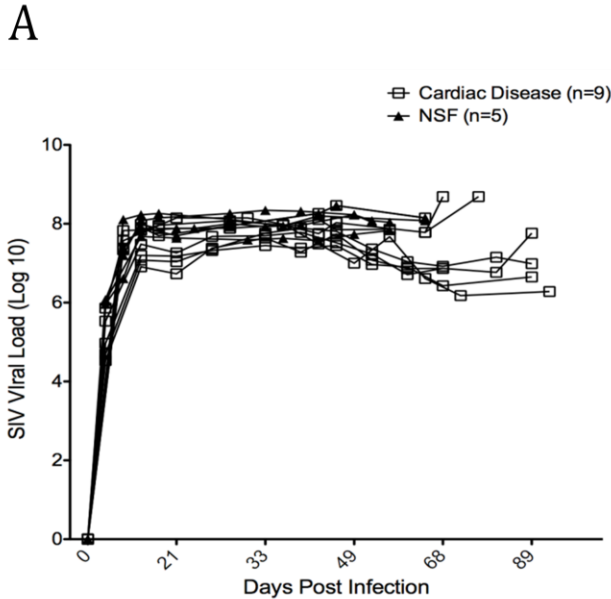


Figure 2.4. Plasma SIV-RNA does not distinguish between animals with and without cardiac disease or with and without SIV encephalitis.

Plasma SIV-RNA was quantified using real time PCR for all animals used in this study. Animals were first grouped based on if they were found to have developed cardiac disease at necropsy (A) and then grouped based on whether or not they developed SIV encephalitis (SIVE) (B).

Plasma SIV-RNA did not distinguish between animals that developed cardiac disease (n=9, open square) and those that had no significant findings in the heart (n=5, closed triangle). Plasma SIV-RNA did not distinguish between animals that developed SIVE (n=7, open circle) and animals that did not develop SIVE (SIV no E) (n=7, closed diamond). By 8 days post infection levels of SIV-RNA peaked and remained consistently elevated during infection for all animals.

Figure 2.5

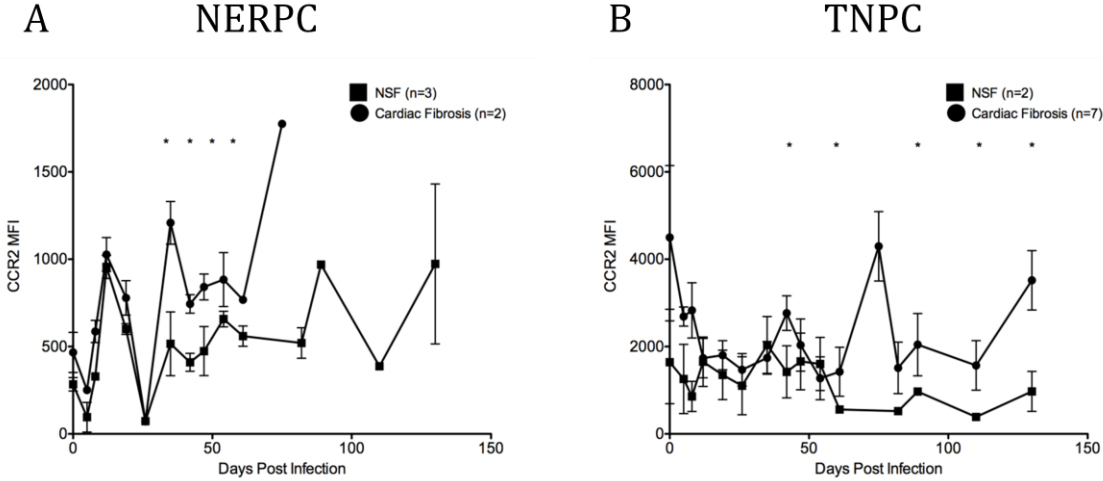


Figure 2.5. Animals with cardiac disease have increased CCR2 expression on activated CD14⁺CD16⁺ monocytes.

Animals in this study were further divided into two cohorts based on if they were housed at the NERPC or TNRPC to examine the expression of the chemokine receptor 2 (CCR2) on activated CD14⁺CD16⁺. (A, B). In both cohorts, there was a significant increase in CCR2 expression on CD14⁺CD16⁺ later during infection in animals with increased cardiac fibrosis compared to those with no significant findings in the heart (*, p<0.05).

REFERENCES

1. Gordon S, Taylor PR. Monocyte and macrophage heterogeneity. *Nat Rev Immunol*. Dec 2005;5(12):953-964.
2. Kim WK, Sun Y, Do H, et al. Monocyte heterogeneity underlying phenotypic changes in monocytes according to SIV disease stage. *J Leukoc Biol*. Apr 2010;87(4):557-567.
3. Ziegler-Heitbrock L, Ancuta P, Crowe S, et al. Nomenclature of monocytes and dendritic cells in blood. *Blood*. Oct 21 2010;116(16):e74-80.
4. Wong KL, Tai JJ, Wong WC, et al. Gene expression profiling reveals the defining features of the classical, intermediate, and nonclassical human monocyte subsets. *Blood*. 2011;118(5):e16-31.
5. Grage-Griebenow E, Flad HD, Ernst M. Heterogeneity of human peripheral blood monocyte subsets. *J Leukoc Biol*. 2001;69(1):11-20.
6. Ziegler-Heitbrock L, Hofer TP. Toward a refined definition of monocyte subsets. *Front Immunol*. 2013;4:23.
7. Ziegler-Heitbrock L. The CD14⁺ CD16⁺ blood monocytes: their role in infection and inflammation. *J Leukoc Biol*. Mar 2007;81(3):584-592.
8. Serbina NV, Jia T, Hohl TM, Pamer EG. Monocyte-mediated defense against microbial pathogens. *Annu Rev Immunol*. 2008;26:421-452.
9. Thieblemont N, Weiss L, Sadeghi HM, Estcourt C, Haeffner-Cavaillon N. CD14^{low}CD16^{high} A cytokine-producing monocyte subset which expands during human immunodeficiency virus infection. *Eur J Immunol*. 1995;25:3418-3424.
10. Fingerle G, Pforte A, Passlick B, Blumenstein M, Ströbel M, Ziegler-Heitbrock HW. The novel subset of CD14⁺/CD16⁺ blood monocytes is expanded in sepsis patients. *Blood*. 1993;82(10):3170-3176.

11. Burdo TH, Soulas C, Orzechowski K, et al. Increased monocyte turnover from bone marrow correlates with severity of SIV encephalitis and CD163 levels in plasma. *PLoS Pathogens*. 2010;6(4):e1000842.
12. Pulliam L, Sun B, Rempel H. Invasive chronic inflammatory monocyte phenotype in subjects with high HIV-1 viral load. *J Neuroimmunol*. Dec 2004;157(1-2):93-98.
13. Ansari AW, Meyer-Olson D, Schmidt RE. Selective expansion of pro-inflammatory chemokine CCL2-loaded CD14+CD16+ monocytes subset in HIV-infected therapy naive individuals. *J Clin Immunol*. Jan 2013;33(1):302-306.
14. Hasegawa A, Liu H, Ling B, et al. The level of monocyte turnover predicts disease progression in the macaque model of AIDS. *Blood*. Oct 1 2009;114(14):2917-2925.
15. Pulliam L, Gascon R, Stubblebine M, McGuire D, McGrath MS. Unique monocyte subset in patients with AIDS dementia. *The Lancet*. 1997;349(9053):692-695.
16. Fischer-Smith T, Croul S, Sverstiuk E, et al. CNS invasion by CD14+ CD16+ peripheral blood-derived monocytes in HIV dementia perivascular accumulation and reservoir of HIV infection. *Journal of NeuroVirology*. 2001;7:528-541.
17. Kania G, Blyszczuk P, Eriksson U. Mechanisms of cardiac fibrosis in inflammatory heart disease. *Trends in Cardiovascular Medicine*. 2009;19(8):247-252.
18. Lech M, Anders HJ. Macrophages and fibrosis: How resident and infiltrating mononuclear phagocytes orchestrate all phases of tissue injury and repair. *Biochim Biophys Acta*. Jul 2013;1832(7):989-997.
19. Patanè S, Marte F, Sturiale M, Dattilo G, Albanese A. Myocarditis and cardiomyopathy HIV associated. *Int J Cardiol*. Feb 3 2011;146(3):e56-57.
20. Wynn TA, Ramalingam TR. Mechanisms of fibrosis: therapeutic translation for fibrotic disease. *Nat Med*. Jul 2012;18(7):1028-1040.

21. Wynn TA, Barron L. Macrophages: master regulators of inflammation and fibrosis. *Semin Liver Dis.* Aug 2010;30(3):245-257.
22. Francis SE, Holden H, Holt CM, Duff GW. Interleukin-1 in myocardium and coronary arteries of patients with dilated cardiomyopathy. *Journal of molecular and cellular cardiology.* 1998;30(2):215-223.
23. Torre-Amione G, Kapadia S, Lee J, et al. Tumor necrosis factor-alpha and tumor necrosis factor receptors in the failing human heart. *Circulation.* Feb 15 1996;93(4):704-711.
24. Habib FM, Springall DR, Davies GJ, Oakley CM, Yacoub MH, Polak JM. Tumour necrosis factor and inducible nitric oxide synthase in dilated cardiomyopathy. *The Lancet.* 1996;347(9009): 1151-1155.
25. Pauschinger M, Knopf D, Petschauer S, et al. Dilated Cardiomyopathy Is Associated With Significant Changes in Collagen Type I/III ratio. *Circulation.* 1999;99(21):2750-2756.
26. Li RK, Li G, Mickle DA, et al. Overexpression of transforming growth factor-beta1 and insulin-like growth factor-I in patients with idiopathic hypertrophic cardiomyopathy. *Circulation.* Aug 5 1997;96(3):874-881.
27. Timonen P, Magga J, Risteli J, et al. Cytokines, interstitial collagen and ventricular remodelling in dilated cardiomyopathy. *Int J Cardiol.* Mar 14 2008;124(3):293-300.
28. Monsuez JJ, Escout L, Teicher E, Charniot JC, Vittecoq D. Cytokines in HIV-associated cardiomyopathy. *Int J Cardiol.* Aug 21 2007;120(2):150-157.
29. Kedzierska K, Crowe SM. Cytokines and HIV-1: interactions and clinical implications. *Antivir Chem Chemother.* May 2001;12(3):133-150.
30. Valdez H, Lederman MM. Cytokines and cytokine therapies in HIV infection. *AIDS Clin Rev.* 1997:187-228.

31. Hemkens LG, Bucher HC. HIV infection and cardiovascular disease. *Eur Heart J*. Jan 21 2014;35(21):1373-1381.
32. Triant VA, Lee H, Hadigan C, Grinspoon SK. Increased acute myocardial infarction rates and cardiovascular risk factors among patients with human immunodeficiency virus disease. *J Clin Endocrinol Metab*. Jul 2007;92(7):2506-2512.
33. Currier JS, Lundgren JD, Carr A, et al. Epidemiological evidence for cardiovascular disease in HIV-infected patients and relationship to highly active antiretroviral therapy. *Circulation*. Jul 8 2008;118(2):e29-35.
34. Hsue PY, Ordovas K, Lee T, et al. Carotid intima-media thickness among human immunodeficiency virus-infected patients without coronary calcium. *Am J Cardiol*. Mar 1 2012;109(5):742-747.
35. Luetkens JA, Doerner J, Thomas DK, et al. Acute myocarditis: multiparametric cardiac MR imaging. *Radiology*. Nov 2014;273(2):383-392.
36. Islam FM, Wu J, Jansson J, Wilson DP. Relative risk of cardiovascular disease among people living with HIV: a systematic review and meta-analysis. *HIV Med*. Sep 2012;13(8):453-468.
37. Duprez DA, Neuhaus J, Kuller LH, et al. Inflammation, coagulation and cardiovascular disease in HIV-infected individuals. *PLoS One*. 2012;7(9):e44454.
38. Esser S, Gelbrich G, Brockmeyer N, et al. Prevalence of cardiovascular diseases in HIV-infected outpatients: results from a prospective, multicenter cohort study. *Clin Res Cardiol*. Mar 2013;102(3):203-213.
39. Khunnawat C, Mukerji S, Havlichek D, Jr., Touma R, Abela GS. Cardiovascular manifestations in human immunodeficiency virus-infected patients. *Am J Cardiol*. Sep 1 2008;102(5):635-642.

40. Cheruvu S, Holloway CJ. Cardiovascular disease in human immunodeficiency virus. *Intern Med J.* Apr 2014;44(4):315-324.
41. Frustaci A, Petrosillo N, Vizza D, et al. Myocardial and microvascular inflammation/infection in patients with HIV-associated pulmonary artery hypertension. *AIDS.* Nov 13 2014;28(17):2541-2549.
42. Remick J, Georgiopolou V, Marti C, et al. Heart failure in patients with human immunodeficiency virus infection: epidemiology, pathophysiology, treatment, and future research. *Circulation.* Apr 29 2014;129(17):1781-1789.
43. Hsue PY, Tawakol A. Inflammation and Fibrosis in HIV: Getting to the Heart of the Matter. *Circ Cardiovasc Imaging.* Mar 2016;9(3):e004427.
44. Holloway CJ, Ntusi N, Suttie J, et al. Comprehensive cardiac magnetic resonance imaging and spectroscopy reveal a high burden of myocardial disease in HIV patients. *Circulation.* Aug 20 2013;128(8):814-822.
45. Cysique LA, Moffat K, Moore DM, et al. HIV, vascular and aging injuries in the brain of clinically stable HIV-infected adults: a (1)H MRS study. *PLoS One.* 2013;8(4):e61738.
46. Kusao I, Shiramizu B, Liang CY, et al. Cognitive performance related to HIV-1-infected monocytes. *J Neuropsychiatry Clin Neurosci.* Winter 2012;24(1):71-80.
47. Shikuma CM, Nakamoto B, Shiramizu B, et al. Antiretroviral monocyte efficacy score linked to cognitive impairment in HIV. *Antivir Ther.* 2012;17(7):1233-1242.
48. Ndhlovu LC, Umaki T, Chew GM, et al. Treatment intensification with maraviroc (CCR5 antagonist) leads to declines in CD16-expressing monocytes in cART-suppressed chronic HIV-infected subjects and is associated with improvements in neurocognitive test performance: implications for HIV-associated neurocognitive disease (HAND). *J Neurovirol.* Dec 2014;20(6):571-582.

49. Lyons JL, Uno H, Ancuta P, et al. Plasma sCD14 is a biomarker associated with impaired neurocognitive test performance in attention and learning domains in HIV infection. *J Acquir Immune Defic Syndr*. Aug 15 2011;57(5):371-379.
50. Burdo TH, Weiffenbach A, Woods SP, Letendre S, Ellis RJ, Williams KC. Elevated sCD163 in plasma but not cerebrospinal fluid is a marker of neurocognitive impairment in HIV infection. *Aids*. Jun 1 2013;27(9):1387-1395.
51. Burdo TH, Lo J, Abbara S, et al. Soluble CD163, a novel marker of activated macrophages, is elevated and associated with noncalcified coronary plaque in HIV-infected patients. *J Infect Dis*. Oct 15 2011;204(8):1227-1236.
52. Subramanian S, Tawakol A, Abbara S, et al. Arterial Inflammation in Patients With HIV. *JAMA*. 2012;308:379-386.
53. Wright EJ, Grund B, Robertson K, et al. Cardiovascular risk factors associated with lower baseline cognitive performance in HIV-positive persons. *Neurology*. 2010;75(10):864-873.
54. O'Leary DH, Polak JF, Kronmal RA, et al. Thickening of the carotid wall. A marker for atherosclerosis in the elderly? Cardiovascular Health Study Collaborative Research Group. *Stroke*. Feb 1996;27(2):224-231.
55. O'Leary DH, Polak JF. Intima-media thickness: a tool for atherosclerosis imaging and event prediction. *The American Journal of Cardiology*. 2002;90(10C):18L-21L.
56. Polak JF, Pencina MJ, Pencina KM, O'Donnell CJ, Wolf PA, D'Agostino RBS. Carotid-Wall Intima–Media Thickness and Cardiovascular Events. *The New England Journal of Medicine*. 2011;365(3):213-221.

57. Volpe GE, Tang AM, Polak JF, Mangili A, Skinner SC, Wanke CA. Progression of Carotid Intima-Media Thickness and Coronary Artery Calcium Over 6 Years in an HIV-Infected Cohort. *Journal of acquired Immune Deficiency Syndromes*. 2013;64(1):51-57.
58. Sander K, Bickel H, Forstl H, et al. Carotid- intima media thickness is independently associated with cognitive decline. The INVADE study. *Int J Geriatr Psychiatry*. Apr 2010;25(4):389-394.
59. Walker JA, Sulciner ML, Nowicki KD, Miller AD, Burdo TH, Williams KC. Elevated numbers of CD163+ macrophages in hearts of simian immunodeficiency virus-infected monkeys correlate with cardiac pathology and fibrosis. *AIDS Res Hum Retroviruses*. Jul 2014;30(7):685-694.
60. Lifson JD, Rossio JL, Piatak M, Jr., et al. Role of CD8(+) lymphocytes in control of simian immunodeficiency virus infection and resistance to rechallenge after transient early antiretroviral treatment. *J Virol*. Nov 2001;75(21):10187-10199.
61. Lackner AA, Smith MO, Munn RJ, et al. Localization of simian immunodeficiency virus in the central nervous system of rhesus monkeys. *American Journal of Pathology*. 1991;139(3):609-621.
62. Sasseville VG, Lackner AA. Neuropathogenesis of simian immunodeficiency virus infection in macaque monkeys. *J Neurovirol*. Feb 1997;3(1):1-9.
63. Westmoreland SV, Halpern E, Lackner AA. Simian immunodeficiency virus encephalitis in rhesus macaques is associated with rapid disease progression. *J Neurovirol*. Jun 1998;4(3):260-268.
64. Walker JA, Beck GA, Campbell JH, Miller AD, Burdo TH, Williams KC. Anti-alpha4 Integrin Antibody Blocks Monocyte/Macrophage Traffic to the Heart and Decreases Cardiac Pathology in a SIV Infection Model of AIDS. *J Am Heart Assoc*. Jul 2015;4(7):e001932.

65. Ruifrok AC, Johnston DA. Quantification of Histochemical Staining by Color Deconvolution. *Analytical and Quantitative Cytology and Histology*. 2001;23:291-299.
66. Brower GL, Gardner JD, Forman MF, et al. The relationship between myocardial extracellular matrix remodeling and ventricular function. *Eur J Cardiothorac Surg*. Oct 2006;30(4):604-610.
67. Kelly KM, Tarwater PM, Karper JM, et al. Diastolic dysfunction is associated with myocardial viral load in simian immunodeficiency virus-infected macaques. *AIDS*. Apr 24 2012;26(7):815-823.
68. Yearley JH, Pearson C, Carville A, Shannon RP, Mansfield K. SIV-Associated Myocarditis: Viral and Cellular Correlates of Inflammation Severity. *AIDS Research and Human Retroviruses*. 2006;22(6):529-540.
69. Yearley JH, Pearson C, Carville A, Shannon RP, Mansfield K. Phenotypic Variation in Myocardial Macrophage Populations Suggests a Role for Macrophage Activation in SIV-Associated Cardiac Disease. *AIDS Research and Human Retroviruses*. 2007;23(4):512-524.
70. Rerkpattanapipat P, Wongpraparut N, Jacobs LE, Kotler MN. cardiac manifestation of acquired immunodeficiency syndrome. *Journal of the American Medical Association Internal Medicine*. 2000;160(5):602-608.
71. Silwa K, Carrington MJ, Becker A, Thienemann F, Ntsekhe M, Stewart S. Contribution of the human immunodeficiency virus acquired immunodeficiency syndrome epidemic to de novo presentations of heart disease in the Heart of Soweto Study cohort. *European Heart Journal*. 2012;33(7):866-874.

- 72.** Luetkens JA, Doerner J, Schwarze-Zander C, et al. Cardiac Magnetic Resonance Reveals Signs of Subclinical Myocardial Inflammation in Asymptomatic HIV-Infected Patients. *Circ Cardiovasc Imaging*. Mar 2016;9(3):e004091.
- 73.** Ntusi N, O'Dwyer E, Dorrell L, et al. HIV-1-Related Cardiovascular Disease Is Associated With Chronic Inflammation, Frequent Pericardial Effusions, and Probable Myocardial Edema. *Circ Cardiovasc Imaging*. Mar 2016;9(3):e004430.
- 74.** Schmitz JE, Kuroda MJ, Santra S, et al. Control of viremia in simian immunodeficiency virus infection by CD8+ lymphocytes. *Science*. Feb 5 1999;283(5403):857-860.
- 75.** Gallimore A, Cranage M, Cook N, et al. Early suppression of SIV replication by CD8+ nef-specific cytotoxic T cells in vaccinated macaques. *Nat Med*. Nov 1995;1(11):1167-1173.
- 76.** Jin X, Bauer DE, Tuttleton SE, et al. Dramatic rise in plasma viremia after CD8(+) T cell depletion in simian immunodeficiency virus-infected macaques. *J Exp Med*. Mar 15 1999;189(6):991-998.
- 77.** Williams KC, Corey S, Westmoreland SV, et al. Perivascular macrophages are the primary cell type productively infected by simian immunodeficiency virus in the brains of macaques: implications for the neuropathogenesis of AIDS. *The Journal of Experimental Medicine*. 2001;193(8):905-915.
- 78.** Clements JE, Babas T, Mankowski JL, et al. The Central Nervous System as a Reservoir for Simian Immunodeficiency Virus (SIV): Steady-State Levels of SIV DNA in Brain from Acute through Asymptomatic Infection. *The Journal of Infectious Diseases*. 2002;186(7):905-913.
- 79.** Soulas C, Conerly C, Kim WK, et al. Recently infiltrating MAC387(+) monocytes/macrophages a third macrophage population involved in SIV and HIV encephalitic lesion formation. *Am J Pathol*. May 2011;178(5):2121-2135.

80. Rogacev KS, Cremers B, Zawada AM, et al. CD14⁺⁺CD16⁺ monocytes independently predict cardiovascular events: a cohort study of 951 patients referred for elective coronary angiography. *J Am Coll Cardiol*. Oct 16 2012;60(16):1512-1520.
81. Rogacev KS, Seiler S, Zawada AM, et al. CD14⁺⁺CD16⁺ monocytes and cardiovascular outcome in patients with chronic kidney disease. *Eur Heart J*. Jan 2011;32(1):84-92.
82. Gratchev A, Sobenin I, Orekhov A, Kzhyshkowska J. Monocytes as a diagnostic marker of cardiovascular diseases. *Immunobiology*. May 2012;217(5):476-482.
83. Berg K, Ljungcrantz I, Andersson L, et al. Elevated CD14⁺⁺CD16⁻ Monocytes Predict Cardiovascular Events. *Circulation. Cardiovascular Genetics*. 2012;5(1):122-131.
84. Barisione C, Garibaldi S, Ghigliotti G, et al. CD14CD16 monocyte subset levels in heart failure patients. *Dis Markers*. 2010;28(2):115-124.
85. Serbina NV, Pamer EG. Monocyte emigration from bone marrow during bacterial infection requires signals mediated by chemokine receptor CCR2. *Nat Immunol*. Mar 2006;7(3):311-317.
86. Charo IF, Ransohoff RM. The many roles of chemokines and chemokine receptors in inflammation. *N Engl J Med*. Feb 9 2006;354(6):610-621.
87. Leuschner F, Courties G, Dutta P, et al. Silencing of CCR2 in myocarditis. *Eur Heart J*. Jun 14 2015;36(23):1478-1488.
88. Veillard NR, Steffens S, Pelli G, et al. Differential influence of chemokine receptors CCR2 and CXCR3 in development of atherosclerosis in vivo. *Circulation*. Aug 9 2005;112(6):870-878.
89. Williams DW, Byrd D, Rubin LH, Anastos K, Morgello S, Berman JW. CCR2 on CD14⁽⁺⁾CD16⁽⁺⁾ monocytes is a biomarker of HIV-associated neurocognitive disorders. *Neurol Neuroimmunol Neuroinflamm*. Oct 2014;1(3):e36.

ACKNOWLEDGEMENTS AND FUNDINGS

We thank the staff at the NEPRC and TNRPC for animal care, pathology residents and staff for assisting with necropsies and tissue collection. We thank Michael Piatek for plasma viral load determination, and Ronald Desrosiers for providing the SIVmac251. This work was supported by funding from the National Institute of Health (NIH) grant: RO1 NS040237 (Williams).

**CHAPTER 3. Elevated Numbers of CD163+ Macrophages in Hearts of SIV Infected Monkeys
Correlates with Cardiac Pathology and Fibrosisⁱ**

Joshua A. Walker, Megan L. Sulciner,

Katherine D. Misgen, Andrew D. Miller,

Tricia H. Burdo, Kenneth C. Williams

ABSTRACT

The role of macrophage activation, traffic, and accumulation on cardiac pathology was examined in twenty-three animals. Seventeen animals were SIV-infected, 12 were CD8-lymphocyte depleted, and the remaining 6 were uninfected controls (2 CD8-lymphocyte depleted, 4 non CD8-depleted). One of five SIV-infected, non-CD8 lymphocyte depleted animals had minor cardiac pathology (20% of animals) with increased numbers of macrophages in ventricular tissue compared to controls. Seven of twelve (58%) SIV-infected, CD8-lymphocyte depleted animals had cardiac pathology in ventricular tissue, including macrophage infiltration and myocardial degeneration. Fibrosis (measured as the percentage of collagen), was increased 41% in animals with cardiac pathology compared to animals without pathological abnormalities in SIV-infected, CD8-depleted animals. CD163+ macrophage numbers increased significantly in SIV-infected, CD8-lymphocyte depleted animals with cardiac pathology compared to ones without (1.66 fold) and controls (5.42 fold). The percent of collagen positively correlated with macrophage numbers in ventricular tissue in SIV-infected animals. There was an influx of BrdU+ monocytes to the heart during late SIV infection, regardless of pathology. These data implicate monocyte/macrophage activation and accumulation in the development of cardiac pathology during SIV infection.

INTRODUCTION

Effective anti-retroviral treatment (ART) has decreased mortality due to HIV infection resulting in an increase survival rate of HIV-infected patients.^{1,2} This increased survival has resulted in new, tissue-specific complications due to HIV infection and chronic immune activation.^{3,4} Previous studies have shown a link between coronary artery disease (CAD) and HIV infection, with HIV-infected individuals having approximately a two-fold increase in the incidence of myocarditis, ventricular dilation and myocardial infarction, compared to age-matched uninfected individuals.⁵⁻⁷ Factors correlating with HIV-associated CAD are likely multifactorial and include anti-retroviral drugs,⁸⁻¹⁰ microbial translocation resulting in chronic immune activation,^{11,12} increased levels of cardiac myosin specific auto-antibodies,¹³ opportunistic infections,^{14,15} and increased inflammation due to immune activation.^{16,17} Consistent observations in HIV infected individuals with CAD include mononuclear cellular infiltrates observed in cardiac parenchymal tissue and coronary vessels.^{12,18}

Monocytes/macrophages have been shown to play a role in SIV- and HIV-associated CAD, in particular atherosclerosis and myocarditis.^{5,19} Developing in the bone marrow, monocytes are released into the blood where they function in immunosurveillance and traffic to specific tissues, normally and in response to infection. Monocytes develop into macrophages in tissues^{5,20} some of which play roles in inflammation while others that are alternatively activated may have anti-inflammatory roles.²¹ Monocytes are prime sources of cytokines and chemokines that can alter cardiac function and,^{22,23} monocyte/macrophage-associated pro-inflammatory cytokines including interleukin (IL)-1, IL-6, and tumor necrosis factor α (TNF- α) are elevated during HIV infection and CAD.^{24,25} The number of CD14+CD16+ pro-inflammatory blood monocytes are increased with CAD and HIV infection, suggesting that chronic immune activation with HIV infection may increase the risk of CAD.^{26,27}

CD163, a hemoglobin/haptoglobin receptor involved in the clearance of hemoglobin is expressed on the surface of monocytes/macrophages^{28,29} and proteolytically cleaved from the surface of activated CD163+ monocytes/macrophages in response to pro-inflammatory signaling.^{30,31} Levels of soluble CD163 (sCD163) in plasma inversely correlate with the levels of membrane bound form of CD163 on monocytes/macrophages³² and is a biomarker for diseases where macrophage activation and inflammation play a central role.³¹ We have shown that sCD163 levels in plasma correlate with the rate of AIDS progression in SIV infected rhesus macaques.³³ Levels of sCD163 in acute (<1 year) and chronic (>1 year) HIV infection functions as a novel marker of HIV activity on monocyte/macrophages activation.³⁴ Additionally, levels of sCD163 in HIV-infected individuals correlated with the percentage of non-calcified, vulnerable, coronary plaques when compared to uninfected age-matched controls, while traditional risk factors of CAD such as d-dimer, C-reactive protein, and IL-6 did not.³⁵ Lastly, there are increased percentages of non-calcified coronary plaques in HIV infected elite controllers not on ART, further underscoring the role of monocytes/macrophages in lesion formation. While causes of CAD in HIV infected individuals are likely multifactorial, we sought to examine the role of macrophage activation and accumulation with SIV-infection on CAD. We used a CD8-lymphocyte depletion model of SIV infection in rhesus macaques, which results in rapid progression to AIDS (3-4 months) with a high rate of macrophage-mediated disease³⁶ as a model to examine the role of macrophage activation in the development of cardiac inflammation and damage during AIDS.

RESULTS

Increased numbers of macrophages in the heart with SIV infection in non-CD8 lymphocyte depleted animals

To investigate the role of monocytes/macrophage activation and traffic on cardiac pathology with SIV infection, twenty-three rhesus macaques were used in this study. Six animals (2 CD8-lymphocyte depleted, 4 non-depleted) were uninfected controls. Seventeen animals were SIV infected, of these 12 were CD8-lymphocyte depleted (Table 3.1). Immunohistochemistry revealed a significant increase in the number of CD163+, CD68+, and MAC387+ macrophages in SIV infected non-CD8 lymphocyte depleted animals compared to uninfected controls. There was a 1.32 fold increase in the number of activated CD163+ macrophages, a 1.91 fold increase in the number of resident CD68+ macrophages, and a 1.45 fold increase in the number of newly infiltrating MAC387+ macrophages in cardiac tissue of SIV-infected non-CD8 lymphocyte depleted animals compared to uninfected controls. In CD8-lymphocyte depleted animals we found a 4.52, 9.44, and 2.36-fold increase ($P < 0.05$) in the number of CD163+, CD68+, and MAC387+ macrophages respectively. CD3+ T-lymphocytes in SIV-infected, CD8-lymphocyte depleted animals were also significantly increased 7.91-fold ($P < 0.05$) compared to uninfected controls (Table 3.2).

Increased numbers of macrophages in the heart of CD8-lymphocyte depleted versus non-CD8 lymphocyte depleted animals

SIV-infected, CD8- lymphocyte depleted animals had significantly elevated numbers of macrophages and T-lymphocytes in cardiac tissue compared to SIV- infected non-lymphocyte depleted rhesus macaques (Table 3.2). CD163+ macrophages were increased 3.41-fold, CD68+ macrophages increased 4.93-fold and MAC387+ cells increased 1.63-fold in SIV-infected, CD8-

depleted animals compared to non-CD8 lymphocyte depleted animals ($P < 0.05$). The number of T lymphocytes in SIV-infected CD8-depleted animals was elevated 4.78-fold over SIV infected non-CD8 lymphocyte depleted animals. Overall, when compared to controls, SIV-infected, CD8-lymphocyte depleted animals show even greater numbers of macrophages and T- lymphocytes in cardiac tissue (Table 3.2).

Increased numbers of macrophages in the hearts of animals with cardiac pathology

SIV-infected, CD8-lymphocyte depleted animals were divided into two groups based on the presence or absence cardiac pathology as determined by a veterinary pathologist. Five of 12 animals had normal histology, while the remaining 7 had mild, moderate, or severe inflammation and degeneration. Animals with cardiac pathology had a 1.66 fold increase of CD163+ macrophages, and CD68+ and MAC387+ macrophages were increased by 2.46 and 1.70-fold, respectively, when compared to SIV-infected, CD8-depleted animals without cardiac pathology ($P < 0.05$). In addition, SIV-infected, CD8-lymphocyte depleted animals with pathology had a 2.51-fold increase in the number of CD3 T-lymphocytes compared to animals without cardiac pathology (Table 3.3).

Correlations between fibrosis and increasing numbers of macrophages in the heart

We quantified the percent of collagen per total tissue area using Masson's trichrome stain, as a measurement of fibrosis. In SIV-infected non-CD8 lymphocyte depleted animals one animal had minor pathology and mild fibrosis with $12.6 \pm 5.6\%$ collagen of total tissue area, as compared to the remaining 4 animals with normal histology with an average of $6.2 \pm 3.8\%$ collagen. The percent collagen in hearts of SIV-infected non-CD8 lymphocyte depleted animals was not significantly different from uninfected controls ($P > 0.05$) (Fig. 3.1B, 3.1C). Overall, SIV-

infected, CD8-lymphocyte depleted animals had increased levels of collagen compared to SIV-infected, non-CD8 depleted animals (14.5 ± 1.81 compared to 7.5 ± 1.39) (Fig. 3.1A, 3.1B). SIV-infected, CD8-lymphocyte depleted animals with cardiac pathology had increased amounts of collagen and numbers of CD163+ macrophages (Fig. 3.1A, 3.1B left). The percent collagen of total tissue area in SIV-infected, CD8-lymphocyte depleted rhesus macaques with cardiac pathology was significantly increased when compared to those without pathology (Fig. 3.1B right) ($19.2 \pm 3.4\%$ vs. $7.93 \pm 4.7\%$, $P < 0.05$). All SIV infected animals had positive correlations between the percentage of collagen as a marker for fibrosis and the numbers of CD163+ (Fig. 3.2A), CD68+ (Fig. 3.2B), and MAC387+ (Fig. 3.2C) macrophages. Animals with severe cardiac pathology had the highest numbers of macrophages in the heart. There was no correlation between the number of CD3+ T-lymphocytes and the amount of fibrosis in SIV-infected animals (Fig. 3.2D).

Absence of SIV viral protein and RNA in the heart of SIV infected animals

Extensive immunohistochemistry and *in situ* hybridization was done on cardiac tissues to determine if SIV-infected cells were present. SIV-p28 and -RNA was found in matched brain and lymph node tissues, but not in cardiac tissues from the same animals (data not shown).

Increased traffic to the heart during late SIV infection

We used BrdU to examine the traffic of recently released macrophages to the heart in SIV-infected, CD8-depleted animals. Animals were grouped based on when they received BrdU, early (6 and 20 dpi) or late (48 dpi and 24 hours prior to necropsy). In animals that received BrdU late we found a 4.72-fold increase in the number of BrdU+ macrophages present compared to animals that received BrdU early (Fig 3.3).

DISCUSSION

We examined in a retrospective study, the role of macrophage activation and traffic to the heart with SIV infection leading to cardiac inflammation and pathology. Examining macrophage populations in SIV infected, non-CD8 lymphocyte depleted rhesus macaques we found increased numbers of macrophages in cardiac tissues compared to uninfected controls. Twenty percent of SIV infected, non-CD8 lymphocyte depleted animals had minor interstitial fibrosis while the remaining had no significant signs of fibrosis when compared to controls. A single animal that had increased levels of fibrosis also had increased numbers of macrophages in the heart when compared to other SIV-infected, non-CD8 lymphocyte depleted animals without fibrosis. This suggests that macrophage accumulation plays a role in the observed cardiac pathology in a subset of SIV infected animals.

Compared to SIV-infected, non-CD8 lymphocyte depleted rhesus macaques CD8-lymphocyte depleted animals had significantly increased numbers of macrophages in the heart and a higher incidence of cardiac pathology. While viral load in plasma has been implicated in the progression of cardiac pathology in SIV-infected animals,⁴¹ we observed no differences in plasma viral load between SIV-infected, CD8-lymphocyte depleted animals with and without cardiac pathology. Additionally, we did not find SIV infected macrophages in the hearts of our animals. Kelly et. al., found scattered SIV-infected macrophages in hearts of a subset of infected animals (12 of 22) using a SIV-gp41 antibody that recognizes productively infected cells.⁴¹ But, the number of infected cells did not correlate with functional decline.⁴¹ Yearley et. al., found 1-4 SIV infected macrophages/mm² in hearts of 7 of 21 animals⁴². These authors used an antibody against SIV-nef that detects latent and productively infected macrophages. We found SIV-p28 and –RNA positive macrophages in brains and lymph nodes of the animals in our study. Results from our study suggest plasma virus, protein, or RNA alone do not drive cardiac pathology, and

other factors, including macrophages, likely do. We found positive correlations between the number of macrophages and the amount of fibrosis as a marker of damage to the heart, where animals with the most severe fibrosis had the highest numbers of macrophages.

While we have reported increased numbers of CD163+ macrophages, in SIV-infected animals with cardiac pathology and fibrosis, others have shown decreased numbers of CD163+ macrophages in the heart of SIV infected animals with active and borderline myocarditis⁴³ and an increase in CD3+ T-lymphocytes.⁴² In these studies, there were increased numbers of CD163+ macrophages in SIV infected animals with normal, uninflamed heart tissue, and fewer CD163+ macrophages in SIV infected animals with active or borderline myocarditis. Because CD163+ macrophages can be considered to be anti-inflammatory, and CD163 is upregulated by the anti-inflammatory cytokines IL-6 and IL-10^{44, 45} these authors concluded that CD163+ macrophages are protective. Their observations are in contrast to ours and others, increased numbers of CD163+ macrophages are present with active inflammation and lesion formation in cardiac and CNS tissues. Another observation to account for differences in the number of CD163+ macrophages in the heart between other studies and ours is that we used CD8-lymphocyte depleted animals which could alter the mechanisms of inflammation with SIV infection. The differing results underscore the fact that, at present, the function of CD163+ macrophages in the heart with SIV infection is not fully understood.

Previous studies have shown that chronic inflammation and T cell activation, without HIV infection, plays a role in the formation of atherosclerotic plaques.⁷ In HIV+ individuals, atherosclerosis is associated with T cell activation and markers of inflammation predict cardiac events.^{46,47} In SIV infected animals CD8+ T-lymphocytes are present and correlate with myocarditis.^{18,42} Animals in our study were persistently CD8+ T-lymphocyte depleted and we found few CD3+ T-lymphocytes in cardiac tissues. Thus, our results show there is cardiac

pathology and fibrosis without CD8+ T-lymphocytes and few CD3+ T-lymphocytes, further underscoring the role of monocytes/macrophages in pathology and fibrosis.

Using FDG-PET imaging, we have shown that increased monocyte/macrophage accumulation in the ascending aorta with HIV infection correlates with the number of non-calcified, vulnerable plaques.⁴⁸ In addition, this accumulation of macrophages is associated with sCD163 in plasma, a marker of macrophage activation.⁴⁸ We have also shown that sCD163 in plasma correlates with the presence of non-calcified, vulnerable, coronary plaques in HIV-infected patients.³⁵ Here, we demonstrate actual macrophage accumulation within ventricular tissue correlates with fibrosis suggesting that macrophage accumulation drives cardiac pathology with SIV infection. While some studies have associated the toxic effects of ART on CAD progression in humans and monkeys,⁸⁻¹⁰ studies examining HIV-1 elite controllers have shown that these individuals have increased rates of atherosclerosis compared to uninfected and chronically HIV-infected individuals.⁴⁹ HIV-1 elite controllers also had elevated levels of sCD163 in plasma⁴⁹. These observations, taken together with data from this study, suggest that immune activation and macrophages play a role in HIV- and SIV-associated cardiac pathology.

Using BrdU, we were able to examine the accumulation of monocytes newly released from the bone marrow. Regardless of cardiac pathology, we show an increase of monocyte/macrophage traffic to the heart during late versus early SIV infection. Due to the low number of animals receiving BrdU we could not determine statistically if increased traffic of macrophages to the heart with SIV infection led to increased damage.

Our studies demonstrated an increase in macrophage numbers in cardiac tissue of SIV infected animals with cardiac pathology. In particular, the numbers of CD163+ macrophages are significantly increased compared to animals without pathology and uninfected controls. We found a strong correlation between numbers of macrophages and the degree of fibrosis

determined by increasing levels of collagen in animals with cardiac pathology. The correlation between fibrosis and increased numbers of CD163+ macrophages demonstrate that the SIV-infected, CD8-lymphocyte depleted animals can be a beneficial model to study the effects of macrophage activation and inflammation on cardiac pathology associated with HIV and SIV infection. Our preliminary studies on HIV+ cardiac tissues also show an increase in the number of CD163+ macrophages in the heart during HIV infection that correlates with fibrosis (data not shown). While the causes of HIV and SIV associated CAD are likely multifactorial, our data suggests that macrophage accumulation and traffic to the heart plays a role in the developing cardiac pathology. Data from this study suggest that therapeutic treatments targeting macrophage activation and traffic, along with effective ART, could potentially reduce inflammation and the resulting damage seen in the heart during infection.

MATERIALS AND METHODS

Ethics Statement

All animals were either housed at Harvard University's New England Regional Primate Research Center or Tulane University's National Primate Center and handled in accordance with Harvard University's or Tulane University's National Primate Research Center Institutional Animal Care and Use Committee (IACUC).

Animals, viral infection and CD8+ T lymphocyte depletion

Twenty-three Rhesus macaques were used in this study. Seventeen were infected with SIVmac251 (SIV p27) by i.v. injection (kindly provided by Ronald Desrosiers, Harvard University). In order to achieve rapid progression to AIDS, 12 of the 17 infected animals were CD8-lymphocyte depleted using a human anti-CD8 antibody, cM-T807, administered s.c (10mg/kg) at 6 days post infection (dpi) and I.V. (5mg/kg) at 8 and 12 dpi, as previously described ⁴. The cM-T807 antibody was provided by the NIH Non-human Primate Reagent Resource (RR016001, A1040101). Six of the twenty-three rhesus macaques served as uninfected controls, 2 of which were CD8-lymphocyte depleted (50mg/kg single bolus I.V. injection). Animals were anesthetized with ketamine-HCL and euthanization with pentobarbital overdose intravenously, and exsanguinated. Following exsanguinations, standard necropsy was performed with a standard set of major organs collected in 10% neutral buffered formalin. Following fixation, all tissues were embedded in paraffin, sectioned at 5 µm, and stained with hematoxylin and eosin. Sections of left ventricular myocardium were blindly analyzed by a board certified veterinary pathologist (Andrew D. Miller, D.V.M, D.A.C.V.P). Cardiac tissues were scored based on ten randomly chosen 400x fields. Pathology was assessed based on the degree of change in the tissue and graded as mild, moderate, or severe inflammation and degeneration.

Plasma Viral Load Determination

SIV RNA in plasma was quantified using real time PCR as previously described.³⁷ Virions were pelleted from 500µL EDTA plasma from infected animals by centrifugation at 20,000 g for 1 hour. The threshold sensitivity was 100 copy Eq/mL. Viral loads peaked at day 8 post infection, and no differences in viral load were observed between SIV infected, CD8-lymphocyte depleted animals.

Immunohistochemistry and In Situ Hybridization for SIV-p28 and -RNA

The presence of SIV viral proteins in heart tissues were identified using SIV gp41 (KK41 1:500, NIH AIDS Research and Reference Reagent Program) and SIV p28 (SIVmac251 1:2500, Fitzgerald Industries), along with *in situ* hybridization with digoxigenin-labeled antisense riboprobes to detect SIV RNA (Lofstrand Labs, Gaithersburg, MD), as previously described.³⁸ Extensive immunohistochemistry and *in situ* hybridization tissue revealed no SIV-p28 or RNA was found in the hearts of SIV infected animals.

5-bromo-2'-deoxyuridine (BrdU) Administration

To study monocyte/macrophage traffic to and accumulation in the heart with SIV infection, BrdU was administered to SIV infected, CD8-lymphocyte depleted animals as previously described.³³ Briefly, a 30 mg/ml BrdU stock solution was prepared with 1X PBS, and was heated to 60°C in a water bath. BrdU was administered as a slow bolus i.v. injection at a dose of 60 mg BrdU/kg body weight. Animals were administered BrdU either early (6 and 20 dpi), or late (48 dpi and 24 hours prior to necropsy).

Immunohistochemistry

Formalin-fixed, paraffin-embedded cardiac tissue were cut in 5 μm sections, air dried overnight, then deparaffinized with xylenes, rehydrated in graded ethanols and finally with deionized water. Following rehydration, antigen binding sites were unmasked using Antigen Unmasking Solution (Vector Laboratories), for antibodies recognizing CD3, CD68, and BrdU with 20 minutes heat exposure followed by 20 minutes cooling at room temperature. Antigen unmasking for HAM56 was accomplished by incubating slides at 37°C for 5 minutes with Proteinase K (Dako). Following antigen unmasking cardiac tissues were blocked with a dual endogenous enzyme block (Dako). Sections were then incubated with biotin solution (Avidin/Biotin block, Vector Laboratories) for fifteen minutes to block endogenous biotin, followed by protein block using serum free protein block (Dako) and incubated for ten minutes for monoclonal antibodies and thirty minutes for polyclonal antibodies. Antibodies used to identify macrophages were the pan macrophage marker mouse monoclonal antibody CD68 (1:400, Dako, clone KP1). The CD163 scavenger receptor was detected using mouse monoclonal CD163 (1:250, Serotec). Recently infiltrated macrophages were identified by staining with mouse monoclonal antibody MAC387, an early marker of monocytes/macrophages (1:100, Dako). Mature macrophages present during chronic inflammation were recognized with a mouse monoclonal MRP8 antibody (BMA Biomedicals). A rabbit polyclonal CD3 antibody (1:300, Dako) was used to identify CD3 T lymphocytes. To assess macrophage traffic to the heart, sections were stained with a mouse monoclonal BrdU antibody (1:100, Dako). Slides were incubated for one hour at room temperature. Sections were incubated with the corresponding anti-mouse or ant-rabbit horseradish peroxidase conjugated secondary antibody for thirty minutes at room temperature. The color reaction product was developed using 3,3'-diaminobenzidine tetrahydrochloride (DAB, Dako). Slides were counterstained in hematoxylin,

dehydrated in washes of increasing concentration of ethanol, followed by xylenes, and mounted. All slides were imaged using a Zeiss Axio Imager M1 microscope (Carl Zeiss MicroImaging Inc., Thornwood, NY) using Plan-Apochromat x20/0.8 Korr objectives. Positive cells were counted manually for 20 random, non-overlapping fields of view to determine number of positive cells/mm² with a field area of 0.148mm²

Massons Trichrome Stain

Cardiac ventricular tissues were stained using a Massons Trichrome Stain kit (Newcomer Supply, Middleton, WI) was used according to manufacturer's protocol and imaged using a Zeiss Axio Imager M1 microscope using Plan-Apochromat x20/0.8 Korr objectives. Twenty random, non-overlapping fields of view were imaged for each slide and the percent of collagen relative to total cardiac tissue area examined was calculated. The percent collagen of total tissue area was quantified using ImageJ analysis software (v1.46, National Institute of Health) and color deconvolution vectors developed for Massons Trichrome that separate histological dyes into individual red, blue, and green colors.³⁹ The area of red and blue dyes corresponding to cytoplasm and collagen were measured to determine the percentage of total tissue area for each. The percentage of collagen serves as a qualitative measurement of fibrosis⁴⁰ and damage to cardiac tissue.

Statistical Analysis

Statistical analyses were performed using Prism version 5.0d (GraphPad Software, Inc., San Diego, CA) software. A Mann-Whitney non-parametric U test was used to compare all groups. Spearman's rank correlation was used for all correlations. Significance was accepted at p<0.05.

Table 3.1. Rhesus Macaques Used in the Study

Animal Type	SIV Status	N	Heart Pathology
Controls	-	6	6 NSF*
non-CD8 depleted	+	5	4 NSF 1 Mild, myocardial fibrosis and immune cell infiltration
CD8-depleted	+	12	5 NSF 3 Mild 3 Moderate 1 Severe, myocardium degeneration, inflammation, and fibrosis

*NSF- No significant findings

Pathology was determined by a veterinary pathologist. Cardiac tissue sections were scored based on ten randomly chosen 400x fields. Inflammation was graded according to mild, moderate, and severe as it related to immunoreactive cells present within the section.

Table 3.2. Comparison of the Numbers of Macrophages and T-lymphocytes in Uninfected, SIV+, and SIV+ CD8-lymphocyte Depleted Rhesus Macaques

Immune Markers	Uninfected (UN) (n=6)	SIV+		p value			Fold Change		
		Non-Depleted (ND) (n=5)	CD8-Depleted (CD8) (n=12)	UN vs. ND	UN vs. CD8	ND vs. CD8	ND/UN	CD8/UN	CD8/ND
CD163	56.33 (±5.30)	74.70 (±3.74)	254.83 (±21.37)	*	**	**	1.32	4.52	3.41
CD68	10.85 (±2.03)	20.76 (±1.63)	102.52 (±23.3)	*	**	**	1.92	9.44	4.93
HAM56	92.50 (±23.20)	77.12 (±10.19)	163.50 (±34.9)	ns	ns	*	-	-	2.12
MAC387	10.92 (±3.20)	15.83 (±1.96)	25.83 (±2.25)	*	*	*	1.45	2.36	1.63
CD3	3.47 (±0.75)	5.74 (±1.07)	27.45 (±7.85)	ns	*	**	-	7.91	4.78

Uninfected controls comprised of 2 uninfected, CD8 T-lymphocyte depleted animals and 4 uninfected, non-depleted animals.

No differences were observed in the number of macrophages and T-lymphocytes between these two groups. Numbers

represent the mean number of positive cells (cells/mm²) ± standard error of the mean (parentheses) based on counts from

20 non-overlapping fields of view using 20X objective. P values were calculated by comparing the mean number of positive

cells for controls and SIV+ animals using a Mann-Whitney U test (*, $p < 0.05$, ** $p < 0.01$). Fold change was calculated based on the ratio of macrophages or T-lymphocytes present in the heart for the indicated groups.

Table 3.3. Increased Number of Macrophages and T-lymphocytes in SIV-Infected CD8+ T-lymphocyte Depleted Rhesus Macaques with Cardiac Pathology Compared to SIV-Infected CD8+ T-lymphocyte Depleted Rhesus Macaques without Cardiac Pathology

Immune Markers	SIV+, CD8 Depleted (n=12)		<i>p value</i>	Fold Change
	w/o Pathology (n=5)	w/ Pathology (n=7)		
CD163	183.40 (±34.20)	305.85 (±14.06)	**	1.66
CD68	55.98 (±12.06)	137.75 (±6.20)	**	2.46
HAM56	196.50 (±14.90)	131.90 (±12.40)	ns	-
MAC387	17.34 (±1.99)	29.48 (±3.01)	*	1.70
CD3	14.60 (±4.72)	36.62 (±12.07)	*	2.51

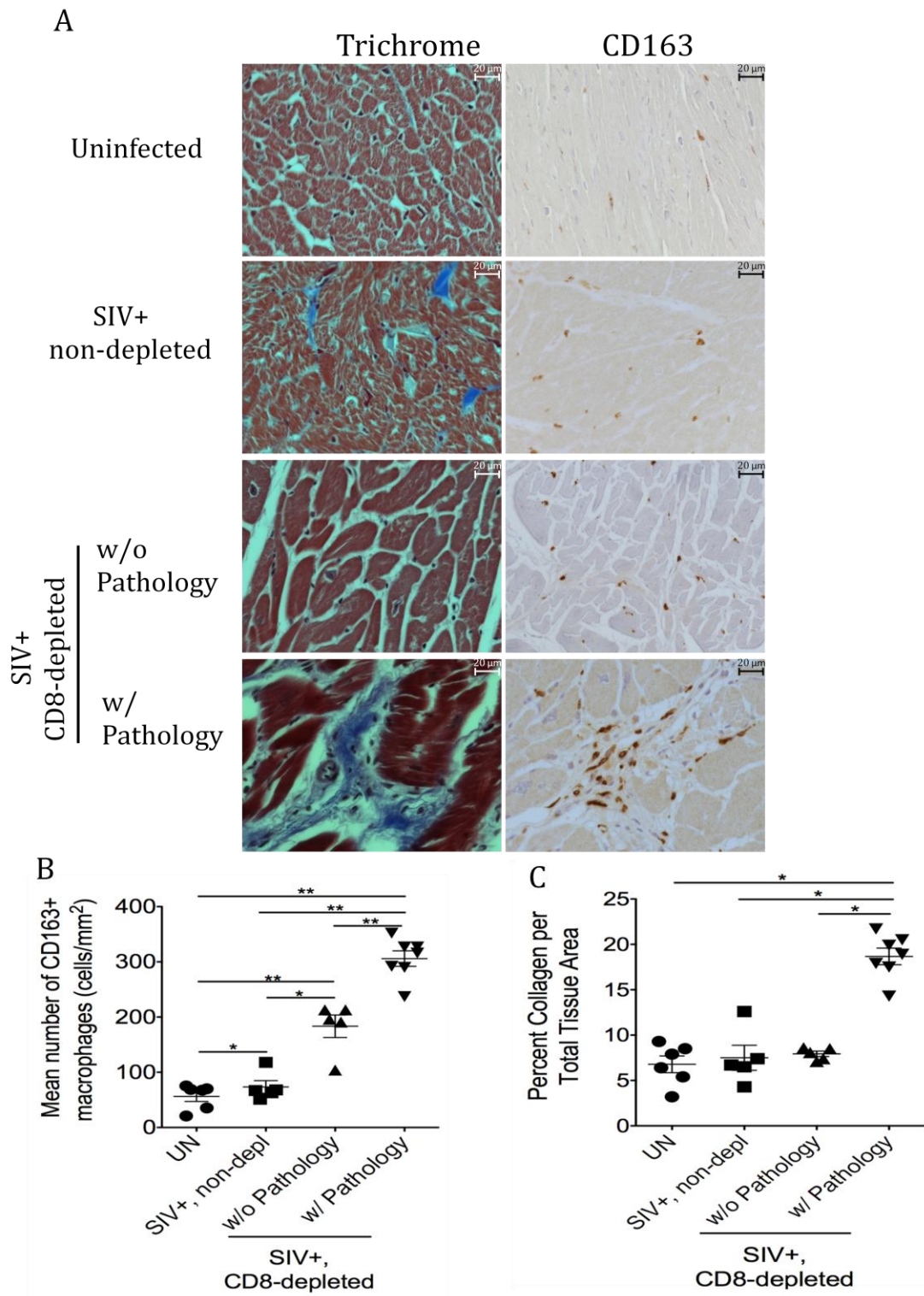
Numbers represent the mean number of positive cells (cells/mm²) ± standard error of the mean (parentheses) based on counts from 20 non-overlapping fields of view using 20X objective. *P* values were calculated by comparing the mean number of positive cells for SIV+, CD8-depleted animals with and without cardiac pathology using a Mann-Whitney U test (* *p*<0.05, ** *p*<0.01). Fold change was calculated based on the ratio of cells in SIV+, CD8-depleted animals with cardiac pathology compared to animals without pathology.

Table 3.4 BrdU+ cells in the heart of SIV-infected, CD8-lymphocyte depleted rhesus macaques are of myeloid lineage

Cell Phenotype	SIV- (n=2)	SIV+ w/o pathology (n=5)	SIV+ w/pathology (n=7)
BrdU+ MAC387+	75.60 (3.71)	84.48 (5.83)	79.25 (4.98)
BrdU+ CD68+	26.75 (7.97)	14.51 (3.92)	19.31 (4.89)
BrdU+ CD163+	9.90 (5.71)	1.24 (0.53)	5.87 (1.80)
BrdU+ CD3+	0.00 (0.00)	0.00 (0.00)	0.00 (0.00)

Note-Phenotype of BrdU+ positive cells in the heart of SIV-infected, CD8-lymphocyte depleted rhesus macaques. All BrdU+ cells were counted for SIV-infected, CD8-lymphocyte depleted animals and the average percentage of double positive cells for each indicated group was calculated for each cell phenotype \pm standard error of the mean, in parentheses.

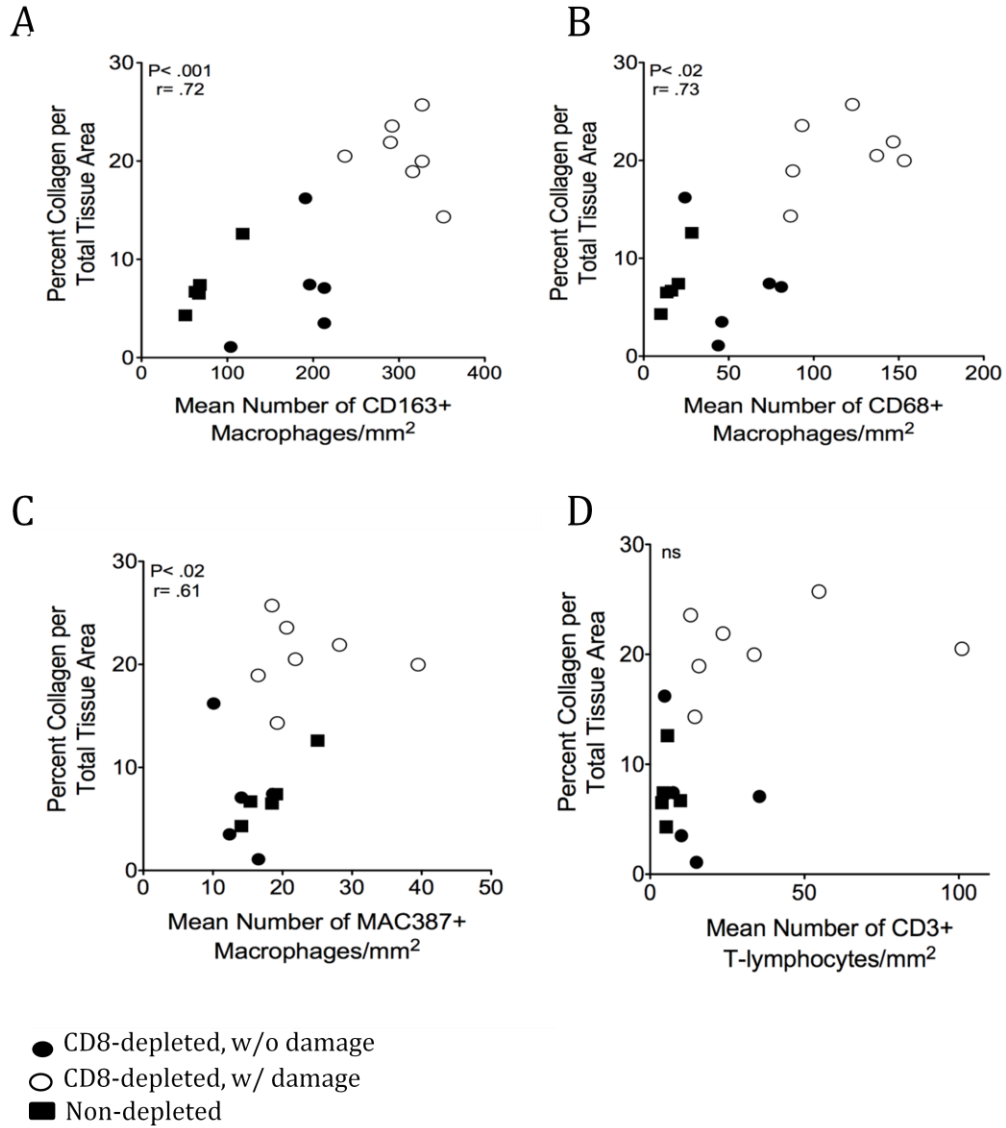
Figure 3.1



*from Walker et al. *AIDS Res Human Retroviruses*, 2014.

Figure 3.1. Increased numbers of CD163+ macrophages and amount of collagen in heart tissue in SIV infected rhesus macaques with cardiac damage Masson's trichrome stain and immunohistochemistry were used to compare the amount of collagen and numbers of CD163+ macrophages present in the heart of uninfected, SIV infected, and SIV infected CD8-depleted rhesus macaques (A). SIV infected, CD8-depleted animals with cardiac pathology show significantly increased levels of collagen ($19.2\pm 3.4\%$) and increased numbers of CD163+ macrophages are present (305.85 ± 14.06) (B, C). Statistical analysis was done between the indicated groups using Mann-Whitney non-parametric U test (*, $p < 0.05$, ** $p < 0.01$).

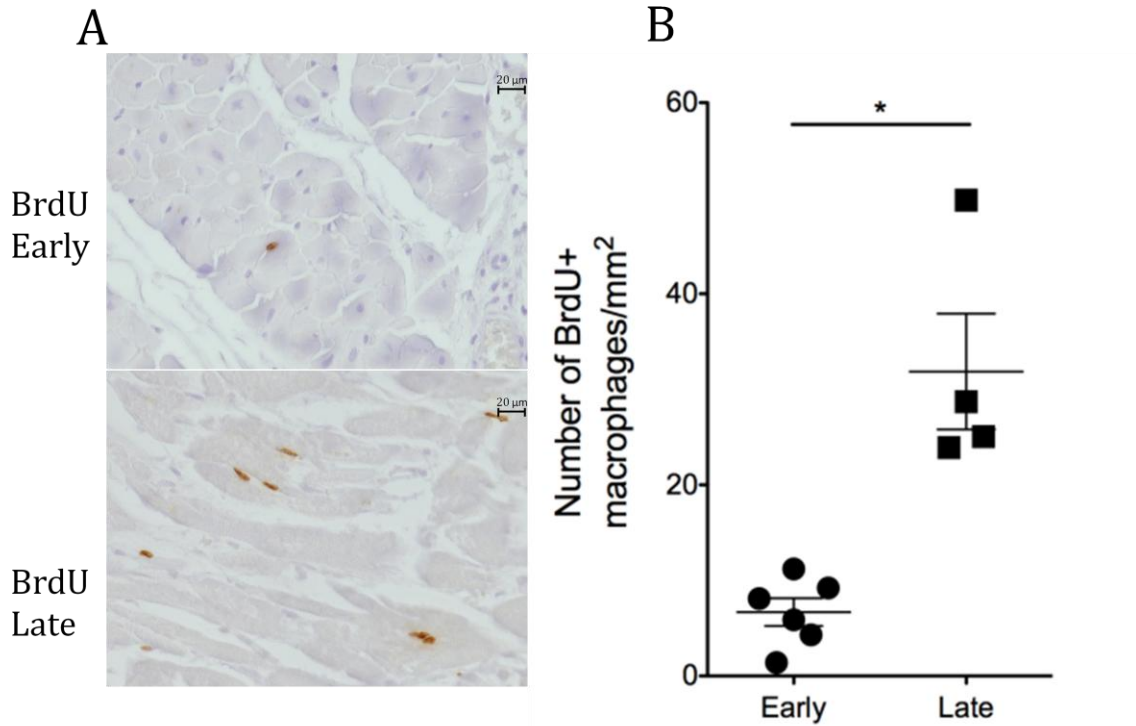
Figure 3.2



*from Walker et al. *AIDS Res Human Retroviruses*, 2014.

Figure 3.2. Correlations between the percentage of collagen per total tissue area and numbers of CD163+, CD68+ and MAC387+ macrophages in SIV infected rhesus macaques Spearman rank test was used to examine if there were correlations between the amount of cardiac damage based on the percentage collagen and the numbers of macrophages in the heart of SIV infected rhesus macaques (closed circle, SIV+ CD8-depleted w/o damage; open circle, SIV+ CD8-depleted w/damage; closed square, SIV+ non-depleted). Positive correlations were found between the amount of damage in each section and the numbers of CD163+ (upper left), CD68+ (upper right), and MAC387 (lower left) macrophages in SIV infected rhesus macaques. No correlations were found between the amount of damage and the number of CD3+ T-lymphocytes (lower right). $r =$ Spearman coefficient. $p < 0.05$.

Figure 3.3



*from Walker et al. *AIDS Res Human Retroviruses*, 2014.

Figure 3.3. Increased traffic of macrophages to the heart during late SIV infection BrdU

experiments were used to examine when macrophages traffic to the heart in SIV-infected, CD8-depleted rhesus macaques. Animals were grouped based on whether they received BrdU early or late. Immunohistochemistry with an anti-BrdU antibody shows increased traffic of BrdU+ macrophages to the heart of SIV-infected, CD8-depleted rhesus macaques that received BrdU late compared to early (A). Animals that received BrdU late during infection had 31.85 ± 14.8 BrdU+ macrophages in the heart compared to 6.68 ± 2.9 BrdU+ macrophages in the heart of animals that received BrdU early.

Figure 3.4

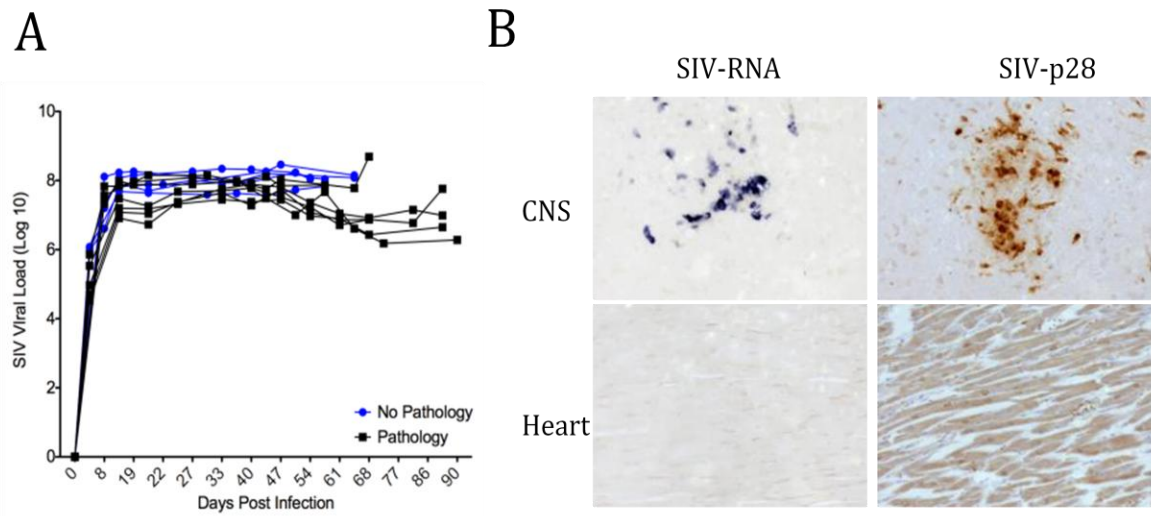


Figure 3.4. SIV plasma virus does not distinguish between animals with and without cardiac pathology SIV plasma viral load was quantified for SIV+ CD8+ T-lymphocyte depleted animals using real-time PCR. (A) For these animals, SIV plasma virus peaked at 8 dpi and remained consistently elevated during the course SIV infection and did not distinguish between animals that did and did not develop cardiac pathology. Sections of cardiac tissue from SIV+ CD8+ T-lymphocyte depleted animals were examined for the presence of SIV-RNA or SIV-p28 viral protein (B). There were no SIV-RNA+ or SIV-p28+ cells found in cardiac tissues of the animals.

REFERENCES

1. Collaboration H-C, Ray M, Logan R, *et al.*: The effect of combined antiretroviral therapy on the overall mortality of HIV-infected individuals. *AIDS* 2010;24:123-137.
2. Coquet I, Pavie J, Palmer P, *et al.*: Survival trends in critically ill HIV-infected patients in the highly active antiretroviral therapy era. *Crit Care* 2010;14:R107.
3. Deeks SG: HIV Infection, Inflammation, Immunosenescence, and Aging. *Annu Rev Med* 2011;62:141-155.
4. Williams K, Westmoreland S, Greco J, *et al.*: Magnetic resonance spectroscopy reveals that activated monocytes contribute to neuronal injury in SIV neuroAIDS. *J Clin Invest* 2005;115:2534-2545.
5. Crowe SM, Westhorpe CL, Mukhamedova N, Jaworowski A, Sviridov D, Bukrinsky M: The macrophage: the intersection between HIV infection and atherosclerosis. *J Leukoc Biol* 2010;87:589-598.
6. Currier JS, Lundgren JD, Carr A, *et al.*: Epidemiological evidence for cardiovascular disease in HIV-infected patients and relationship to highly active antiretroviral therapy. *Circulation* 2008;118:e29-35.
7. Ho JE, Hsue PY: Cardiovascular manifestations of HIV infection. *Heart* 2009;95:1193-1202.
8. Annamalai L, Westmoreland SV, Domingues HG, Walsh DG, Gonzalez RG, O'Neil SP: Myocarditis in CD8-Depleted SIV-Infected Rhesus Macaques after Short-Term Dual Therapy with Nucleoside and Nucleotide Reverse Transcriptase Inhibitors. *PLoS One* 2010;5:e14429.
9. Friis-Møller N, Reiss P, Sabin CA, *et al.*: Class of antiretroviral drugs and the risk of myocardial infarction. *N Engl J Med* 2007;356:1723-1735.

10. Friis-Møller N, Sabin CA, Weber R, *et al.*: Combination Antiretroviral Therapy and the Risk of Myocardial Infarction. *N Engl J Med* 2003;349:1993-2003.
11. Brenchley JM, Price DA, Schacker TW, *et al.*: Microbial translocation is a cause of systemic immune activation in chronic HIV infection. *Nat Med* 2006;12:1365-1371.
12. Pandrea I, Cornell E, Wilson C, *et al.*: Coagulation biomarkers predict disease progression in SIV-infected nonhuman primates. *Blood* 2012;120:1357-1366.
13. Currie PF, Goldman JH, Caforio ALP, *et al.*: Cardiac autoimmunity in HIV related heart muscle disease. *Heart* 1998;79:599-604.
14. Yanai T, Lackner AA, Sakai H, Masegi T, Simon MA: Systemic arteriopathy in SIV-infected rhesus macaques (*Macaca mulatta*). *J Med Primatol* 2006;35:106-112.
15. Liu R, Moroi M, Yamamoto M, *et al.*: Presence and Severity of Chlamydia and pneumoniae and Cytomegalovirus Infection in Coronary Plaques Are Associated With Acute Coronary Syndromes. *Int Heart J* 2006;47:511-519.
16. Roivainen M, Viik-Kajander M, Palosuo T, *et al.*: Infections, Inflammation, and the Risk of Coronary Heart Disease. *Circulation* 2000;101:252-257.
17. Stein JH, Hsue PY: Inflammation, Immune Activation, and CVD Risk in Individuals With HIV Infection. *JAMA* 2012;308:405-406.
18. Shannon RP, Simon MA, Mathier MA, Geng YJ, Mankad S, Lackner AA: Dilated Cardiomyopathy Associated With Simian AIDS in Nonhuman Primates. *Circulation* 2000;101:185-193.
19. Crowe SM, Hoy JF: Are monocytes the canary in the coal mine for HIV-related atherosclerosis? *J Infect Dis* 2012;206:1491-1493.

20. Auffray C, Sieweke MH, Geissmann F: Blood monocytes: development, heterogeneity, and relationship with dendritic cells. *Annu Rev Immunol* 2009;27:669-692.
21. Martinez FO, Helming L, Gordon S: Alternative activation of macrophages: an immunologic functional perspective. *Annu Rev Immunol* 2009;27:451-483.
22. Prabhu SD: Cytokine-induced modulation of cardiac function. *Circ Res* 2004;95:1140-1153.
23. Monsuez JJ, Escaut L, Teicher E, Charniot JC, Vittecoq D: Cytokines in HIV-associated cardiomyopathy. *Int J Cardiol* 2007;120:150-157.
24. Barbaro G, Di Lorenzo G, Soldini M, *et al.*: Clinical course of cardiomyopathy in HIV-infected patients with or without encephalopathy related to the myocardial expression of tumor necrosis factor- α and nitric oxide synthase. *AIDS* 2000;14:827-838.
25. Fisher SD, Bowles NE, Towbin JA, Lipshultz SE: Mediators in HIV-associated cardiovascular disease a focus on cytokines and genes. *AIDS* 2003;17:S29-35.
26. Thieblemont N, Weiss L, Sadeghi HM, Estcourt C, Haeffner-Cavaillon N: CD14^{low}CD16^{high} A cytokine-producing monocyte subset which expands during human immunodeficiency virus infection. *Eur J Immunol* 1995;25:3418-3424.
27. Barisione C, Garibaldi S, Ghigliotti G, *et al.*: CD14CD16 monocyte subset levels in heart failure patients. *Dis Markers* 2010;28:115-124.
28. Kristiansen M, Graversen JH, Jacobsen C, Hoffmann E, Lawskov SKA, Moestrup SK: Identification of the haemoglobin scavenger receptor. *Nature* 2001;409:1999-2002.
29. Onofre G, Koláčková M, Jankovičová K, Krejsek J: Scavenger Receptor CD163 and its Biological Function. *Acta Medica* 2009;52:57-61.

30. Buechler C, Ritter M, Orsó E, Langmann T, Klucken J, Schmitz G: Regulation of scavenger receptor CD163 expression in human monocytes and macrophages by pro- and antiinflammatory stimuli. *J Leukoc Biol* 2000;67:97-103.
31. Etzerodt A, Moestrup SK: CD163 and inflammation: biological, diagnostic, and therapeutic aspects. *Antioxid Redox Signal* 2013;18:2352-2363.
32. Davis BH, Zarev PV: Human monocyte CD163 expression inversely correlates with soluble CD163 plasma levels. *Cytometry B Clin Cytom* 2005;63:16-22.
33. Burdo TH, Soulas C, Orzechowski K, *et al.*: Increased Monocyte Turnover from Bone Marrow Correlates with Severity of SIV Encephalitis and CD163 Levels in Plasma. *PLoS Pathog* 2010;6:e1000842.
34. Burdo TH, Lentz MR, Autissier P, *et al.*: Soluble CD163 made by monocyte/macrophages is a novel marker of HIV activity in early and chronic infection prior to and after anti-retroviral therapy. *J Infect Dis* 2011;204:154-163.
35. Burdo TH, Lo J, Abbara S, *et al.*: Soluble CD163, a novel marker of activated macrophages, is elevated and associated with noncalcified coronary plaque in HIV-infected patients. *J Infect Dis* 2011;204:1227-1236.
36. Schmitz JE, Simon MA, Kuroda MJ, *et al.*: A Nonhuman Primate Model for the Selective Elimination of CD8+ Lymphocytes Using a Mouse-Human Chimeric Monoclonal Antibody. *Am J Pathol* 1999;154:1923-1932.
37. Lifson JD, Rossio JL, Piatak M, Jr., *et al.*: Role of CD8(+) lymphocytes in control of simian immunodeficiency virus infection and resistance to rechallenge after transient early antiretroviral treatment. *J Virol* 2001;75:10187-10199.

38. Williams K, Schwartz A, Corey S, *et al.*: Proliferating Cellular Nuclear Antigen Expression as a Marker of Perivascular Macrophages in Simian Immunodeficiency Virus Encephalitis. *Am J Pathol* 2002;161:575-585.
39. Ruifrok AC, Johnston DA: Quantification of Histochemical Staining by Color Deconvolution. *Anal Quant Cytol Hist* 2001;23:291-299.
40. Brower GL, Gardner JD, Forman MF, *et al.*: The relationship between myocardial extracellular matrix remodeling and ventricular function. *Eur J Cardiothorac Surg* 2006;30:604-610.
41. Kelly KM, Tarwater PM, Karper JM, *et al.*: Diastolic dysfunction is associated with myocardial viral load in simian immunodeficiency virus-infected macaques. *AIDS* 2012;26:815-823.
42. Yearley JH, Pearson C, Carville A, Shannon RP, Mansfield K: SIV-Associated Myocarditis: Viral and Cellular Correlates of Inflammation Severity. *AIDS Res Hum Retroviruses* 2006;22:529-540.
43. Yearley JH, Pearson C, Carville A, Shannon RP, Mansfield K: Phenotypic Variation in Myocardial Macrophage Populations Suggests a Role for Macrophage Activation in SIV-Associated Cardiac Disease. *AIDS Res Hum Retroviruses* 2007;23:512-524.
44. Moestrup SK, Møller HJ: CD163: a regulated hemoglobin scavenger receptor with a role in the anti-inflammatory response. *Ann Med* 2004;36:347-354.
45. Moller HJ. Soluble CD163: *Scand J Clin Lab Invest* 2012;72:1-13.
46. Baker JV, Henry WK, Patel P, *et al.*: Progression of carotid intima-media thickness in a contemporary human immunodeficiency virus cohort. *Clin Infect Dis* 2011;53:826-835.
47. Kaplan RC, Sinclair E, Landay AL, *et al.*: T cell activation and senescence predict subclinical carotid artery disease in HIV-infected women. *J Infect Dis* 2011;203:452-463.

48. Subramanian S, Tawakol A, Abbara S, *et al.*: Arterial Inflammation in Patients With HIV.
JAMA 2012;308:379-386.
49. Pereyra F, Lo J, Triant V, *et al.*: Increased coronary atherosclerosis and immune activation in HIV-1 elite controllers. AIDS 2012;26:2409-2415.

ACKNOWLEDGEMENTS AND FUNDING

We thank the staff at the NEPRC for animal care, pathology residents and staff for assisting with necropsies and tissue collection. We thank Michael Piatek and Jeffrey Lifson for plasma viral load determination, and Ronald Desrosiers for providing the SIVmac25. This work was supported by the following NIH grants R01 NS040237 (K.C.W.), R01 NS082116 (T.H.B.) and a pilot grant from the Tulane National Primate Research Center NIH P51-RR00164 (T.H.B), and a NERPC base grant NIH OD011103.

CHAPTER 4. Increased Aortic Intima Media Thickness and Cardiac Fibrosis Correlates with Soluble CD163: A Role for Monocytes/Macrophages in HIV-Associated Cardiovascular Disease Progression

Joshua A. Walker, Graham A. Beck,

Jennifer H. Campbell, Katherine D. Nowicki,

Andrew D. Miller, Tricia H. Burdo,

Kenneth C. Williams

ABSTRACT

HIV+ individuals have an increased risk of cardiovascular disease (CVD) where chronic immune activation and monocyte/macrophage inflammation may play a role. We examined matched aorta, left ventricle (cardiac tissue), and plasma from 16 chronically infected HIV+ individuals on combination antiretroviral therapy (cART) and 16 age and sex matched HIV -individuals. Aorta and cardiac tissue were assessed for numbers of inflammatory macrophages and T-lymphocytes. Aortic intima-media thickness (aIMT) and cardiac fibrosis were measured following a modified Verhoeff Van Gieson and Modified Massons trichrome stain. Plasma soluble CD163 (sCD163), a marker of monocyte/macrophage activation with HIV infection was measured by ELISA. We found significant increases in the numbers of CD163+, CD68+, CD206+, and MAC387+ macrophages in aorta and cardiac tissue with HIV infection. The number of macrophages in aorta correlated with numbers of macrophages in cardiac tissues. There was a positive correlation between plasma sCD163 and numbers of all macrophages in aorta and cardiac tissues. Soluble CD163 correlated with the percentage of collagen (fibrosis) and aIMT. These data underscore the role of monocyte/macrophage activation and inflammation in increased aIMT and cardiac fibrosis with HIV infection and point to the necessity to target monocytes/macrophages to reduce CVD inflammation and pathology with HIV.

INTRODUCTION

Monocytes/macrophages are mediators of cardiovascular disease (CVD) with HIV infection and are mediators in fibrosis,¹ myocarditis^{2,3} and atherosclerotic plaque progression. Monocytes can traffic to cardiovascular tissues and differentiate into macrophages where they phagocitize low density lipoprotein (LDL) and develop into foam cells,⁴ this drives the development of the atheroma core.^{5,6} A range of monocyte phenotypes are present within an atherosclerotic plaque, where M1 inflammatory macrophages are thought to be involved in plaque rupture⁷. In contrast, alternatively activated M2 macrophages are thought to be athero-protective.⁸ Monocytes/macrophages can influence the stability of an atherosclerotic plaque.⁹ Macrophages within atherosclerotic plaques can secrete matrix metalloproteinases (MMPs) that promote plaque instability and rupture.^{10,11} Studies using optical coherence tomography show that vulnerable plaques are characterized by a larger lipid rich core and increased macrophage accumulation in the cap and shoulder regions compared to stable plaques within the same individual.¹² While traditional risk factors of CVD are present among HIV+ individuals, they do not fully account for the increased risk of CVD among HIV+ individuals.^{13,14} It is thought that the increased CVD risk seen among this population is due in part to increased immune activation and monocyte/macrophage accumulation.¹⁵⁻¹⁷ In this population, there is an increase in vulnerable, non-calcified plaques that are prone to rupture.^{18,19}

Among HIV+ individuals with controlled viremia circulating CD14+CD16+ monocytes, are predictive of coronary artery calcium (CAC) progression, suggesting that they are pro-atherogenic and associated with CVD.²⁰ Monocyte chemoattractant protein-1 (MCP-1), tumor necrosis factor- α (TNF- α)²¹, and soluble CD14 (sCD14)²² also predict CAC progression independent of traditional CVD risk factors.²¹ We have shown that levels of soluble CD163 (sCD163), a marker of monocyte/macrophage activation, is elevated with HIV infection and

correlate with the number of non-calcified, vulnerable plaques.^{18,19} In addition to increased inflammation, there is also an increase in high-risk plaque morphology defined as an increase in the number of low attenuated plaques and positive remodeling, and that inflammation in the aorta is representative of inflammation in the rest of the arterial tree.²³ To date, correlations between sCD163 and macrophage inflammation in the aorta and heart have not been done.

In this study we examined matched aorta, left ventricle (cardiac tissue), and plasma from age and sex matched HIV- and HIV+ individuals to determine if HIV infection results in increased monocyte/macrophage inflammation, increased aortic intima-media thickness (aIMT) and cardiac fibrosis than HIV- individuals. We measured levels of sCD163 to determine if it correlated with increased aIMT and cardiac fibrosis with HIV infection. We found that HIV+ individuals on combination anti-retroviral therapy (cART) had greater aortic and cardiac inflammation and increased aIMT and cardiac fibrosis. Soluble CD163 positively correlated with increased aIMT and cardiac fibrosis, providing evidence that chronic immune activation plays a role in the development of HIV-associated CVD.

RESULTS

HIV infection results in increased macrophage inflammation in the aorta and cardiac tissue.

Paired aorta and cardiac tissue sections were stained immunohistochemically with antibodies recognizing CD163+, CD68+, CD206+, and MAC387+ macrophages (Fig. 4.1). We found a significant 2.02-fold increase in numbers of CD163+ macrophages, a 1.57-fold increase numbers of CD68+ macrophages, 1.59-fold increase in numbers of CD206+ macrophages, and a 1.84-fold increase in numbers of MAC387+ macrophages in HIV+ aortic tissues compared to HIV- aortic tissues (Table 1, Fig. 4.1B *left*) (Mann-Whitney t-test). In cardiac tissue we found a significant 2.05-fold increase in CD163+ macrophages, a 2.02-fold increase in CD68+ macrophages, a 2.21-fold increase in CD206+ macrophages, and a 1.87-fold increase in MAC387+ macrophages in HIV+ cardiac tissues compared to HIV- cardiac tissues (Table 4.2, Fig. 4.1B *right*) (Mann-Whitney t-test). There were no differences observed between the numbers of CD3+ T-lymphocytes in the aorta and cardiac tissues between HIV- and HIV+ individuals. Using Spearman rank correlation we found positive correlations between numbers of CD163+ ($r=.70$, $p<0.01$), CD68+ ($r=.67$, $p<0.01$), CD206+ ($r=.57$, $p<0.01$) and MAC387+ macrophages ($r=.58$, $p<0.01$) in aorta and cardiac tissue. (Fig.4. 1C).

Increased numbers of macrophages in the aorta correlate with increased aortic intima-media thickness

With HIV infection there is a significant 1.51-fold increase in aIMT compared to HIV- individuals (Fig. 4.2A, 4.2B) (Mann-Whitney t-test, $*p<0.05$). Using a Spearman rank correlation we found that increased aIMT positively correlated with increased numbers of CD163+ ($r=.58$, $p<0.05$), CD68+ ($r=.56$, $p<0.05$), CD206+ ($r=.47$, $p<0.05$), and MAC387+ macrophages ($r=.53$, $p<0.05$) (Fig. 4.2C).

Increased numbers of macrophages in cardiac tissues correlate with increased levels of fibrosis

Cardiac tissues from HIV+ individuals had a significant increase in the percentage of collagen per total tissue area compared to HIV- cardiac tissues (Fig. 4.3A). There was a significant 1.62-fold increase in the percentage of collagen in HIV+ cardiac tissues ($31.52 \pm 2.03\%$) compared to HIV- cardiac tissues ($19.44 \pm 3.4\%$) (Fig. 4.3B) (Mann-Whitney t-test, $**p < 0.01$). Additionally, there was a positive correlation between increased numbers of CD163+ ($r = .56$, $p < 0.05$), CD68+ ($r = .52$, $p < 0.05$), CD206+ ($r = .75$, $p < 0.01$) and MAC387+ macrophages ($r = .53$, $p < 0.05$) and increased percentage of collagen per total tissue area (Fig. 4.3C).

Increased plasma soluble CD163 correlated with macrophage inflammation, increased aortic intima-media thickness, and cardiac fibrosis

There was a significant 1.73-fold increase in plasma sCD163 from HIV+ individuals compared to HIV- individuals (Fig. 4.4A) (Mann-Whitney t-test). There were positive correlations between plasma sCD163 and macrophage inflammation in the matched aorta (Fig. 4.4B) and cardiac tissues (Fig. 4.4C). Positive correlations were found between plasma sCD163 and increased aIMT (Fig. 4.4D *left*) cardiac fibrosis aIMT were found (Fig. 4.4D *right*).

DISCUSSION

Despite effective cART HIV+ individuals still suffer from chronic immune activation²⁸⁻³⁰ and secondary co-morbidities where activated monocytes/macrophages are implicated.^{9,16,30,31} HIV+ individuals are at an increased risk of atherosclerosis compared to the general population.³²⁻³⁴ We have previously shown that sCD14 and sCD163 but not traditional cardiovascular risk factors (D-dimer, interleukin (IL)-6, and C-reactive protein (CRP)) were associated with atherosclerotic plaques with HIV infection¹⁸, suggesting that chronic immune activation is playing a role in CVD development. There is also an increased risk of myocarditis and cardiomyopathy where 40-50% of AIDS patients at necropsy showed signs of the diseases.³⁵ However, while this rate has declined in the cART era, myocarditis is still present, along with myocardial fibrosis shown through magnetic resonance imaging (MRI) and spectroscopy (MRS).³⁶⁻³⁸ Data from our study supports this, showing that increased inflammation in the heart is still present in HIV+ individuals.

In this study we found significant increases in the numbers of macrophages in the aorta and cardiac tissues of HIV+ individuals compared to controls. In particular, we see a significant increase in alternatively activated CD163+ and CD206+ macrophages. It has previously been shown that these macrophages accumulate in the shoulder and cap regions of unstable atherosclerotic plaques.³⁹ While CD163 and CD206 are thought to be markers of M2 polarized macrophages that are anti-inflammatory, it is possible that their accumulation leads to a weakening of the atherosclerotic plaque making it prone to rupture. In rodent models, M2 macrophage accumulation in the aorta results in increased fibrosis and elastin loss.⁴⁰ Macrophages also control fibrosis in cardiac tissues. By themselves, macrophages control fibrosis by secreting MMPs, however studies on the heart are needed to determine what pro-fibrotic factors are expressed by macrophages specifically. Data from our studies support this in

the heart, where we found that increased numbers of macrophages correlate with increased cardiac fibrosis. Additionally, we found positive correlations between the levels of inflammation in cardiac tissues and the aorta, suggesting that there is progressive and systemic inflammation in the cardiovascular system.

Previous studies have examined associations between soluble markers of immune activation and surrogate markers of CVD, in particular CAC and aIMT. Studies have shown increased levels of sCD14 are associated with CAC progression with HIV infection²² and sCD14 and sCD163 are increased and associated with atherosclerosis.⁴¹ Imaging studies have investigated the relationship between plasma markers and monocyte/macrophage accumulation in the aorta and cardiac tissues with HIV. FDG-PET imaging showed increased arterial inflammation which is associated with elevated levels of sCD163,¹⁹ but it was not possible to colocalize glucose uptake with macrophage markers. We showed that sCD163 correlates with increased macrophage inflammation with HIV infection in aorta and heart using post-mortem tissues. Levels of sCD163 also correlated with fibrosis and aIMT, actual markers of CVD. These data support evidence that monocyte/macrophage activation plays a role in the development of HIV-associated CVD, and that sCD163 could potentially be a diagnostic marker and predictive of fibrosis and aIMT. However, longitudinal studies would need to be examined to indeed see if sCD163 is increased along with markers of CVD with HIV infection.

Data from these experiments provide evidence supporting the notion that chronic immune activation plays a role in the development of HIV-associated CVD. While cART is effective in decreasing viremia to undetectable levels, it does not target monocytes/macrophages that play a role in the development of CVD. Studies have begun to examine therapeutic agents that effect monocyte/macrophage activation and could be beneficial in decreasing CVD. Inhibitors of 3-hydroxy-3-methylglutaryl-coenzyme A reductase

inhibitors (statins) have been beneficial in decreasing levels of interleukin-6 (IL-6), interleukin-8 (IL-8), and TNF- α , serum markers of immune activation and monocyte/macrophage activation.⁴² A recent study using atorvastatin did not decrease arterial inflammation in HIV+ men with subclinical atherosclerosis and arterial inflammation, but it did decrease the volume of non-calcified plaques.⁴³

In this study we found that HIV infection results in significant aortic and cardiac tissue inflammation. While we only examined the aorta, inflammation in the aorta has been shown to be representative of the arterial tree,²³ suggesting that increased inflammation could be present in other arteries. Additionally, we show that soluble factors of immune activation correlate with increased fibrosis in the heart and increased intima-media thickness of the aorta. Overall, our data support the growing evidence that HIV+ individuals are at an increased risk for CVD where activated monocytes/macrophages play a role.

MATERIALS AND METHODS

Cardiac tissues and plasma

Matched tissue samples of aorta, left ventricle (cardiac tissue), and blood plasma from 16 HIV- and 16 HIV+ males were provided by the National NeuroAIDS Tissue Consortium (NNTC) and the National Disease Research Institute (NDRI). Samples from HIV- individuals had no history of CVD or inflammatory conditions. The average age for the HIV- cohort was 53.3 ± 3.55 years and the average age for the HIV+ cohort was 50.8 ± 2.70 years and there was no significant differences between the average ages of the groups. The average duration for HIV infection 10.6 ± 1.33 years, with HIV+ individuals being on cART for an average of 8.6 ± 2.43 years with no detectable virus.

Immunohistochemistry

Formalin-fixed, paraffin-embedded tissue sections of paired aorta and cardiac tissues were assessed for CD163+, CD68+, CD206+, and MAC387+ macrophages, CD3+ T-lymphocytes as previously described.²⁴ Slides were imaged using a Zeiss Axio Imager M1 microscope (Carl Zeiss MicroImaging Inc., Thornwood, NY) using Plan-Apochromat .20/0.8 Korr objectives. Positive cells were counted manually from twenty random, non-overlapping 200X fields of view (Corresponding to a field area of 0.147mm^2) and results presented as the number of positive cells/ mm^2 . The average number of positive cells was expressed as plus or minus the standard error of the mean (SEM).

Measurement of Aorta Intima-Media Thickness (aIMT)

A modified Verhoeff Van Gieson elastic stain (Sigma) was used to differentiate the intima, media, and the adventitia of the aortic wall.²⁵ Tissue sections were rehydrated in

xylenes and graded ethanols and stained following the manufacturer's protocol. Sections of aorta were incubated with a ferric chloride solution to differentiate the layers of the vessel wall. Differentiation was stopped when the internal and external elastic lamina were distinct from background tissue by incubating the sections in water. Aortic intima-media thickness (aIMT) was determined by optical measurement using ImageJ Analysis software and calipers. The aIMT was measured on ten non-overlapping 400x fields of view (corresponding to a field area of 1.15mm²) and expressed as plus or minus the SEM.

Quantification of Cardiac Fibrosis

Cardiac tissue fibrosis was measured as the percentage of collagen per total tissue area²⁶, using a modified Massons Trichrome stain (Newcomer Supply, Middleton, WI) according to the manufacturer's protocol. The percentage of collagen (blue) per total tissue area was determined using ImageJ Analysis Software.²⁶

sCD163 ELISA

Soluble CD163 (sCD163) in plasma was quantified by ELISA according to manufacturer's protocol (Trillium Diagnostics) and as previously described.²⁷ Sample plasma was diluted 1:500.

Statistical Analysis

Statistical analyses were performed using Prism version 5.0 (Graphpad Software Inc., San Diego, CA). Comparisons were made between HIV- and HIV+ groups using a non-parametric Mann-Whitney t-test with significance accepted at p<0.05. A non-parametric Spearman rank test was used to determine if there were correlations between the numbers of macrophages and levels of fibrosis in cardiac tissue and aIMT

Table 4.1. Increased number of macrophages in the aorta and cardiac tissues with HIV infection

Immune Marker	Aorta				Left Ventricle			
	HIV- (n=16)	HIV+ (n=16)	<i>p</i> value	Fold Change	HIV- (n=16)	HIV+ (n=16)	<i>p</i> value	Fold Change
CD163	22.04 (±2.75)	44.67 (±3.07)	*	2.02	38.52 (±4.73)	76.18 (±3.15)	**	2.05
CD68	16.48 (±1.59)	25.73 (±2.11)	**	1.57	24.47 (±3.03)	49.53 (±3.51)	**	2.02
CD206	14.27 (±1.62)	22.77 (±1.85)	*	2.21	35.88 (±4.09)	79.27 (±4.13)	**	2.21
MAC387	8.29 (±0.89)	15.32 (±0.99)	*	1.84	11.97 (±1.21)	22.41 (±1.16)	*	1.87

Mean number of positive cells (cells/mm²) ± standard error of the mean (in brackets) in aorta and cardiac tissues from HIV- and HIV+ individuals. Numbers of positive cells were counted from twenty, non-overlapping 200X fields of view for each tissue section with the mean number of positive cells being shown. A non-parametric Mann-Whitney t-test was used to statistically compare the mean number of positive cells in the HIV- and HIV+ individuals (* *p*<0.05, ** *p*<0.01).

Figure 4.1

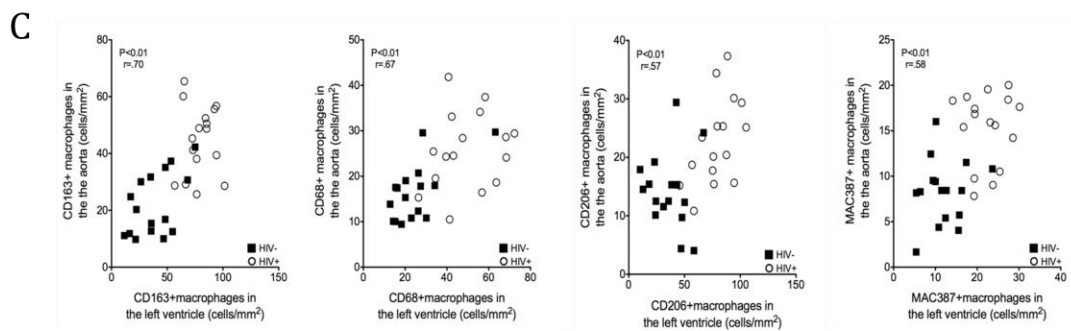
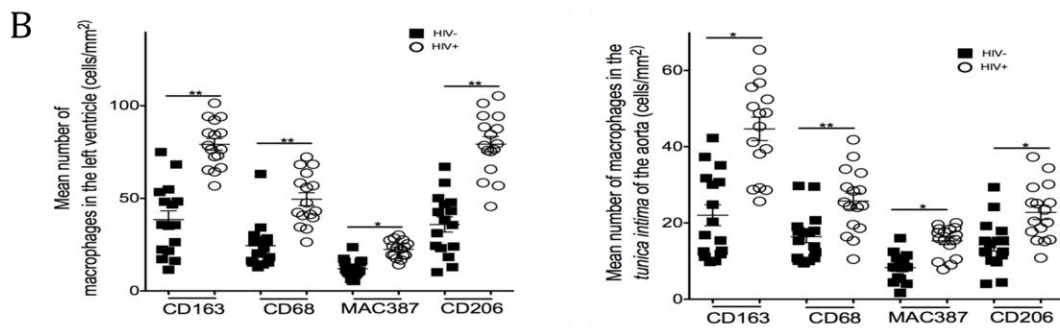
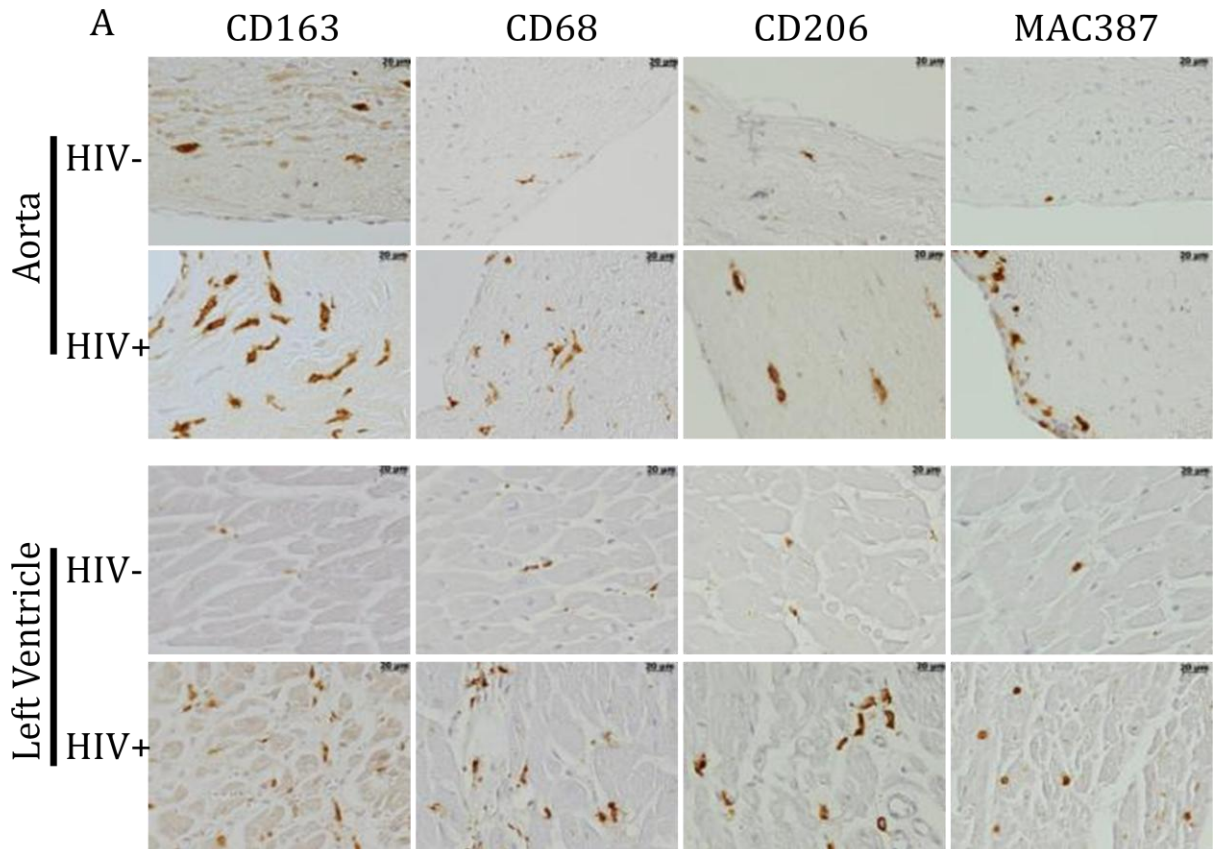


Figure 4.1. HIV infection results in increased macrophage inflammation in aorta and cardiac tissue compared to uninfected individuals.

(A) Sections of aorta and left ventricle (cardiac tissue) from HIV+ and HIV- individuals were immunohistochemically stained with antibodies against CD163+, CD68+, CD206+, and MAC387+ macrophages. (B) HIV infection resulted in significantly increased numbers of CD163+, CD68+, CD206+, and MAC387+ macrophages in the aorta and cardiac tissues compared to uninfected controls. Statistical analysis was done a Mann-Whitney t-test with significance accepted at $p < 0.05$ (* $p < 0.05$, ** $p < 0.01$). Twenty random, non-overlapping 200X fields of view were imaged and positive macrophages were counted for each individual with the mean and standard error of the mean calculated. (C) There is a positive correlation between the numbers of CD163+, CD68+, CD206+, and MAC387+ macrophages in sections aorta and cardiac tissue in HIV- (*closed square*) and HIV+ (*open circle*). (Spearman rank correlation, $r = \text{Spearman coefficient}$, $p < 0.05$). Scale bar= 20 microns, 400X magnification. Vertical bars represent the mean plus or minus the standard error of the mean.

Figure 4.2

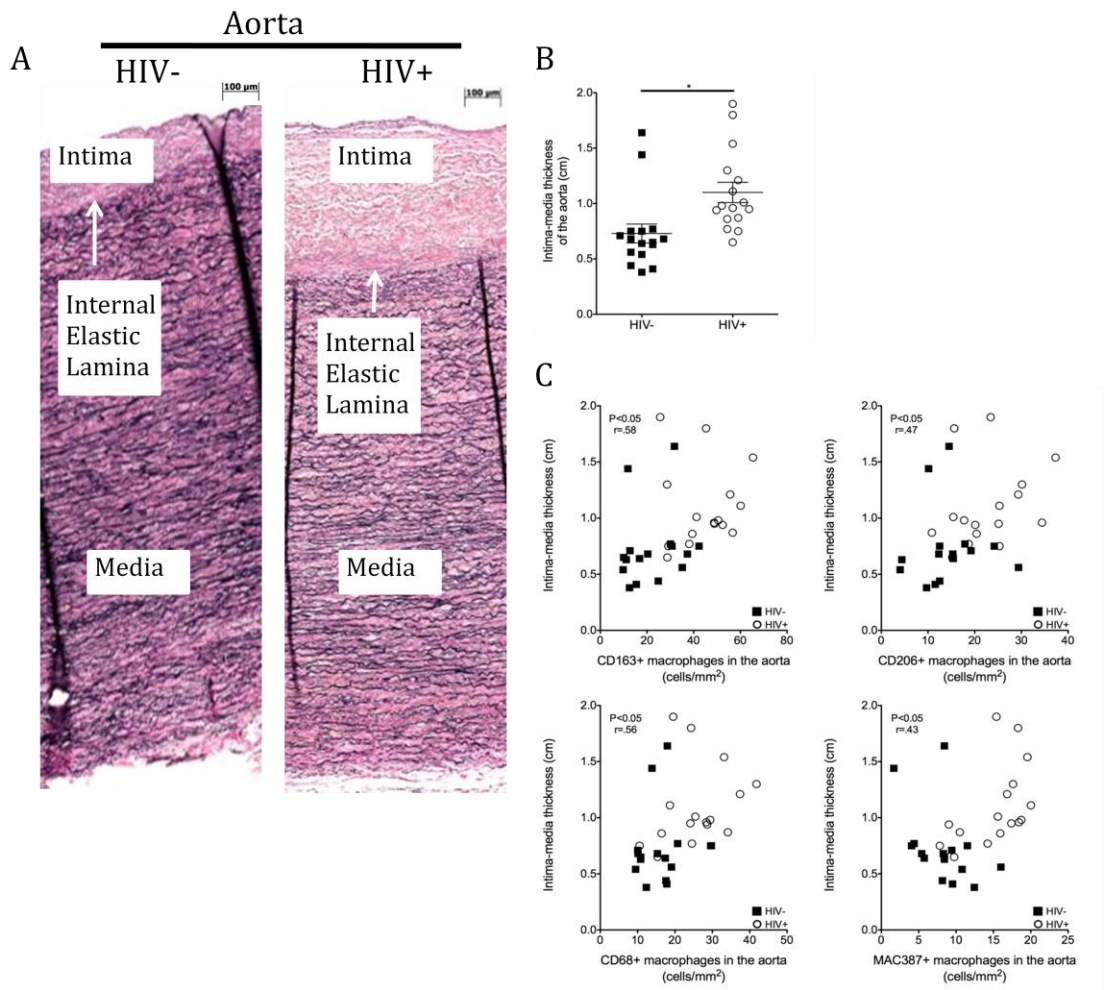


Figure 4.2. HIV infection results in an increased intima-media thickness of the aorta that correlates with increasing numbers of macrophages.

(A) A modified Verhoeff Van Gieson elastic stain kit was used to quantify aortic intima-media thickness (aIMT) in HIV- (*left*) and HIV+ (*right*) individuals. B) There was a significant 1.5-fold increase in aIMT in HIV+ individuals compared to uninfected controls (Mann-Whitney t-test, * $p < 0.05$). Vertical bars represent the mean plus or minus the standard error of the mean. (C) There were positive correlations between the number of CD163+, CD68+, CD206+, and MAC387+ macrophages and increased aIMT with HIV infection. $r =$ Spearman coefficient, $p < 0.05$.

Figure 4.3

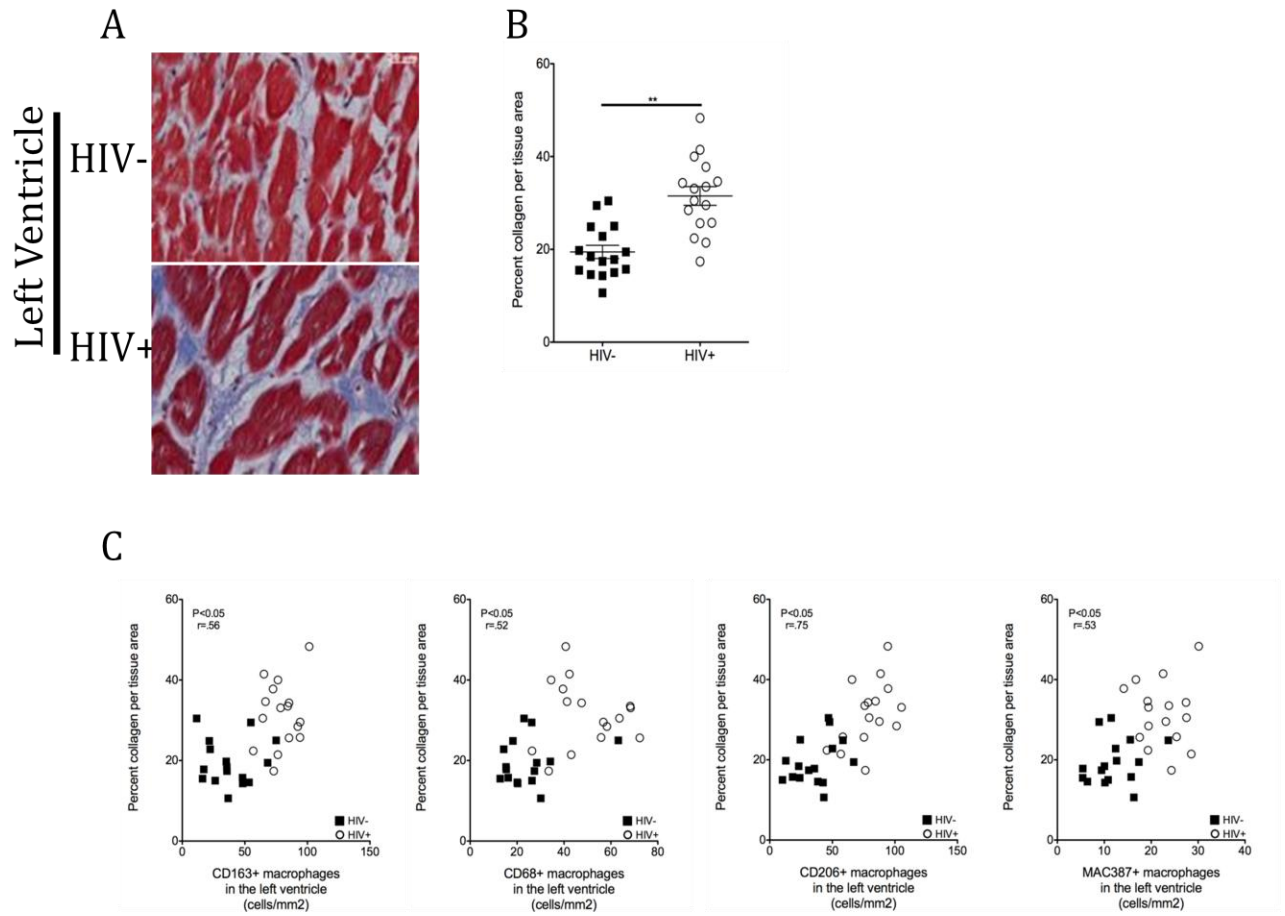
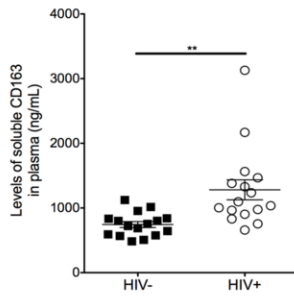


Figure 4.3. HIV infection results in increased cardiac fibrosis that correlates with elevated numbers of macrophages.

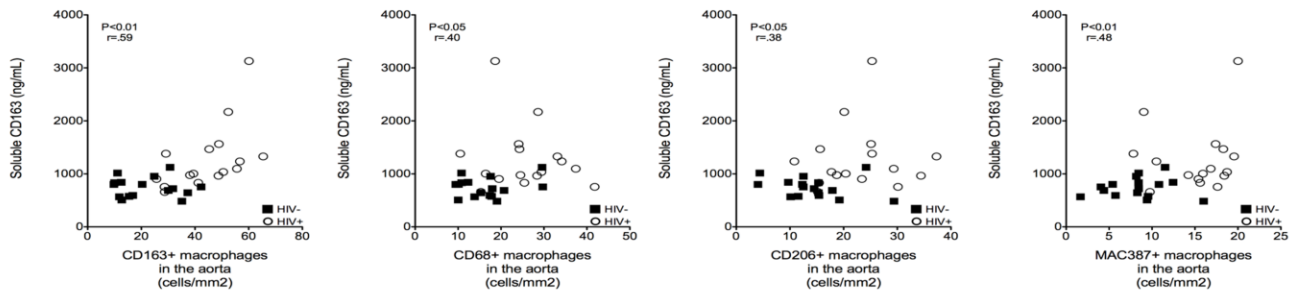
(A) Massons trichrome stain was used to measure the percentage of collagen (fibrosis) in cardiac tissues. (B) There was a significant 1.62-fold increase in the percentage of collagen per total tissue area cardiac tissues from HIV+ individuals compared to HIV- individuals (Mann-Whitney t-test, ** $p < 0.01$). (C) We found positive correlations between increased numbers of CD163+, CD68+, CD206+ and MAC387+ macrophages present and increasing levels of fibrosis in HIV+ individuals (*square*) compared to HIV- individuals (*circle*). $r =$ Spearman coefficient, $p < 0.05$.

Figure 4.4

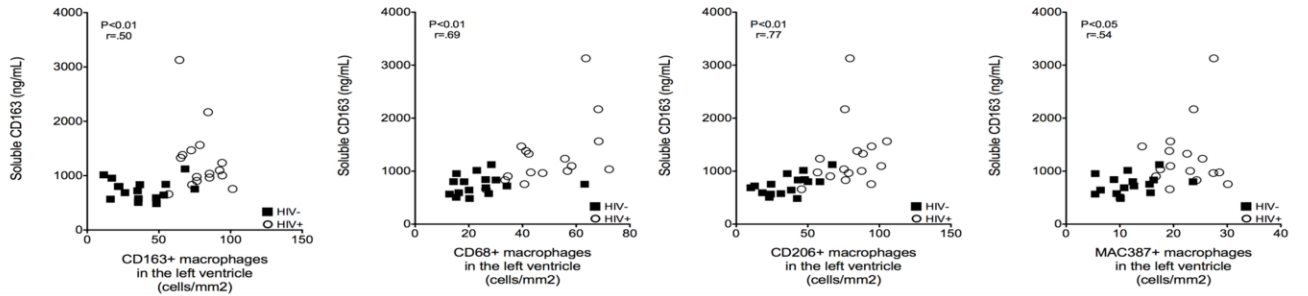
A



B



C



D

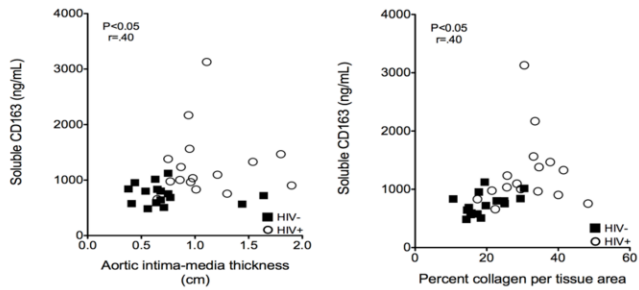


Figure 4.4. Soluble plasma CD163 correlates with increased inflammation, fibrosis, and aIMT in aorta and cardiac tissues.

(A) Soluble CD163 (sCD163) were measured in plasma from HIV- and HIV+ individuals using an ELISA. HIV infection resulted in a significant 1.7-fold increase in sCD163 in plasma in HIV+ individuals compared to seronegative individuals (Mann-Whitney t-test, * $p < 0.05$). Vertical bars represent the mean plus or minus the standard error of the mean. Increased sCD163 positively correlates with macrophage inflammation in the aorta (B) and cardiac tissue (C) with HIV infection. (D) Soluble CD163 positively correlates with increased aIMT (*left*) and increased cardiac fibrosis. ($r =$ Spearman coefficient, $p < 0.05$.)

REFERENCES

1. Lech M, Anders HJ. Macrophages and fibrosis: How resident and infiltrating mononuclear phagocytes orchestrate all phases of tissue injury and repair. *Biochim Biophys Acta*. 2013;1832(7):989-997.
2. Patanè S, Marte F, Sturiale M, Dattilo G, Albanese A. Myocarditis and cardiomyopathy HIV associated. *Int J Cardiol*. 2011;146(3):e56-57.
3. Esser S, Gelbrich G, Brockmeyer N, et al. Prevalence of cardiovascular diseases in HIV-infected outpatients: results from a prospective, multicenter cohort study. *Clin Res Cardiol*. 2013;102(3):203-213.
4. Dushkin MI. Macrophage/foam cell is an attribute of inflammation: mechanisms of formation and functional role. *Biochemistry. Biokhimiia*. 2012;77(4):327-338.
5. Fernandez-Velasco M, Gonzalez-Ramos S, Bosca L. Involvement of monocytes/macrophages as key factors in the development and progression of cardiovascular diseases. *Biochem J*. 2014;458(2):187-193.
6. Woollard KJ. Immunological aspects of atherosclerosis. *Clin Sci (Lond)*. 2013;125(5):221-235.
7. Bobryshev YV. Dendritic cells and their role in atherogenesis. *Lab Invest*. 2010;90(7):970-984.
8. Bouhlel MA, Derudas B, Rigamonti E, et al. PPARgamma activation primes human monocytes into alternative M2 macrophages with anti-inflammatory properties. *Cell Metab*. 2007;6(2):137-143.
9. Medbury HJ, James V, Ngo J, et al. Differing association of macrophage subsets with atherosclerotic plaque stability. *Int J Angiol*. 2013;32(1):74-84.

10. Tan C, Liu Y, Li W, et al. Associations of matrix metalloproteinase-9 and monocyte chemoattractant protein-1 concentrations with carotid atherosclerosis, based on measurements of plaque and intima-media thickness. *Atherosclerosis*. 2014;232(1):199-203.
11. Ma Y, Yabluchanskiy A, Hall ME, Lindsey ML. Using plasma matrix metalloproteinase-9 and monocyte chemoattractant protein-1 to predict future cardiovascular events in subjects with carotid atherosclerosis. *Atherosclerosis*. 2014;232(1):231-233.
12. MacNeill BD, Jang IK, Bouma BE, et al. Focal and multi-focal plaque macrophage distributions in patients with acute and stable presentations of coronary artery disease. *J Am Coll Cardiol*. 2004;44(5):972-979.
13. Triant VA, Lee H, Hadigan C, Grinspoon SK. Increased acute myocardial infarction rates and cardiovascular risk factors among patients with human immunodeficiency virus disease. *J Clin Endocrinol Metab*. 2007;92(7):2506-2512.
14. Freiberg MS, Chang CC, Kuller LH, et al. HIV infection and the risk of acute myocardial infarction. *JAMA Intern Med*. 2013;173(8):614-622.
15. Crowe SM, Westhorpe CL, Mukhamedova N, Jaworowski A, Sviridov D, Bukrinsky M. The macrophage: the intersection between HIV infection and atherosclerosis. *J Leukoc Biol*. 2010;87(4):589-598.
16. Anzinger JJ, Butterfield TR, Angelovich TA, Crowe SM, Palmer CS. Monocytes as regulators of inflammation and HIV-related comorbidities during cART. *J Immunol Res*. 2014;2014:569819.
17. van der Wal AC, Becker AE, van der Loos CM, Das PK. Site of Intimal Rupture or Erosion of Thrombosed Coronary Atherosclerotic Plaques Is Characterized by an Inflammatory Process irrespective of the Dominant Plaque Morphology. *Circulation*. 1994;89(1):36-44.

18. Burdo TH, Lo J, Abbara S, et al. Soluble CD163, a novel marker of activated macrophages, is elevated and associated with noncalcified coronary plaque in HIV-infected patients. *J Infect Dis.* 2011;204(8):1227-1236.
19. Subramanian S, Tawakol A, Abbara S, et al. Arterial Inflammation in Patients With HIV. *JAMA.* 2012;308:379-386.
20. Baker JV, Hullsiek KH, Singh A, et al. Immunologic predictors of coronary artery calcium progression in a contemporary HIV cohort. *Aids.* 2014;28(6):831-840.
21. Shikuma CM, Barbour JD, Ndhlovu LC, et al. Plasma Monocyte Chemoattractant Protein-1 and Tumor Necrosis Factor- α Levels Predict the Presence of Coronary Artery Calcium in HIV-Infected Individuals Independent of Traditional Cardiovascular Risk Factors. *AIDS Res Hum Retroviruses.* 2014;30(2):142-146.
22. Longenecker CT, Jiang Y, Orringer CE, et al. Soluble CD14 is independently associated with coronary calcification and extent of subclinical vascular disease in treated HIV infection. *Aids.* 2014;28(7):969-977.
23. Tawakol A, Lo J, Zanni MV, et al. Increased Arterial Inflammation Relates to High-risk Coronary Plaque Morphology in HIV-Infected Patients. *J Acquir Immune Defic Syndr.* 2014;66(2):164-171.
24. Walker JA, Sulciner ML, Nowicki KD, Miller AD, Burdo TH, Williams KC. Elevated numbers of CD163+ macrophages in hearts of simian immunodeficiency virus-infected monkeys correlate with cardiac pathology and fibrosis. *AIDS Res Hum Retroviruses.* 2014;30(7):685-694.
25. Deopukari R, Dixit A. The study of age related changes in coronary arteries and its relevance to the atherosclerosis. *J Anat Soc India.* 2010;59(2):192-196.

26. Brower GL, Gardner JD, Forman MF, et al. The relationship between myocardial extracellular matrix remodeling and ventricular function. *Eur J Cardiothorac Surg.* 2006;30(4):604-610.
27. Burdo TH, Soulas C, Orzechowski K, et al. Increased monocyte turnover from bone marrow correlates with severity of SIV encephalitis and CD163 levels in plasma. *PLoS Pathog.* 2010;6(4):e1000842.
28. Lichtfuss GF, Cheng WJ, Farsakoglu Y, et al. Virologically suppressed HIV patients show activation of NK cells and persistent innate immune activation. *J Immunol.* 2012;189(3):1491-1499.
29. Dornadula G, Zhang H, VanUitert B, et al. Residual HIV-1 RNA in Blood Plasma of Patients Taking Suppressive Highly Active Antiretroviral Therapy. *JAMA.* 1999;282(17):1627-1632.
30. Neuhaus J, Angus B, Kowalska JD, et al. Risk of all-cause mortality associated with nonfatal AIDS and serious non-AIDS events among adults infected with HIV. *Aids.* 2010;24(5):697-706.
31. Rodriguez-Penney AT, Iudicello JE, Riggs PK, et al. Co-morbidities in persons infected with HIV: increased burden with older age and negative effects on health-related quality of life. *AIDS Patient Care STDS.* 2013;27(1):5-16.
32. Lo J, Abbara S, Shturman L, et al. Increased prevalence of subclinical coronary atherosclerosis detected by coronary computed tomography angiography in HIV-infected men. *Aids.* 2010;24(2):243-253.
33. Baker JV, Henry WK, Patel P, et al. Progression of carotid intima-media thickness in a contemporary human immunodeficiency virus cohort. *Clin Infect Dis.* 2011;53(8):826-835.

34. Post WS, Budoff M, Kingsley L, et al. Associations Between HIV Infection and Subclinical Coronary Atherosclerosis. *Ann Intern Med.* 2014;160(7):458-467.
35. Khunnawat C, Mukerji S, Havlichek D, Jr., Touma R, Abela GS. Cardiovascular manifestations in human immunodeficiency virus-infected patients. *Am J Cardiol.* 2008;102(5):635-642.
36. Holloway CJ, Ntusi N, Suttie J, et al. Comprehensive cardiac magnetic resonance imaging and spectroscopy reveal a high burden of myocardial disease in HIV patients. *Circulation.* 2013;128(8):814-822.
37. Cheruvu S, Holloway CJ. Cardiovascular disease in human immunodeficiency virus. *Intern Med J.* 2014;44(4):315-324.
38. Frustaci A, Petrosillo N, Vizza D, et al. Myocardial and microvascular inflammation/infection in patients with HIV-associated pulmonary artery hypertension. *Aids.* 2014;28(17):2541-2549.
39. Tahara N, Mukherjee J, de Haas HJ, et al. 2-deoxy-2-[F]fluoro-d-mannose positron emission tomography imaging in atherosclerosis. *Nat Med.* 2014;20(2):215-219.
40. Moore JP, Vinh A, Tuck KL, et al. M2 macrophage accumulation in the aortic wall during angiotensin II infusion in mice is associated with fibrosis, elastin loss, and elevated blood pressure. *American journal of physiology. Heart and circulatory physiology.* 2015;309(5):H906-917.
41. McKibben RA, Margolick JB, Grinspoon S, et al. Elevated Levels of Monocyte Activation Markers Are Associated With Subclinical Atherosclerosis in Men With and Those Without HIV Infection. *J Infect Dis.* 2015;211(8):1219-1228.

42. Calza L, Trapani F, Bartoletti M, et al. Statin therapy decreases serum levels of high-sensitivity C-reactive protein and tumor necrosis factor-alpha in HIV-infected patients treated with ritonavir-boosted protease inhibitors. *HIV Clin Trials*. 2012;13(3):153-161.
43. Lo J, Lu MT, Ihenachor EJ, et al. Effects of statin therapy on coronary artery plaque volume and high-risk plaque morphology in HIV-infected patients with subclinical atherosclerosis: a randomised, double-blind, placebo-controlled trial. *Lancet HIV*. 2015;2(2):e52–e63.

ACKNOWLEDGEMENTS and FUNDINGS

We would like to thank the NNTC and the NDRI for the procurement of samples from HIV- and HIV+ individuals used in this study. This work was supported by NIH R01 NS040237 (KCW) and MSINAD 5 R25 MH080663-07.

**CHAPTER 5. An Anti- α 4 Antibody Blocks Monocyte/Macrophage Traffic to the Heart and
Decreases Cardiac Pathology in a SIV Infection Model of AIDSⁱⁱ**

Joshua A. Walker, Graham A. Beck,

Jennifer H. Campbell, Andrew D. Miller,

Tricia H. Burdo, Kenneth C. Williams

ABSTRACT

Cardiovascular disease (CVD), myocarditis and fibrosis are co-morbidities of HIV+ individuals on durable anti-retroviral therapy (ART). Although mechanisms for these vary, monocytes/macrophages are increasingly demonstrated to be key players. We directly blocked monocyte/macrophage traffic to the heart in an SIV model of AIDS using an anti-alpha-4 integrin antibody (natalizumab). Nineteen Rhesus macaques were with SIVmac251 infected and CD8-lymphocyte depleted for rapid AIDS. Ten animals received natalizumab once a week, for three weeks, and were sacrificed one week later. Six animals began treatment at the time of infection (early) and the remaining four began treatment 28 days post infection (late), a time point we have previously established when significant cardiac inflammation occurs. Nine animals were untreated controls, of these three were sacrificed early and six were sacrificed late. At necropsy we found decreased SIV-associated cardiac pathology in late natalizumab treated animals compared to untreated controls. Early and late treatment resulted in significant reductions in numbers of CD163+ and CD68+ macrophages in cardiac tissues compared to untreated controls, and a trend in decreasing numbers of newly recruited MAC387+ and BrdU+ (recruited) monocytes/macrophages. In late treated animals, decreased macrophage numbers in cardiac tissues correlated with decreased fibrosis. Early and late treatment resulted in decreased cardiomyocyte damage. These data demonstrate the role of macrophages in the development of cardiac inflammation and fibrosis and suggest blocking monocyte/macrophage traffic to the heart can alleviate HIV and SIV-associated myocarditis and fibrosis. They underscore the importance of targeting macrophage activation and traffic as an adjunctive therapy in HIV infection.

INTRODUCTION

Combination anti-retroviral therapy (cART) has increased the life expectancy of HIV+ individuals but co-morbidities including neurological,¹ renal,² bone,³ and cardiovascular disease⁴⁻⁹ exist.¹⁰⁻¹² HIV-associated cardiovascular disease is a leading cause of HIV-associated mortality where there is a two-fold increase in the relative risk compared to non infected, age matched individuals.¹³ HIV-associated cardiovascular disease, that includes atherosclerosis, dilated cardiomyopathy, myocarditis, and myocardial infarction^{7,14,15}, likely has multiple etiologies including toxic effects of cART,¹⁶ opportunistic infections,¹⁷ and chronic immune activation¹⁸ but monocyte/macrophages are emerging as central players.

Dilated cardiomyopathy and myocarditis with HIV infection was evident in 40-50% of AIDS patients at necropsy in the pre-cART era.¹⁹ With effective cART in developed countries the incidence has decreased approximately 30% suggesting that dilated cardiomyopathy and myocarditis with HIV and cART has declined.^{7,19,20} Despite this, magnetic resonance imaging (MRI) and spectroscopy (MRS) show that HIV+ individuals continue to have subclinical myocardial disease with myocardial fibrosis and alterations in cardiac function.^{21,22} Recent data comparing the rates of mortality in the pre- and post-cART era support these findings, where HIV+ individuals had a 6.3-fold increase in mortality due to cardiomyopathy and myocarditis in the post-cART era. Additionally, a recent study examining myocardial and microvascular inflammation showed that myocarditis is still present with HIV infection.²³ This suggests that HIV infection with effective cART can still lead to increased cardiac fibrosis and myocarditis.

SIV-infected rhesus macaques are an excellent model to study the effects of SIV on cardiac inflammation and fibrosis. Previous work established that SIV-infected monkeys have dilated cardiomyopathy and myocarditis.^{24,25} Overall few SIV- or HIV- RNA or protein positive cells are found in cardiac tissues similar to what is found in HIV infected human cardiac

tissues.^{26,27} Despite this, levels of SIV-RNA correlate with diastolic dysfunction underscoring the role of lentiviral infection and cardiac dysfunction with AIDS.²⁷ We have previously demonstrated that SIV-infected, CD8-lymphocyte depleted animals develop rapid and consistent AIDS with macrophage accumulation in the heart, cardiomyocyte damage, and fibrosis²⁸ and accumulation of CD163+ macrophages correlated with increased fibrosis.^{28,29} In these studies, BrdU labeled monocyte/macrophages, that were labeled in the bone marrow and traffic to the heart, were increased late in infection. Overall, these observations support the hypothesis that macrophage activation and accumulation with SIV and HIV infection play a critical role in the development of cardiac pathology. To date, no studies have directly blocked monocyte/macrophage traffic to the heart in experimental infection with SIV.

While no studies have directly blocked monocyte/macrophage traffic to the heart with SIV or HIV infection, data from experimental and clinical studies that diminished macrophage activation or accumulation in the heart, support the notion that these cells are major players in cardiac pathogenesis. Thus, studies that blocked chemokine receptor-5 (CCR5) using CCL5-RANTES resulted in decreased monocyte/macrophage and T-lymphocyte accumulation^{30,31} likely by indirect mechanisms. Similarly, blocking CCR5 with the anti-CCR5 antibody maraviroc resulted in reduced cardiac CD163 expression by macrophages and prevented diastolic dysfunction in SIV-infected monkeys.³² Similarly, studies blocking macrophage inhibitory factor (MIP) showed decreased T-cell and macrophage migration and inhibition of the onset of myocarditis in a rodent model of experimental autoimmune myocarditis.³³ Treatment with the statin pravastatin decreased macrophage numbers in abdominal aortic plaques of uninfected monkeys.³⁴ Another statin, atorvastatin that did not reduce aortic inflammation in HIV+ infected individuals, did decrease the volume and high-risk features of noncalcified plaques.³⁵ In humans with coronary artery disease, angiotensin receptor blocker (ARB) treatment resulted in

decreased numbers of atherosclerotic lesions and significantly decreasing levels of soluble markers of inflammation C-reactive protein, Interleukin-6 (IL-6), and monocyte chemoattractant protein-1 (MCP-1).^{36, 37}

In this study we examined whether directly blocking leukocyte and monocyte/macrophage traffic to cardiac tissues with the anti- α 4 integrin antibody, natalizumab, decreased SIV-associated cardiac pathology (inflammation, fibrosis, and cardiomyocyte damage). Natalizumab is an anti- α 4 antibody that binds to the α 4 subunit of α 4 β 1 and α 4 β 7 integrins and blocks the interactions between α 4 and its ligands.³⁸ Natalizumab has been used effectively to treat Multiple Sclerosis³⁹ and Crohn's disease,⁴⁰ blocking accumulation of lymphocytes and monocytes/macrophages in the brain and gut, but not lymph nodes. In rodents, blocking α 4 integrins reduced macrophage homing to atherosclerotic plaques.⁴¹ We have shown that natalizumab treatment in SIV-infected rhesus macaques with AIDS blocked monocyte/macrophage traffic to the central nervous system (CNS) and leukocytes to the gut resulting in decreased numbers of SIV-RNA and SIV-p28 positive cells.⁴² Further, natalizumab treatment of monkeys at the time of SIV infection resulted in undetectable SIV- RNA, -DNA and -p28+ cells in the CNS and gut in the majority of animals, and the absence of leukocyte inflammation. In the current study, we examined if natalizumab treatment decreased monocyte/macrophage accumulation in the heart and whether such treatment decreased cardiac fibrosis and myocyte damage.

RESULTS

Natalizumab treatment decreases the frequency and severity of pathology in SIV-infected, CD8-lymphocyte depleted rhesus macaque cardiac tissues

The relative degree of pathology in cardiac tissues was assessed based on the levels of inflammation, fibrosis, and cardiomyocyte degeneration. Normal sections were scored as having no significant findings (NSF). When present, inflammation, fibrosis, and cardiomyocyte degeneration were scored as mild, moderate, or severe. We found no significant changes in the pathology of cardiac tissues in early natalizumab treated animals compared to untreated controls. Of three SIV-infected untreated animals sacrificed early, 21 dpi (n=3), two had no significant findings with regards to inflammation or fibrosis. The remaining SIV-infected untreated controls, sacrificed at 21 dpi, had mild inflammation and mild fibrosis. In the early natalizumab treated group (n=6), sacrificed at 21 dpi, 4 animals had no significant findings in regards to inflammation and fibrosis and two animals had mild inflammation and fibrosis (Table 5.1).

Overall, natalizumab treatment decreased cardiac pathology in late treated animals (n=4), compared to late untreated controls (n=6) (Table 1). Three of 4 late treated animals had no significant findings with respect to cardiomyocyte degeneration, and 2 of 4 had no significant findings with regard to fibrosis. SIV-infected, untreated late control animals with cardiac pathology (n=3), had an increased severity compared to late treated SIV-infected animals (Table 5.1). Two of the late controls with pathology had moderate inflammation and one had mild inflammation. All three late controls with pathology had moderate fibrosis while two had mild and one had moderate cardiomyocyte degeneration. Compared to the late controls with pathology, the severity of pathology in SIV-infected, late natalizumab treated animals (n=4) was diminished (Table 5.1). Three late treated animals had mild inflammation while the remaining

had moderate inflammation. Two late treated animals had no inflammation and two had only mild inflammation. Three late treated animals had no significant findings with regard to cardiomyocyte degeneration and one had mild cardiomyocyte degeneration (Table 5.1).

Natalizumab treatment decreases the number of macrophages present in cardiac tissue in early and late treated animals.

In animals that began natalizumab treatment early at 0 dpi, there was a significant decrease in the number of CD163+ and CD68+ macrophages in heart tissues compared to untreated controls sacrificed at the same time point (Fig. 5.1). There was a significant 3.35-fold and 3.74-fold decrease in the numbers of CD163+ and CD68+ macrophages, respectively, in cardiac tissue in early natalizumab treated animals compared to controls (Fig. 5.1B, Table 2, non-parametric Mann-Whitney t-test, * p<0.05). While not significant, there were decreased numbers of newly infiltrating macrophages MAC387+ macrophages and CD3 T-lymphocytes in early treated animals (Fig. 5.1B, Table 2).

Natalizumab treatment beginning on 28 dpi (late) resulted in a significant decrease in the numbers of CD163+ and CD68+ macrophages when compared to all SIV-infected untreated late control animals (Fig. 5.1). We found a 3.53-fold and a 1.19-fold decrease in the numbers of CD163+ and CD68+ macrophages respectively in cardiac tissues of late natalizumab treated tissues compared to controls (Table 5.2, non-parametric Mann-Whitney t -test, *p<0.05, ** p<0.01). We next examined if the numbers of macrophages in late natalizumab treated animals differed between late untreated control animals with and without cardiac pathology.

Late treated animals had decreased numbers of CD163+ macrophages compared to untreated late controls without cardiac pathology (Fig. 5.1A). There was a 2.51-fold decrease in the number of CD163+ macrophages in cardiac tissue in late treated animals compared to

controls without cardiac pathology (Fig. 5.1B, Table 3, non-parametric Mann-Whitney t-test, * $p < 0.05$). There were no differences in numbers of CD68+, MAC387+ macrophages and CD3 T-lymphocytes in cardiac tissues of late natalizumab treated animals and untreated controls without pathology (Table 5.3).

Significant reductions in the number of CD163+ and CD68+ macrophages were found in late treated animals compared to late untreated controls with cardiac pathology (Fig. 5.1A). There was a 4.53-fold and 1.59-fold decrease in the numbers of CD163+ and CD68+ macrophages present in cardiac tissues compared to late natalizumab treated animals (Fig 5.1C, Table 5.3, non-parametric Mann-Whitney t-test, * $p < 0.05$, ** $p < 0.01$). Similar to early treated animals, late treated animals had a trend of decreased numbers of newly infiltrating macrophages expressing MAC387 and CD3 T-lymphocytes compared to late untreated animals with cardiac pathology (Table 5.3).

Natalizumab treatment blocks traffic of macrophages to the cardiac tissues

BrdU experiments were used to further determine if natalizumab treatment blocks traffic of monocyte/macrophages to the heart. Previously, we have shown that the majority of BrdU+ macrophages in the heart are MAC387+ macrophages.²⁸ In early natalizumab treated animals there were few BrdU+ cells (4.38 ± 0.64 cells/mm²) and a trend of decreasing numbers of BrdU+ cells compared to untreated controls (9.31 ± 1.57 cells/mm²) (Fig. 5.1A, 5.1B, Table 5.2). Animals that began natalizumab treatment at 28 dpi, had decreased number of BrdU+ cells (16.42 ± 3.19 cells/mm²) compared to untreated animals with cardiac pathology (22.51 ± 5.23 cells/mm²) (Fig. 5.1A, 5.1C, Table 5.3). The number of BrdU+ cells in late natalizumab treated animals did not differ when compared to untreated animals without cardiac pathology (Fig. 5.1A, 5.1C, Table 5.3).

Decreased fibrosis in cardiac tissues of natalizumab treated animals correlates with significant decreases in macrophage numbers.

Using a modified Masson's trichrome stain, the percent collagen per total tissue area in cardiac tissues of natalizumab treated animals and untreated controls was quantified (Fig. 5.2A, 5.2B). Compared to controls, both early and late natalizumab treated animals had decreased amounts of collagen (Fig. 5.2C). In early natalizumab treated animals, the average percent collagen per total tissue area was $5.58 \pm 2.56\%$ compared to $9.6 \pm 2.06\%$ for untreated controls, a significant 1.72-fold decrease in the percent collagen (Fig. 5.2C, left, * $p < 0.05$, non-parametric Mann-Whitney t-test).

Animals that began natalizumab treatment at 28 dpi (late) had a significantly higher average percentage of collagen per tissue area in the left ventricle ($8.66 \pm 2.31\%$) compared to animals that began treatment early (5.58 ± 1.47) (Fig. 5.2C, right, * $p < 0.05$, non-parametric Mann-Whitney t-test). Late natalizumab treated animals had no significant differences in the percent of collagen per total tissue area compared to untreated animals without cardiac pathology ($8.66 \pm 2.31\%$ vs. $10.33 \pm 1.84\%$). However, when compared to untreated animals with cardiac pathology, there was a significant decrease in the percentage of collagen per tissue area. While late natalizumab treated animals had an average percentage of collagen of $8.66 \pm 2.31\%$, untreated animals with cardiac pathology had an average of $19.91 \pm 1.85\%$, a significant 2.29-fold decrease in the average percent collagen per total tissue area (Fig. 5.2C, right, * $p < 0.05$, non-parametric Mann-Whitney t-test).

We next examined if there was a correlation between decreased fibrosis in natalizumab treated animals and changes in macrophage numbers in cardiac tissues if significant differences in macrophage numbers were found between groups. There was a correlation between increased fibrosis and increased numbers of CD163+ ($r = .9$, $p < 0.05$) and CD68+ ($r = .86$, $p < 0.05$)

macrophages in untreated controls sacrificed at 21 dpi compared to early natalizumab treated animals (Fig. 5.2D). A correlation also existed in late natalizumab treated animals compared to all late untreated controls for CD163+ ($r=.85$, $p<0.05$), CD68+ ($r=.55$, $p<0.05$) macrophages and fibrosis (Fig. 5.2E.)

DISCUSSION

Chronic inflammation persists within HIV infected individuals despite effective cART and decreased plasma viral load to undetectable levels.⁴⁶⁻⁴⁸ With chronic inflammation, there are increased co-morbidities compared to the general non HIV-infected population.⁴⁹⁻⁵¹ In particular there is an increased incidence of CVD⁴ where monocytes/macrophages are increasingly considered to play a role.^{52, 53} Previously, we have shown that SIV-infected, CD8-lymphocyte depleted monkeys have increased numbers of macrophages (CD163+, CD68+, and MAC387+) in cardiac tissues that positively correlate increased fibrosis.²⁸ In this study we examined if an anti- α 4 antibody, natalizumab, diminishes leukocyte and monocyte/macrophage traffic to the heart resulting in decreased fibrosis.

Natalizumab blocks the interaction between α 4 integrin and its ligand, vascular cell adhesion molecule-1 (VCAM-1).³⁸ VCAM-1 is expressed on endothelial cells of the arterial lumen with atherosclerosis.⁵⁴ Studies in mice showed that inhibiting the interaction between α 4 and VCAM-1 decreased macrophage recruitment to atherosclerotic plaques.⁴¹ Previously we have shown that there is a higher level of macrophages traffic to the heart later in SIV infection (>21 dpi) and that there are few macrophages present in untreated animals sacrificed at 21 dpi.²⁸ In the current study we found that natalizumab treatment beginning at 0 dpi resulted in decreased numbers of CD163+ and CD68+ macrophages compared to uninfected controls but cardiac pathology in early infection is minimal and most of the pathology occurred in the later stages of infection.

When compared to untreated controls with cardiac pathology, late treated animals had significant decreases in the number of CD163+ and CD68+ macrophages. In fact, the numbers of macrophages in late natalizumab treated animals were similar to untreated animals without cardiac pathology. Additionally, we found a correlation between decreased macrophage

numbers in natalizumab treated animals with decreased cardiac fibrosis. Overall, these data show that blocking monocyte/macrophage traffic to the heart alleviates HIV and SIV-associated cardiac pathology resulted in reduced inflammation, fibrosis, and cardiomyocyte degeneration.

While not significant, we found a trend of decreasing numbers of MAC387+ macrophages in the left ventricle of late treated animals compared to untreated animals with cardiac pathology. The finding of a decrease in newly recruited macrophages is supported our observation of fewer BrdU labeled macrophages (that traffic from the bone marrow); suggesting that macrophage traffic to the heart results in increased fibrosis. While previous research showed natalizumab decreased traffic of CD3 T-lymphocytes and MAC387+ to the brain and gut,⁴² in the current study, we do not find significant differences in the number of CD3 T-lymphocytes or MAC387+ macrophages in cardiac tissues of SIV infected animals with or without natalizumab treatment. This possibly suggests that CD3+ T-lymphocytes and MAC387+ macrophages use different integrins to traffic to the heart than to the brain or gut, however we have previously shown that MAC387+ macrophages and not CD3+ T-lymphocytes correlate with increased fibrosis in cardiac tissues.²⁸ Our lack of finding a statistically significant reduction in the number MAC387+ macrophages may be due to the relatively few numbers of those cells in cardiac tissues.

Previously, we have shown that the rate of monocyte/macrophage traffic to the heart is increased later in infection (after 48 dpi) as opposed to early infection.²⁸ Using BrdU labeling we found a trend of decreased traffic of monocytes/macrophages to the heart in late natalizumab treated animals compared to untreated animals that developed cardiac pathology. Late natalizumab treated animals had a similar rate of traffic of newly released monocytes/macrophages from bone marrow to the heart as untreated animals without cardiac

pathology. This provides evidence that potentially blocking traffic of monocyte/macrophages later during SIV infection can alleviate SIV-associated cardiac pathology.

While cART can decrease HIV to non-detectable levels in plasma, it does not necessarily target monocyte/macrophages that play a role in the development of cardiac pathology and cardiovascular disease.³² Chronic immune activation with HIV infected is posited to play a role in HIV-associated cardiovascular pathology. Previous studies show that HIV infected individuals have increased inflammation in the ascending aorta that correlates with levels of sCD163 in plasma.⁵⁵ Increased inflammation in the aorta is also been linked to high-risk noncalcified plaques that are prone to rupture.⁸ FDG-PET imaging studies have demonstrated that such plaque areas are comprised of areas with accumulation of macrophages.^{8, 56, 57} While macrophage accumulation in the aorta and cardiac plaques are critical in HIV associated cardiac disease, it is not surprising that also there is increased macrophage inflammation in cardiac tissues at the same time. Unpublished data from our laboratory (Chapter 4), using matched cardiac tissues (left ventricle) and aorta from HIV- and HIV+ individuals, shows that with HIV infection there is increased macrophage inflammation in ventricular tissues and the aorta. Moreover, increased macrophage inflammation in cardiac tissues correlates with increased fibrosis, macrophage accumulation in the aorta, and increased aortic intima-media thickness. To date, there are few therapies that target macrophages specifically or indirectly to diminish HIV-associated cardiovascular pathology. Emergent data underscores the importance of such therapy strategies.

Therapeutic agents that have been successful in the treatment noncalcified cardiac plaque in HIV+ individuals include 3-hydroxy-3-methylglutaryl-coenzyme A reductase inhibitors (statins), which fortuitously have anti-inflammatory effects on macrophages.^{58, 59} Statin therapy in conjunction with cART reduced serum levels of inflammatory markers including interleukin-6,

interleukin-8 and tumor necrosis factor- α , more so than cART alone.⁶⁰ Statins have similarly been used in monkeys where they decreased the macrophage content in plaques in the abdominal aorta.³⁴ A recent study in HIV infected individuals showed that statins significantly decreased the volume on noncalcified plaques but whether statin use in this study directly affected monocyte and/or macrophage activation and traffic was not studied.³⁵ In rodent models of experimental autoimmune myocarditis (EAM) rosuvastatin reduced numbers of macrophages, T-lymphocytes and multinucleated giant cells in the heart resulted in decreased numbers of apoptotic cardiomyocytes. The effects of statins on myocarditis with HIV infection have not been examined.⁶¹

Other studies found maraviroc treatment decreased chemotaxis of monocyte/macrophages, *in vitro*,⁶² but in clinical studies with advanced HIV, it did not affect the development of immune reconstitution inflammatory syndrome (IRIS),⁶³ Maraviroc is used primarily to inhibit viral replication of R5-tropic HIV by blocking interactions between the virus and CCR5 on host cells.^{64, 65} Studies using maraviroc in SIV-infected monkeys demonstrated fewer CD163+ macrophages in the heart, but this could have been due to a decreased CD163 expression (activation) on macrophages already present in the heart and not a decrease in inflammatory cells. All together, these experiments add further evidence to the role that monocyte/macrophages play in cardiac pathology with HIV and SIV infection, and suggest that therapies blocking monocyte/macrophage traffic to the heart could diminish HIV-associated cardiac pathology.

In this study we showed that directly blocking monocyte/macrophage traffic to cardiac tissues with natalizumab successfully decreased the numbers of macrophages present in tissues. Studies examining if blocking traffic to vessels result in decreased in high risk vascular plaques with HIV infection are warranted. Our data suggest that studies examining the efficacy of

blocking monocyte/macrophage traffic, or directly targeting monocyte/macrophage activation as an adjunctive therapy with cART, should be examined with an aim to decrease HIV-associated cardiac pathology.

MATERIALS AND METHODS

Ethical treatment of animals

The treatment of animals in this study was in accordance with the Guide for the Care and Use of Laboratory Animals, 8th edition. Animals were housed at The New England Regional Primate Center (NERPC) (Southborough, MA), Tulane National Primate Research Center (TNPRC) (Covington, LA), or BIOQUAL (Baltimore, MD). The NEPRC Protocol Number for this study is 04420 and the Animal Welfare Assurance Number is A3431-01. The TNPRC Number for this study is 3497 and the Animal Welfare Assurance Number is A4499-01. Animals were monitored daily for evidence of disease progression and changes in appetite or behavior, with clinical support administered under the direction of an attending veterinarian.

Animals, SIV Infection, CD8 lymphocyte depletion

Nineteen rhesus macaques (*Macaca mulatta*) were infected with SIV mac251 (2ng of SIV-p27) intravenously (kindly provided by Ronald Desrosiers, University of Miami) (Table 1). All animals were CD8-lymphocyte depleted using cM-T807, a human anti-CD8 antibody, administered subcutaneously (10mg/kg) on day 6 post infection (pi) and intravenously (5 mg/kg) on days 8 and 12 pi, as previously described¹. Ten animals (n=4 late natalizumab treated, n=6 untreated) were sacrificed at similar time points with progression to AIDS (49 to 65 dpi). All CD8 –lymphocyte depleted animals had high viral load at peak viremia that remained elevated and was not different between early and late treated animals and controls. Six early natalizumab treated animals were sacrificed at 21 dpi and three untreated controls sacrificed at 22 dpi. Sections of left ventricular myocardium (hereafter referred to as cardiac tissue) were analyzed by a board certified veterinary pathologist (ADM), and scored based on the degree of inflammation, fibrosis, and cardiomyocyte degeneration. Sections were scored as either no

significant findings (NSF), mild, moderate, or severe, based on the degree of change in cardiac tissues as previously described.²⁸

Anti- α 4 integrin (natalizumab) and BrdU administration

The anti- α 4 integrin mAB (natalizumab) was provided by Biogen Idec (Cambridge, MA) in a sterile concentrated solution. Natalizumab has specificity for the α 4 subunit of α 4 β 1 and α 4 β 7 integrins expressed on surfaces of all leukocytes, except neutrophils.⁴³ Natalizumab was administered weekly for three weeks beginning on the day of infection (0 dpi, n=6) or on 28 dpi (n=4), as previously described.⁴² This treatment regimen maintains high levels of natalizumab in serum of rhesus macaques during treatment⁴⁴. To study monocyte/macrophage traffic to the heart animals were administered BrdU (30mg/kg) at indicated time points (Table 5.1) as previously described.⁴²

Immunohistochemistry

The numbers of macrophages and T-lymphocytes present in formalin-fixed, paraffin-embedded tissues were determined by immunohistochemistry and cell counting. Cardiac tissues were stained with antibodies against CD163 (1:250, Serotec), CD68 (1:200, Dako), MAC387 (1:100, Dako) macrophages and CD3+ T-lymphocytes (1:300, Dako). The number of macrophages that traffic to cardiac tissues was determined using a mouse monoclonal BrdU antibody (1:50), as previously described.²⁸ Twenty random, non-overlapping 200X microscopic fields of view were taken for each animal and the number of positive cells/mm² calculated for each. The data are represented as the average number of positive cells/mm² from the twenty random fields.

Masson's Trichrome Stain

The percent of collagen per tissue area used as a marker of fibrosis,²⁹ was measured using a modified Massons Trichrome Stain kit (Newcomer Supply, Middleton, WI) according to the manufacturer's recommendation. Tissue sections were imaged using a Zeiss Axio Imager M1 microscope using Plan-Apochromat x20/0.8 Korr objectives, as previously described.^{28, 45} The area of red and blue dyes corresponding to cytoplasm and collagen, respectively, were measured to determine the percentage of total tissue area.

Statistical Analysis

Statistical analyses were conducted using Prism version 6.0 (GraphPad Software, Inc.). P values were calculated using the non-parametric Mann-Whitney t-test with significance accepted at $p < 0.05$ when comparing early and late natalizumab treated animals to early and late untreated controls. Analysis of variance (ANOVA) was used to compare late natalizumab treated animals to late untreated animals with and without cardiac pathology. If the ANOVA was significant ($p < 0.05$), then a post-hoc non-parametric Mann-Whitney t-test were performed. To determine if changes in numbers of macrophages in the cardiac tissues correlates with changes in fibrosis, a non-parametric Spearman rank correlation was used where $p < 0.05$ was significant.

Table 5.1. Cardiac Pathology of Natalizumab Treated and Control Animals Used in this Study

Animal Groups	ID	Primate Center	Start of natalizumab (dpi)	BrdU Admin. (dpi)	Survival (dpi)	Cardiac Pathology		
						Inflammation	Fibrosis	Cardiomyocyte degeneration
Early untreated n=3	A1	TNPRC	-	6,20	22	NSF	NSF	NSF
	A2	TNPRC	-	6,20	22	NSF	NSF	NSF
	A3	TNRPC	-	22	22	Mild	Mild	NSF
Early natalizumab n=6	A4	NERPC	0	6,20	21	NSF	NSF	NSF
	A5	NERPC	0	6,20	21	NSF	NSF	NSF
	A6	BIOQUAL	0	6,20	21	NSF	NSF	NSF
	A7	BIOQUAL	0	6,20	21	NSF	NSF	NSF
	A8	BIOQUAL	0	6,20	21	Mild	Mild	Mild
	A9	BIOQUAL	0	6,20	21	Mild	Mild	NSF
Late untreated without cardiac pathology n=3	A10	NERPC	-	49	56	NSF	NSF	NSF
	A11	NERPC	-	pre, 7, 20, 41, 54	56	NSF	NSF	NSF
	A12	NERPC	-	pre, 7, 20, 41, 54	55	Mild	Mild	NSF
Late untreated with cardiac Pathology n=3	A13	TNPRC	-	pre, 7, 26, 55	56	Moderate	Moderate	Mild
	A14	TNPRC	-	pre, 7, 26, 55	65	Moderate	Moderate	Mild
	A15	NERPC	-	6, 20	60	Severe	Moderate	Moderate
Late natalizumab n=4	A16	NERPC	28	pre, 26, 47	49	Mild	NSF	NSF
	A17	NERPC	28	pre, 26, 47	49	Mild	NSF	NSF
	A18	NERPC	28	33, 47	49	Mild	Mild	NSF
	A19	NERPC	28	33, 47	49	Moderate	Mild	Mild

Nineteen animals were used in this study, housed at either The New England Regional Primate Center (NERPC), Tulane National Primate Research Center (TNPRC), or BIOQUAL, as indicated. Six animals began natalizumab treatment at the time of infection at 0 days post infection (dpi) and were sacrificed at 21 dpi. Three early untreated controls were sacrificed at 22 dpi. Four late natalizumab treated animals began treatment at 28 dpi and were sacrificed at 49 dpi. Three animals each for late untreated controls without cardiac pathology and with cardiac pathology were sacrificed at 56-65 dpi. Pathology was assessed based on the degree of inflammation, fibrosis, and cardiomyocyte degeneration. To investigate if blocking monocyte/macrophage traffic to the heart decreased SIV-associated cardiac pathology, 10 randomly chosen, 200X fields of view were chosen and analyzed blindly by a veterinary pathologist. Sections of cardiac tissue were scored based on the degree of change as having no significant findings (NSF), mild, moderate, or severe inflammation, fibrosis, and cardiomyocyte degeneration.

Table 5.2. Numbers of Macrophages and T-lymphocytes in Natalizumab Treated and Control Animals

Immune Markers	Early				Late			
	Untreated (n=3)	NZ (n=6)	<i>P</i> value	Fold Change	Untreated (n=6)	NZ (n=4)	<i>p</i> value	Fold Change
CD163	158.84 (±55.78)	47.36 (±18.77)	*	3.35	282.45 (±36.97)	80.06 (±10.95)	**	3.53
CD68	84.34 (±16.67)	22.54 (±5.09)	*	3.74	63.01 (±4.71)	52.87 (±10.83)	*	1.19
MAC387	9.33 (±1.17)	7.43 (±3.19)	ns	-	18.25 (±2.11)	15.91 (±7.46)	ns	-
CD3	8.05 (±2.13)	5.13 (±3.02)	ns	-	15.55 (±3.60)	12.27 (±5.42)	ns	-
BrdU	9.31 (±1.57)	4.39 (±0.64)	ns	-	21.19 (±5.85)	16.42 (±3.19)	ns	-

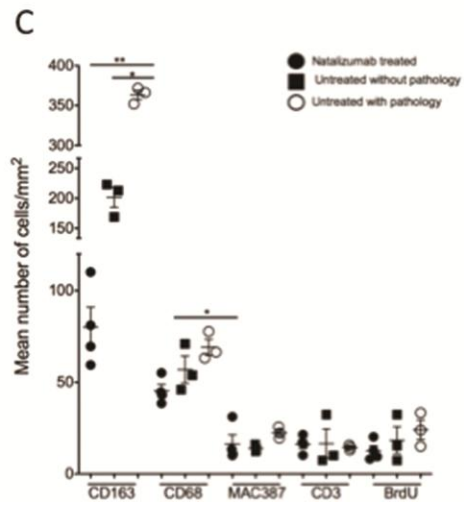
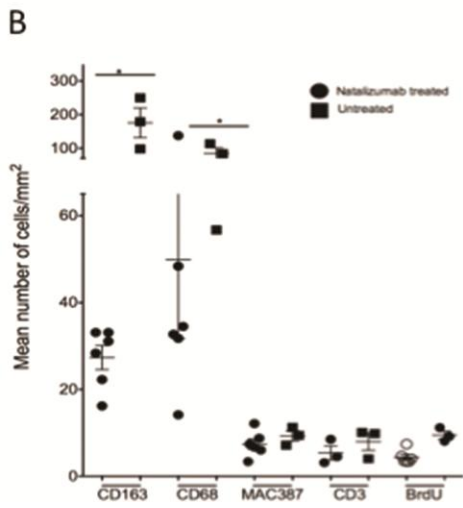
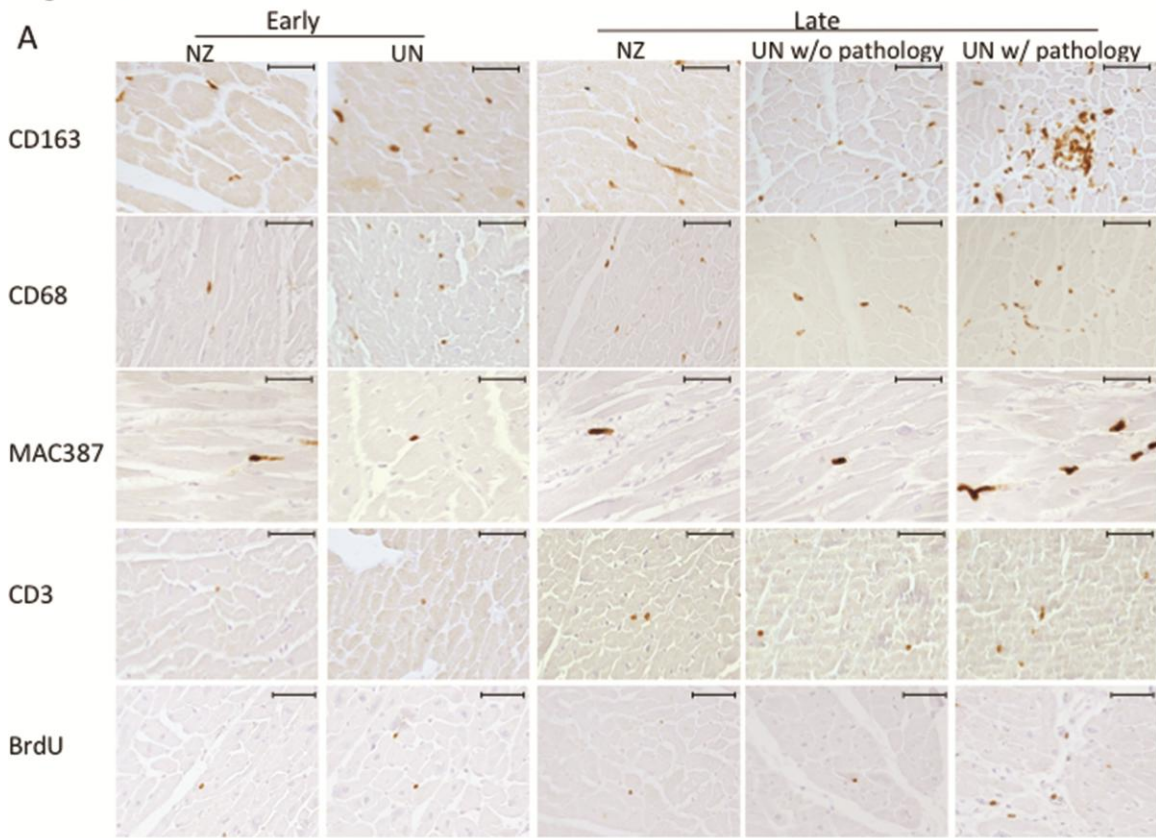
Numbers represent the mean number of positive cells (cells/mm²) ± the standard error of the mean, in bracket. All animals were SIV-infected and CD8-lymphocyte depleted, with 10 of the animals receiving natalizumab. Twenty random, non-overlapping, 200X fields of view were counted for each animal and the average number of positive cells/mm² calculated. *P* values were calculated by comparing the mean number of positive cells for the indicated groups using the non-parametric Mann-Whitney t-test (* *p*<0.05, ** *p*<0.01). The fold change was calculated for the numbers of cells where there was a significant difference between the indicated groups. Early natalizumab treated animals began treatment at the time of infection, 0 days post infection (dpi). Late natalizumab treated animals began treatment 28 dpi. All treated animals were treated weekly for three weeks with a dose of 30 mg/kg of α-VLA-4. NZ=Natalizumab treated. Ns=No significance

Table 5.3 Numbers of macrophages and T-lymphocytes in late natalizumab treated animals and controls without and with cardiac pathology

	Late		NZ n=4	<i>p</i> value NZ vs. w/o	<i>p</i> value NZ vs. w/	Fold Change NZ vs. w/o	Fold Change NZ vs. w/
	Untreated w/o pathology n=3	Untreated w/ pathology n=3					
Immune Markers							
CD163	195.33 (±16.37)	363.23 (±15.87)	80.06 (±10.95)	*	**	2.51	4.53
CD68	56.96 (±7.37)	84.13 (±4.38)	52.87 (±10.83)	ns	*	-	1.59
MAC387	14.01 (±1.09)	22.51 (±1.77)	15.91 (±7.46)	ns	ns	-	-
CD3	13.17 (±3.76)	16.63 (±7.92)	12.27 (±5.42)	ns	ns	-	-
BrdU	19.86 (±10.08)	22.51 (±5.23)	16.17 (±3.19)	ns	ns	-	-

Numbers represent the mean number of positive cells (cells/mm²) ± the standard error of the mean, in bracket. All animals were SIV-infected and CD8-lymphocyte depleted. Twenty random, non-overlapping, 200X fields of view were counted for each animal and the average number of positive cells/mm² calculated. Analysis of variance (ANOVA) was used to compare late natalizumab treated animals to late untreated animals with and without cardiac pathology. If the ANOVA was significant (p<0.05), then a post-hoc Mann-Whitney t-tests were performed. NZ= natalizumab treated, w/o= untreated without cardiac pathology, w/ = untreated with cardiac pathology. *p<0.05, **p<0.01. Ns=no significance.

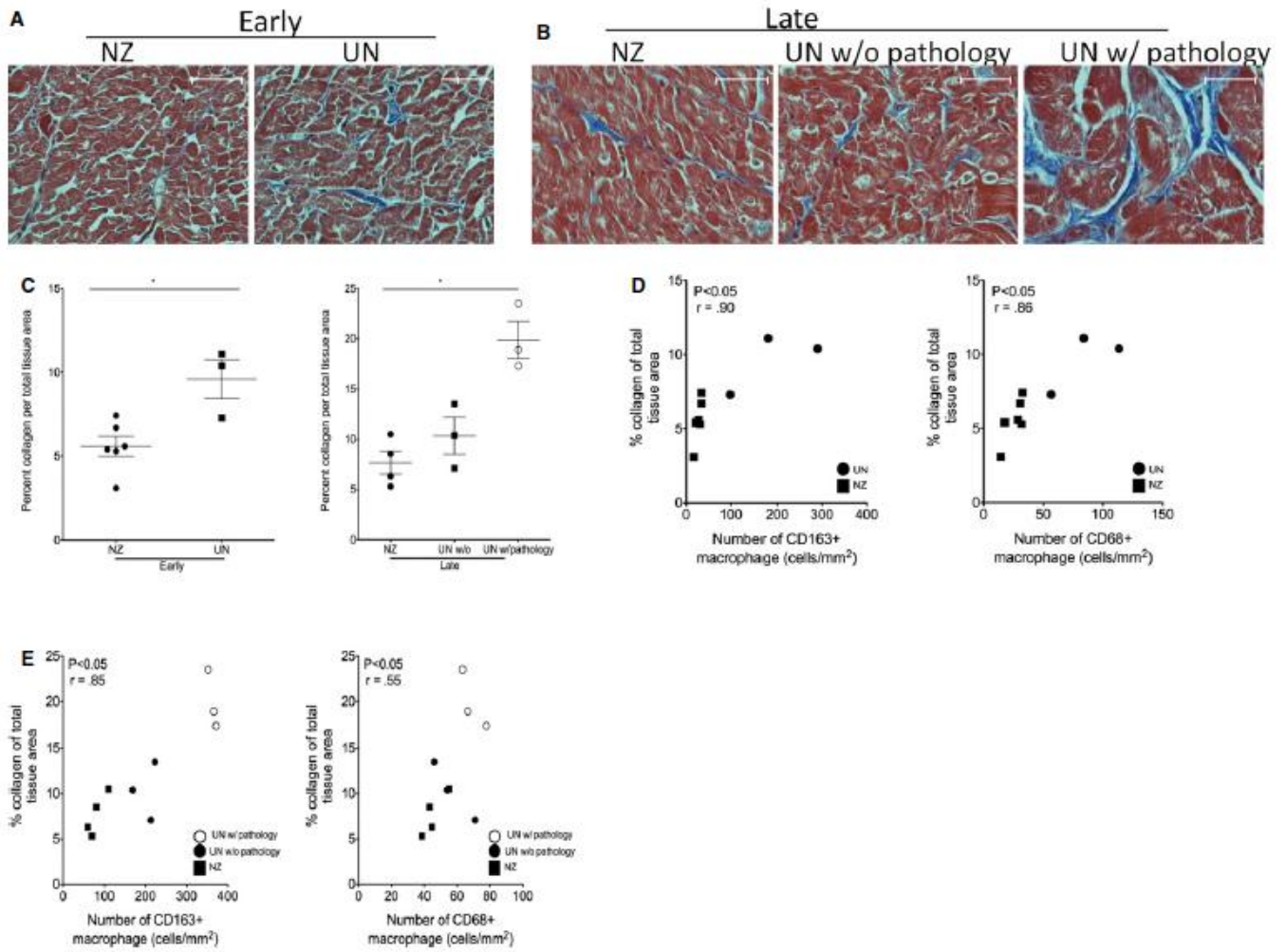
Figure 1



*from Walker et al. *JAMA*, 2015.

Figure 5.1. Natalizumab treatment decreases the number of macrophages in cardiac tissues in SIV-infected, CD8-lymphocyte depleted rhesus macaques.

(A) Sections of left ventricular tissues from early and late natalizumab treated animals and matched controls were immunohistochemically stained with antibodies recognizing CD163+, CD68+, and MAC387+ macrophages and CD3+ T-lymphocytes. (B, C) Twenty random, non-overlapping 200X fields of view were taken for each animal and the average number of cells/mm² calculated. In both early and late natalizumab treated animals there is a decrease in the numbers of CD163+ and CD68+ macrophages when compared to controls, with no differences in T-lymphocytes detected. Statistical analysis between early natalizumab treated animals and controls was done using a non-parametric Mann-Whitney t-test. For late natalizumab treated animals and untreated controls with and without cardiac pathology an ANOVA was performed first, and if significant, a post-hoc non-parametric Mann-Whitney t-test was performed (*, p<0.05, **, p<0.01). Scale bar= 50 microns, 400X magnification. Error bars represent the average number of positive cells/mm² ± the standard error of the mean (SEM). NZ, Natalizumab treated. UN, untreated. Early, treatment began at 0 dpi. Late, treatment began at 21 dpi.



*from Walker et al. *JAHA*, 2015.

Figure 5.2. Natalizumab treatment decreases fibrosis in the left ventricle of SIV-infected, CD8-lymphocyte depleted rhesus macaques.

(A, B) Modified Masson's trichrome stain was used to compare the percent collagen per total tissue area, a marker of fibrosis, in the left ventricle of early and late natalizumab treated animals compared to untreated controls. (C) Natalizumab treatment resulted in decreased fibrosis in cardiac tissues compared to controls regardless of when treatment began. In animals that began natalizumab treatment at 0 dpi there was a significant decrease in the amount of collagen per tissue area ($5.58 \pm 2.56\%$) compared to untreated controls ($9.6 \pm 2.06\%$, non-parametric Mann-Whitney t-test, $p < 0.05$). Animals that began natalizumab treated at 28 dpi also showed a significant decrease in the amount of collagen per total tissue area ($8.66 \pm 2.31\%$) when compared to untreated controls with cardiac pathology ($19.91 \pm 1.85\%$). There was no difference in the percent collagen per total tissue area in animals late natalizumab treated animals compared to untreated controls without cardiac pathology. Spearman rank test was used to determine if there was a correlation between decreased fibrosis in natalizumab treated animals and decreased numbers of macrophages. (D) In early natalizumab treated animals (*closed square*) there is a correlation between the decrease in numbers of CD163+ and CD68+ macrophages and decreases in fibrosis when compared to untreated controls (*closed circle*). (E) In late natalizumab treated animals (*closed square*), there is a correlation between decreases in CD163+ and CD68+ macrophages compared to untreated controls with (*open circle*) and untreated controls without pathology (*closed circle*). $r =$ spearman coefficient, $p < 0.05$. Statistical analysis between early natalizumab treated animals and controls was done using a non-parametric Mann-Whitney t-test. For late natalizumab treated animals and untreated controls with and without cardiac pathology an ANOVA was performed first, and if significant, a post-hoc non-parametric Mann-Whitney t-test was performed (*, $p < 0.05$). Scale bar= 50

microns, 400X magnification. Error bars represent the average number of positive cells/mm² ± the standard error of the mean (SEM).

REFERENCES

1. Williams K, Westmoreland S, Greco J, Ratai E, Lentz M, Kim WK, Fuller RA, Kim JP, Autissier P, Sehgal PK, Schinazi RF, Bischofberger N, Piatak M, Lifson JD, Masliah E, Gonzalez RG. Magnetic resonance spectroscopy reveals that activated monocytes contribute to neuronal injury in hiv neuroaids. *J Clin Invest*. 2005;115:2534-2545.
2. Mocroft A, Kirk O, Gatell J, Reiss P, Gargalianos P, Zilmer K, Beniowski M, Viard JP, Staszewski S, Lundgren JD. Chronic renal failure among hiv-1-infected patients. *Aids*. 2007;21:1119-1127.
3. Cazanave C, Dupon M, Lavignolle-Aurillac V, Barthe N, Lawson-Ayayi S, Mehnen N, Mercie P, Morlat P, Thiebaut R, Dabis F, Groupe d'Epidemiologie Clinique du SeA. Reduced bone mineral density in hiv-infected patients: Prevalence and associated factors. *Aids*. 2008;22:395-402.
4. Ho JE, Hsue PY. Cardiovascular manifestations of hiv infection. *Heart*. 2009;95:1193-1202.
5. Zaaqq AM, Khasawneh FA, Smalligan RD. Cardiovascular complications of hiv-associated immune dysfunction. *Cardio Res Pract*. 2015;2015:1-8.
6. Freiberg MS, Chang CC, Kuller LH, Skanderson M, Lowy E, Kraemer KL, Butt AA, Bidwell Goetz M, Leaf D, Oursler KA, Rimland D, Rodriguez Barradas M, Brown S, Gibert C, McGinnis K, Crothers K, Sico J, Crane H, Warner A, Gottlieb S, Gottdiener J, Tracy RP, Budoff M, Watson C, Armah KA, Doebler D, Bryant K, Justice AC. Hiv infection and the risk of acute myocardial infarction. *JAMA Intern Med*. 2013;173:614-622.
7. Esser S, Gelbrich G, Brockmeyer N, Goehler A, Schadendorf D, Erbel R, Neumann T, Reinsch N. Prevalence of cardiovascular diseases in hiv-infected outpatients: Results from a prospective, multicenter cohort study. *Clin Res Cardiol*. 2013;102:203-213.

8. Tawakol A, Lo J, Zanni MV, Marmarelis E, Ihenachor EJ, MacNabb M, Wai B, Hoffmann U, Abbara S, Grinspoon S. Increased arterial inflammation relates to high-risk coronary plaque morphology in hiv-infected patients. *J Acquir Immune Defic Syndr*. 2014;66:164-171.
9. Zanni MV, Schouten J, Grinspoon SK, Reiss P. Risk of coronary heart disease in patients with hiv infection. *Nat Rev Cardiol*. 2014;11:728-741.
10. Ray M, Logan R, Sterne JA, Hernandez-Diaz S, Robins JM, Sabin C, Bansi L, van Sighem A, de Wolf F, Costagliola D, Lanoy E, Bucher HC, von Wyl V, Esteve A, Casbona J, del Amo J, Moreno S, Justice A, Goulet J, Lodi S, Phillips A, Seng R, Meyer L, Perez-Hoyos S, Garcia de Olalla P, Hernan MA. The effect of combined antiretroviral therapy on the overall mortality of hiv-infected individuals. *Aids*. 2010;24:123-137.
11. Coquet I, Pavie J, Palmer P, Barbier F, Legriel S, Mayaux J, Molina JM, Schlemmer B, Azoulay E. Survival trends in critically ill hiv-infected patients in the highly active antiretroviral therapy era. *Crit Care*. 2010;14:R107.
12. Guaraldi G, Orlando G, Zona S, Menozzi M, Carli F, Garlassi E, Berti A, Rossi E, Roverato A, Palella F. Premature age-related comorbidities among hiv-infected persons compared with the general population. *Clin Infect Dis*. 2011;53:1120-1126.
13. Hemkens LG, Bucher HC. Hiv infection and cardiovascular disease. *Eur Heart J*. 2014;35:1373-1381.
14. Barbaro G, Fisher SD, Lipshultz SE. Pathogenesis of hiv-associated cardiovascular complications. *Lancet Infect Dis*. 2001;1:115-124.
15. Patanè S, Marte F, Sturiale M, Dattilo G, Albanese A. Myocarditis and cardiomyopathy hiv associated. *Int J Cardiol*. 2011;146:e56-57.

16. Friis-Møller N, Reiss P, Sabin CA, Weber R, d'Arminio Monforte A, El-Sadr W, Thiébaud R, De Wit S, Kirk O, Fontas E, Law MG, Phillips A, Lundgren JD. Class of antiretroviral drugs and the risk of myocardial infarction. *N Engl J Med*. 2007;356:1723-1735.
17. Liu R, Moroi M, Yamamoto M, Kubota T, Ono T, Funatsu A, Komatsu H, Tsuji T, Hara H, Nakamura M, Hirai H, Yamaguchi T. Presence and severity of chlamydia and pneumoniae and cytomegalovirus infection in coronary plaques are associated with acute coronary syndromes. *Int Heart J*. 2006;47:511-519.
18. Stein JH, Hsue PY. Inflammation, immune activation, and cvd risk in individuals with hiv infection. *JAMA*. 2012;308:405-406.
19. Khunnawat C, Mukerji S, Havlichek D, Jr., Touma R, Abela GS. Cardiovascular manifestations in human immunodeficiency virus-infected patients. *Am J Cardiol*. 2008;102:635-642.
20. Silwa K, Carrington MJ, Becker A, Thienemann F, Ntsekhe M, Stewart S. Contribution of the human immunodeficiency virus acquired immunodeficiency syndrome epidemic to de novo presentations of heart disease in the heart of soweto study cohort. *Eur Heart J*. 2012;33:866-874.
21. Holloway CJ, Ntusi N, Suttie J, Mahmood M, Wainwright E, Clutton G, Hancock G, Beak P, Tajar A, Piechnik SK, Schneider JE, Angus B, Clarke K, Dorrell L, Neubauer S. Comprehensive cardiac magnetic resonance imaging and spectroscopy reveal a high burden of myocardial disease in hiv patients. *Circulation*. 2013;128:814-822.
22. Cheruvu S, Holloway CJ. Cardiovascular disease in human immunodeficiency virus. *Int Med J*. 2014;44:315-324.

23. Frustaci A, Petrosillo N, Vizza D, Francone M, Badagliacca R, Verardo R, Fedele F, Ippolito G, Chimenti C. Myocardial and microvascular inflammation/infection in patients with hiv-associated pulmonary artery hypertension. *Aids*. 2014;28:2541-2549.
24. Shannon RP. Siv cardiomyopathy in non-human primates. *Trends Cardiovasc Med*. 2011;11:242-246.
25. Shannon RP, Simon MA, Mathier MA, Geng YJ, Mankad S, Lackner AA. Dilated cardiomyopathy associated with simian aids in nonhuman primates. *Circulation*. 2000;101:185-193.
26. Yearley JH, Pearson C, Carville A, Shannon RP, Mansfield K. Phenotypic variation in myocardial macrophage populations suggests a role for macrophage activation in siv-associated cardiac disease. *AIDS Res Hum Retroviruses*. 2007;23:512-524.
27. Kelly KM, Tarwater PM, Karper JM, Bedja D, Queen SE, Tunin RS, Adams RJ, Kass DA, Mankowski JL. Diastolic dysfunction is associated with myocardial viral load in simian immunodeficiency virus-infected macaques. *Aids*. 2012;26:815-823.
28. Walker JA, Sulciner ML, Nowicki KD, Miller AD, Burdo TH, Williams KC. Elevated numbers of cd163+ macrophages in hearts of simian immunodeficiency virus-infected monkeys correlate with cardiac pathology and fibrosis. *AIDS Res Hum Retroviruses*. 2014;30:685-694.
29. Brower GL, Gardner JD, Forman MF, Murray DB, Voloshenyuk T, Levick SP, Janicki JS. The relationship between myocardial extracellular matrix remodeling and ventricular function. *Eur J Cardiothorac Surg*. 2006;30:604-610.
30. Schall TJ, Bacon K, Toy KJ, Goeddel DV. Selective attraction of monocytes and t lymphocytes of the memory phenotype by cytokine rantes. *Nature*. 1990;347:669-671.

31. Montecucco F, Braunersreuther V, Lenglet S, Delattre BM, Pelli G, Buatois V, Guilhot F, Galan K, Vuilleumier N, Ferlin W, Fischer N, Vallee JP, Kosco-Vilbois M, Mach F. Cc chemokine ccl5 plays a central role impacting infarct size and post-infarction heart failure in mice. *Eur Heart J*. 2012;33:1964-1974.
32. Kelly KM, Tocchetti CG, Lyashkov A, Tarwater PM, Bedja D, Graham DR, Beck SE, Metcalf Pate KA, Queen SE, Adams RJ, Paolocci N, Mankowski JL. Ccr5 inhibition prevents cardiac dysfunction in the siv/macaque model of hiv. *J Am Heart Assoc*. 2014;3:e000874.
33. Matsui Y, Okamoto H, Jia N, Akino M, Uede T, Kitabatake A, Nishihira J. Blockade of macrophage migration inhibitory factor ameliorates experimental autoimmune myocarditis. *J Mol Cell Cardiol*. 2004;37:557-566.
34. Sukhova GK. Statins reduce inflammation in atheroma of nonhuman primates independent of effects on serum cholesterol. *Arterioscler Thromb Vasc Biol*. 2002;22:1452-1458.
35. Lo J, Lu MT, Ihenachor EJ, Wei J, Looby SE, Fitch KV, Oh J, Zimmerman CO, Hwang J, Abbara S, Plutzky J, Robbins G, Tawakol A, Hoffmann U, Grinspoon SK. Effects of statin therapy on coronary artery plaque volume and high-risk plaque morphology in hiv-infected patients with subclinical atherosclerosis: A randomised, double-blind, placebo-controlled trial. *The Lancet HIV*. 2015;2:e52–e63.
36. Fliser D, Buchholz K, Haller H. Antiinflammatory effects of angiotensin ii subtype 1 receptor blockade in hypertensive patients with microinflammation. *Circulation*. 2004;110:1103-1107.
37. Navalkar S, Parthasarathy S, Santanam N, Khan BV. Irbesartan, an angiotensin type 1 receptor inhibitor, regulates markers of inflammation in patients with premature atherosclerosis. *J Am Coll Cardiol*. 2001;37:440-444.

38. Yu Y, Schurpf T, Springer TA. How natalizumab binds and antagonizes alpha4 integrins. *J Biol Chem*. 2013;288:32314-32325.
39. Polma CH, O'Connor PW, Havrdova E, Hutchinson M, Kappos L, Miller DH, Phillips JT, Lublin FD, Giovannoni G, Wajgt A, Toal M, Lynn F, Panzara MA, Sandrock AW. A randomized, placebo-controlled trial of natalizumab for relapsing multiple sclerosis. *N Engl J Med*. 2006;354:899-910.
40. Kane SV, Horst S, Sandborn WJ, Becker B, Neis B, Moscardrew M, Hanson KA, Tremaine WJ, Bruining DH, Faubion WA, Pardi DS, Harmsen WS, Zinsmeister AR, Loftus EV. Natalizumab for moderate to severe crohn's disease in clinical practice: The mayo clinic rochester experience. *Inflamm Bowel Dis*. 2012;18:2203-2208.'
41. Patel SS, Thiagarajan R, Willerson JT, Yeh ETH. Inhibition of α 4 integrin and icam-1 markedly attenuate macrophage homing to atherosclerotic plaques in apoe-deficient mice. *Circulation*. 1998;97:75-81.
42. Campbell JH, Ratai E-M, Autissier P, Nolan DJ, Tse S, Miller AD, González RG, Salemi M, Burdo TH, Williams KC. Anti- α 4 antibody treatment blocks virus traffic to the brain and gut early, and stabilizes cns injury late in infection. *PLoS Pathogs*. 2014;10:e1004533.
43. Stuve O, Marra CM, Jerome KR, Cook L, Cravens PD, Cepok S, Frohman EM, Phillips JT, Arendt G, Hemmer B, Monson NL, Racke MK. Immune surveillance in multiple sclerosis patients treated with natalizumab. *Ann Neurol*. 2006;59:743-747.
44. Sasseville VG, Newmna W, Brodie SJ, Hesterberg P, Pauley D, Ringler DJ. Monocyte adhesion to endothelium in simian immunodeficiency virus-induced aids encephalitis is mediated by vascular cell adhesion molecule-1/ α 4 beta 1 integrin interactions. *Am J Pathol*. 1994;144:27-40.

45. Ruifrok AC, Johnston DA. Quantification of histochemical staining by color deconvolution. *Anal Quant Cytol.* 2001;23:291-299.
46. Lambotte O, Taoufik Y, de Goer MG, Wallon C, Goujard C, Delfraissy JF. Detection of infectious hiv in circulating monocytes from patients on prolonged highly active antiretroviral therapy. *J Acquir Immune Defic Syndr.* 2000;23:114-119.
47. Dornadula G, Zhang H, VanUitert B, Stern J, Livornese Jr. L, Ingerman MJ, Witek J, Kedanis RJ, Natkin J, DeSimone J, Pomerantz RJ. Residual hiv-1 rna in blood plasma of patients taking suppressive highly active antiretroviral therapy. *JAMA.* 1999;282:1627-1632.
48. Lichtfuss GF, Cheng WJ, Farsakoglu Y, Paukovics G, Rajasuriar R, Velayudham P, Kramski M, Hearps AC, Cameron PU, Lewin SR, Crowe SM, Jaworowski A. Virologically suppressed hiv patients show activation of nk cells and persistent innate immune activation. *J Immunol.* 2012;189:1491-1499.
49. Neuhaus J, Angus B, Kowalska JD, La Rosa A, Sampson J, Wentworth D, Mocroft A, Insight S, groups Es. Risk of all-cause mortality associated with nonfatal aids and serious non-aids events among adults infected with hiv. *Aids.* 2010;24:697-706.
50. Rodriguez-Penney AT, Iudicello JE, Riggs PK, Doyle K, Ellis RJ, Letendre SL, Grant I, Woods SP, Group HIVNRPH. Co-morbidities in persons infected with hiv: Increased burden with older age and negative effects on health-related quality of life. *AIDS Patient Care STDs.* 2013;27:5-16.
51. Anzinger JJ, Butterfield TR, Angelovich TA, Crowe SM, Palmer CS. Monocytes as regulators of inflammation and hiv-related comorbidities during cart. *J Immunol Res.* 2014;2014:569819.

52. Medbury HJ, James V, Ngo J, Hitos K, Wang Y, Harris D, Fletcher JP. Differing association of macrophage subsets with atherosclerotic plaque stability. *Int Angiol.* 2013;32:74-84.
53. Pamukcu B, Lip GYH, devitt A, Griffiths H, Shantsila E. The role of monocytes in atherosclerotic coronary artery disease. *Ann Med.* 2010;42:394-403.
54. OBrien KD, Allen MD, McDonald TO, Chait A, Harlan JM, Fishbein D, McCarty J, Ferguson M, Hudkins K, Benjamin CD, Lobb R, Alpers CE. Vascular cell adhesion molecule-1 is expressed in human coronary atherosclerotic plaques. Implications for the mode of progression of advanced coronary atherosclerosis. *J Clin Invest.* 1993;92:945-951.
55. Subramanian S, Tawakol A, Abbara S, Wei J, Vijayakumar J, Corsini E, Abdelbaky A, Zanni MV, Hoffman U, Williams KC, Lo J, Grinspoon SK. Arterial inflammation in patients with hiv. *JAMA.* 2012;308:379-386.
56. Abdelbaky A, Corsini E, Figueroa AL, Subramanian S, Fontanez S, Emami H, Hoffmann U, Narula J, Tawakol A. Early aortic valve inflammation precedes calcification: A longitudinal fdg-pet/ct study. *Atherosclerosis.* 2015;238:165-172.
57. Tahara N, Mukherjee J, de Haas HJ, Petrov AD, Tawakol A, Haider N, Tahara A, Constantinescu CC, Zhou J, Boersma HH, Imaizumi T, Nakano M, Finn A, Fayad Z, Virmani R, Fuster V, Bosca L, Narula J. 2-deoxy-2-[f]fluoro-d-mannose positron emission tomography imaging in atherosclerosis. *Nat Med.* 2014;20:215-219.
58. Giguere JF, Tremblay MJ. Statin compounds reduce human immunodeficiency virus type 1 replication by preventing the interaction between virion-associated host intercellular adhesion molecule 1 and its natural cell surface ligand Ifa-1. *J Virol.* 2004;78:12062-12065.
59. Calza L, Trapani F, Bartoletti M, Manfredi R, Colangeli V, Borderi M, Grossi G, Motta R, Viale P. Statin therapy decreases serum levels of high-sensitivity c-reactive protein and

- tumor necrosis factor-alpha in hiv-infected patients treated with ritonavir-boosted protease inhibitors. *HIV Clin Trials*. 2012;13:153-161.
60. Calza L, Vanino E, Salvadori C, Manfredi R, Colangeli V, Cascavilla A, Di Bari MA, Motta R, Viale P. Tenofovir/emtricitabine/efavirenz plus rosuvastatin decrease serum levels of inflammatory markers more than antiretroviral drugs alone in antiretroviral therapy-naive hiv-infected patients. *HIV Clin Trials*. 2014;15:1-13.
61. Liu X, Li B, Wang W, Zhang C, Zhang M, Zhang Y, Xia Y, Dong Z, Guo Y, An F. Effects of hmg-coa reductase inhibitor on experimental autoimmune myocarditis. *Cardiovasc Drugs Ther*. 2012;26:121-130.
62. Rossi R, Lichtner M, De Rosa A, Sauzullo I, Mengoni F, Massetti AP, Mastroianni CM, Vullo V. In vitro effect of anti-human immunodeficiency virus ccr5 antagonist maraviroc on chemotactic activity of monocytes, macrophages and dendritic cells. *Clin Exp Immunol*. 2011;166:184-190.
63. Sierra-Madero JG, Ellenberg SS, Rassool MS, Tierney A, Belaunzarán-Zamudio PF, López-Martínez A, Piñeirúa-Menéndez A, Montaner LJ, Azzoni L, Benítez CR, Sereti I, Andrade-Villanueva J, Mosqueda-Gómez JL, Rodriguez B, Sanne I, Lederman MM. Effect of the ccr5 antagonist maraviroc on the occurrence of immune reconstitution inflammatory syndrome in hiv (cadiris): A double-blind, randomised, placebo-controlled trial. *The Lancet HIV*. 2014;1:e60-e67.
64. MacArthur RD, Novak RM. Maraviroc: The first of a new class of antiretroviral agents. *Clin Infect Dis*. 2008;47:236-241.
65. Soriano V, Geretti AM, Perno CF, Fatkenheuer G, Pillay D, Reynes J, Tambussi G, Calvez V, Alami J, Rockstroh J. Optimal use of maraviroc in clinical practice. *Aids*. 2008;22:2231-2240.

ACKNOWLEDGEMENTS and FUNDING

We thank Biogen Idec (Cambridge, MA) for providing natalizumab for use in this study. In vivo CD8 depletion antibodies were kindly provided by the NIH Nonhuman Primate Reagent Resource. This work was supported by the following NIH grants R01 NS040237 (KCW) and R01 NS082116 (THB).

**CHAPTER 6. Direct Targeting of Macrophages with Methylglyoxal-Bis-Guanylhydrazone
Decreases SIV-Associated Cardiovascular Inflammation and Pathologyⁱⁱⁱ**

Joshua A. Walker, Andrew D. Miller,

Tricia H. Burdo, Michael S. McGrath

Kenneth C. Williams

ABSTRACT

Despite effective combination antiretroviral therapy (cART) HIV+ individuals develop co-morbidities including cardiovascular disease (CVD), where activated macrophages play a key role. To date, few therapies target activated monocytes and macrophages. We evaluated a novel oral form of the polyamine biosynthesis inhibitor methylglyoxal-bis-guanylhydrazone (MGBG) on cardiovascular inflammation, carotid artery intima-media thickness (cIMT), and fibrosis in a SIV infection model of AIDS. Eleven SIV-infected animals received MGBG (30 mg/kg) once daily and 8 received a placebo control both beginning at 21 dpi. Animals were time sacrificed (49 dpi), when matched placebos developed AIDS, or at the study endpoint (84 dpi). Cardiac arteries and tissues were analyzed. Quantitative analysis of macrophage populations and T-lymphocytes were done and correlated with cIMT and fibrosis. MGBG treatment resulted in a 2.19 (CD163+), 1.86 (CD68+), 2.31 (CD206+), and 2.12-fold (MAC387+) decrease in macrophages in carotid arteries and a significant 2.07 (CD163+), 1.61 (CD68+), 1.95 (MAC387+) and 1.62-fold (CD206+) decrease in macrophages in cardiac tissues compared to controls. CIMT (1.49-fold) and fibrosis (2.05-fold) were significantly decreased in treated animals compared to controls. Cardiac macrophage numbers and fibrosis in treated animals were similar to uninfected animals. There was a correlation between decreased macrophage numbers in the carotid artery and cIMT and cardiac macrophages and fibrosis. These data demonstrate directly targeting macrophages with MGBG can reduce cardiovascular inflammation, IMT, and fibrosis. They suggest therapies targeting macrophages with HIV should be used in conjunction with cART.

INTRODUCTION

Effective combination anti-retroviral therapy (cART) has increased the lifespan of HIV+ individuals¹⁻³ and can successfully decrease viral load to low or undetectable levels.^{4,5} While effective in reducing plasma viral load chronic immune activation and inflammation persist leading to non-AIDS morbidities, including cardiovascular disease (CVD).⁶ HIV+ individuals on cART have elevated levels of soluble CD14, C-reactive protein, tumor necrosis factor (TNF)- α , and soluble CD163 (sCD163) many of which are myeloid derived, and activated monocytes and macrophages.⁷ Similar findings are reported in elite controllers, who have never been on cART, and have elevated sCD163, activated monocyte/macrophages and CVD, despite having low levels of viremia.⁸⁻¹⁰

HIV+ individuals have increased risk of cardiovascular disease (CVD) compared to the general population.^{11,12} Growing evidence suggests that chronic immune activation and inflammation are a cause for increased CVD risk.^{13,14} HIV+ individuals have increased percentages of activated nonclassical (CD14+CD16++) and intermediate (CD14++CD16+) monocytes similar to non HIV infected individuals with CVD.¹⁵ Using FDG-PET imaging, we have shown increased arterial inflammation in the ascending aorta that correlates with levels of plasma sCD163, a marker of monocyte/macrophage activation.¹⁶ Additionally, monocyte activation markers sCD163, sCD14 and CCL2 were elevated in plasma of HIV+ individuals and associated with atherosclerosis.¹⁷

Monocytes/macrophages play roles in the development of atherosclerosis, vascular calcification, and myocarditis. Macrophages secrete tumor necrosis factor alpha (TNF- α) and transforming growth factor beta (TGF- β), which can enhance calcification *in vitro*¹⁸. Studies showed that macrophages are associated with calcium deposits in carotid plaques¹⁹ and longitudinal studies provided evidence that inflammation precedes calcification.^{20,21} In the

heart, macrophages secrete pro-inflammatory and pro-fibrotic factors which correlate with the extent of fibrosis.²² Unpublished data from our lab (Chapter 4) showed increased macrophage accumulation in the aorta with HIV infection and levels of sCD163 in plasma correlate with increased aortic intima-media thickness (aIMT). Using a SIV-infected, CD8+ T-lymphocyte depletion model of rapid and consistent AIDS, we found macrophage infiltration of cardiac parenchymal tissue correlates with increased cardiac fibrosis.²³ Directly blocking monocyte/macrophage traffic to the heart, using an anti- α 4 antibody, decreased macrophage accumulation in cardiac tissues and cardiac fibrosis.²⁴ These results suggest that by targeting macrophages it is possible to decrease HIV-associated cardiovascular inflammation and decrease HIV-associated CVD.

Few therapies directly targeting macrophages and residual immune activation in conjunction with cART in HIV infection have been described.⁶ Glucocorticoid treatment of SIV-infected animals depleted pro-inflammatory and pro-thrombic CD14+CD16++ monocytes.²⁵ Minocycline, a tetracycline antibiotic, previously was shown to prevent the development of SIV encephalitis (SIVE),^{26,27} decrease circulating activated monocytes that correlated with neuroprotection, and decrease monocyte/macrophage inflammation in lymph nodes.²⁸ However minocycline treatment in humans was not effective.²⁹⁻³¹ SIV-infected monkeys treated with maraviroc, a CCR5 inhibitor, had decreased CD163 expression on macrophages in the myocardium³² and in humans, maraviroc in conjunction with effective cART decreased vascular cell adhesion molecule-1 (VCAM-1). A clinical trial using low dose methotrexate treatment to reduce inflammation has been initiated (NCT01949116).

Methylglyoxal-bis-guanylhydrazone (MGBG) is a polyamine biosynthesis inhibitor that inhibits S-adenosine methionine decarboxylase (SAMDC) resulting in decreased intracellular concentrations of spermine and spermidine in monocytes/macrophages.^{33,34} Polyamines are

necessary for macrophage activation, proliferation, and differentiation, suggesting MGBG might be useful in targeting macrophages to alleviate macrophage-mediated diseases associated with HIV infection.^{35,36} Previously, MGBG injected intravenously (i.v.) was used to treat HIV-associated lymphomas³⁷ but was discontinued.³⁸ More recently the effects of MGBG, *in vitro*, on HIV expression in human macrophages have been studied. MGBG inhibited HIV-p24 expression and DNA integration in human monocytes/macrophages without cell associated toxicities.³⁹ Interestingly, MGBG is taken up and concentrated within macrophages, but not by T-lymphocytes. To date, most ART agents target T-lymphocytes and have limited uptake and or penetration into macrophages which are more resistant to antiretroviral agents.⁴⁰

We have used a CD8+ T-lymphocyte depletion model of rapid AIDS with consistent CNS and cardiac pathology and found that increased macrophage accumulation in cardiac tissues and vessels leads to cardiac fibrosis and cardiomyocyte damage.²³ We used 19 SIV-infected, CD8+ T-lymphocyte depleted rhesus macaques and 6 uninfected controls, to examine if a novel oral form of MGBG treatment decreased inflammation in the aorta, carotid artery, and left ventricle (cardiac tissue) by directly targeting macrophages. We sought to determine if decreased cardiac inflammation would decrease intima-media thickness and cardiac fibrosis. MGBG treatment significantly decreased macrophage associated inflammation and fibrosis in cardiac tissues to levels similar to that of uninfected animals. Compared to placebo controls, MGBG treatment resulted in a trend towards decreased inflammation in the carotid artery and a significant decrease in cIMT. These results suggest that therapies directly targeting monocyte/macrophages with HIV infection potentially could reduce HIV-associated CVD.

RESULTS

MGBG treatment decreases cardiovascular pathology in SIV-infected rhesus macaques

Aorta and carotid artery

Cardiovascular pathology was assessed for the aorta, carotid artery, and cardiac tissue for all animals. Both MGBG treated and placebo control animals had no significant findings in the aorta for all animals. MGBG treatment resulted in decreased inflammation in the carotid artery. Five of 9 (55%) MGBG treated animals had no inflammation in the carotid artery compared to 2 of 6 (33%) placebo controls. The remaining MGBG treated (4 of 9, 44%) and placebo controls (4 of 6, 66%) all had mild inflammation. Six of 9 (66%) of MGBG treated had no significant carotid artery degeneration, compared to 3 of 6 placebo controls (50%). Intimal thickening was noted in only 1 of 9 (11%) MGBG treated animals compared to 3 of 6 (50%) placebo controls (Table 6.2).

Cardiac Tissue

Cardiac tissues were assessed based on inflammation, fibrosis, and cardiomyocyte degeneration. MGBG treatment reduced the frequency and severity of inflammation in cardiac tissues. Five of 11 (45%) MGBG treated animals had no inflammation while placebo controls had either mild (7 of 8, 87%) or moderate (1 of 8, 13%) inflammation. Seven of 11 (63%) of MGBG treated animals had no cardiac fibrosis compared to only 2 of 8 (25%) of placebo controls. Four of 11 (37%) MGBG treated animals had mild fibrosis and 6 of 8 (75%) remaining placebo controls had mild to moderate fibrosis. Five of 11 (45%) MGBG treated animals had no cardiomyocyte degeneration compared to only 1 of 8 (13%) of the placebo control animals, suggesting that MGBG decreased the frequency of cardiomyocyte degeneration.

MGBG decreases macrophage inflammation in the carotid artery and cardiac tissue in SIV-infected rhesus macaques

MGBG treatment resulted in a trend of decreased macrophage numbers in the carotid artery compared to placebo controls. There was a 2.19-fold (CD163+), 1.86-fold (CD68+), 2.12-fold (MAC387+), and 2.31-fold (CD206) decrease in the numbers of macrophages in the carotid artery of MGBG treated animals compared to placebo controls (Fig. 6.1A). There were no differences between the numbers of CD3+ T-lymphocytes present in the carotid artery in placebo controls compared to MGBG treated animals.

MGBG treatment significantly decreased cardiac tissue macrophages compared to placebo controls. There was a significant 2.07-fold (CD163+), 1.61-fold (CD68+), 1.95-fold (MAC387+) and 1.62-fold (CD206+) decrease in numbers of macrophages in cardiac tissues of MGBG treated animals (Fig. 6.1B). Similar to the carotid artery, there was no difference in numbers of CD3+ T-lymphocytes in cardiac tissues of placebo controls and treated animals.

There were significantly increased numbers of macrophages in placebo controls compared to uninfected animals. We did not find differences in the numbers of CD163+, MAC387+ and CD206+ macrophages in cardiac tissues of treated compared to uninfected animals. We did find CD68 was significantly increased (2.71-fold increase) in treatment compared to uninfected animals (Fig. 6.1B).

MGBG treatment results in a reduction of carotid artery intima-media

MGBG treatment resulted in a significant 1.49-fold decrease of carotid artery intima-media thickness (cIMT) compared to placebo controls. The average cIMT for placebo controls was 0.41 ± 0.05 mm (n=6) compared to 0.28 ± 0.02 mm MGBG treated animals (n=9) (Fig. 6.2A, 6.2B). Spearman rank correlation analysis of tissues from placebo controls and MGBG treated

animals demonstrated a positive correlation between increased numbers of CD68+ ($r=.52$, $p<0.05$), CD206+, and MAC387+ ($r=.42$, $p<0.05$) macrophages present in the carotid artery and increased cIMT. There was no correlation between the number of CD163+ macrophages and increased cIMT (Fig. 6.2C).

MGBG treatment results in decreased cardiac fibrosis in SIV-infected rhesus macaques

There was a significant 2.05-fold decrease in the percent collagen per tissue area in MGBG treated animals compared to placebo controls. The average percent collagen per tissue area for MGBG treated animals was $5.79\pm 0.67\%$ ($n= 11$) compared to $11.85\pm 0.98\%$ for placebo controls ($n=8$) (Fig. 6.3). SIV negative animals had a mean percent collagen per tissue area of $6.74\pm 1.91\%$ ($n=6$). Placebo control animals had a significant 1.76-fold increase in the percent collagen per tissue area compared to uninfected animals. MGBG treated animals showed no significant differences in the percent collagen per tissue area compared to uninfected animals. Spearman rank analysis of tissues from uninfected, placebo controls, and MGBG treated animals demonstrated positive correlations between increased numbers of CD163+ ($r=0.69$, $p<0.01$), CD68+ ($r=0.63$, $p<0.05$), CD206+ ($r=0.54$, $p<0.01$), and MAC387+ ($r=0.53$, $p<0.05$) macrophages in cardiac tissues and increased fibrosis in cardiac tissues (Fig. 6.3C).

In situ hybridization for SIV-RNA

We did not find SIV-RNA or SIV-p28+ cells in the carotid artery or cardiac tissues of SIV-infected placebo controls or MGBG treated animals at the study endpoint (84 dpi), consistent with previous findings.²³ Viral loads in all animals peaked at 8 dpi and remained elevated in MGBG treated or placebo controls (data not shown).

DISCUSSION

With effective combination anti-retroviral therapy (cART) mortality due to AIDS related causes has decreased,^{2,47} however secondary co-morbidities have increased.³ While cART decreases plasma virus to low or undetectable levels, chronic immune activation that potentially drives the progression of cardiovascular disease persists.⁴⁸ Statins, that are likely to have a mild immune suppressive effect on myeloid cells,⁴⁹ have been used successfully to decrease CVD with HIV infection⁵⁰⁻⁵² Two studies used rosuvastatin in uninfected individuals⁵⁰ and HIV+ individuals on cART with a moderate cardiovascular risk⁵¹ found a reduced rate of cIMT progression. Additionally atorvastatin reduced non-calcified plaque volume and high-risk coronary plaque features (positive remodeling and low attenuation of plaques) among HIV+ individuals with arterial inflammation.⁵² Statins do not directly target macrophages that are key players in HIV- and SIV-associated CVD⁵³⁻⁵⁵ and myocarditis^{56,57} and to date few therapies target them.

We and our collaborators previously showed that traditional risk factors of CVD are not associated with atherosclerotic plaques, but markers of monocyte/macrophage immune activation, sCD14 and sCD163⁵⁸ are, suggesting that chronic immune activation with HIV infection plays a role in the development of HIV-associated CVD. Increased sCD14⁵⁹ and monocyte chemoattractant protein 1 (MCP-1) and tumor necrosis factor alpha (TNF- α)⁶⁰ also associated with increased coronary artery calcium (CAC), a marker of coronary atherosclerosis. FDG-PET imaging showed that with HIV infection there is increased arterial inflammation in the ascending aorta that correlated with levels of sCD163,¹⁶ and an increase in high-risk plaque morphology.⁶¹ Soluble CD163 made by activated monocytes and macrophages also was associated with non-calcified plaques in HIV+ individuals.⁵⁸ High-risk, non-calcified plaques tend to have large necrotic lipid rich cores and increased macrophage numbers compared to stable

plaques.⁵³ HIV elite controllers, who control viremia, have elevated myeloid markers of immune activation^{8,62} and an increased prevalence of non-calcified coronary plaques further suggesting a link between monocyte/macrophage activation and HIV-associated CVD.¹⁰

Previously our lab showed that the SIV-infected, CD8+ T-lymphocyte depletion model of rapid AIDS in rhesus macaques can be used to study the effects of SIV on the development of cardiac fibrosis.²³ We found that directly blocking macrophage traffic to the heart, using an anti- α 4 antibody, decreased overall cardiac pathology, macrophage inflammation, and cardiac fibrosis.²⁴ The anti-alpha 4 antibody is less useful long term in HIV+ individuals because of the emergence of JC virus infection with long term usage seen in patients with MS and Crohns.^{63,64} In the current study, we examined the effects of an oral formulation of methylglyoxal-bis-guanylhydrazone (MGBG), that is specifically taken up by and concentrated in monocytes/macrophages³⁹ and not T-lymphocytes. We investigated the effects of oral administration of MGBG on SIV-associated cardiovascular inflammation in the carotid artery and heart, cIMT, and cardiac fibrosis. Animal groups consisting of placebo and MGBG treated animals were sacrificed early, when placebo controls developed AIDS, or study endpoint.

We found a trend of decreased inflammation in carotid arteries of MGBG treated animals compared to placebo controls, as well as a significant decrease in the cIMT. Carotid artery intima-media thickness, a marker of atherosclerosis and subclinical cardiovascular disease⁶⁵⁻⁶⁷ is associated with myocardial infarction and stroke.^{68,69} cIMT increases more rapidly in HIV+ individuals compared to age-matched control individuals^{70,71} and is associated with a low CD4+ T-lymphocyte count ($<200\text{cells}/\text{mm}^3$)⁷². A limitation of the current study is not having carotid arteries from uninfected animals to compare to MGBG treated animals.

MGBG treatment decreased macrophage inflammation in cardiac tissues and cardiac fibrosis compared to placebo controls. Cardiac inflammation and fibrosis in MGBG treated

animals was similar to levels seen in uninfected animals. We did not find any effect of MGBG on the number of CD3+ T-lymphocytes present in cardiac tissues consistent with our findings that MGBG is selectively taken up and concentrated in monocytes and macrophages, and not T lymphocytes.³⁹ We have previously shown in our rapid AIDS model that the accumulation of macrophages, and not T-lymphocytes nor viral infected cells, best correlates with cardiac fibrosis and cardiomyocyte damage.²³ Plasma viral load for all placebo and MGBG treated animals in this study were not statistically different as these animals were CD8+ T-lymphocyte depleted and lacked early control of viremia. We did not find SIV-RNA+ cells in the hearts of our monkeys, a result that is consistent with prior reports of low or scattered SIV- and HIV-infected macrophages in cardiac tissues.^{73,74} Together, these data underscore the role of macrophages in the development of SIV-associated CVD. Targeting macrophages directly might be a possible way to diminish inflammation in the heart and cardiac fibrosis. While the incidence of cardiac fibrosis has declined in the cART era among HIV+ individuals,^{75,76} recent studies demonstrate it is still prevalent among HIV+ individuals.^{77,78} Some animals in this study that received MGBG developed AIDS, others receiving the drug did not possibly due to animals being time sacrificed at the end of the study. However, there were no differences in the levels of fibrosis and cIMT in MGBG treated animals with and without AIDS suggesting that disease progression is not the sole cause of cardiovascular disease, adding evidence that chronic inflammation with SIV and HIV infection likely plays a more central role.

In this study we examined the effects MGBG has on SIV-associated cardiovascular inflammation and cardiac fibrosis by directly targeting macrophages. Animals receiving daily doses of MGBG showed decreased inflammation in the carotid artery and cardiac tissue when compared to placebo controls. MGBG treatment also prevented an increase in cIMT and cardiac fibrosis that remained at levels similar to SIV negative animals. These data suggest that

therapies designed to target chronic inflammation and immune activation seen with HIV infection could be used as adjunctive therapies to cART to alleviate HIV-associated cardiovascular disease.

MATERIALS AND METHODS

Ethics Statement

All animals used in this study were handled in strict accordance with the American Association for Accreditation of Laboratory Animal Care with the approval of the Institutional Animal Care and Use Committee of Harvard University and housed at the New England Primate Research Center (NERPC) (Southborough, MA). The NEPRC Protocol Number for this study was 04420 and the Animal Welfare Assurance Number was A3431-01. All animals were anesthetized with ketamine-HCl and euthanized by an intravenous pentobarbital overdose and exsanguinated. The development of simian AIDS was determined post-mortem by the presence of opportunistic infections and presence of AIDS-defining lesions.

Animals, SIV infection, CD8+ T-lymphocyte depletion, MGBG treatment

Twenty-five animals were used in this study. Six animals were uninfected controls and 19 animals SIV-infected and CD8 lymphocyte depleted. Of these, 11 received MGBG (30 mg/kg) (provided by Pathologica, LLC; formulated as syrup by Wedgewood Pharmacy, Swedesboro, NJ) orally, once daily beginning at 21 days post infection (dpi), when significant CNS and cardiovascular inflammation is known to occur in this model.^{24,41} Eight received on oral placebo control at the same time point. Previous experiments showed that an effective dose of 0.7µM MGBG in plasma and tissues was reached in animals that received a daily oral dose of 30mg/kg.³⁹ Infected animals receiving MGBG or placebo were assigned to one of six groups with at least one placebo control per group. Six uninfected animals were group 1. Animals in each group were sacrificed at 49 dpi (Group 2), when placebo controls developed AIDS (Groups 3-6), or at the end of the study (84 days) (Group 7) (Table 6.1).

Assessment of cardiovascular pathology

Following exsanguination a full SIV necropsy was performed and major organs were collected in 10% neutral buffered formalin, embedded in paraffin, and sectioned at 5 μm . Sections of the carotid artery, aorta, and left ventricle (cardiac tissue) were stained with hematoxylin and eosin and graded blindly by a veterinary pathologist. The carotid artery and aorta was assessed based on two criteria; inflammation and carotid artery or aortic degeneration. Degeneration of the carotid artery or aorta was based on the alignment of smooth muscle fibers in the tunica intima. Cardiac tissues were assessed based on the degree of inflammation, fibrosis, and cardiomyocyte degeneration. Sections were graded for each category based on the degree of change in cardiac tissues and scored as either having no significant findings (NSF) or being mild, moderate, or severe.

Immunohistochemistry

Numbers of macrophages in the carotid artery (n=11 MGBG treated, n=8 placebo) and left ventricle (cardiac tissue) (n=11 MGBG treated, n=8 placebo, n=6 SIV negative) were assessed using immunohistochemistry and cell counting as previously described.²⁴ Formalin-fixed, paraffin-embedded sections of carotid artery and cardiac tissue were deparaffinized in xylenes and rehydrated in graded ethanols, followed by incubation with peroxidase block (Dako) for 5 minutes. Sections were incubated with serum free protein block (Dako) for 30 minutes then incubated with antibodies against CD163+, CD68+, CD206+, MAC387+ macrophage markers, and CD3+ T-lymphocytes for 1 hour at RT or overnight at 4°C. Tissue sections were rinsed and incubated with an anti-mouse secondary antibody conjugated to horseradish peroxidase (Dako). The reaction product was visualized using 3, 3'-diaminobenzidine tetrahydrochloride (DAB, Dako). The average number of immune positive macrophages/ mm^2 plus or minus the standard

error of the mean (SEM) was determined by counting the number of positive macrophages from twenty non-overlapping 200x fields of view (field area=0.148mm²) per section, using a Zeiss Axio Imager M1 microscope with Plan-Apochromat x20/0.8 Korr objectives (Carl Zeiss Microimaging Inc., Thornwood, NY).

Measurement of carotid artery intima-media thickness

Sections of carotid artery were deparaffinized and rehydrated in xylenes and graded ethanols, followed by staining with a Verhoeff Van Gieson elastic stain (Sigma) to differentiate the intima, media, and adventitia of the carotid artery wall.⁴² The cIMT was measured optically using ImageJ Analysis Software for 10 non-overlapping fields of view per section. Data were expressed as the average cIMT plus or minus the SEM.

Measurement of cardiac fibrosis

Cardiac tissue were stained using a modified Massons Trichrome (Newcomer Supply, Middleton, WI) to determine the percent of collagen per tissue area.^{43,44} The percent collagen (blue dye) per tissue area was determined using ImageJ Analysis software from 20 non-overlapping 200x fields of view (field area=0.148mm²). Data were expressed as the average percent collagen per tissue area plus or minus the SEM.

In situ hybridization for SIV-RNA

In situ hybridization for SIV-RNA was performed using digoxigenin-labeled antisense riboprobes from Lofstrand Labs (Gaithersburg, MD), as previously described.⁴⁵ Formalin-fixed, paraffin-embedded sections of carotid artery and cardiac tissues were deparaffinized and rehydrated in xylenes and graded ethanols. Sections were treated with antigen unmasking

solution (Vector Labs, Burlingame, CA) for 20 minutes at high heat, washed, and prehybridized at 45°C for 1 hour with prehybridization buffer containing denatured herring sperm DNA and yeast tRNA at concentrations of 10mg/mL. Digoxigenin-labeled probes (10ng/mL) were diluted in hybridization buffer and hybridized overnight at 45°C. Following stringency washes with decreasing concentrations of SSC buffer, sections were blocked with a 1% blocking solution (Roche Diagnostics) for 30 minutes. Digoxigenin-labeled probes were detected with NBT/BCIP (Roche Diagnostics) with levamisole (Dako) to inhibit alkaline phosphatases. The NBT/BCIP substrate produces a visible blue reaction product.

Plasma SIV-RNA was quantified using real-time PCR for all animals used in this study, as previously described.⁴⁶ 500µL of EDTA plasma was collected and SIV virions were pelleted by centrifugation at 20,000 g for 1 hour. The threshold sensitivity was 100 copy Eq/mL, with an average interassay coefficient variation of less than 25%.

Statistical Analysis

Statistical analyses were done using Prism version 5.0 (Graphpad Software Inc., San Diego, CA). For the carotid artery, comparisons of the mean number of macrophages/mm² and carotid artery intima-media thickness (cIMT) were made between SIV-infected placebo controls, and SIV-infected MGBG treated animals using a non-parametric Mann-Whitney t-test with significance accepted at p<0.05. For cardiac tissues, comparisons of the mean number of macrophages/mm² and the percent collagen per tissue area were made between uninfected animals, SIV-infected placebo controls, and SIV-infected MGBG treated animals using analysis of variance (ANOVA). If the ANOVA was significant (p<0.05) a posthoc non-parametric Mann-Whitney t-test was performed. A Spearman rank correlation analysis was used to determine if

changes in cIMT and the percent collagen per total tissue area correlated with decreased macrophage numbers in the carotid artery and cardiac tissues of MGBG treated animals

Table 6.1. MGBG and Placebo Control Animals Used in this Study

	Animal ID	Survival (dpi)	SIV/AIDS	Tissue Sections		Treatment
				Carotid Artery	Left Ventricle	
Group 1	373-03	NA	SIV-	N	Y	-
	257-00	NA	SIV-	N	Y	-
	417-08	NA	SIV-	N	Y	-
	454-08	NA	SIV-	N	Y	-
	96-10	NA	SIV-	N	Y	-
	428-08	NA	SIV-	N	Y	-
Group 2	5035	49	SIV+, SIVE	N	Y	Placebo
	5038	49	SIV+, SIVE	N	Y	Placebo
	5041	49	SIV+, AIDS	N	Y	MGBG
	5042	49	SIV+, No AIDS	N	Y	MGBG
Group 3	299-10	63	SIV+, AIDS	Y	Y	Placebo
	264-10	63	SIV+, AIDS	Y	Y	MGBG
	186-10	63	SIV+, No AIDS	Y	Y	MGBG
Group 4	296-10	70	SIV+ SIVE	Y	Y	Placebo
	291-10	70	SIV+, No AIDS	Y	Y	MGBG
	273-10	70	SIV+, No AIDS	Y	Y	MGBG
Group 5	291-09	77	SIV+, SIVE	Y	Y	Placebo
	257-10	77	SIV+, AIDS	Y	Y	MGBG
	328-10	77	SIV+ No AIDS	Y	Y	MGBG
Group 6	326-10	83	SIV+, AIDS	Y	Y	Placebo
	201-10	83	SIV+, No AIDS	Y	Y	MGBG
	272-10	83	SIV+, AIDS	Y	Y	MGBG
Group 7	434-10	84	SIV+, AIDS	Y	Y	Placebo
	262-09	84	SIV+, No AIDS	Y	Y	Placebo
	272-09	84	SIV+, No AIDS	Y	Y	MGBG

Twenty-five animals were used in this study to examine the effects of MGBG treatment on cardiovascular inflammation. Six animals were uninfected (group 1). The remaining 19 animals (groups 2-7) were either treated daily with MGBG or given a placebo control. Animals were grouped and sacrificed at the indicated days post infection (dpi) when placebo controls

developed AIDS or at the end of the study (83, 84 dpi). SIVE, SIV-encephalitis. For tissue sections, N indicate no section was available, Y indicates that a tissue section was available.

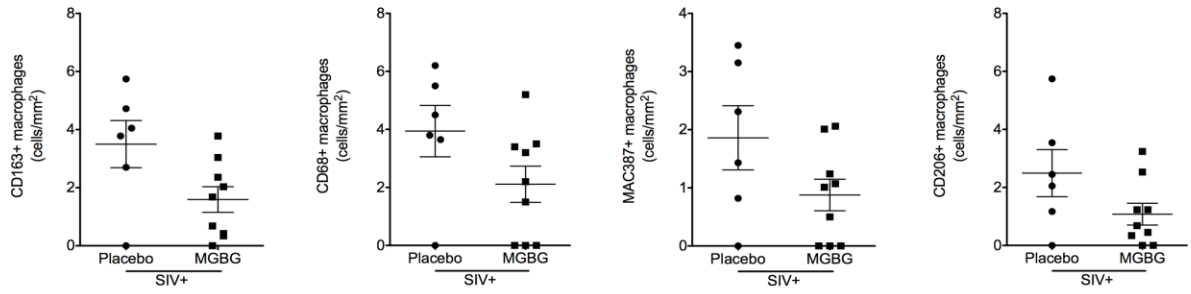
Table 6.2. Cardiovascular Pathology of MGBG and Placebo Control Animals

	Animal ID	Aorta (n=15)		Carotid Artery (n=15)		Cardiac Tissue (n=25)		
		Inflammation	Degeneration	Inflammation	Degeneration	Inflammation	Fibrosis	Degeneration
Uninfected	373-03	NA	NA	NA	NA	NSF	NSF	NSF
	257-00	NA	NA	NA	NA	NSF	NSF	NSF
	417-08	NA	NA	NA	NA	NSF	NSF	NSF
	454-08	NA	NA	NA	NA	NSF	NSF	NSF
	96-10	NA	NA	NA	NA	NSF	NSF	NSF
	428-08	NA	NA	NA	NA	Mild	Mild	NSF
SIV-infected, CD8+ T-lymphocyte depleted placebo control	5035	NA	NA	NA	NA	Mild	Mild	Mild
	5038	NA	NA	NA	NA	Mild	NSF	NSF
	299-10	NSF	NSF	Mild	NSF	Mild	NSF	Mild
	296-10	NSF	NSF	NSF	NSF	Mild	Mild	Mild
	291-09	NSF	NSF	Mild	Mild, with intimal thickening	Moderate	Moderate	Mild
	326-10	NSF	NSF	Mild	Mild, with intimal thickening	Mild	Mild	Mild
	434-10	NSF	NSF	Mild	Mild, with intimal thickening	Mild	Mild	Moderate
	262-09	NSF	NSF	NSF	NSF	Mild	Mild	Mild
SIV-infected, CD8+ T-lymphocyte depleted MGBG treated	5041	NA	NA	NA	NA	NSF	NSF	NSF
	5042	NA	NA	NA	NA	NSF	NSF	NSF
	264-10	NSF	NSF	NSF	NSF	NSF	NSF	NSF
	186-10	NSF	NSF	Mild	NSF	NSF	NSF	NSF
	291-10	NSF	NSF	Mild	Mild	Mild	NSF	Mild
	273-10	NSF	NSF	NSF	NSF	Mild	Mild	Mild
	257-10	NSF	NSF	NSF	NSF	NSF	Mild	Moderate
	328-10	NSF	NSF	NSF	NSF	Mild	NSF	Mild
	201-10	NSF	NSF	NSF	NSF	Mild	Mild	Mild
	272-10	NSF	NSF	Mild	Mild, with isolated thickening	Mild	Mild	Mild
	272-09	NSF	NSF	Mild	Mild	Mild	NSF	NSF

Hematoxylin and eosin stained sections of matched aorta, carotid artery, and cardiac tissue were graded blindly by a board certified pathologist. Sections of carotid artery and aorta were graded based on the following criteria; inflammation and degeneration with intimal thickening noted if present. Degeneration was assessed based on the degree of alignment of smooth muscles fibers in the tunica intima. Cardiac tissues were graded based on the following criteria; inflammation, fibrosis, and cardiomyocyte degeneration. Sections were graded as having no significant findings (NSF) if they appeared normal or as either being mild, moderate, or severe, based on the degree of change in the tissue. NA= not available. Sections of the aorta and carotid artery were not available for analysis from all SIV negative animals and two placebo control and two MGBG treated animals, as indicated.

Figure 6.1

A



B

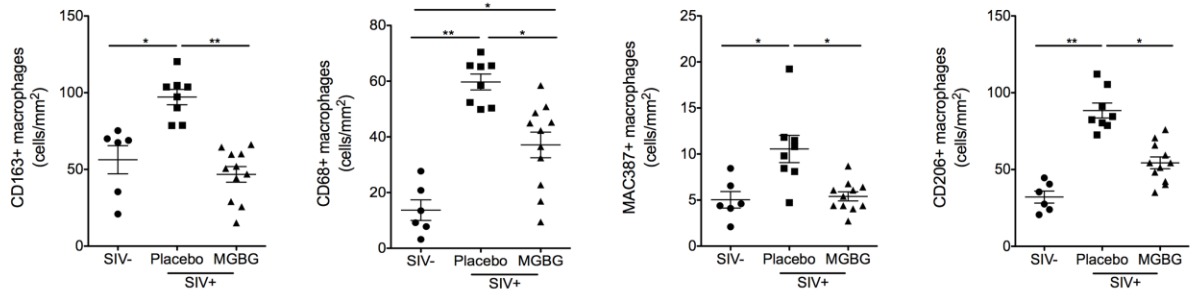


Figure 6.1. Daily treatment with MGBG results in a trend of decreased inflammation in the carotid artery and a significant decrease in inflammation in cardiac tissues from SIV-infected CD8+ T-lymphocyte depleted rhesus macaques.

(A) Sections of carotid artery from MGBG treated (n=9) and placebo control (n=6) SIV-infected CD8+ T-lymphocyte rhesus macaques were immunohistochemically stained with antibodies recognizing CD163+, CD68+, CD206+, and MAC387+ macrophages. MGBG treatment resulted in a trend of decreased numbers of CD163+ (2.19-fold), CD68+ (1.86-fold), MAC387+ (2.12-fold), and CD206+ (2.31-fold) macrophages present in the carotid artery when compared to placebo controls. Statistical analysis was performed using a non-parametric Mann-Whitney t-test with significance accepted at $p < 0.05$. (B) Sections of cardiac tissue from SIV- (n=6) MGBG treated (n=11) and placebo controls (n=8) rhesus macaques were immunohistochemically stained with the same antibodies. MGBG treated animals had significantly decreased numbers of CD163+ (2.07-fold), CD68+ (1.61-fold), and MAC387+ (1.95-fold) and CD206+ (1.62-fold) macrophages when compared to placebo controls. There was no difference in numbers of CD163+, MAC387+, and CD206+ macrophages when comparing uninfected and MGBG treated animals. For cardiac tissues statistical analysis was performed between uninfected animals, SIV-infected placebo controls, and SIV-infected MGBG treated animals using analysis of variance (ANOVA). If the ANOVA was significant ($p < 0.05$) between two groups, a posthoc non-parametric Mann-Whitney t-test was performed. * $p < 0.05$, ** $p < 0.01$.

Figure 6.2

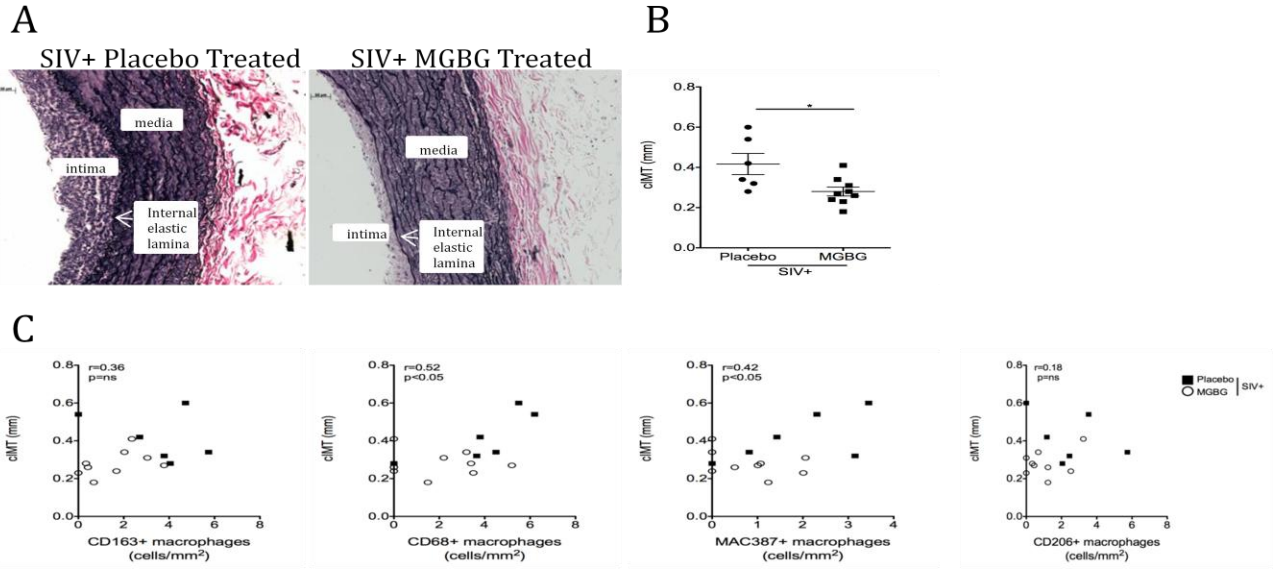


Figure 6.2 MGBG treatment prevents an increase in carotid artery intima-media thickness which correlates with a decreased trend in macrophage inflammation.

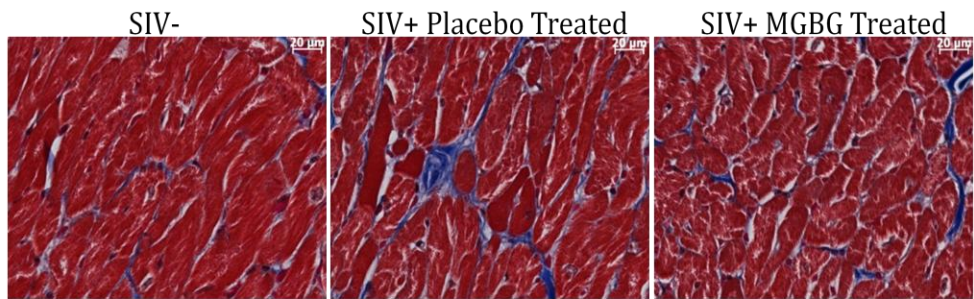
(A) Sections of carotid artery were stained with a Verhoeff Van Gieson elastic stain in order to measure the carotid artery intima-media thickness (cIMT). The cIMT was measured using calipers and ImageJ Analysis Software from 10 random non-overlapping fields of view with average cIMT calculated and expressed as plus or minus the standard error of the mean (SEM).

(B) There was a significant 1.49-fold decrease in cIMT when comparing placebo control animals to MGBG treated animals. Statistical analysis was performed using a non-parametric Mann-Whitney t-test comparing placebo controls to MGBG treated animals with significance accepted at $p < 0.05$.

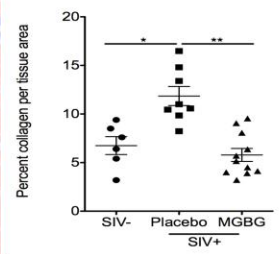
(C) Using a Spearman rank correlation analysis, in the carotid artery, there was a positive correlation between increased numbers of CD68+ ($r=0.52$) and MAC387+ ($r=0.42$) macrophages and increasing cIMT. There was no correlation between numbers of CD163+ and CD206+ macrophages and cIMT. * $p < 0.05$. Scale bar equals 50 μm .

Figure 6.3

A



B



C

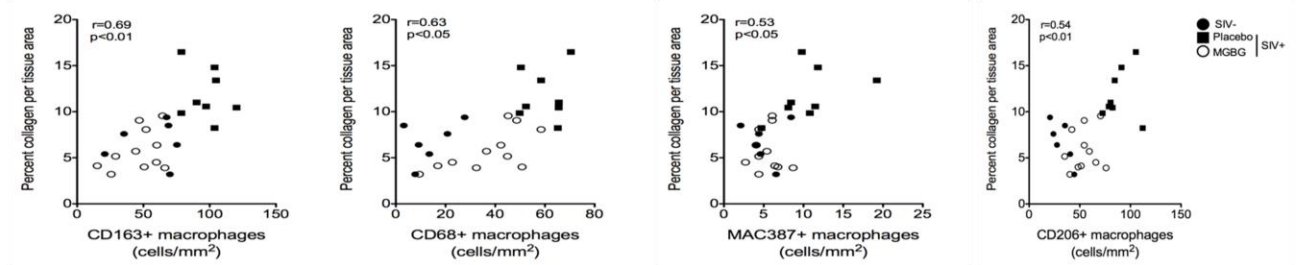


Figure 6.3. MGBG treatment prevents an increase in cardiac fibrosis in cardiac tissues similar to levels seen in uninfected controls.

(A) Collagen, a marker of fibrosis, in cardiac tissues was measured by staining cardiac tissue with a trichrome stain. ImageJ Analysis software was used to determine the percent collagen (blue dye) per total tissue area from 20 200x non-overlapping fields of view with the average percent collagen per total tissue area calculated for each animal. (B) There was a significant 2.05-fold decrease in the percent collagen per total tissue area when comparing placebo controls to MGBG treated animals. There was no significant difference between the percent collagen per total tissue area between uninfected and MGBG treated animals. Statistical analysis was performed using analysis of variance (ANOVA). If the ANOVA was significant ($p < 0.05$) between two groups, a posthoc non-parametric Mann-Whitney *t*-test was performed. (C) Using Spearman rank correlation analysis, we found positive correlations between increasing numbers of CD163+ ($r = 0.69$), CD68+ ($r = 0.63$), MAC387+ ($r = 0.53$) and CD206+ ($r = 0.54$) macrophages and increasing percent collagen per total tissue area. * $p < 0.05$, ** $p < 0.01$. Scale bar equals 20 μm .

REFERENCES

1. Coquet I, Pavie J, Palmer P, et al. Survival trends in critically ill HIV-infected patients in the highly active antiretroviral therapy era. *Crit Care*. 2010;14:R107.
2. Landay A, Miller CJ, Baker JV, et al. Adjudicated Morbidity and Mortality Outcomes by Age among Individuals with HIV Infection on Suppressive Antiretroviral Therapy. *PLoS One*. 2014;9:e95061.
3. Hasse B, Ledergerber B, Furrer H, et al. Morbidity and Aging in HIV-Infected Persons The Swiss HIV Cohort Study. *Clin Infect Dis*. 2011;53:1130-1139.
4. Maldarelli F, Palmer S, King MS, et al. ART suppresses plasma HIV-1 RNA to a stable set point predicted by pretherapy viremia. *PLoS Pathog*. 2007;3:e46.
5. French MA, King MS, Tschampa JM, da Silva BA, Landay AL. Serum immune activation markers are persistently increased in patients with HIV infection after 6 years of antiretroviral therapy despite suppression of viral replication and reconstitution of CD4+ T cells. *J Infect Dis*. 2009;200:1212-1215.
6. Deeks SG. HIV Infection, Inflammation, Immunosenescence, and Aging. *Annu Rev Med*. 2011;62:141-155.
7. Wada NI, Jacobson LP, Margolick JB, et al. The effect of HAART-induced HIV suppression on circulating markers of inflammation and immune activation. *Aids*. 2015;29:463-471.
8. Li JZ, Arnold KB, Lo J, et al. Differential Levels of Soluble Inflammatory Markers by Human Immunodeficiency Virus Controller Status and Demographics. *Open Forum Infect Dis*. 2014;2:ofu117-ofu117.
9. Krishnan S, Wilson EM, Sheikh V, et al. Evidence for innate immune system activation in HIV type 1-infected elite controllers. *J Infect Dis*. 2014;209:931-939.

10. Pereyra F, Lo J, Triant V, et al. Increased coronary atherosclerosis and immune activation in HIV-1 elite controllers. *Aids*. 2012;26:2409-2415.
11. Feinstein MJ, Bahiru E, Achenbach C, et al. Patterns of Cardiovascular Mortality for HIV-Infected Adults in the United States: 1999-2013. *Am J Cardiol*. 2016;117:214-220.
12. Petoumenos K, Reiss P, Ryom L, et al. Increased risk of cardiovascular disease (CVD) with age in HIV-positive men: a comparison of the D:A:D CVD risk equation and general population CVD risk equations. *HIV Med*. 2014;15:595-603.
13. Stein JH, Hsue PY. Inflammation, Immune Activation, and CVD Risk in Individuals With HIV Infection. *JAMA*. 2012;308:405-406.
14. Kuller LH, Tracy R, Belloso W, et al. Inflammatory and coagulation biomarkers and mortality in patients with HIV infection. *PLoS Med*. 2008;5:e203.
15. Funderburg NT, Zidar DA, Shive C, et al. Shared monocyte subset phenotypes in HIV-1 infection and in uninfected subjects with acute coronary syndrome. *Blood*. 2012;120:4599-4608.
16. Subramanian S, Tawakol A, Abbara S, et al. Arterial Inflammation in Patients With HIV. *JAMA*. 2012;308:379-386.
17. McKibben RA, Margolick JB, Grinspoon S, et al. Elevated Levels of Monocyte Activation Markers Are Associated With Subclinical Atherosclerosis in Men With and Those Without HIV Infection. *J Infect Dis*. 2015;211:1219-1228.
18. Tintut Y, Patel J, Territo M, Saini T, Parhami F, Demer LL. Monocyte/macrophage regulation of vascular calcification in vitro. *Circulation*. 2002;105:650-655.
19. Jeziorska M, McCollum C, Woolley DE. Calcification in atherosclerotic plaque of human carotid arteries: associations with mast cells and macrophages. *J Pathol*. 1998;185:10-17.

20. Abdelbaky A, Corsini E, Figueroa AL, et al. Early aortic valve inflammation precedes calcification: A longitudinal FDG-PET/CT study. *Atherosclerosis*. 2015;238:165-172.
21. Abdelbaky A, Corsini E, Figueroa AL, et al. Focal arterial inflammation precedes subsequent calcification in the same location: a longitudinal FDG-PET/CT study. *Circ Cardiovasc Imaging*. 2013;6:747-754.
22. Timonen P, Magga J, Risteli J, et al. Cytokines, interstitial collagen and ventricular remodelling in dilated cardiomyopathy. *Int J Cardiol*. 2008;124:293-300.
23. Walker JA, Sulciner ML, Nowicki KD, Miller AD, Burdo TH, Williams KC. Elevated numbers of CD163+ macrophages in hearts of simian immunodeficiency virus-infected monkeys correlate with cardiac pathology and fibrosis. *AIDS Res Hum Retroviruses*. 2014;30:685-694.
24. Walker JA, Beck GA, Campbell JH, Miller AD, Burdo TH, Williams KC. Anti-alpha4 Integrin Antibody Blocks Monocyte/Macrophage Traffic to the Heart and Decreases Cardiac Pathology in a SIV Infection Model of AIDS. *J Am Heart Assoc*. 2015;4:e001932.
25. Moniuszko M, Liyanage NPM, Doster MN, et al. Glucocorticoid Treatment at Moderate Doses of SIVmac251-Infected Rhesus Macaques Decreases the Frequency of Circulating CD14+CD16++Monocytes But Does Not Alter the Tissue Virus Reservoir. *AIDS Res Hum Retroviruses*. 2015;31:115-126.
26. Ratai EM, Bombardier JP, Joo CG, et al. Proton magnetic resonance spectroscopy reveals neuroprotection by oral minocycline in a nonhuman primate model of accelerated NeuroAIDS. *PLoS One*. 2010;5:e10523.
27. Zink MC, Uhrlaub J, DeWitt J, et al. Neuroprotective and anti-human immunodeficiency virus activity of minocycline. *JAMA*. 2005;293:2003-2011.

28. Campbell JH, Burdo TH, Autissier P, et al. Minocycline inhibition of monocyte activation correlates with neuronal protection in SIV neuroAIDS. *PLoS One*. 2011;6:e18688.
29. Ho EL, Spudich SS, Lee E, Fuchs D, Sinclair E, Price RW. Minocycline fails to modulate cerebrospinal fluid HIV infection or immune activation in chronic untreated HIV-1 infection: results of a pilot study. *AIDS Res Ther*. 2011;8:17-17.
30. Nakasujja N, Miyahara S, Evans S, et al. Randomized trial of minocycline in the treatment of HIV-associated cognitive impairment. *Neurology*. 2013;80:196-202.
31. Sacktor N, Miyahara S, Deng L, et al. Minocycline treatment for HIV-associated cognitive impairment: Results from a randomized trial. *Neurology*. 2011;77:1135-1142.
32. Kelly KM, Tocchetti CG, Lyashkov A, et al. CCR5 Inhibition Prevents Cardiac Dysfunction in the SIV/Macaque Model of HIV. *J Am Heart Assoc*. 2014;3:e000874.
33. Corti A, Dave C, Williams-Ashman HG, Mihich E, Schenone A. Specific inhibition of the enzymic decarboxylation of S-adenosylmethionine by methylglyoxal bis(guanylhydrazone) and related substances. *Biochem J*. 1974;139:351-357.
34. Williams-Ashman HG, Schenone A. Methyl glyoxal bis(guanylhydrazone) as a potent inhibitor of mammalian and yeast S-adenosylmethionine decarboxylases. *Biochem Biophys Res Commun*. 1972;46:288-295.
35. Pegg AE. Mammalian polyamine metabolism and function. *IUBMB life*. 2009;61:880-894.
36. Janne J, Holtta E, Kallio A, Kapyaho K. Role of polyamines and their antimetabolites in clinical medicine. *Spec Top Endocrinol Metab*. 1983;5:227-293.
37. Tulpule A, Espina B, Pedro Santabarbara AB, et al. Treatment of AIDS related non-Hodgkin's lymphoma with combination mitoguazone dihydrochloride and low dose CHOP chemotherapy: results of a phase II study. *Invest New Drugs*. 2004;22:63-68.

38. Gerner EW, Meyskens FL, Jr. Polyamines and cancer: old molecules, new understanding. *Nat Rev Cancer*. 2004;4:781-792.
39. Jin X, McGrath MS, Xu H. Inhibition of HIV Expression and Integration in Macrophages by Methylglyoxal-Bis-Guanylhydrazone. *J Virol*. 2015;89:11176-11189.
40. Gavegnano C, Detorio MA, Bassit L, Hurwitz SJ, North TW, Schinazi RF. Cellular pharmacology and potency of HIV-1 nucleoside analogs in primary human macrophages. *Antimicrob Agents Chemother*. 2013;57:1262-1269.
41. Soulas C, Conerly C, Kim WK, et al. Recently infiltrating MAC387(+) monocytes/macrophages a third macrophage population involved in SIV and HIV encephalitic lesion formation. *Am J Pathol*. 2011;178:2121-2135.
42. Deopukari R, Dixit A. The study of age related changes in coronary arteries and its relevance to the atherosclerosis. *J Anat Soc India*. 2010;59:192-196.
43. Brower GL, Gardner JD, Forman MF, et al. The relationship between myocardial extracellular matrix remodeling and ventricular function. *Eur J Cardiothorac Surg*. 2006;30:604-610.
44. Ruifrok AC, Johnston DA. Quantification of Histochemical Staining by Color Deconvolution. *Anal Quant Cytol Histol*. 2001;23:291-299.
45. Williams K, Schwartz A, Corey S, et al. Proliferating Cellular Nuclear Antigen Expression as a Marker of Perivascular Macrophages in Simian Immunodeficiency Virus Encephalitis. *Am J Pathol*. 2002;161:575-585.
46. Lifson JD, Rossio JL, Piatak M, Jr., et al. Role of CD8(+) lymphocytes in control of simian immunodeficiency virus infection and resistance to rechallenge after transient early antiretroviral treatment. *J Virol*. 2001;75:10187-10199.

47. Engsig FN, Zangerle R, Katsarou O, et al. Long-term mortality in HIV-positive individuals virally suppressed for >3 years with incomplete CD4 recovery. *Clin Infect Dis*. 2014;58:1312-1321.
48. Beltran LM, Rubio-Navarro A, Amaro-Villalobos JM, Egado J, Garcia-Puig J, Moreno JA. Influence of immune activation and inflammatory response on cardiovascular risk associated with the human immunodeficiency virus. *Vasc Health Risk Manag*. 2015;11:35-48.
49. Yadav A, Betts MR, Collman RG. Statin modulation of monocyte phenotype and function: implications for HIV-1-associated neurocognitive disorders. [published online March 28, 2016]. *J Neurovirol*. doi: 10.1007/s13365-016-0433-8.
50. Crouse JR, 3rd, Raichlen JS, Riley WA, et al. Effect of rosuvastatin on progression of carotid intima-media thickness in low-risk individuals with subclinical atherosclerosis: the METEOR Trial. *JAMA*. 2007;297:1344-1353.
51. Calza L, Manfredi R, Colangeli V, et al. Two-year treatment with rosuvastatin reduces carotid intima-media thickness in HIV type 1-infected patients receiving highly active antiretroviral therapy with asymptomatic atherosclerosis and moderate cardiovascular risk. *AIDS Res Hum Retroviruses*. 2013;29:547-556.
52. Lo J, Lu MT, Ihenachor EJ, et al. Effects of statin therapy on coronary artery plaque volume and high-risk plaque morphology in HIV-infected patients with subclinical atherosclerosis: a randomised, double-blind, placebo-controlled trial. *Lancet HIV*. 2015;2:e52–e63.
53. Tahara N, Mukherjee J, de Haas HJ, et al. 2-deoxy-2-[F]fluoro-d-mannose positron emission tomography imaging in atherosclerosis. *Nat Med*. 2014;20:215-219.

54. Fenyo IM, Gafencu AV. The involvement of the monocytes/macrophages in chronic inflammation associated with atherosclerosis. *Immunobiology*. 2013;218:1376-1384.
55. Moore KJ, Sheedy FJ, Fisher EA. Macrophages in atherosclerosis: a dynamic balance. *Nat Rev Immunol*. 2013;13:709-721.
56. Yang M, Zheng J, Miao Y, et al. Serum-glucocorticoid regulated kinase 1 regulates alternatively activated macrophage polarization contributing to angiotensin II-induced inflammation and cardiac fibrosis. *Arterioscler Thromb Vasc Biol*. 2012;32:1675-1686.
57. Falkenham A, de Antueno R, Rosin N, et al. Nonclassical resident macrophages are important determinants in the development of myocardial fibrosis. *Am J Pathol*. 2015;185:927-942.
58. Burdo TH, Lo J, Abbara S, et al. Soluble CD163, a novel marker of activated macrophages, is elevated and associated with noncalcified coronary plaque in HIV-infected patients. *J Infect Dis*. 2011;204:1227-1236.
59. Longenecker CT, Jiang Y, Orringer CE, et al. Soluble CD14 is independently associated with coronary calcification and extent of subclinical vascular disease in treated HIV infection. *Aids*. 2014;28:969-977.
60. Shikuma CM, Barbour JD, Ndhlovu LC, et al. Plasma Monocyte Chemoattractant Protein-1 and Tumor Necrosis Factor- α Levels Predict the Presence of Coronary Artery Calcium in HIV-Infected Individuals Independent of Traditional Cardiovascular Risk Factors. *AIDS Res Hum Retroviruses*. 2014;30:142-146.
61. Tawakol A, Lo J, Zanni MV, et al. Increased Arterial Inflammation Relates to High-risk Coronary Plaque Morphology in HIV-Infected Patients. *J Acquir Immune Defic Syndr*. 2014;66:164-171.

62. Pereyra F, Palmer S, Miura T, et al. Persistent low-level viremia in HIV-1 elite controllers and relationship to immunologic parameters. *J Infect Dis.* 2009;200:984-990.
63. Van Assche G, Van Ranst M, Sciot R, et al. Progressive Multifocal Leukoencephalopathy after Natalizumab Therapy for Crohn's Disease. *N Engl J Med.* 2005;353:362-380.
64. Jilek S, Jaquiéry E, Hirsch HH, et al. Immune responses to JC virus in patients with multiple sclerosis treated with natalizumab: a cross-sectional and longitudinal study. *Lancet Neurol.* 2010;9:264-272.
65. O'Leary DH, Polak JF, Kronmal RA, et al. Thickening of the carotid wall. A marker for atherosclerosis in the elderly? Cardiovascular Health Study Collaborative Research Group. *Stroke.* 1996;27:224-231.
66. O'Leary DH, Polak JF. Intima-media thickness: a tool for atherosclerosis imaging and event prediction. *Am J Cardiol.* 2002;90:18L-21L.
67. Polak JF, Pencina MJ, Pencina KM, O'Donnell CJ, Wolf PA, D'Agostino RBS. Carotid-Wall Intima–Media Thickness and Cardiovascular Events. *N Engl J Med.* 2011;365:213-221.
68. Chambless LE, Folsom AR, Clegg LX, et al. Carotid wall thickness is predictive of incident clinical stroke: the Atherosclerosis Risk in Communities (ARIC) study. *Am J Epidemiol.* 2000;151:478-487.
69. O'Leary DH, Polak JF, Kronmal RA, Manolio TA, Burke GL, Wolfson SK, Jr. Carotid-artery intima and media thickness as a risk factor for myocardial infarction and stroke in older adults. Cardiovascular Health Study Collaborative Research Group. *N Engl J Med.* 1999;340:14-22.
70. Volpe GE, Tang AM, Polak JF, Mangili A, Skinner SC, Wanke CA. Progression of Carotid Intima-Media Thickness and Coronary Artery Calcium Over 6 Years in an HIV-Infected Cohort. *J Acquir Immune Defic Syndr.* 2013;64:51-57.

71. Hsue PY, Ordovas K, Lee T, et al. Carotid intima-media thickness among human immunodeficiency virus-infected patients without coronary calcium. *Am J Cardiol.* 2012;109:742-747.
72. Hsue PY, Lo JC, Franklin A, et al. Progression of atherosclerosis as assessed by carotid intima-media thickness in patients with HIV infection. *Circulation.* 2004;109:1603-1608.
73. Kelly KM, Tarwater PM, Karper JM, et al. Diastolic dysfunction is associated with myocardial viral load in simian immunodeficiency virus-infected macaques. *Aids.* 2012;26:815-823.
74. Yearley JH, Pearson C, Carville A, Shannon RP, Mansfield K. SIV-Associated Myocarditis: Viral and Cellular Correlates of Inflammation Severity. *AIDS Res Hum Retroviruses.* 2006;22:529-540.
75. Silwa K, Carrington MJ, Becker A, Thienemann F, Ntsekhe M, Stewart S. Contribution of the human immunodeficiency virus acquired immunodeficiency syndrome epidemic to de novo presentations of heart disease in the Heart of Soweto Study cohort. *Eur Heart J.* 2012;33:866-874.
76. Khunnawat C, Mukerji S, Havlichek D, Jr., Touma R, Abela GS. Cardiovascular manifestations in human immunodeficiency virus-infected patients. *Am J Cardiol.* 2008;102:635-642.
77. Cheruvu S, Holloway CJ. Cardiovascular disease in human immunodeficiency virus. *Intern Med J.* 2014;44:315-324.
78. Frustaci A, Petrosillo N, Vizza D, et al. Myocardial and microvascular inflammation/infection in patients with HIV-associated pulmonary artery hypertension. *Aids.* 2014;28:2541-2549.

ACKNOWLEDGMENTS AND FUNDING

We would like to thank Wedgwood Pharmacy for formulating MGBG and placebo. This work was supported by the following grants: R01 NS040237 (Williams), R01 NS082116 (Burdo) and U19MH08183 (McGrath).

CHAPTER 7. Summary and Discussion

Data in this thesis provide evidence supporting the role of monocyte/macrophage activation in the development of HIV and SIV-associated cardiovascular pathogenesis. We show in Chapter 2 there are early differences in the numbers of activated monocytes that potentially predict the development of cardiac fibrosis in an SIV infection model of rapid AIDS. We also found a correlation between cardiac and CNS inflammation, linked by immune activation and monocyte/macrophage activation and traffic. Previously, cross sectional studies have found that increased monocyte activation correlates with cardiovascular disease development¹⁻⁴. The experiments in Chapter 2 are the first to examine whether longitudinal changes in monocyte activation correlate with cardiac fibrosis in SIV+ macaques. While we show a positive correlation between monocyte activation as early as 8 dpi and cardiac fibrosis at necropsy it will be of particular interest in future studies, in humans and animals, to see if early changes in monocyte activation correlate with other markers of cardiovascular disease, such as intima-media thickness. Additionally, studies showed that SIV infection resulted in functional decline of the heart muscle itself using Doppler echocardiography⁵. As we show that early changes in monocyte activation (8 dpi) can distinguish between animals that did develop cardiac fibrosis and those that do not, it is possible that monocyte activation could be used to predict subclinical cardiovascular disease before there are any physical manifestations. This would need to be confirmed by analyzing changes in monocyte phenotypes in HIV+ individuals and examining if they correlate with predictors of CVD using non-invasive methods such as cardiac MRS or B-mode ultrasound for carotid artery intima-media thickness. This would allow the individual to begin early therapy to treat cardiovascular disease before symptoms manifest.

Having demonstrated a link between monocyte activation and macrophage inflammation in cardiac tissues, we examined in Chapter 3, cardiac tissues from SIV-infected

CD8+ T-lymphocyte depleted rhesus macaques to compare cardiac pathology with SIV-infected nondepleted animals and to determine if there is a correlation between increased cardiac inflammation and cardiac pathology. We showed that with CD8 depletion there is a higher degree of cardiac inflammation and fibrosis compared to nondepleted and uninfected animals. We showed that increased macrophage inflammation in SIV-infected CD8+ T-lymphocyte depleted animals correlated with increased fibrosis, suggesting a role for monocytes/macrophages in cardiac fibrosis. In the studies in Chapter 3, we show that uninfected animals and SIV+ nondepleted animals have few resident cardiac tissue macrophages that express CD68 and little cardiac fibrosis. Immunohistochemistry showed there is an increase in newly infiltrating monocytes/macrophages that express MAC387 in SIV+, CD8+ T-lymphocyte depleted animals compared to uninfected and SIV+ nondepleted animals. Along with BrdU experiments that showed increased traffic to the heart later during SIV infection (>21 dpi) this suggests that ongoing macrophage infiltration plays a role in the development of cardiac fibrosis.

In Chapter 4 we examined post-mortem cardiovascular tissues from HIV+ individuals on durable cART. We found a correlation between macrophage aortic and cardiac inflammation with increased aortic intima-media thickness (aIMT) and cardiac fibrosis. Additionally, we found increased levels of sCD163 in plasma of HIV+ individuals correlated with increased aIMT and cardiac fibrosis. It is interesting that in the studies in Chapter 4 involving post-mortem human samples that we see evidence of aortic inflammation when in the animal studies in Chapter 6 the aorta of all animals appeared normal. This is possibly due to aortic disease not being present in nonhuman primate models unless they are fed a high-fat, “western” diet which would lead to the development of atherosclerosis.

In Chapters 3 and 4 we show that there are increased numbers of M2 macrophages that express CD163 and CD206. Recent studies found that M2 polarized macrophages are present in unstable atherosclerotic plaques that occur in HIV+ individuals^{6,7}. Studies have begun to use radiolabeled labeled ligands against CD206 (Tilmanocept) in conjunction with PET imaging to target these macrophages specifically in order to image and stage atherosclerotic plaques⁸. Preliminary data from our lab shows that in Tilmanocept has a high degree of specificity for CD206+ macrophages in the aorta (Appendix A) Tilmanocept and PET imaging, in theory, could also be used to visualize specific macrophage inflammation in vasculature as well as the heart. Knowing that there are specific macrophage subsets that are present in cardiovascular inflammation with HIV infection, therapies could be designed as well to target those specific macrophages in order to decrease their activation or expression of pro-inflammatory and pro-fibrotic cytokines. It is possible that other macrophage subsets are present in vulnerable atherosclerotic plaques. Identifying specific surface markers on macrophage subsets would potentially allow them to be targeting by specific therapies or to be imaged as well. Double label immunohistochemistry on post-mortem samples would also be beneficial to examine if other surface macrophage markers are present on CD206+ macrophages or if they are a unique population.

In the final two chapters we examined the effects of blocking monocyte/macrophage traffic to the heart (Chapter 4) and the effects of targeting monocyte/macrophage activation directly (Chapter 5). Blocking monocyte/macrophage traffic to the heart decreased cardiac fibrosis (Chapter 4) and using MGBG to target monocyte/macrophage activation directly we found that decreased inflammation in carotid arteries and cardiac tissues resulted in decreased intima-media thickness and cardiac fibrosis. In both chapters we show that blocking leukocyte traffic to the heart correlated with decreased cardiac fibrosis (Chapter 4), and that targeting

monocyte/macrophage directly (Chapter 5) we not only decreased cardiac inflammation and fibrosis, but also demonstrated a trend of decreased macrophage numbers in carotid arteries and decreased carotid artery intima-media thickness. In the studies in Chapter 5 we did not find any difference in pathology, inflammation, or IMT in that aorta of placebo controls and treated animals, possibly be due to the model of acute infection we used. It is also possible that diet might directly influence the pathology of the aorta in SIV+ animals and as these animals were not fed a high-fat diet it is likely that they would not spontaneously develop aortic disease. While cART does not decrease marker of immune activation, in fact they remain elevated during infection, these studies show that therapeutics targeting macrophages specifically used in conjunction with cART could be effective in decreasing inflammation and alleviating not only cardiovascular disease but also other macrophage mediated diseases associated with HIV infection including neurological, renal, and bone disorders.

The data in this thesis adds evidence to the role of monocyte/macrophage activation in the development of HIV-associated cardiovascular disease. While HIV has become a chronic condition with effective cART the lifespan of an infected individual will increase, but the prevalence of cardiovascular disease among this population is expected to rise. Already current prediction models appear to underestimate the risk of cardiovascular disease development, likely due to the fact that they do not include HIV specific factors in their prediction algorithms. As the number of HIV infected individuals with cardiovascular disease continues to grow it will be important in the future to treat the symptoms of cardiovascular disease in order to continue to improve mortality of HIV+ individuals. Here we show that significant macrophage inflammation is present in cardiovascular tissues and provide evidence of possible therapeutics to use as an intervention in developing cardiovascular disease.

REFERENCES

1. Hristov M, Leyendecker T, Schuhmann C, et al. Circulating monocyte subsets and cardiovascular risk factors in coronary artery disease. *Thromb Haemost.* 2010;104(2):412-414.
2. Libby P, Nahrendorf M, Swirski FK. Monocyte Heterogeneity in cardiovascular disease. *Semin Immunopathol.* 2013;35:553-562.
3. Schlitt A, Heine GH, Blankenberg S, et al. CD14+CD16+ monocytes in coronary artery disease and their relationship to serum TNF-alpha levels. *Thromb Haemost.* 2004;92(2):419-424.
4. Gratchev A, Sobenin I, Orekhov A, Kzhyshkowska J. Monocytes as a diagnostic marker of cardiovascular diseases. *Immunobiology.* 2012;217(5):476-482.
5. Kelly KM, Tarwater PM, Karper JM, et al. Diastolic dysfunction is associated with myocardial viral load in simian immunodeficiency virus-infected macaques. *Aids.* 2012;26(7):815-823.
6. Tahara N, Mukherjee J, de Haas HJ, et al. 2-deoxy-2-[F]fluoro-d-mannose positron emission tomography imaging in atherosclerosis. *Nat Med.* 2014;20(2):215-219.
7. Burdo TH, Lo J, Abbara S, et al. Soluble CD163, a novel marker of activated macrophages, is elevated and associated with noncalcified coronary plaque in HIV-infected patients. *J Infect Dis.* 2011;204(8):1227-1236.
8. Cope FO, Abbruzzese B, Sanders J, et al. The inextricable axis of targeted diagnostic imaging and therapy: An immunological natural history approach. *Nucl Med Biol.* 2016;43(3):215-225.

APPENDIX A. Tilmanocept as a diagnostic imaging agent

INTRODUCTION

^{99m}Tc-tilmanocept (Lymphoseek®, Navidea Biopharmaceuticals, Inc.) is a diagnostic imaging agent that is approved for the identification of sentinel lymph nodes in multiple solid tumors.¹⁻³ Mechanistically, Tilmanocept recognizes and binds to CD206 receptors on macrophages and dendritic cells. In many diseases, cancers rheumatoid arthritis, cardiovascular disease, expression of CD206 is increased. Combined with multiple binding sites for Tilmanocept, the high turnover rate of CD206 receptors on macrophages, and the upregulation of CD206+ macrophages in unstable atherosclerotic plaques⁴ the specificity of Tilmanocept for CD206 potentially makes this imaging agent useful in imaging HIV-associated cardiovascular disease.⁵ Previously, we and our collaborators published results using ¹⁸F-FDG-PET imaging to assess arterial wall inflammation in HIV+ individuals. In this study we found that with HIV there was a significant increase in inflammation in the ascending aorta compared to controls that correlated with levels of soluble CD163 (sCD163).⁶ Now, patients from the same study are undergoing imaging with ^{99m}Tc-tilmanocept. Here, we show preliminary data from 16 sections of aorta (n= 10, HIV-, n=10 HIV+) and 3 sections of carotid artery with atherosclerotic plaques that there is a high degree of co-localization between CD206 and CD163 on macrophages and that Tilmanocept specifically targets CD206+ macrophages.

METHODS

Single Label Immunohistochemistry

Single label immunohistochemistry for CD163⁺ and CD206⁺ macrophages was performed on formalin-fixed paraffin embedded sections of aorta from HIV- (n=10) and HIV+ (n=10) individuals and carotid artery (n=3) with atherosclerotic plaques, from different donors. Sections were provided by the National NeuroAIDS Tissue Consortium (NNTC) and the National Disease Research Institute (NDRI). Tissue sections were deparaffinized and rehydrated in xylenes and graded ethanols followed by antigen retrieval (Vector) using high heat for 20 mins. Sections were then incubated with peroxidase block (Dako), washed in TBS-T, followed by a 30 minute protein block. Sections of the aorta were incubated with monoclonal antibodies recognizing CD163⁺ macrophage (Serotec) or CD206 (R&D Systems) for 1hr at RT (CD163) or overnight at 4°C (CD206). Sections were washed in TBS-T and incubated with an anti-mouse secondary antibody conjugated to horseradish peroxidase (Dako). The reaction product was visualized using 3, 3'-diaminobenzidine tetrahydrochloride (DAB, Dako). The average number of immune positive macrophages/mm² plus or minus the standard error of the mean (SEM) was determined by counting the number of positive macrophages from twenty non-overlapping 200x fields of view (field area=0.148mm²) per section, using a Zeiss Axio Imager M1 microscope with Plan-Apochromat x20/0.8 Korr objectives (Carl Zeiss Microimaging Inc., Thornwood, NY).

Immunofluorescence

Double label immunofluorescence was performed on formalin-fixed paraffin embedded sections of aorta from 10 HIV- and 10 HIV+ individuals using antibodies against CD163 and CD206 and fluorescently labeled Tilmanocept. Tissue sections were permeabilized in 0.1% TritonX-100/PBS/fish skin gelatin (FSG) and washed with PBS/FSG. They were subsequently

blocked in PBS/FSG with 10% normal goat serum (NGS), followed by 1 hour or overnight incubation with primary antibodies diluted in PBS/FSG/normal goat serum. After primary incubation sections were washed in PBS/FSG before adding the fluorescent secondary antibody diluted in PBS/FSG normal goat serum. Finally the sections were washed in PBS/FSG and incubated in copper sulfate in ammonium acetate for 45 minutes to quench auto fluorescence. Tissue sections were stained with a combination of CD163 and CD206, CD163 and Tilmanocept, and CD206 and Tilmanocept antibodies and visualized using a Zeiss Axio Imager.Z2 with Apotome filter and x200 objective.

For sections double labeled with CD163 and CD206 antibodies, the percentage of CD163⁺CD206⁺, CD163⁺CD206⁻, and CD163⁻CD206⁺ cells was determined by counting the number of positive cells for each phenotype divided by the total number of cells in the field of view. The average percentage was calculated from 20 random, non-overlapping x200 fields of view. For sections double labeled with CD203 and Tilmanocept the percentage of Tilmanocept⁺ CD206⁺ and Tilmanocept⁻ CD206⁺ was determined by counting the number of positive cells for each phenotype divided by the total number of CD206⁺ cells.

RESULTS

Increased expression of CD163 and CD206 in the aorta with HIV infection

In the aorta there was increased expression of CD163⁺ and CD206⁺ macrophages with HIV infection. The mean number of CD163⁺ macrophages/mm² for HIV- individuals was 22.95±3.66 compared to 46.78±5.40 for HIV+ individuals, a significant 2.03-fold increase (Fig. 1A). The mean number of CD206⁺ macrophages/mm² for HIV- was 14.74±5.64 compared to 30.08±6.27 for HIV+ individuals, a significant 2.13-fold increase (Fig. 1B).

Co-localization of CD163 and CD206 on macrophages in the aorta

Sections of aorta from HIV- (n=10) and HIV+ (n=10) individuals were double labeled with antibodies against CD163⁺ and CD206⁺ macrophages. There was a high degree of colocalization between CD163 and CD206 in sections from HIV- and HIV+ individuals. The percentage of CD163⁺CD206⁺ macrophages in the aorta for HIV- individuals was 88.24±4.5% and 90.01±6.3% for HIV+ individuals. The percentage of CD163⁺CD206⁻ was 10.75±5.1 and 9.98±3.3%, respectively. There were no cells in sections of the aorta from HIV- or HIV+ individuals that had a CD163⁻CD206⁺ (Fig. 1C).

Co-localization of CD206 and Tilmanocept on macrophages in the aorta

Sections of aorta were double labeled with an antibody against CD206⁺ macrophages and its ligand, fluorescently labeled Tilmanocept. The percentage of colocalization was determined by counting CD206⁺ macrophages and determining if they were also positive for Tilmanocept. There was a similar degree of colocalization of Tilmanocept and CD206 in sections from HIV- and HIV+ individuals. There was 89.03±3.7% colocalization between Tilmanocept and CD206 in sections of aorta from HIV- individuals and 91.73±6.4% in sections from HIV+

individuals. The percentage of Tilmanocept⁻CD206⁺ was 8.27±4.2 and 8.54±3.5% for sections of aorta from HIV- and HIV+ individuals, respectively (Fig. 1 D).

Co-localization of CD163 and CD206 on macrophages in carotid arteries

Sections of carotid artery with atherosclerotic plaques (Fig. 2A) from individuals were double labeled with antibodies against CD163⁺ and CD206⁺ macrophages. There was a high degree of co-localization between CD163⁺ and CD206⁺ macrophages in the shoulder and cap regions of plaques. The percentage of CD163⁺CD206⁺ macrophages was 84.59±1.35%. The percentage of CD163⁺CD206⁻ was 14.56±3.45. The percentage of CD163⁻CD206⁺ macrophages was 0.84±0.43%.

Co-localization of CD206 and Tilmanocept on macrophages in carotid arteries

Sections of carotid artery (n=3) were double labeled with an antibody against CD206⁺ macrophages and its ligand, fluorescently labeled Tilmanocept (Fig. 2B). In shoulder and cap regions of plaques in the carotid artery there was a high degree of co-localization between CD206 and Tilmanocept. We found that the percentage of Tilmanocept⁺CD206⁺ was 87.94±4.26% and the percentage of Tilmanocept⁻CD206⁺ was 12.03±3.27%.

Discussion

In this preliminary study we confirmed that with HIV infection there is an increase in CD163 and CD206 expression in the aorta compared to controls, and demonstrated a high degree of co-localization between CD206 and Tilmanocept in macrophages in the aorta and carotid artery. Currently there are several diagnostic techniques that can be used to detect cardiovascular inflammation associated with HIV; however, many of them do not target a specific macrophage subset. Cardiac magnetic resonance (CMR) can be used to gain information about the presence of inflammation and fibrosis in the heart^{7,8} and FDG-PET can assess arterial inflammation⁶, but this technique labels all metabolically active cells, likely macrophages. However, in this preliminary data we show that Tilmanocept specifically targets CD206+ macrophages in arteries. Previous research showed that CD206 expression is upregulated in unstable atherosclerotic plaques.⁴ Using ^{99m}Tc-tilmanocept it is possible that only those specific macrophages involved in plaque instability and rupture could be identified and discriminate between stable and unstable atherosclerotic plaques.

REFERENCES

1. Leong SP, Kim J, Ross M, et al. A phase 2 study of (99m)Tc-tilmanocept in the detection of sentinel lymph nodes in melanoma and breast cancer. *Ann Surg Oncol*. Apr 2011;18(4):961-969.
2. Sondak VK, King DW, Zager JS, et al. Combined analysis of phase III trials evaluating [(99m)Tc]tilmanocept and vital blue dye for identification of sentinel lymph nodes in clinically node-negative cutaneous melanoma. *Ann Surg Oncol*. Feb 2013;20(2):680-688.
3. Wallace AM, Hoh CK, Ellner SJ, Darrah DD, Schulteis G, Vera DR. Lymphoseek a molecular imaging agent for melanoma sentinel lymph node mapping. *Annals of Surgical Oncology*. 2007;14(2):913-921.
4. Tahara N, Mukherjee J, de Haas HJ, et al. 2-deoxy-2-[F]fluoro-d-mannose positron emission tomography imaging in atherosclerosis. *Nat Med*. Jan 12 2014;20(2):215-219.
5. Cope FO, Abbruzzese B, Sanders J, et al. The inextricable axis of targeted diagnostic imaging and therapy: An immunological natural history approach. *Nuclear Medicine and Biology*. 2016;43(3):215-225.
6. Subramanian S, Tawakol A, Abbara S, et al. Arterial Inflammation in Patients With HIV. *JAMA*. 2012;308:379-386.
7. Luetkens JA, Doerner J, Thomas DK, et al. Acute myocarditis: multiparametric cardiac MR imaging. *Radiology*. Nov 2014;273(2):383-392.
8. Luetkens JA, Doerner J, Schwarze-Zander C, et al. Cardiac Magnetic Resonance Reveals Signs of Subclinical Myocardial Inflammation in Asymptomatic HIV-Infected Patients. *Circ Cardiovasc Imaging*. Mar 2016;9(3):e004091.

Figure A.1

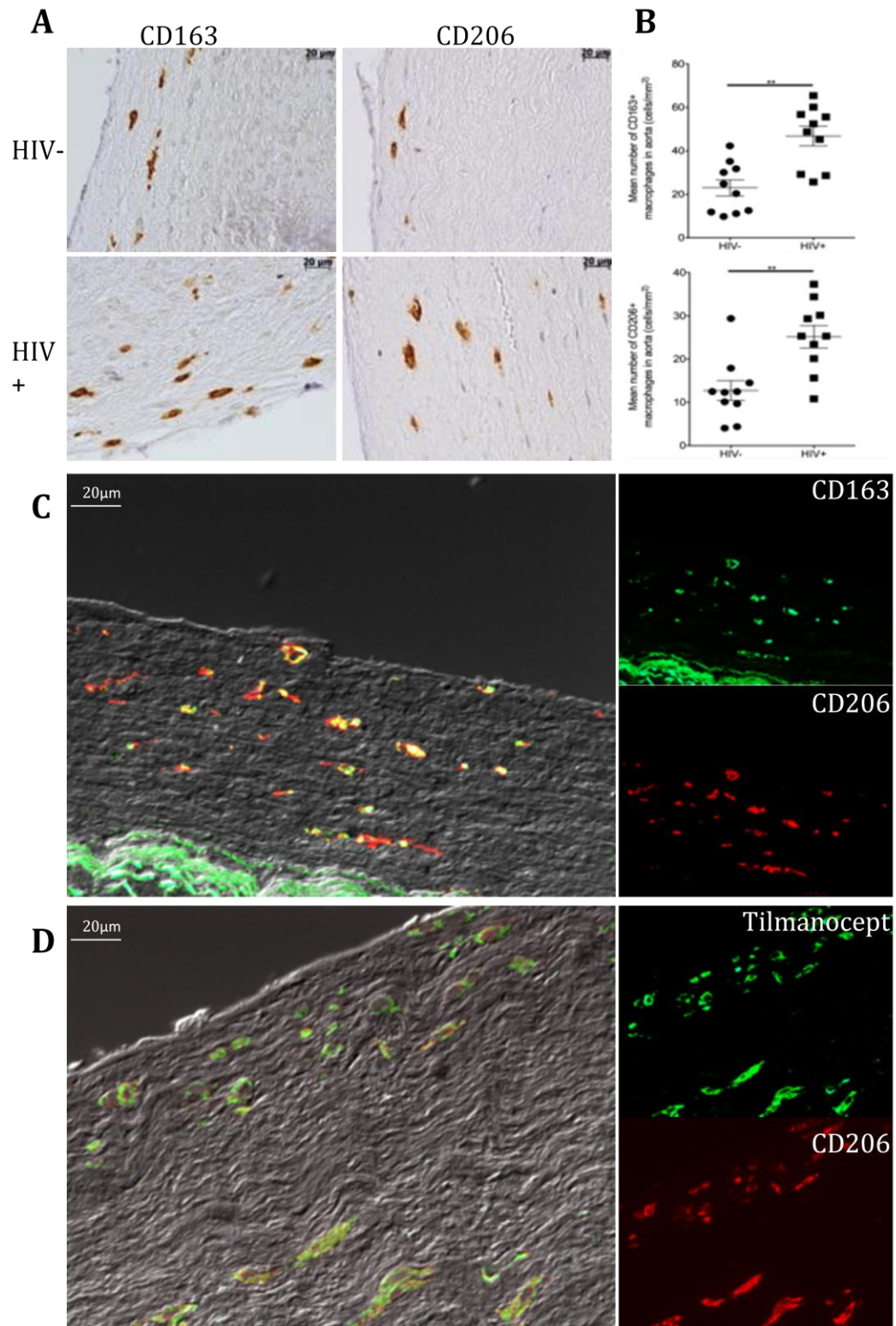
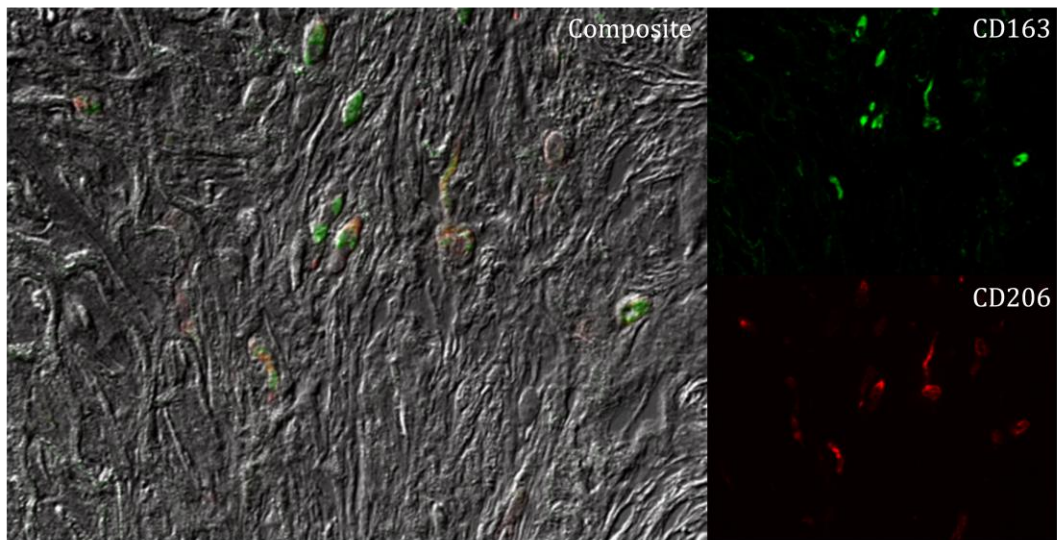


Figure A.1. Tilmanocept shows a high degree of specificity in targeting CD206+ macrophages in the intima of the aorta.

(A) Sections of aorta from HIV⁻ (top, n=10) and HIV⁺ (bottom, n=10) were stained with antibodies recognizing CD163⁺ and CD206⁺ macrophages. (B) There was a significant 2.03 and 2.13-fold increase in numbers of CD163⁺ and CD206⁺ macrophages in the aorta of HIV⁺ individuals compared to controls (*p<0.05). (C) Double label immunofluorescence showed a high degree of co-localization between CD163 and CD206 in the aorta of HIV⁻ and HIV⁺ individuals. The percentage of CD163⁺CD206⁺ macrophages in the aorta for HIV⁻ individuals was 88.24±4.5% and 90.01±6.3% for HIV⁺ individuals. The percentage of CD163⁺CD206⁻ was 10.75±5.1 and 9.98±3.3%, respectively. There were no cells in sections of the aorta from HIV⁻ or HIV⁺ individuals that had a CD163⁻CD206⁺. (D) Fluorescently labeled tilmanocept shows a high level of colocalization with CD206⁺ macrophages in the aorta. There was 89.03±3.7% colocalization between Tilmanocept and CD206 in sections of aorta from HIV⁻ individuals and 91.73±6.4% in sections from HIV⁺ individuals. The percentage of Tilmanocept⁻CD206⁺ was 8.27±4.2 and 8.54±3.5% for sections of aorta from HIV⁻ and HIV⁺ individuals, respectively.

Figure A.2

A



B

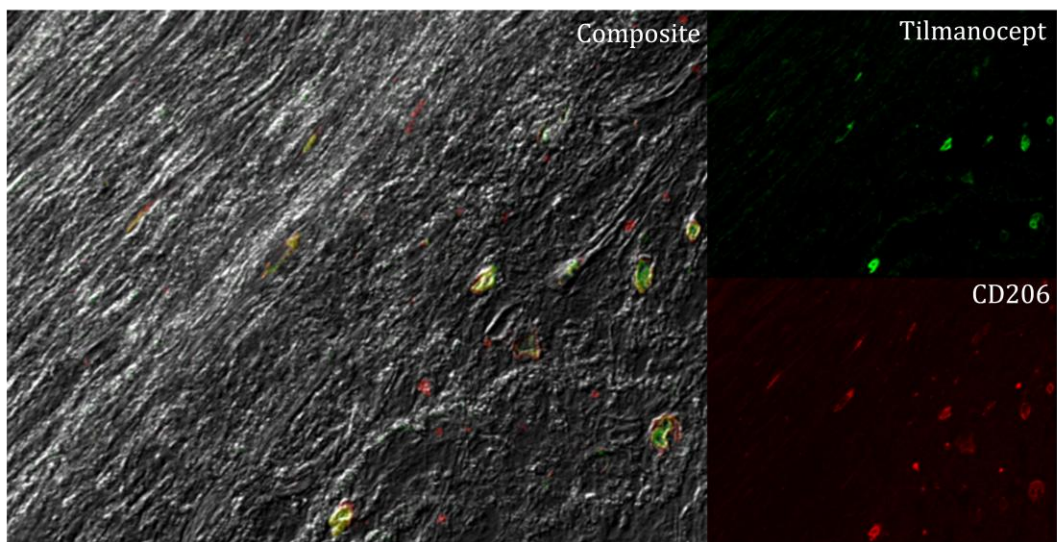


Figure A.2. Tilmanocept shows a high degree of specificity in targeting CD206+ macrophages in the carotid artery with atherosclerotic plaque.

(A) Double label immunofluorescence showed a high degree of co-localization between CD163 and CD206 in the aorta of HIV⁻ and HIV⁺ individuals. . The percentage of CD163⁺CD206⁺ macrophages was 84.59±1.35%. The percentage of CD163⁺CD206⁻ was 14.56±3.45. The percentage of CD163⁻CD206⁺ macrophages was 0.84±0.43%. (B) Fluorescently labeled tilmanocept shows a high level of colocalization with CD206⁺ macrophages in the aorta. We found that the percentage of Tilmanocept⁺CD206⁺ was 87.94±4.26% and the percentage of Tilmanocept⁻CD206⁺ was 12.03±3.27%.

APPENDIX B. Publications

Publications

F. O. Cope, B. Abbruzzese, J. Sanders, W. Metz, K. Sturms, D. Ralph, M. Blue, J. Zhang, P. Bracci, W. Bshara, S. Behr, T. Mauer, K. Williams, **J. A. Walker**, A. Beverly, B. Blay, A. Damughatla, M. Larsen, C. Mountain, E. Neylon, K. Parcel, K. Raghuramen, K. Ricks, L. Rose, A. Sivakumar, N. Streck, B. Wang, C. Wacco, A. Williams, M. McGrath. (2016). The Inextricable Axis of Targeted Diagnostics Imaging and therapy: An Immunological Natural History Approach. *Nuclear Medicine and Biology*.

T. H. Burdo, **J. A. Walker**, K. C. Williams. (2015). Macrophage Polarization in AIDS: Dynamic Interface between Anti-Viral and Anti-Inflammatory Macrophages during Acute and Chronic Infection. *Journal of Clinical and Cellular Immunology*.

J. A. Walker, G. A. Beck, J. H. Campbell, A. D. Miller, T. H. Burdo, K. C. Williams (2015). Anti- $\alpha 4$ Antibody Blocks Monocyte/Macrophage Traffic to the Heart and Decreases Cardiac Pathology in a SIV Infection Model of AIDS. *Journal of the American Heart Association*.

J. A. Walker, M. L. Sulciner, K. D. Nowicki, A. D. Miller, T. H. Burdo, K. C. Williams (2014). Elevated Numbers of CD163+ Macrophages in Hearts of Simian Immunodeficiency Virus-Infected Monkeys Correlate with Cardiac Pathology and Fibrosis. *AIDS Research and Human Retroviruses*.

Under submission or to be submitted

J.A. Walker, A. D. Miller, T. H. Burdo, M. S. McGrath, K. C. Williams (2016). Direct targeting of macrophages with MGBG Decreases SIV-Associated Cardiovascular Inflammation and Pathology. *Under Review. Journal of Acquired Immune Deficiency Syndromes*

J.A. Walker, J. Wang, A. D. Miller, P. Autissier, K.C. Williams (2016). Expansion of CD14⁺CD16⁺ Monocyte Subset Correlates with Increased Cardiac Fibrosis, Inflammation, and Encephalitis in SIV-infected Rhesus Macaques. *To be submitted*

J. A. Walker, G. A. Beck, J. H. Campbell, K. D. Nowicki, A. D. Miller, T. H. Burdo, K. C. Williams
(2016). Increased Aortic Intima Media Thickness and Cardiac Fibrosis Correlates with Soluble
CD163: A Role for Monocytes/Macrophages in HIV-Associated Cardiovascular Disease
Progression. *To be submitted*

APPENDIX C. Conferences and Awards

Grant and Awards

Young Investigator Award: 22nd Conference on Retroviruses and Opportunistic Infections. Seattle, WA. 2015 *“Soluble CD163 Correlates with Intima-Media Thickness and Macrophages in the Aorta and Cardiac Tissues with HIV Infection”*

Young Investigator Award: 20th Conference on Retroviruses and Opportunistic Infections. Atlanta, GA. 2013. *“Elevated Numbers of CD163+ Macrophages In Hearts Of SIV+ Rhesus Macaques With Cardiac Disease Are Decreased With MGBG Treatment”*

Oral Presentations

20th Conference on Retroviruses and Opportunistic Infections. Atlanta, GA. 2013. *“Elevated Numbers of CD163+ Macrophages In Hearts Of SIV+ Rhesus Macaques With Cardiac Disease Are Decreased With MGBG Treatment”*

Poster Presentations

23rd Conference on Retroviruses and Opportunistic Infections. Boston, MA. 2016. *“SIV-Associated Pathogenesis Modulation with Macrophage Targeted MGBG”*

22nd Conference on Retroviruses and Opportunistic Infections. Seattle, WA. 2015. *“sCD163 in Plasma Correlates with Increased Intima-Media Thickness and Fibrosis in Aorta and Heart with HIV Infection”*

13th International Symposium on NeuroVirology. San Diego, CA. 2015. *“Macrophage Infiltration and Chronic Immune Activation Correlates with Encephalitis and Cardiac Fibrosis”*

32nd Annual Symposium on Nonhuman Primate Model of AIDS. Portland, OR. 2014. *“Increased Numbers of CD206+ Macrophages with SIV-Associated Cardiovascular Pathology”*

29th Annual Symposium on Nonhuman Primate Model of AIDS. Seattle, WA. 2011. “Elevated Numbers of CD163+ Macrophages in Cardiac Tissues of SIV Infected Rhesus Macaques with Cardiac Pathology”

ⁱ This research was originally published in *AIDS Research and Human Retroviruses*. Joshua A. Walker, Megan L. Sulciner, Katherine D. Nowicki, Andrew D. Miller, Tricia H. Burdo, Kenneth C. Williams. Elevated numbers of CD163+ macrophages in hearts of simian immunodeficiency virus-infected monkeys correlate with cardiac pathology and fibrosis. *AIDS Research and Human Retroviruses*. 2014;30:685-694.

ⁱⁱ This research was originally published in *Journal of the American Heart Association*. Joshua A. Walker, Graham A. Beck, Jennifer H. Campbell, Andrew D. Miller, Tricia H. Burdo, Kenneth C. Williams. Anti-alpha4 integrin antibody blocks monocyte/macrophage traffic to the heart and decreases cardiac pathology in a SIV infection model of AIDS. *Journal of the American Heart Association*. 2015;4:e001932.

ⁱⁱⁱ This research is currently under submission at *Journal of Acquired Immune Deficiency Syndromes*.